Chapter 2: Part I

Pharmacophore I: Amidines and Amide Adducts

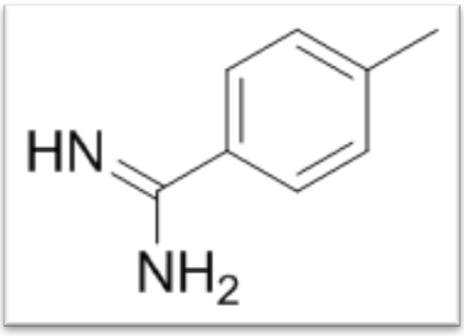

Abstract:

Amidines, due to their unique biocompatibility and desirable physical characteristics, have been the functionality of choice as a scaffold for large number of drug synthesis. Still synthesis of amidines in presence of other active functional groups or pharmacophore, remained a challenge. In this work, a simple and reliable protocol for conversion of nitrile-amide to unsubstituted amidine-amide is developed using metal amide and/or ammonia gas. The scope and efficiency of this synthetic strategy is demonstrated on a number of substrates which differ in functional groups will be discussed. The designing of synthesized molecules is in accordance with docking studies performed on PRMT1. In this process, ten novel aryl amidines in good yields (upto 85%) were synthesized. Biological evaluation revealed that compound 4-(aminoiminomethyl)-N-(2-furanyl methyl) benzamide (IC_{50}=9μM) and 4-(aminoiminomethyl)-*N*-(3-pyridinylmethyl) benzamide (73.36% growth inhibition) showed moderate efficacy for cancer cells.

2.1.1 Introduction

As discussed in the preceding chapter, the importance of working with pharmacophore based drug designing appears to be very useful in the present world. This has led to many successful drugs in market.

Protein arginine methyl transferase (PRMT) as a therapeutic target plays an important role not only in cancer but also for other diseases such as cardiovascular diseases, virus related diseases and endothelial cell (EC) inflammatory responses [1]. Therefore, the critical functions of PRMTs in oncogenesis make the PRMT family of enzymes, promising therapeutic targets in drug discovery [2].

One strategy to control anti-proliferative activity is to design PRMT inhibitors with a varying pharmacophore. In literature, these inhibitors are divided into two groups. The first group consists of peptide derivatives having critical role of 'amide' pharmacophore [3-6]. The second class consists of inhibitors derived out of small organic molecules, which are normally obtained from random or target based screening such as AMI-1, stilbamidine, allantodapsone, RM-65 and SAM derivatives (Figure 2.1) [7-9]. Most of these targeted compounds have diamidine structure in them.

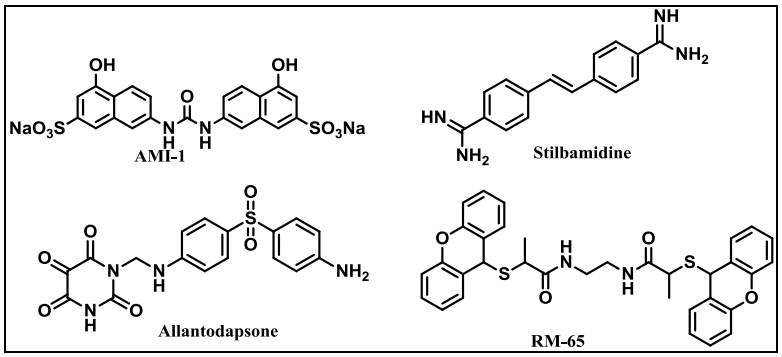

Figure 2.1.1: PRMT inhibitors

Amidine functionality serves as a synthon for the synthesis of variety of heterocyclic compounds [10]. On the other hand, amidines with their unique structural properties and bio-compatibility are present in various active pharmaceuticals ingredients (API) employed for antiviral, anti-inflamatory and anticancer [11]. This latter aspect will open up new scope for amidines as a pharmacophore.

Synthesis of amidines has been explored by many scientists in the past. Out of the various reagents available for the synthesis of amidine, single step conversion of nitrile to amidine remained the choice of synthetic chemists. In the reported methods, the nitrile functionality is activated by electron withdrawing groups or lewis acids [12-13] to give the desired products.

Pinner reaction, to the best of our knowledge, happens to be the most commonly used technique for the amidine synthesis from the parent nitrile compound [14]. Contemplating the mechanism, first step being the cyanide activation using dry HCl gas in dry methanol, leads to the formation of amidinates as shown in *Scheme 2.1.1*. Ammonia attack is the next step which leads to amidine, the desired product, in good yield. Key step in this process remains the activation of nitrile group by HCl. This may lead to unwanted chemical reactions if additional functional groups are present on substrate. This is what is observed in our case, nitrile-amide system, where functional group started reacting prior to nitrile acitivation and it leads to the formation of undesired products. Hence for our substrate, there is a need to find an alternative methodology where nitrile group is activated prior to the amide linkage.

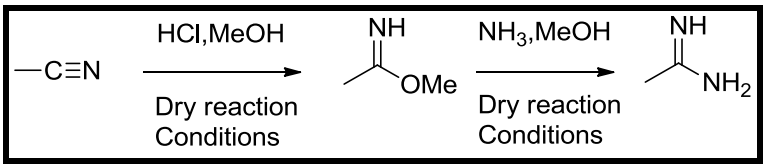

Scheme 2.1.1: Pinner reaction conditions

Further literature search resulted in few more alternative methods where scientists have used different reagents/reaction conditions for the conversion of nitrile to amidine (*Scheme 2.1.2*) [12,15-16]. Cornell et al (1928) reported the synthesis of aliphatic and aromatic amidines from their parent nitriles using liquefied ammonia gas with various metal amides [17]. Criticality of this reaction was the difficulty in handling liquefied ammonia gas in standard synthetic laboratory. Newbery et al (1947) used same reagent (metal amides) but with slightly milder conditions, using benzene as solvent at high temperatures [18]. The drawback of using this method is the solubility of the parent nitriles in benzene and also the toxicity of the solvent [19]. Interestingly, today's drug

design challenge revolves around presence of more than one functional group (pharmacophores) on a single API [20].

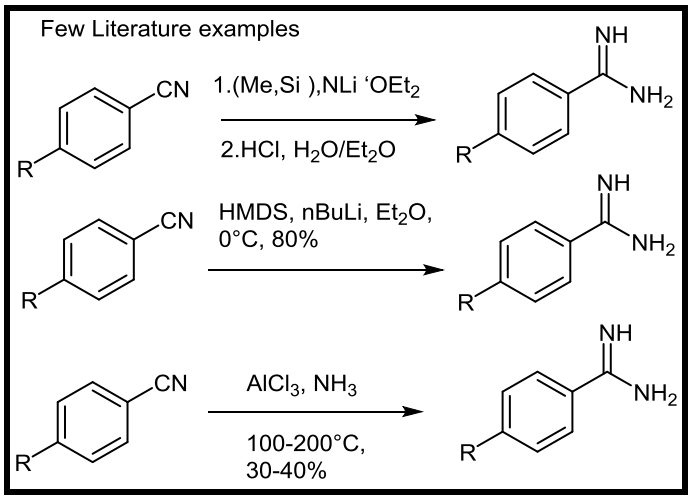

Scheme 2.1.2: Literature of amidine synthesis from nitriles

2.1.2 Our Strategy:

Keeping the above literature survey in mind, our efforts were focused on amidine synthesis in the presence of amide ($R.CO.NH_2$) functionality (*Figure 2.1.1 and Figure 2.1.2*).

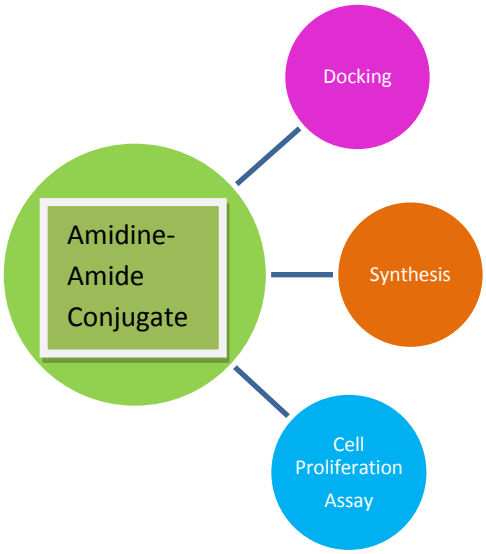

Figure2.1.1: Overall Strategy

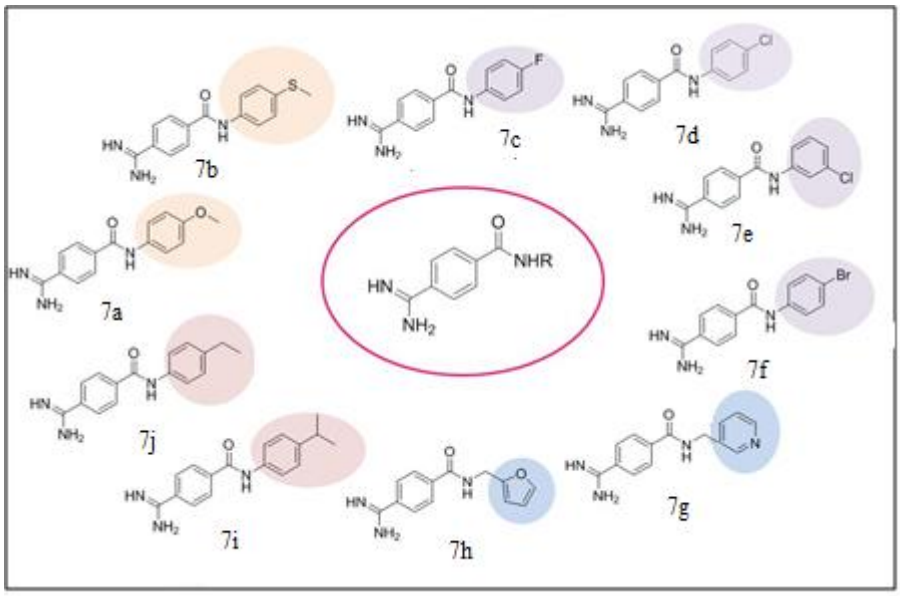

Figure2.1.2: Our strategy for the synthesis of novel amidines

2.1.3 Results and Discussion:

A. Docking Studies:

Due to the immense pharmacological activity of diamidines, it has attracted attention of many medicinal chemists to identify its inhibitory properties against PRMT1. In a pioneering study by Spannhoff et al. [21], it has been found that, a diamidine compound, stilbamidine, inhibited PRMT1 activity at the micromolar level. Second to this report, Yan et al [22] also developed some novel derivatives resembling amidine of the guanidine moiety of the substrate arginine to maintain the substrate-specificity. Results of the study confirmed that the presence of positively charged amidine functional group serves as an anchor to engage the peptidic site of PRMT. It leads to the stabilization of the ligand at the target site necessary for inhibitory activity. As X-ray crystal structure information for human PRMT1 is not yet available, structural data for the homologous rat proteins PRMT1 (sequence identity 95.1%) (PDB:3Q7E; www.pdb.org) was used for our studies. The rat and human PRMT1 differ only at one position (H161 is Y in human) [23]. The file contains arginine methyltransferase co-crystallized with its ligand (S-adenosyl methionine).

Results of the docking study have been elucidated in *Table 2.1.1*. It has been found that, the entire set of the molecules show considerable affinity against PRMT1, which may serve as the probable cause for its significant anticancer activity. Almost all compounds show the formation of hydrogen bonds (H-bonds) with key catalytic residue of Lys90, except compound **7c**, which show an additional bond with Lys116. Whereas, no H-bond was revealed in the case of compound **7f** having substitution of bromine at *para*-position. It is surprising to note that, Lys 90 was again found as predominant residue for creation of π-cation interaction, except in the case of **7h** and **7j** (Lys116), whereas, compound **7a** and **7i** showed no such bonds. As explained by CDOCKER interaction energy, these compounds are energetically proficient enough to engage key catalytic residues viz. Lys90 and Lys116. To better understand the structural features imperative for PRMT1 inhibition and to exemplify the key structural parameter necessary for bioactivity, the docked orientation of most promising and least active inhibitors were examined, compound **7h** and **7a**, respectively. As shown in *Figure 2.1.3*, it was found that, the most active compound **7h** showed the formation of additional π-cation interaction with Lys116 along with formation of H-bond. While, this similar interaction was absent in compound **7a**. On close inspection of above oriented ligands, it was shown that, compound **7h** was found to be oriented in a U-shape, while compound **7a** does not attain such confirmation and this may be work out as a probable reason for its inactivity. In order to validate the orientation of these two ligands at the target site, the Root Mean Square Deviation (R.M.S.D) value has been identified between two molecules. The R.M.S.D. value has been found $>$2Å suggesting the ligands bind to active site of the PRMT1 in a similar fashion. Thus, this study has suggested that, small structural variation may induce marked influence on the orientation which in turn influences the bioactivity of the tested compound.

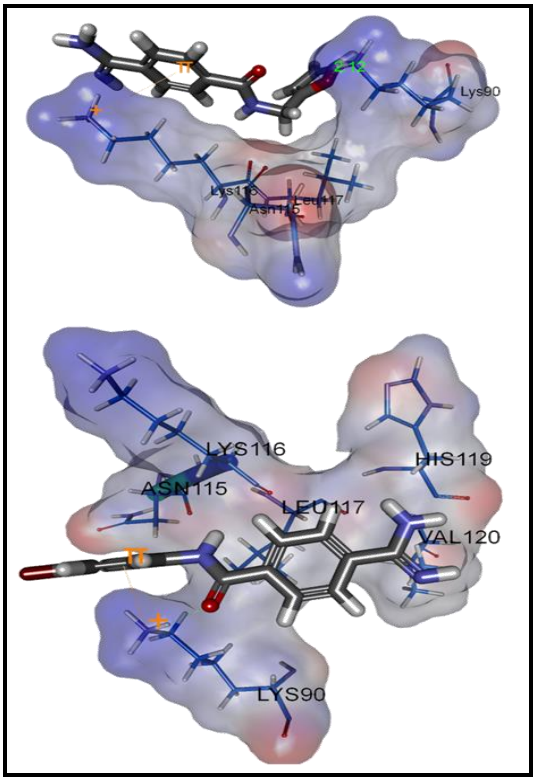

Figure 2.1.3: Interaction of 7h and 7a with PRMT-1.

Table 2.1.1: Tabulation of Docking Results

Entry	H-bonds	π-cation	CDOCKER interaction energy (kcal mol^{-1})	Remarks
7a	Lys90, Lys116	no	22.21	Least active compound
7b	Lys90		6.59	
7c	Lys90, Lys116	Lys90	15.61	
7d	Lys90	Lys90	18.91	
7e	Lys90	Lys90	23.50	
7f	No	Lys90	10.17	
7g	Lys90	Lys90	21.68	
7h	Lys90,	Lys116	29.34	Most active compound
7i	Lys90	no	22.94	

7j	Ala90	Lys116	16.13

B. Synthesis:

Amidine Synthesis:

The first step for us was to synthesize the amidine group. Literature survey for this revealed that the best way to obtain amidine is from the conversion of cyano group. This conversion has been done by ancient traditional synthesis Pinner reaction as shown in the scheme below (*Scheme 2.1.3*).

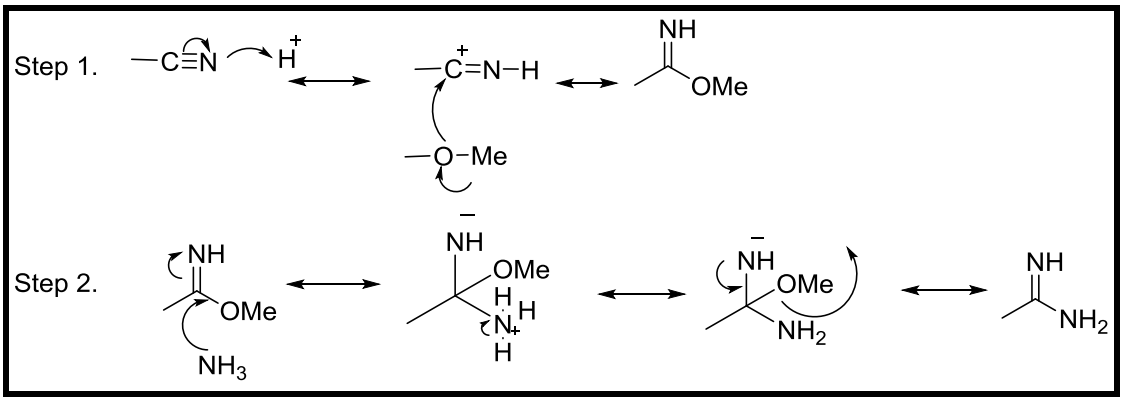

Scheme 2.1.3: Mechanism of Pinner reaction in general

As we can see in the above mechanism, the first step is the activation of cyano group using proton ion, making the carbon more electron deficient and then the attack of methanol's oxygen to give the imidate as intermediate. Next step here is the nucleophilic substitution of $-NH_2^-$ with -OMe.

For our substrate the first step, activation step, can be done at two sites: 1. Cyano 2. Amide's carbonyl carbon (*Figure 2.1.4*). This is what observed. When the standard Pinner reaction conditions were employed to our substrate the activation of amide's carbonyl carbon was observed leaving behind the undesired cleaved product (Cyanobenzene + Aniline derivatives) (*Figure 2.1.5*). Hence there was an urgent need to check for this solution.

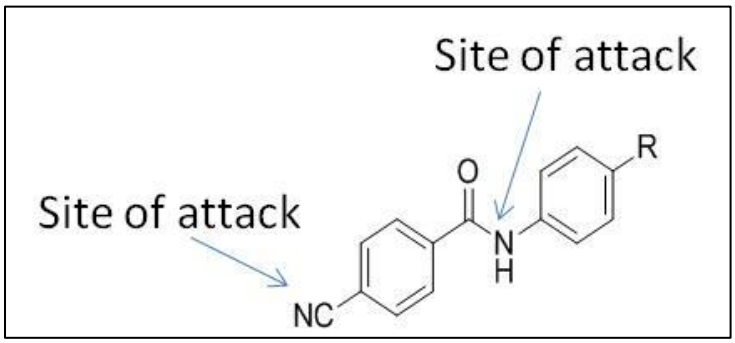

Figure 2.1.4: Probable sites in our substrate for nucleophilic attack

Mechanism:

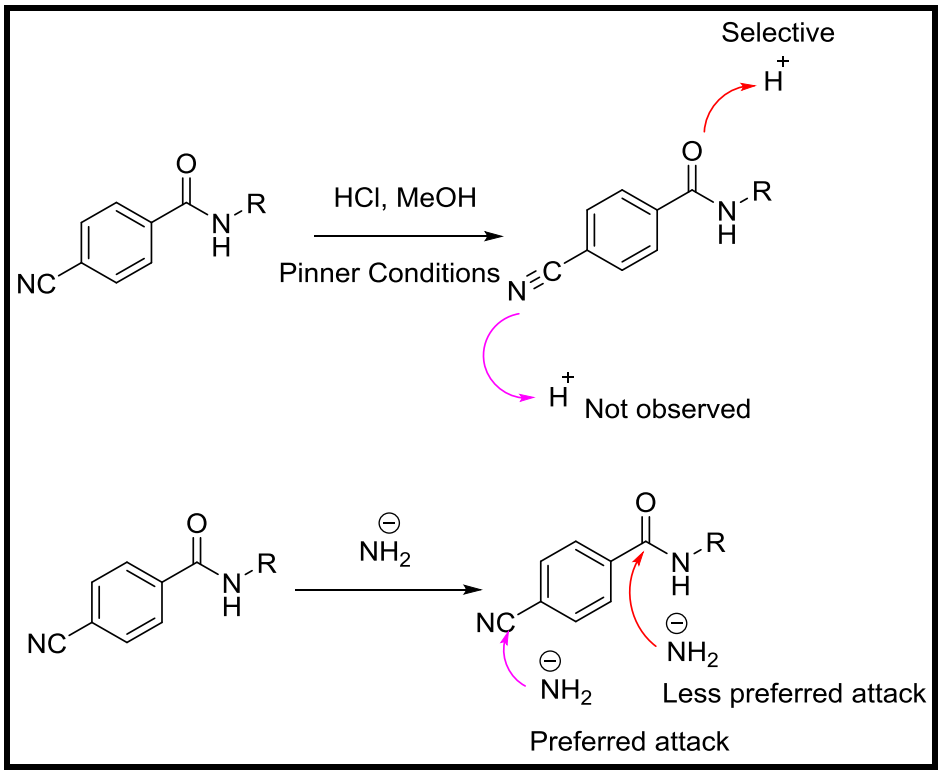

Figure 2.1.5: Selectivity of reaction justifying our synthetic methodology

Our reaction conditions: The only solution was to use a reagent where the amide anion could be generated or directly used (NH_2^-). This process can be considered as a 'direct'

amidine formation method, since it requires no prior activation of nitrile functionality. Now, NH_2^- can be generated in-situ as well as ex-situ. Therefore, both the methods were used: Method 1- in-situ generation: dry NH_3 (g) with sodium hydride in DMSO, and Method 2- ex-situ generation: Sodamide in DMSO (*Scheme 2.1.4*). The role of sodium hydride in the Method-1 is to abstract proton from ammonia and form NH_2^- (in-situ generation). Both these methods, when carried out at room temperature (16-25°C), gave good yields with substantial reduction in the time of the reaction as compared to literature. Interestingly, bottle-neck for both these modified methods remains is the contact time of sodamide and nitrile functionality, which can be controlled by tailoring the reaction conditions.

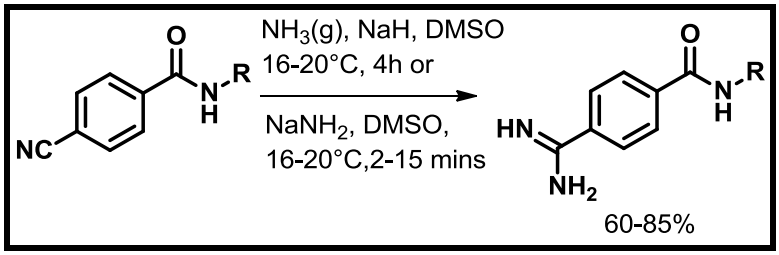

Scheme 2.1.4: Our reaction conditions for the synthesis of new amidine-amide adduct

Reaction conditions were explored. *Table 2.1.1* shows results of screening different reaction conditions for both these methods on 4-(aminoiminomethyl)-benzamide, a standard substrate with presence of amide functionality with nitrile. Thus, standardized optimum conditions were employed for the synthesis of ten new compounds with amidine-amide linkages. As we can see in table 2.1.1, dipolar aprotic solvents DMF and DMSO favors the reaction, although DMF favors side reactions also, giving rise to the reduced yields. This could be because $-NH_2^-$ intermediate is stabilized by the polar solvents facilitating the reaction in the forward direction.

Table 2.1.1 : Reaction Conditions tried for amidination

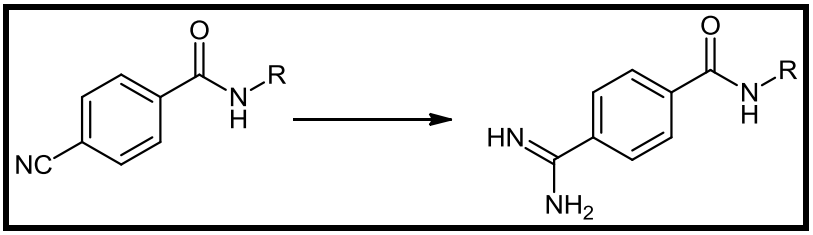

Entry	Reagent[b]	Solvent	Yield[c] %
1	Na, NH_4Cl	MeOH	No reaction
2	HCl(g), EtOH/NH_3(g)	EtOH	No reaction
3	$NH_2OH.HCl$,TEA/NH_3(g)	EtOH	No reaction
4	NH_4Cl, Si[d]	MeOH	No reaction
5	EtOH.HCl/NH_4Cl	MeOH	No reaction
6	NH_3(g), NaH	THF	15
7	NH_3(g), NaH	DMF	35
8	NH_3(g), NaH	Toluene	No reaction
9	NH_4Cl, NaH	Toluene	No reaction
10	NH_4Cl, NaH	DMSO	No reaction
11	NH_3(g), NaH	DMSO	80-85
12	$NaNH_2$	DMSO	80-85

[b] Reactions were performed based on the literature procedure.

[c] Yield of the isolated product after column chromatography

[d] Reaction was performed in a sealed tube.

Overall Synthesis of the amidine and amide adducts:

Synthesis starts with 4-iodo-*N*-(4-methoxyphenyl) benzamide **5a** was obtained from 4-iodobenzoic acid **4** (*Scheme 2.1.5*) in two stages, treatment with thionyl chloride in first step and DMAP/R-NH_2 [22-24] in second step. For the latter step, variety of bases triethyl amine (TEA), diethyl amine (DEA) and (dimethyl amino pyridine) DMAP along with number of solvents such as dry ACN, MDC, $CHCl_3$ and CCl_4 was employed. The best yields were obtained with MDC and DMAP. Traditionally, Iodo/nitrile exchange employs NaCN or KCN but in our present strategy we preferred 'green' nitrile source in the form of cuprous cyanide (CuCN). Good yield of 4-cyano-*N*-(4-methoxyphenyl) benzamide **(6a-j)** were accessed by reacting 4-iodo-*N*-(4-methoxyphenyl) benzamide (**5a-j)** with the requisite CuCN as the nitrile source in dry DMF.

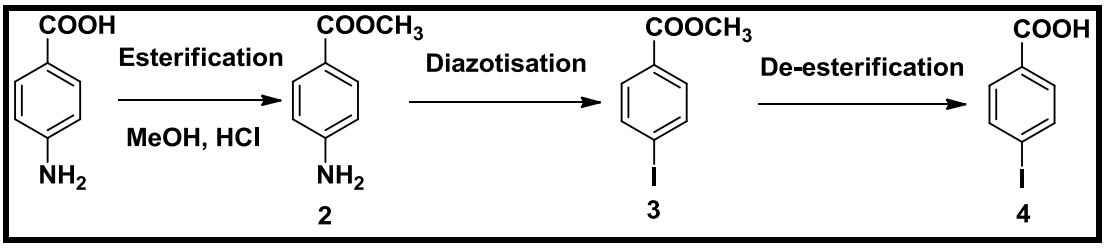

Scheme 2.1.5: Synthesis of 4-iodo benzoic acid

The synthesis of 4-(aminoiminomethyl)-benzamide, one of the standard lead compounds, was carried out using *Scheme 2.1.6*. To validate this synthetic procedure different substituents in the form of halogens, heterocycles were introduced near amide functionality. These structures are tabulated in table 1. While tailoring the structures with different substituent, PAINS (Pan Assay Interference Compounds) were kept in mind [21]. PAINS functionality doesn't discriminate between target and non-target moieties leading to a plethora of side effects. We observed key step during the synthesis of this series compounds remained in the formation of amidine from parent nitrile functionality.

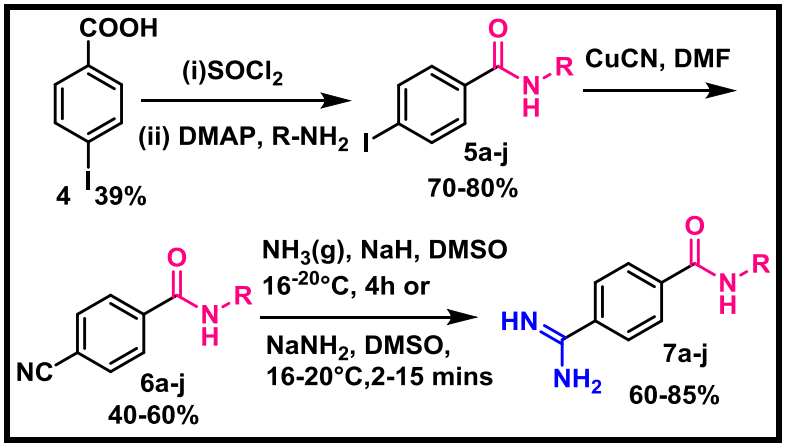

Scheme 2.1.6: Synthesis of new amidine and amide adducts

C. Characterization:

Spectral Analysis

All the new compounds were characterized by micro analysis, FT-IR, ^{1}H NMR, ^{13}C NMR and mass spectrometry. Spectra analyses were consistent with the assigned structures. Details of each structure with its characterization are presented in the experimental section.

Single crystal XRD analysis

The crystallographic data, details of data collection and some important features of the refinement for compound **7j** is given in *Table 2.1.3*. Crystals of suitable size of the molecule **7j** were obtained by slow evaporation of the solvent. The data were collected on Oxford X-CALIBUR-S diffractometer with CuKα radiation(λ= 1.541841Å) at 293K. The data interpretations were processed with CrysAlis Pro, Agilent Technologies, Version 1.171.35.19. An absorption correction based on multi-scan method was applied. All structures were solved by direct methods and refined by the full matrix least-square based on F^2 technique using SHELXL-97 program package. All calculations were carried out using WinGX system Ver- 1.64.

4-(aminoiminomethyl)-*N*-(4-ethylphenyl)benzamide **7j** got crystallized in triclinic crystal system with P1 space group, with only one molecule in an asymmetric unit (*Figure 2.1.6*).

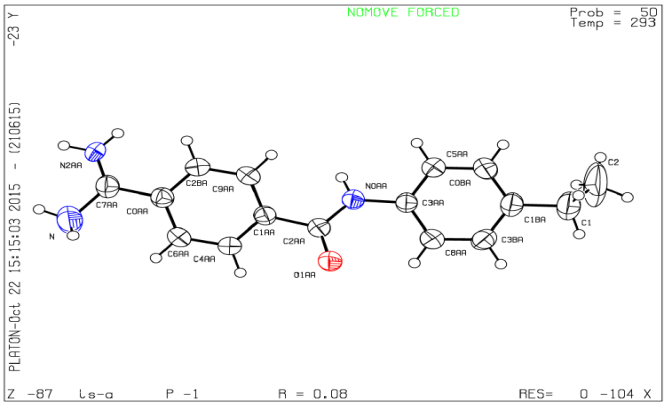

Figure 2.1.6: Molecular view of compound 7j having thermal ellipsoid are shown with 50% probability

Table 2.1.3: Crystallographic data and structure refinements for 7j

	7j
CCDC	1432792
Chemical formula	$C_{16}H_{17}N_3O$
Exact Mass	267.137
Temperature/K	293(2)
Crystal system	triclinic
Space Group	P-1
a (Å)	5.4233(3)
b (Å)	7.8624(6)
C (Å)	16.8873(12)
α /°	103.398(6)
β /°	90.103(5)
γ /°	97.215(5)
Volume/Å^3	694.58(8)
Z	13
ρcalcmg/mm3	1.211
μ/mm-1	0.642
F(000)	268.0
Crystal size/mm3	
2Θ range for data collection	10.78 to 143.78°
Index ranges	$-4 \le h \le 6, -8 \le k \le 9, -20 \le l \le 20$
Reflections collected	4085
Independent reflections	2654[R(int) = 0.0137]
Data/restraints/parameters	2654/0/174
Goodness-of-fit on F^2	2.044
Final R indexes [I>=2σ (I)]	R1 = 0.1438, wR2 = 0.4226
Final R indexes [all data]	R1 = 0.1536, wR2 = 0.4449

There was no prominent hydrogen bonding in spite of the presence of strong hydrogen donor and hydrogen acceptor groups. Two expected short contacts amongst (a) amidine groups (b) amide linkage (C-O-H-N) and (c) aromatic C-H linkages were observed. Although these interactions are considered to be weak in nature but, it is reported that they play an important role in the protein- drug binding [16]. Here, latter mode of short contact helps in keeping planarity of two aromatic rings. The angle between the two planes passing through two phenyl rings is 1.68°, this is due to the amide linkage between the rings. Also, the amide linkage causes the criss-cross arrangement of the molecules. The centroid distance for the two oppositely placed molecules is 3.6 Å. In spite of the possibility of 'aromatic donor-acceptor interaction' between the amidine phenyl ring and ethyl phenyl ring, the face-centered stacking is not observed. The reason for this is the slight bending in the planarity due to intermediate amide linkage. Hunter and Sanders [29] have provided a rational way of looking at polarized aromatic ring systems (*Figure 2.1.7*).

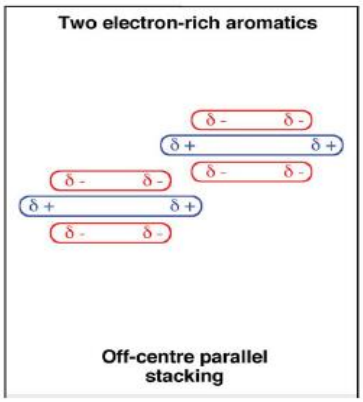

Figure 2.1.7: Hunter and Sanders representation for off-center parallel stacking

The distance between the plane passing through one ethyl end ring and the other amidine end ring is 0.977 Å, for the two amidine ring it is 2.599Å, this suggests that the arrangement of molecule is having off-center parallel stacking. Also, the two have parallel off-set pairs. It can also be described as the sheet structure, where we can imagine the sheets to be anti parallel of each other when viewed from front (*Figure 2.1.8*). The centroid distance between the ethyl ring and amidine ring is 6.360 Å and that of two amidine ring is 5.423 Å. This also suggests that the four near proximity ring forms

the hexagonal arrangement when it is viewed from side with 3.938Å distance as shown in the Figure below.

Figure 2.1.8: Description of crystal structure of 7j

Thermo gravimetric Analysis:

Thermal stability of API (Active Pharmaceutical Ingredient) is one of the major concerns in drug industry. The TG-DTA data reveals that all the compounds are stable at and below 200°C. Two of the derivatives **7h** and **7j** didn't give a good graph (*Figure 2.1.4*).

Table 2.1.4: TG-DTA data

Entry	Melting Point (°C)	Mass Loss % (Temperature range °C)	Residual Content	DTG °C
7a	200-202	124-226°C (20.7%) 240-335 (59.8%)	Mass loss continued after 500°C	305.7
7b	230-232	251-359°C (91.1%)		342
7c	204-205	200-300°C (100%)		
7d	198-200	116-239°C (21.1%) 240-324°C (68.7%)	Zero	307.3
7e	135-140	209-314 °C (71.7%)	Mass loss continued after 500°C	298
7f	220-222	205-324°C (92.8%)		
7g	156-158	236-347°C (70.4%) 347-417°C (13.1%)	Mass loss continued after 500°C	322.6, 391.5

7i	170-172	224-329°C (85.79%)	310.5

D. Antiproliferative Assay:

MTT Analysis:

Cytotoxicity studies [30] on HeLa cell line was performed for all the new compounds. Cis-platin was used as the reference drug. Percentage cell viability of synthesized compounds on HeLa cell line at various concentrations was checked and then from that IC_{50} was calculated (One way ANOVA (non-parametric test was carried out. P value= 0.0062(**)). *Table 2.1.5* and *Figure 2.1.9* shows results of IC_{50} in mM concentrations.

Table 2.1.5: IC_{50} values of all newly synthesized compounds

Code	IC_{50}(mM)
7a	1.208
7b	1.354
7c	0.825
7d	0.153
7e	1.825
7f	ND
7g	0.842
7h	0.009
7i	1.035
cis-Platin	0.028

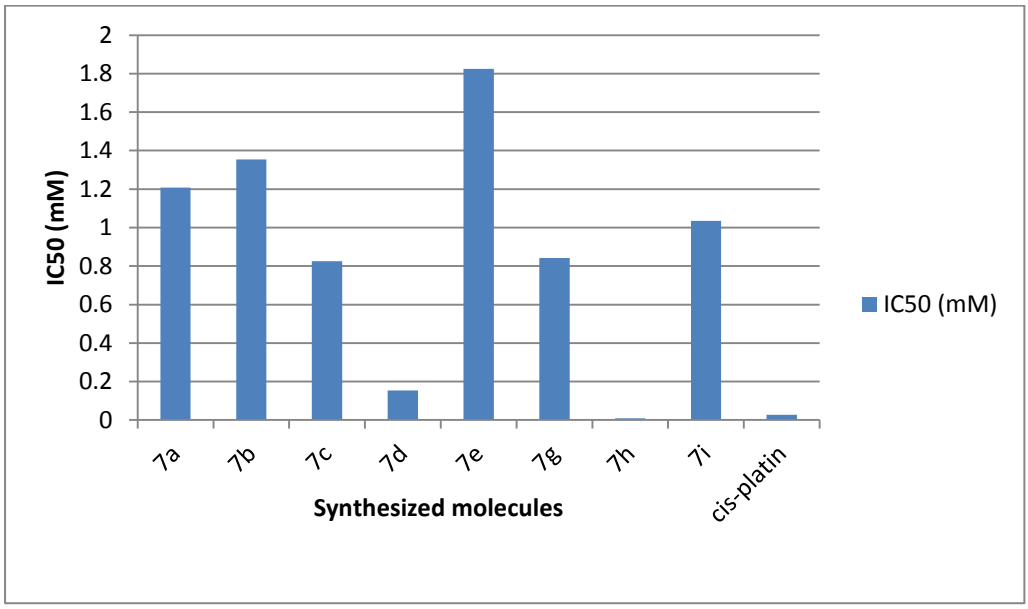

Figure 2.1.9: Cytotoxicity studies on HeLa cell line was performed for all the new compounds. Cis-platin was used as the reference drug. Percentage cell viability of synthesized compounds on HeLa cell line at various concentrations was checked and then from that IC_{50} was calculated (One way ANOVA (non-parametric test was carried out. P value= 0.0062(**)).

NCI 60 cell line screen:

All molecules were initially screened for anti-proliferative activity *in silico* by National Cancer Institute (NCI), USA. Out of this, compounds **7b**, **7c**, **7d** and **7g** were further selected for actual screening anti-proliferative activity at 10µM concentration. Graph below (*Figure 2.1.10*) shows comparative study of compounds **7b**, **7c**, **7d** and **7g** on selected human derived cell lines NCI-H522 (Non-Small cell lung cancer), HCT-116 (Colon cancer), SF-539 (CNS cancer), OVCAR-8 (Ovarian cancer) and SN-12 (Renal cancer). **7g** shows 73.36% growth inhibition in HCT-116 colon cancer cell line (mean growth inhibition) at 10μM concentration.

Two heterocyclic structure containing derivatives of furan and picolyamine were found to be most potent among all. Both compounds **7g** and **7h** have a heterocycle in conjugation with NH side of amide linkage, but also have flexible -CH_2 bridge. Thus, from an anti-cancer activity it can be concluded that 4-(aminoiminomethyl)-*N*-(3-pyridinylmethyl) benzamide **(7g)** and 4-(aminoiminomethyl)-*N*-(2-furanylmethyl) benzamide **(7h)** can be investigated further for the development as new leads.

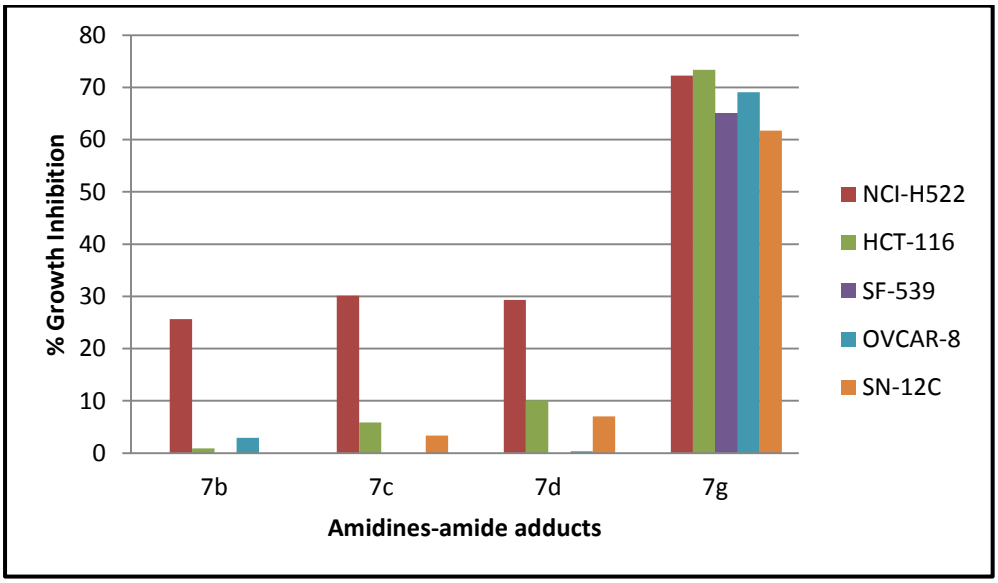

Figure 2.1.10: % Growth Inhibition on selected cell lines at 10µM concentration NCI-H522: Non-Small cell lung cancer cell line; HCT-116: Colon cancer cell line; SF-539: CNS cancer cell line; OVCAR-8: Ovarian cancer cell line; SN-12: Renal cancer cell line

Amidine-amide pharmacophore was studied by 'inserting' additional changes in the molecule in the form of halogens, heterocycle so as to increase solubility, as well as activity. In this respect, **7j**, because of its poor solubility in DMSO could not be tested for its anti-cancer activity using MTT assay. For halogenated derivatives, compound **7d** (4-chloro derivative) showed the highest potency as compared to **7c**, **7e** and **7f**, which are fluoro, 3-chloro and bromo derivatives, respectively. Compound **7f** with bromo substitution was the least potent among the reported compounds. Two heterocyclic structures containing derivatives of furan and picolyamine were found to be the most potent among all. MTT data showed that the furan ring containing mono amidine **7h** showed better activity as compared to the standard anticancer drug *cis*-platin. As per docking scores, **7h** furan derivative was best interacting with the protein PRMT1. NCI-60 human cancer cell line study shows **7g** as a probable candidate for future study. Both compounds **7g**, **7h** have not only have a cyclic heterocycle in conjugation with NH side of amide linkage, but also have flexible -CH_2 bridge. Such flexibility might play a crucial role in modulating antitumor activity. In conclusion, amidines affinity for PRMT1 was the basis of this work, which led to the anti-proliferative activity. Thus, it can be concluded that 4-(aminoiminomethyl)-*N*-(3-pyridinylmethyl) benzamide **(7g)** and 4-(aminoiminomethyl)-*N*-(2-furanylmethyl) benzamide **(7h)** can be modified and investigated further for the development of new leads.

2.1.4 Conclusion:

Novelty in this section lies in the synthesis of ten new molecules by conjoining two pharmacophores amidine and amide together. In this section, we have described the relevant literature and our results with experiments. Conversion from nitrile to amidine can be achieved effectively in a single step and in the presence of amide functionality using metal amide and/or ammonia gas. This method is extended for the synthesis of amidines-amide conjugates where strategy works effectively in the presence of heterocyclic functionality as well. Apart from nearing room temperature, most of the times yield observed in the modified reaction conditions clocks above 70% for nitrile to amidine conversion. Our preliminary results confirmed that in the present strategy, amidine-amide conjugates can act as anti-proliferative active compounds, similar to what is observed in literature [31]. In short, this study paves a way to synthesize not only novel amidines but also amidine-amide conjugates, a strategy for future drug design [32]. All the compounds were well characterized using CHN, FT-IR, NMR and Mass analysis. Docking studies performed on PRMT1 showed **7h** gets U type bend inside the cavity for extra π-cation interaction. Single crystal for one of the compounds was developed and solved. The MTT assay was performed on HeLa cell line to check their anti-proliferative activity. Also, these compounds were screened on 60 cancer cell lines for broader aspect. Our results manifest that heterocyclic derivatives bridged by –methylene groups, similar to five membered ring containing furfuryl derivative (**7h)** and six membered ring containing picolyl derivative **(7g),** to amidine-amide system should be worth investigating as potential anticancer agents.

2.1.5 Experimental

2.1.5A Materials and Methods:

All the compounds were purified using column chromatography (2000- 400 mesh silica) before characterization. TLC analysis was done using pre-coated silica on aluminum sheets. Melting points were recorded in Thiele's tube using paraffin oil and are uncorrected. FT-IR (KBr pellets) spectra were recorded in the 4000-400 cm^{-1} range using a Perkin-Elmer FT-IR spectrometer. The NMR spectra were obtained on a Bruker AV-III

400 MHz spectrometer using TMS as an internal standard. The chemical shifts were reported in parts per million (ppm), coupling constants (*J*) were expressed in hertz (Hz) and signals were described as singlet (s), doublet(d), triplet(t), broad (b) as well as multiplet (m). The microanalysis was carried out using a Perkin-Elmer IA 2400 series elemental analyzer. The mass spectra were recorded on Thermo scientific DSQ-II. All chemicals and solvents were of commercial grade and were used without further purification. Single crystal data was collected with Xcalibur, EoS, Gemini.

2.1.5B Synthesis of compounds:

Synthesis of 4-iodo benzoic acid (4):

4-iodo benzoic acid (**4**) was prepared according to the literature procedure, starting with 4-amino benzoic acid. Compound 1 was esterified using methanol (as a solvent and reagent) and conc. H_2SO_4 to give compound **2**. Yield-91%. Compound **2** was then subjected to diazotization followed by hydrolysis to give compound **4**[33-35].

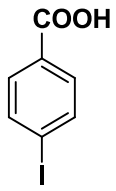 4 $C_7H_5IO_2$ (248)	Yield: 39% M.P: 266-269°C (literature mp: 269-272°C)

Synthesis of 4-iodo-*N*-(4-methoxyphenyl) benzamide (5a-j):

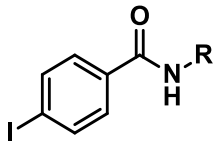

Synthesis of compound 5a was done in two steps. A mixture of compound 4 and thionyl chloride was heated at 70-75°C for 3hrs. Acyl derivative was obtained by distilling excesses thionyl chloride [36-39]. In a separate round bottom flask mixture of 4-methoxy aniline (0.496g, 0.00403 mol) and DMAP (0.492g, 0.004032 mol) and MDC (5ml) was stirred at 20-25°C for 30 min. Acyl derivative(1.074g, 0.004032) was then slowly added in 15mins at 20-25°C and further stirred for 16-20 hrs. Compound was then isolated and further purified by column chromatography to afford desired compound 5a as a white solid.

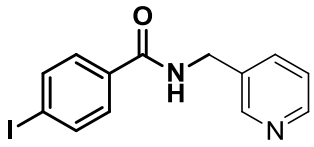 4-iodo-*N*-(pyridin-3-ylmethyl)benzamide $C_{13}H_{11}IN_2O$ 338.1437	Yield: 72% MS (m/z) (M+1): 338.8834

Yield: 74-80%.

Using the above procedure of compound 5a rest of the compounds 5b-j was synthesized.

Synthesis of 4-cyano-*N*-(4-methoxyphenyl) benzamide (6a-j):

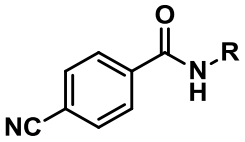

A suspension of compound **5a** (0.500g, 0.001416 mol) and copper cyanide (0.634g, 0.007082 mol) were stirred in dry DMF at 150°C for 4hrs. After the reaction was completed (monitored by TLC, eluent, petroleum ether/ ethyl acetate, 1/1,v/v) , water was added and the residue was basified and extracted in ethyl acetate (3x20ml), dried over sodium sulphate and purified by silica gel column chromatography (eluent, petroleum ether/ethyl acetate 1/1, v/v) to afford compound **6a** as off-white to pale-yellow solid.

Yield: 40-60%.

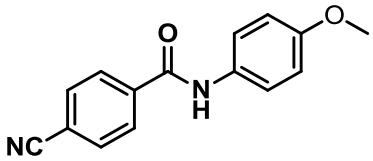 4-cyano-*N*-(4-methoxyphenyl)benzamide $C_{15}H_{12}N_2O_2$ (252.2680)	Yield: 60% MS(m/z) (M+1): 253.0165
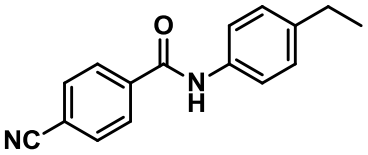 4-cyano-*N*-(4-ethylphenyl)benzamide $C_{16}H_{14}N_2O$ (250.2952)	Yield: 58% MS(m/z) (M+1): 251.0263
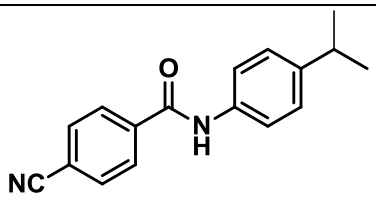 4-cyano-*N*-(4-isopropylphenyl)benzamide $C_{17}H_{16}N_2O$ (264.3217)	Yield: 60% MS(m/z) (M+1): 265.0459
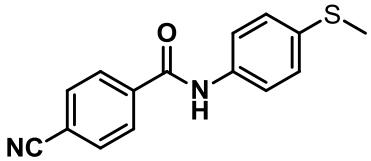 4-cyano-*N*-(4-(methylthio)phenyl)benzamide $C_{15}H_{12}N_2OS$ (268.3336)	Yield: 55% MS(m/z) (M+1): 268.9787
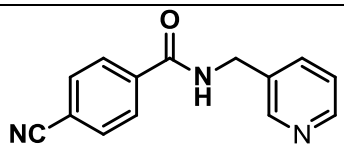 4-cyano-*N*-(pyridin-3-ylmethyl)benzamide $C_{14}H_{11}N_3O$ (237.2566)	Yield: 42% MS(m/z) (M+1): 237.9835

Using the above procedure of compound **6a** rest of its derivatives was synthesized.

General procedure for the synthesis of compound 7a-j:

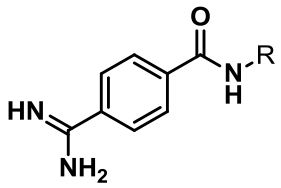

The compound under heading can be synthesized by two methods in good isolated yields.

Procedure 1: Dry DMSO and NaH (60% suspension in oil, 0.100mg,0.0025 mol) were stirred at 16-20°C for 15mins. Compound **6a** was then added and ammonia gas was purged in it till the completion of the reaction (monitored by TLC, eluent, petroleum ether/ethyl acetate, 1/4, V/V), cooled the reaction. Then the water was added slowly such that temperature of the reaction should not exceed 30°C. Residue was extracted with ethyl actetate (3x10ml) and purified by neutral alumina column chromatography (eluent, petroleum ether/ ethyl acetate, 1/4, v/v) to afford compound **7a** as off white solid.

Yield: 82%.

Melting point: 200-202°C.

Procedure 2: Dry DMSO and compound **6a** were stirred at 25°C for 5mins, sodamide was added in it and stirred for 2-15mins at the same temperature. Reaction was monitored by TLC (eluent, petroleum ether/ethyl acetate, 1/4, v/v), cooled the reaction and water was added slowly such that temperature of reaction should not exceed 30°C. Residue was extracted with ethylacetate (3x10ml) and purified by neutral alumina column chromatography (eluent: petroleum ether/ethylacetate, 1/4, v/v) to afford compound **7a** as off-white solid.

Yield: 80%

Synthesis of 4-(aminoiminomethyl)-*N*-(4-Methoxyphenyl) benzamide (7a):

The title compound was synthesized according to the general as given above procedure.

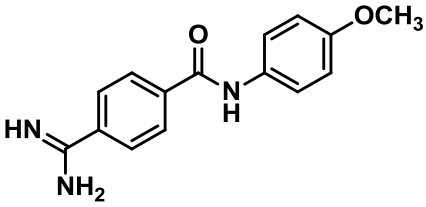 7a $C_{15}H_{15}N_3O_2$ (269)	Off-white solid **Yield**: 82%; **M.P**: 200-202°C **Anal. Calc. for $C_{15}H_{15}N_3O_2$**: C, 66.90; H, 5.61; N, 15.60 %; Found: C, 67.20; H, 5.40; N, 15.82 % **^{1}H NMR (400MHz,DMSO-d6) δ:** 10.31(s, NH), 8.09-8.04(m, 4H), 7.70-7.67(m, 2H), 6.96-6.93(m, 2H), 3.75(s,3H), 2.64(s,3H,amidine) ppm **^{13}C NMR (100MHz, DMSO-d6) δ:** 198.9(C=NH), 165.3(C=O), 156.3(C-O), 139.1(C-C=O), 131.8(C-C=NH), 128.7(2C), 128.2(2C), 122.9(2C), 114.3(2C), 55.6(O-CH_3) ppm **FT-IR(KBr) γ:** 3336.77(amidine-NH), 2923 (w), 1681.31(C=O), 1647.57(C=N), 1534.10(NH), 1269.39(C-N), 1249.80(C-O), 1031.31(C-O amide), 824.13(*para* substitution) cm^{-1} **MS(m/z):** (M^+) 269.15 (*Figure 2.1.12, 2.1.22, 2.1.32, 2.1.42, 2.1.52*)

Synthesis of 4-(aminoiminomethyl)-*N*-{(4-Methylthio) phenyl} benzamide (7b)

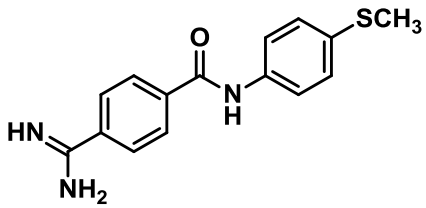 7b $C_{15}H_{15}N_3OS$ (285)	Off-white solid. **Yield:** 85%; **M.P:** 230-232°C ; **Anal. Calc. for $C_{15}H_{15}N_3OS$**: C, 63.13; H, 5.30; N, 14.73 %; Found: C, 63.05; H, 5.45; N, 14.90 % **^{1}H NMR (400MHz,DMSO-d6) δ:** 10.41(s,NH), 8.09-8.05(s, 4H), 7.76-7.74(d, 2H, *J*=8.4 Hz), 7.29-7.27(d, 2H, *J*=8.8 Hz), 2.64(s, 3H, amidine), 2.47(s,3H) ppm **^{13}C NMR (100MHz, DMSO-d6) δ:** 198.1(C=NH), 165.0(C=O), 139.3, 139.1, 136.8, 133.1, 128.6, 128.4, 127.2, 121.5, 121.4, 15.8 (S-CH_3) ppm **FT-IR(KBr) γ:** 3333.49(Amide-NH), 1682.59(C=O), 1651.41(C=N), 1588.98,1522.75(aromatic C=C), 1399.97, 856.10, 816.20(para substitution) cm^{-1} **MS(m/z):** (M^+) 285 (*Figure 2.1.13, 2.1.23, 2.1.33, 2.1.43, 2.1.53*)

Synthesis of 4-(aminoiminomethyl)-*N*-(4-Florophenyl) benzamide (7c)

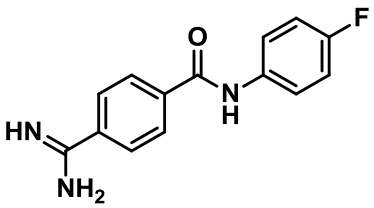 7c $C_{14}H_{12}FN_3O$ (257)	White solid. **Yield:** 74%; **M.P:** 204-205°C ; **Anal. Calc. for $C_{14}H_{12}FN_3O$**: C, 65.36; H, 4.70; N, 16.33 %; Found: C, 65.55; H, 4.30; N, 16.50 % **^{1}H NMR (400MHz,DMSO-d6) δ:** 10.46(s, NH), 8.10-8.05(m, 4H), 7.82-7.78(m, 2H), 7.23-7.19(m, 2H), 2.64 (s, 3H, amidine) ppm **^{13}C NMR (100MHz, DMSO-d6) δ:** 198.1(C=NH), 165.1(C=O), [160.0,157.6] (C-F, $^1J_{C-F}$=239 Hz),139.3, 139.0, 135.7, 128.6, 128.4, [122.7,122.6] ($^3J_{C-F}$=7.7 Hz), [115.8,115.6] ($^2J_{C-F}$=22 Hz) ppm **FT-IR(KBr) γ:** 3335.41(s, N-H), 1683.35(C=O), 1644.32(C=N), 1611.86(N-H, stretch), 1533.76(C-F), 1516.23(aromatic C=C), 1407.82, 1360.67, 1215.81(N-H, bend), 831.90 (para substitution)cm^{-1} **MS(m/z):** (M^+) 257 (*Figure 2.1.14*, *2.1.24*, *2.1.34*, *2.1.44*)

Synthesis of 4-(aminoiminomethyl)-*N*-(4-Chlorophenyl)benzamide (7d)

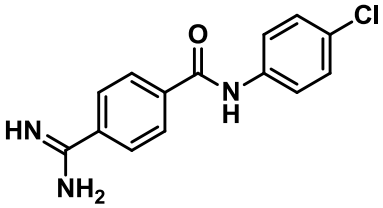 7d $C_{14}H_{12}ClN_3O$ (273.5)	White solid. **Yield:** 78%; **M.P:** 198-200°C ; **Anal. Calc. for $C_{14}H_{12}ClN_3O$**: C, 61.43; H, 4.42; N, 15.35 %; Found: C, 61.60; H, 4.30; N, 15.20 % **^{1}H NMR (400MHz,DMSO-d6) δ:** 10.55(s, NH),8.11-8.05(m, 4H), 7.84-7.82(d, 2H, J=8.0 Hz), 7.44-7.42(d, 2H, *J*=8.0 Hz), 2.65(s, 3H, amidine) ppm **^{13}C NMR (100MHz, DMSO-d6) δ:** 198.1(C=NH), 165.3(C=O), 139.3, 138.9, 138.3, 129.0, 128.6, 128.5, 128.0, 122.3 ppm **FT-IR(KBr) γ:** 3359.19 (Amide-NH), 1682.92(C=O), 1654.24(C=N), 1594.50, 1522.42(aromatic C=C), 823.15(para substitution), 511.62(C-Cl) cm^{-1} **MS(m/z)**: (M^+) 273.5 (*Figure 2.1.15*, *2.1.25*, *2.1.35*, *2.1.45*, *2.1.54*)

Synthesis of 4-(aminoiminomethyl)-*N*-(3-Chlorophenyl) benzamide (7e)

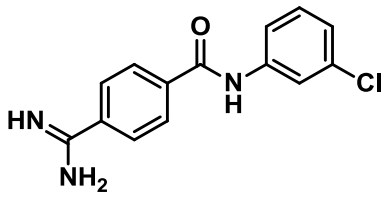 7e $C_{14}H_{12}ClN_3O$ (273.5)	White solid. **Yield:** 70%; **M.P :**135-140°C ; **Anal. Calc. for $C_{14}H_{12}ClN_3O$**: C, 61.43; H, 4.42; N, 15.35 %; Found: C, 61.20; H, 4.50; N, 15.20 % **^{1}H NMR (400MHz,DMSO-d6) *δ*:** 10.59(s, NH), 8.11-8.06(m, 4H), 7.98-7.97(s, 1H), 7.73-7.71(d, 1H, *J*=7.6 Hz),7.42-7.38 (t,1H), 7.20-7.18(d, 2H, *J*=7.6 Hz) 2.65(s, 3H, amidine) ppm **^{13}C NMR (100MHz, DMSO-d6) *δ*:** 198.1(C=NH), 165.4(C=O), 140.8, 139.4, 138.7, 133.4, 130.8, 128.7, 128.5, 124.1, 120.2, 119.1 ppm **FT-IR(KBr) *γ*:** 3353.31(Amide-NH), 1671.09(C=O), 1593.50 (C=N),1530.26(aromatic C=C),1483.06, 1421.54, 1313.21, 777.74(C-Cl), 684.02(meta substitution) cm^{-1} **MS(m/z):** (M^+) 273.5 (*Figure 2.1.16, 2.1.26, 2.1.36, 2.1.46, 2.1.55*)

Synthesis of 4-(aminoiminomethyl)-*N*-(4-Bromophenyl)benzamide (7f)

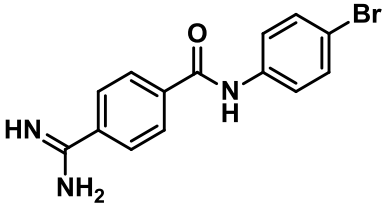 7f $C_{14}H_{12}BrN_3O$ (318)	Off-white solid. **Yield:** 60%; **M.P :**220-222°C ; **Anal. Calc. for $C_{14}H_{12}ClN_3O$**: C, 61.43; H, 4.42; N, 15.35 %; Found: C, 61.20; H, 4.50; N, 15.20 % **^{1}H NMR (400MHz,DMSO-d6) δ:** 10.59 (s, NH), 8.06-8.03(d, 2H, *J*=8.8), 8.00-7.98(d, 2H, *J*=8.4), 7.68-7.66 (d, 2H, *J*=8.8 Hz), 7.54-7.51(d,2H, *J*=8.8 Hz), 2.60(s, 3H, amidine) ppm **^{13}C NMR (100MHz, DMSO-d6) δ:** 198.0(C=NH), 187.8, 165.9(C=O), 139.4, 138.8, 138.3, 132.0, 128.7, 128.4, 123.1 ppm **FT-IR(KBr) γ:** 3360.85(Amide-NH), 1681.84(C=O), 1654.89(C=N), 1594.13,1527.86(aromatic C=C), 820.69(para substitution), 509.88(C-Br) cm^{-1} **MS(m/z):** (M^+) 317 (*Figure 2.1.17*, *2.1.27*, *2.1.37*, *2.1.47*, *2.1.56*)

Synthesis of 4-(aminoiminomethyl)-*N*-(3-pyridinylmethyl)benzamide (7g)

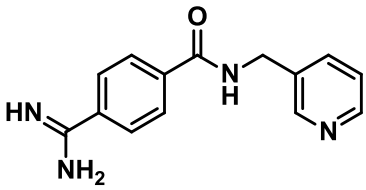 7g $C_{14}H_{14}N_4O$ (254)	White solid. **Yield:** 65%; **M.P :** 156-158°C; **Anal. Calc. for $C_{14}H_{14}N_4O$**: C, 66.13; H, 5.55; N, 22.03 %; Found: C, 66.25; H, 5.20; N, 22.15 % **^{1}H NMR (400MHz,DMSO-d6) δ:** 9.28-9.25(t, NH), 8.56(s, 1H), 8.47-8.46(d, 1H, *J*=6.0 Hz), 8.05-7.98(m, 4H), 7.75-7.72(d, 1H, *J*=6 Hz),7.38-7.35(m, 1H), 4.52-4.51(s, 2H), 2.62(s, 3H, amidine) ppm **^{13}C NMR (100MHz,DMSO-d6)δ:** 198.1(C=NH),166.0 (C=O), 149.3, 148.6, 139.2, 138.3, 135.6, 135.3, 128.6, 128.0, 123.9, 40.9, ppm **FT-IR(KBr) γ:** 3202.57(Amide-NH),3063.16, 1681.28(C=O), 1647.91, 1545.77 (C=N), 1432.39, 1328.20,1296.67, 1267.00, 862.32, 712.87, 681.94 cm^{-1} **MS(m/z):** (M^+) 254 (*Figure 2.1.18, 2.1.28, 2.1.38, 2.1.48, 2.1.57*)

Synthesis of 4-(aminoiminomethyl)-*N*-(2-furanylmethyl)benzamide (7h)

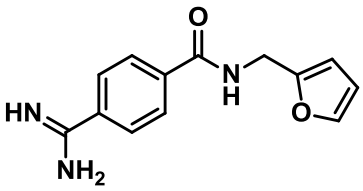 7h $C_{13}H_{13}N_3O_2$ (243)	White solid. **Yield:** 75%; **M.P :** 144-145°C ; **Anal. Calc. for $C_{13}H_{13}N_3O_2$**: C, 64.19; H, 5.39; N, 17.27 %; Found: C, 64.30; H, 5.45; N, 17.15 % **^{1}H NMR (400MHz, DMSO-d6) δ:** 9.16-9.15(s,NH), 8.04-7.97(m, 4H), 7.58(s, 1H), 6.41-6.39(s, 1H),6.30-6.29(s, 1H), 4.49-4.47(s, 2H), 2.61(s, 3H, amidine) ppm **^{13}C NMR (100MHz, DMSO-d6) δ:** 198.1(C=NH), 165.7(C=O), 152.5, 142.5, 139.1, 138.3, 128.6, 128.0, 110.9, 107.4, 36.5 ppm **FT-IR(KBr)γ:**3303.30(Amide-NH), 1685.99(C=O),1639.62,1556.43(C=N),1427.65,1252.65, 1012.11,770.84, 752.22, 667.36 cm^{-1} **MS(m/z):** (M^+) 243 (*Figure 2.1.19, 2.1.29, 2.1.39, 2.1.49*)

Synthesis of 4-(aminoiminomethyl)-*N*-(4-(2-propane)phenyl)benzamide (7i)

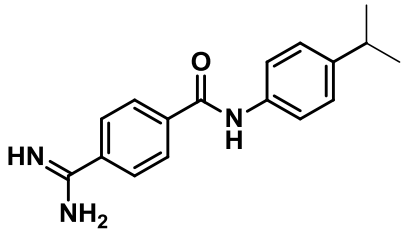

7i

$C_{17}H_{19}N_3O$ (281)

Light brown solid.

Yield: 83%;

M.P : 170-172°C ;

Anal. Calc. for $C_{17}H_{19}N_3O$: C, 72.57; H, 6.81; N, 14.94 %; Found: C, 72.45; H, 6.61; N, 15.10 %

^{1}H NMR (400MHz,DMSO-d6) δ: 10.36 (s, 1H), 8.08-8.05(m, 4H), 7.69-7.67 (d, 2H, *J*=8.4Hz), 7.24-7.22 (d,2H, *J*=8.4 Hz), 2.90-2.83 (septate, 1H, *J*=6.8Hz), 2.64 (s, 3H, amidine), 1.21-1.19 (d, 6H, *J*=6.8Hz) ppm

^{13}C NMR (100MHz, DMSO-d6) δ: 198.3 (C=NH), 165.2 (C=O), 144.5, 139.3, 137.1, 128.6, 128.4, 126.8, 121.0, 33.3 (CH), 24.4 (CH_3) ppm

FT-IR(KBr) γ: 3338.31(Amide-NH),2956.62(2-propane methyl symmetric stretch), 2923.33(2-propane asymmetric stretch), 1686.48(C=O stretch), 1648.81(C=N stretch), 1595.46,1519.10(aromatic C=C),1411.59,1318.87, 823.75(*para* substitution) cm^{-1}

MS(m/z): (M^+) 281

(*Figure 2.1.20, 2.1.30, 2.1.40, 2.1.50, 2.1.58*)

Synthesis of 4-(aminoiminomethyl)-*N*-(4-ethylphenyl)benzamide (7j)

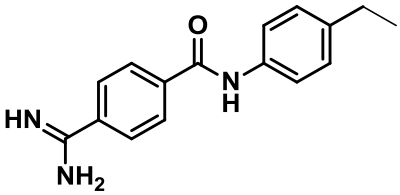 7j $C_{16}H_{17}N_3O$ (267)	White solid. **Yield:** 72%; **M.P :** 180-183°C ; **Anal. Calc. for $C_{16}H_{17}N_3O$**: C, 71.89; H, 6.41; N, 15.72 %; Found: C, 71.85; H, 6.30; N, 15.86 % **^{1}H NMR (400MHz,DMSO-d6) δ:** 10.36(s,NH), 8.07(m, 4H), 7.69-7.67(d, 2H, *J*=8.0 Hz), 7.21-7.19(d, 2H, *J*=8.0 Hz), 2.64(s, 3H, amidine), 2.61-2.55(q, 2H), 1.19-1.16(t,3H) ppm **^{13}C NMR (100MHz, DMSO-d6) δ:** 198.2(C=NH), 164.9(C=O), 139.8, 139.2, 137.0, 128.6, 128.4, 128.3, 120.9, 28.1(CH_2), 16.1(CH_3) ppm **FT-IR(KBr)γ:** 3344.20 (Amide-NH) ,2965.61, 1682.69 (C=O), 1650.00(C=N), 1596.51,1528.63 (aromatic C=C),1410.91, 1265.39, 828.12 (*para* substitution) cm^{-1} **MS(m/z):** (M^+) 267 (*Figure 2.1.21*, *2.1.31*, *2.1.41*, *2.1.51*, *2.1.59*)

2.1.5C *In-Cellulo assays:*

In-cellulo studies also come under the *in-vitro* studies with the only distinction that these studies are carried out within a cellular environment. Cell-based assays are often used for screening the compounds for their potency for cytotoxicity. There are a variety of assay methods exploiting different cellular properties for different targets.

Cytotoxicity on HeLa cell line (Human cancer cell line):

Concept and principle of MTT assay:

This assay is the colorimetric assay that measures the reduction of yellow 3-(4,5-dimethythiazol- 2-yl)-2,5-diphenyl tetrazolium bromide (MTT) into an insoluble, coloured (dark purple) formazan product within the cell (*Fig.2.1.11*). The cells are then solubilized with an organic solvent (e.g. DMSO) and the released, solubilized formazan reagent with an absorbance maximum near 570 nm is measured spectrophotometrically. Reduction of MTT occurs in metabolically active cells, the level of activity is a measure of the viability of the cells. Viable cells with active metabolism convert MTT into formazan product but when cells die, they lose the ability to convert MTT into formazan, thus color formation serves as a useful and convenient marker of only the viable cells. The exact cellular mechanism of MTT reduction into formazan is not well understood. Speculation in the early literature involving specific mitochondrial enzymes has led to the assumption that MTT is a measure of mitochondrial activity, the reduction being caused by mitochondrial succinate dehydrogenase, but most likely involves reaction with NADH or similar reducing molecules that transfer electrons to MTT [40-42].

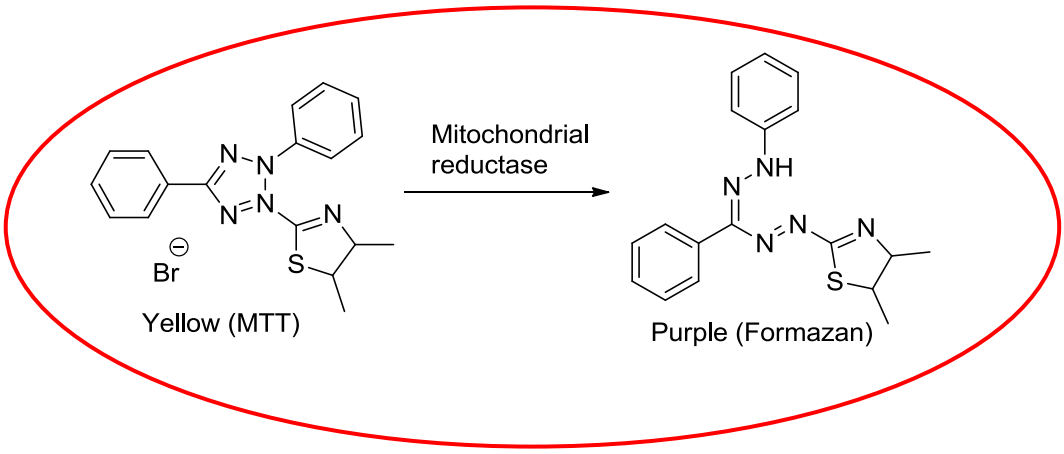

Figure 2.1.11: Structure of MTT and colored formazen product

Materials and instrumentation:

The cell lines were cultured in Dulbecco's Modified Eagle Medium (DMEM), while Phosphate Buffer Saline (PBS) was used for washing purposes. The stock solutions of compounds (1 mg/ml) were prepared by first dissolving in minimum volume of DMSO (50µl) and then diluting the concentrated DMSO solution with DMEM media to 1 ml. Further dilutions from the stock solution were made using DMEM for subsequent dosing. Both DMEM and PBS were purchased from Hi-Media. The MTT dye was purchased from SRL (Sisco research laboratory, Mumbai, India.). DMSO used to prepare stock solution as well as to dissolve formazan crystals was of analytical grade and purchased from Merck. 96-well culture plates were purchased from Tarson India Pvt. Ltd. The cell lines were procured from National Centre for Cell Science (NCCS), Pune, India.

The spectrophotometric detection of culture plates was done by Biotek-ELX universal ELISA reader (Bio-Tek instruments, Inc., Winooski, VT). The data so obtained were converted into percentage viability and were analyzed and plotted with the help of the software Graphpad Prism 3 using one-way ANOVA as the statistical tool.

Experimental:

The MTT reduction assay was the first homogeneous cell viability assay developed for a 96-well format [31]. The MTT tetrazolium assay technology has been widely adapted and remains popular in academic labs as evidenced by thousands of published articles.

In the present study cervical cancer cell line HeLa has been used. Cytotoxicity of all the newly synthesized compounds was tested on HeLa cell line.

According to the standard assay, the cancer cells (HeLa) with a cell density of 5.0×10^3 cells per well were placed in 96-well culture plates (Tarson India Pvt. Ltd.) and grown overnight at 37°C in a 5% CO_2 incubator. Compounds to be tested were then added to the wells to achieve a final concentrations as per the doses fixed (the final dosing was fixed per compound as per the results of subsequent trials). Control wells were prepared by addition of culture medium without the compounds. The plates were incubated at 37°C in

a 5% CO_2 incubator for 48 h. Upon completion of incubation, MTT dye solution (prepared using serum free culture medium) was added to each well to a final concentration of 0.5 mg/ml. After 4 h of incubation with MTT, the culture media was discarded and the wells were washed with Phosphate Buffer Saline, followed by addition of DMSO to dissolve the formazan crystals so formed and subsequent incubation for 30 min. The plates were then analyzed on a microplate reader (Thermo Scientific Multiskan EX) at 570 nm with a reference reading at 620nm to determine the absorbance of the samples. The IC50 values were determined by plotting the percentage viability *versus* concentration and reading off the concentration at which 50% of cells remained viable relative to the control. Each experiment was repeated six times to obtain mean values.

Methodology for 60 human cancer cell line assays:

The 60 human cancer cell line assay as mentioned earlier was carried out by NCI. The process is adapted from the web page; **www.dtp.nci.nih.gov**. Cancer cell lines are grown in RPMI 1640 medium containing 5% fetal bovine serum and 2mM L-glutamine. For screening experiments, cells are inoculated into 96 well microtiter plated in 100 µL

The human tumor cell lines of the cancer screening panel are grown in RPMI 1640 medium containing 5% fetal bovine serum and 2 mM L-glutamine. For a typical screening experiment, cells are inoculated into 96 well microtiter plates in 100 µL at plating densities ranging from 5,000 to 40,000 cells/well depending on the doubling time of individual cell lines. After cell inoculation, the microtiter plates are incubated at 37 °C, 5% CO_2, 95% air and 100% relative humidity for 24 h prior to the addition of experimental drugs (Chaudhary et al., 2011). After 24 h, two plates of each cell line are fixed in situ with TCA, to represent a measurement of the cell population for each cell line at the time of drug addition (Tz). Experimental drugs are solubilized in dimethyl sulfoxide at 400-fold the desired final maximum test concentration and stored frozen prior to use. At the time of drug addition, an aliquot of frozen concentrate is thawed and diluted to twice the desired final maximum test concentration with complete medium containing 50 µg/ml gentamicin. Additional four, 10-fold or ½ log serial dilutions are made to provide a total of five drug concentrations plus control. Aliquots of 100 µL of

these different drug dilutions are added to the appropriate microtiter wells already containing 100 µL of medium, resulting in the required final drug concentrations. Following drug addition, the plates are incubated for an additional 48 h at 37 °C, 5% CO_2, 95% air, and 100% relative humidity. For adherent cells, the assay is terminated by the addition of cold TCA. Cells are fixed in situ by the gentle addition of 50 µL of cold 50% (w/v) TCA (final concentration, 10% TCA) and incubated for 60 min at 4°C. The supernatant is discarded, and the plates are washed five times with tap water and air dried. Sulforhodamine B (SRB) solution (100 µL) at 0.4% (w/v) in 1% acetic acid is added to each well, and plates are incubated for 10 min at room temperature. After staining, unbound dye is removed by washing five times with 1% acetic acid and the plates are air dried. Bound stain is subsequently solubilized with 10 mM trizma base, and the absorbance is read on an automated plate reader at a wavelength of 515 nm. For suspension cells, the methodology is the same except that the assay is terminated by fixing settled cells at the bottom of the wells by gently adding 50 µL of 80% TCA. The values are the mean of three independent observed values (**www.dtp.nci.nih.gov**).

2.1.6 Selected Spectra

^{1}H NMR Data of compounds 7a-7j

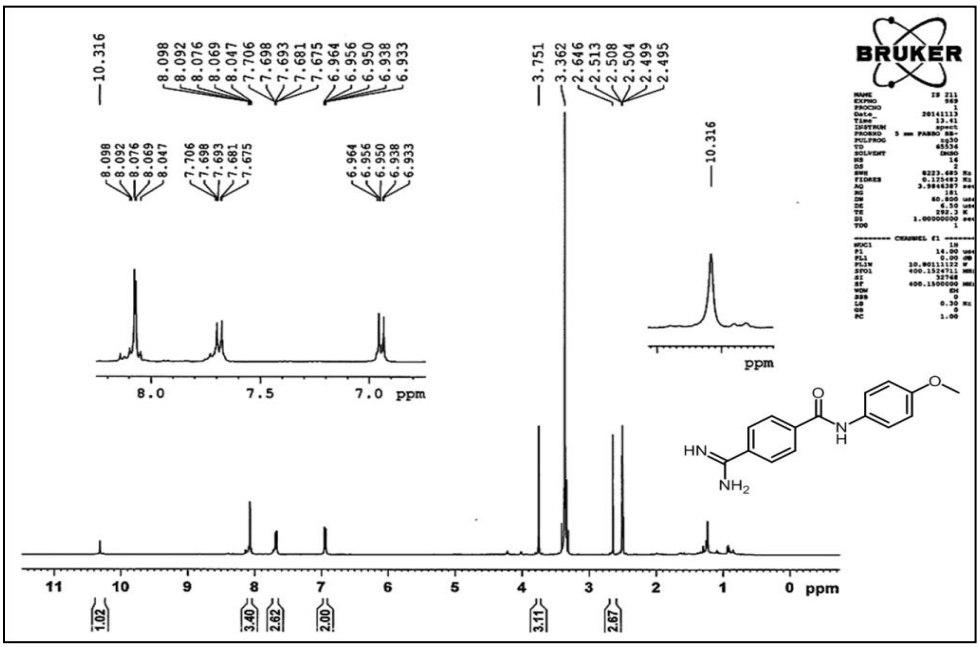

Figure 2.1.12: ^{1}H NMR spectra of 7a

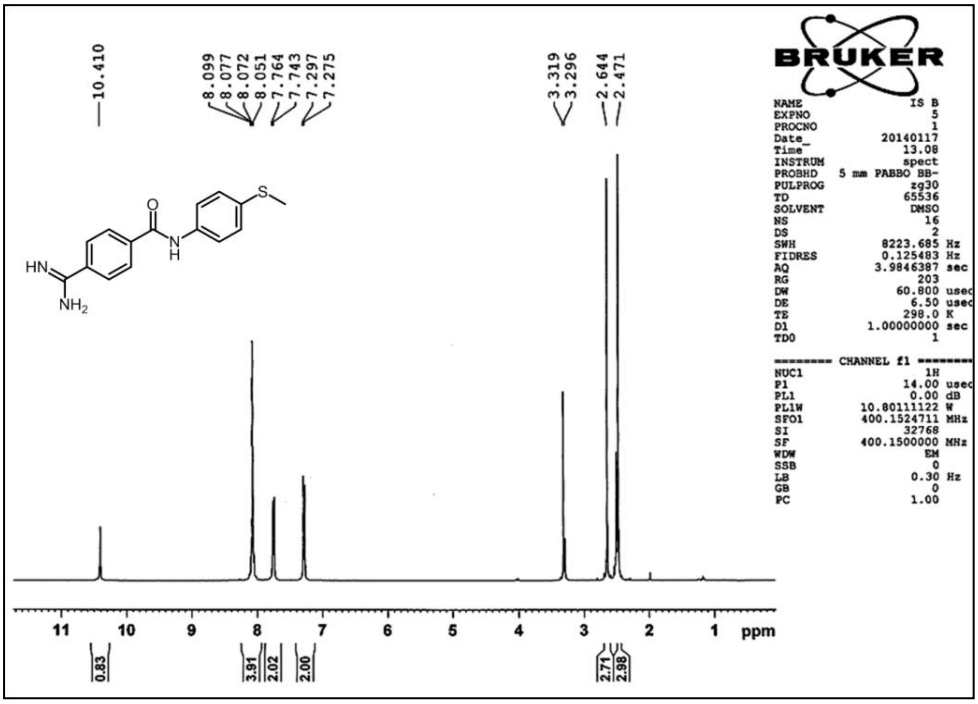

Figure 2.1.13: ^{1}H NMR spectra of 7b

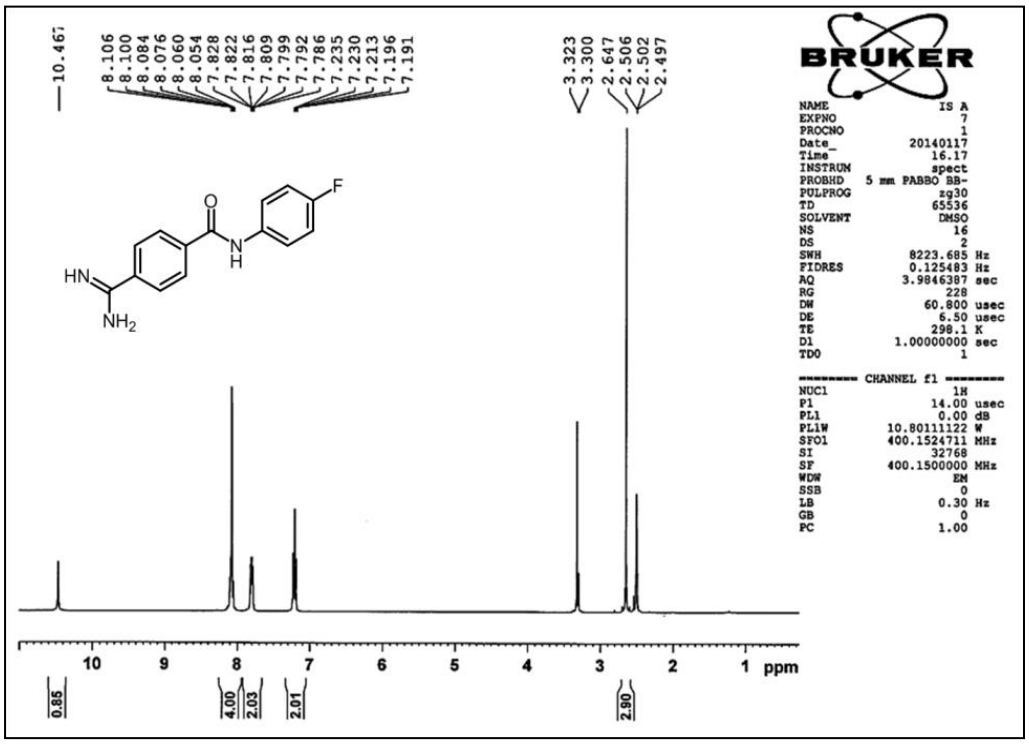

Figure 2.1.14: ^{1}H NMR spectra of 7c

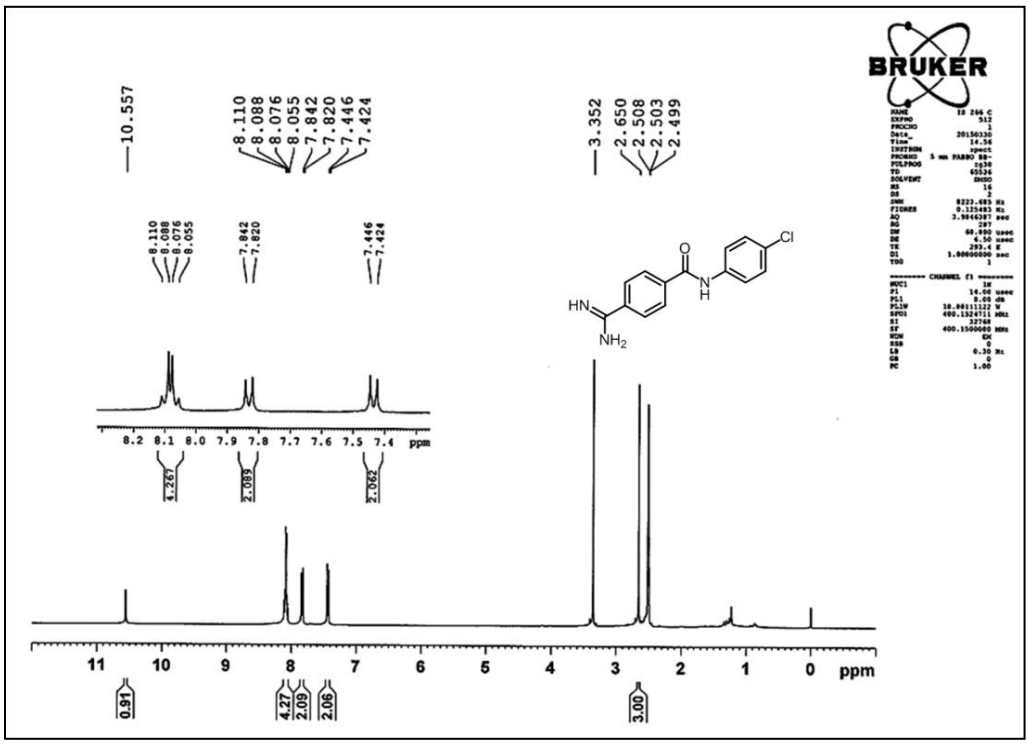

Figure 2.1.15: ^{1}H NMR spectra of 7d

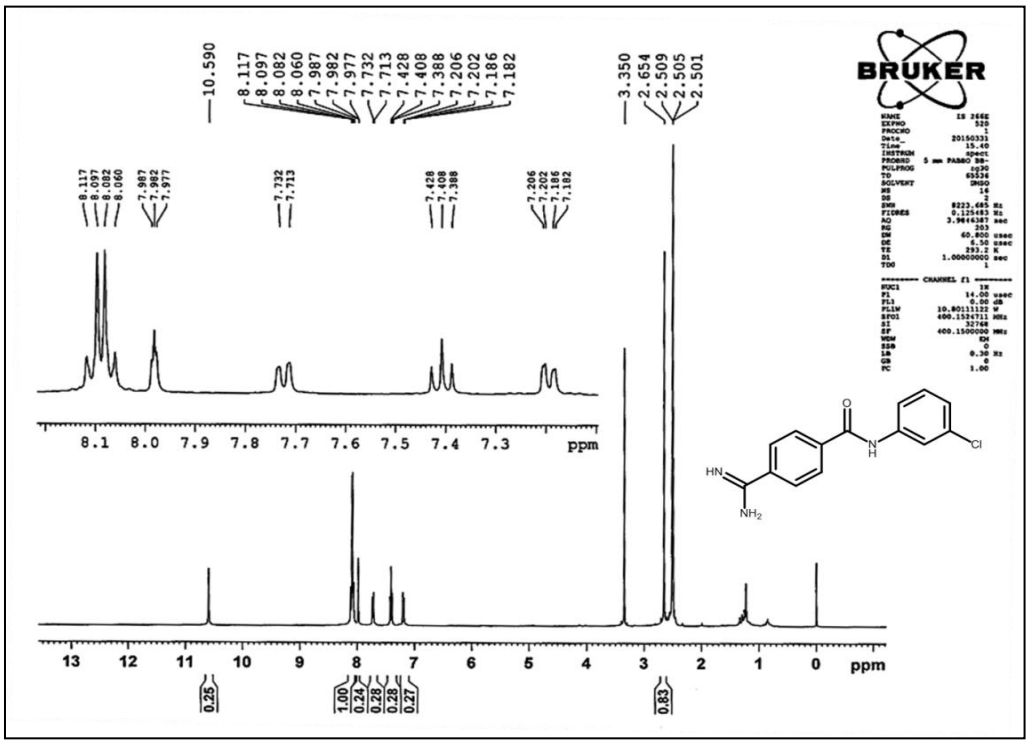

Figure 2.1.16: ^{1}H NMR spectra of 7e

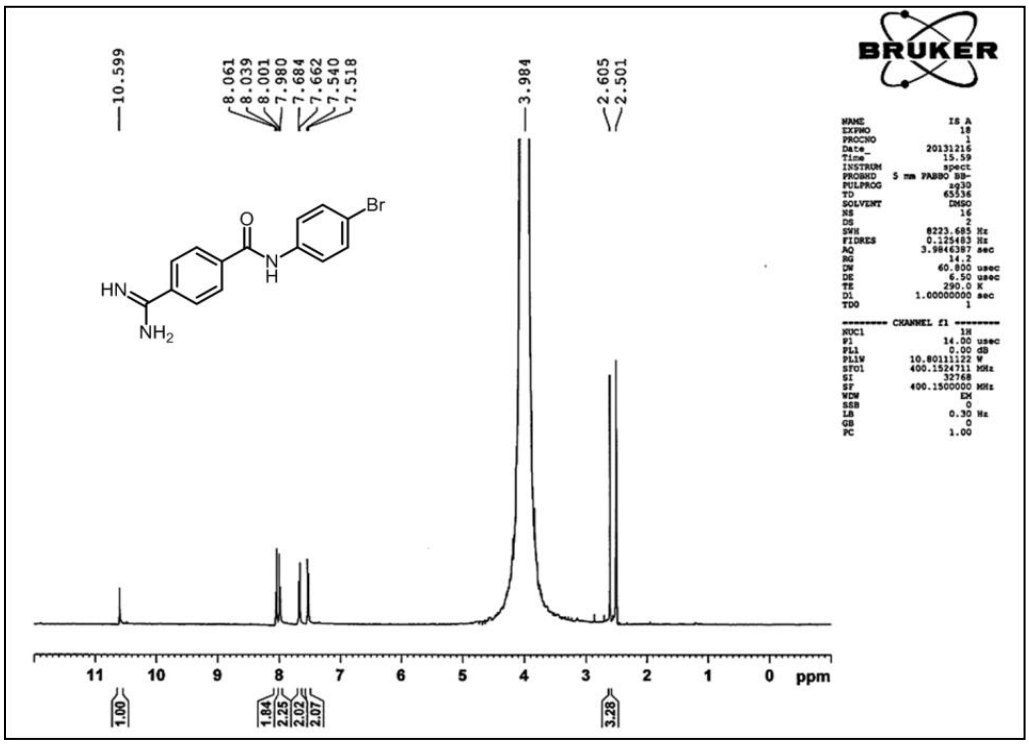

Figure 2.1.17: ^{1}H NMR spectra of 7f

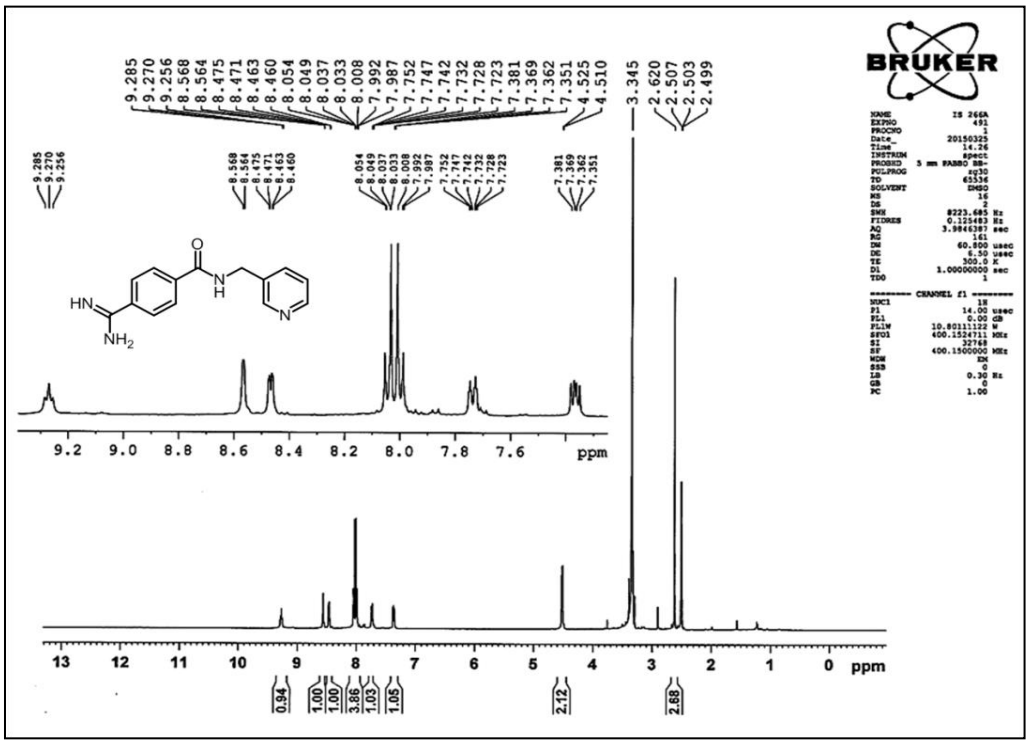

Figure 2.1.18: ^{1}H NMR spectra of 7g

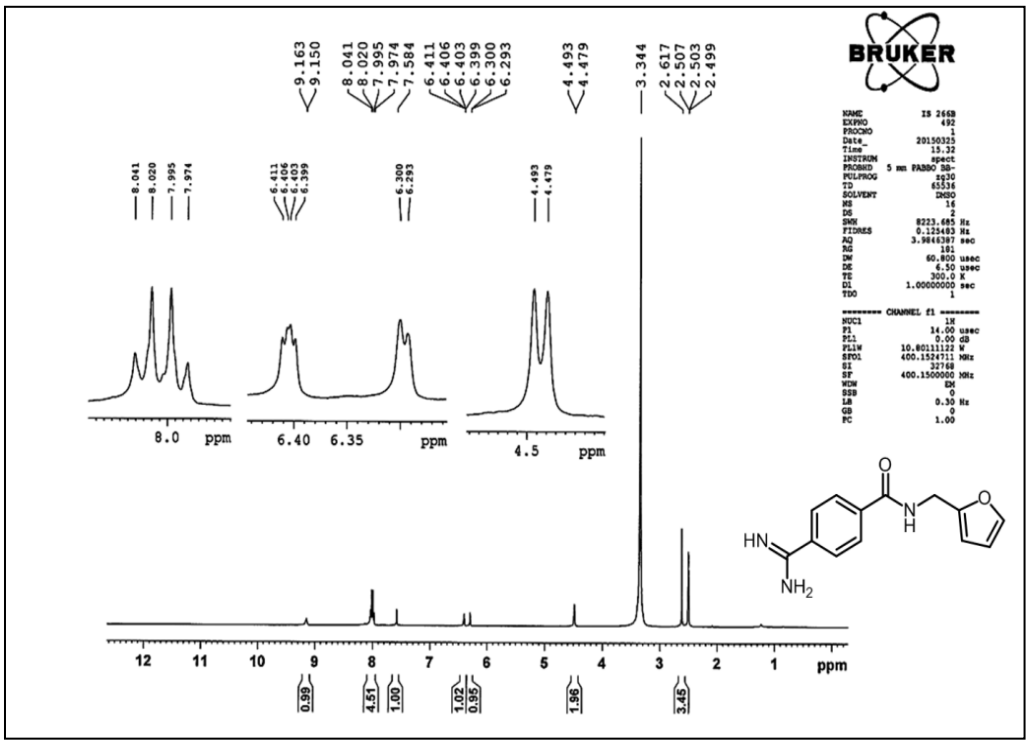

Figure 2.1.19: ^{1}H NMR spectra of 7h

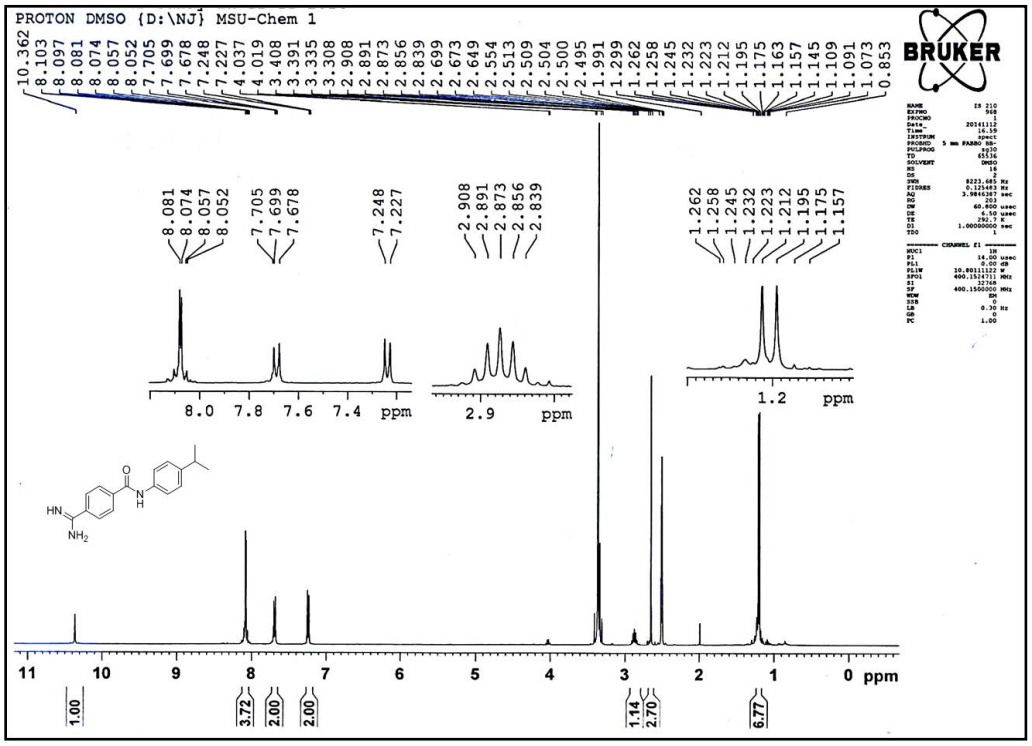

Figure 2.1.20: ^{1}H NMR spectra of 7i

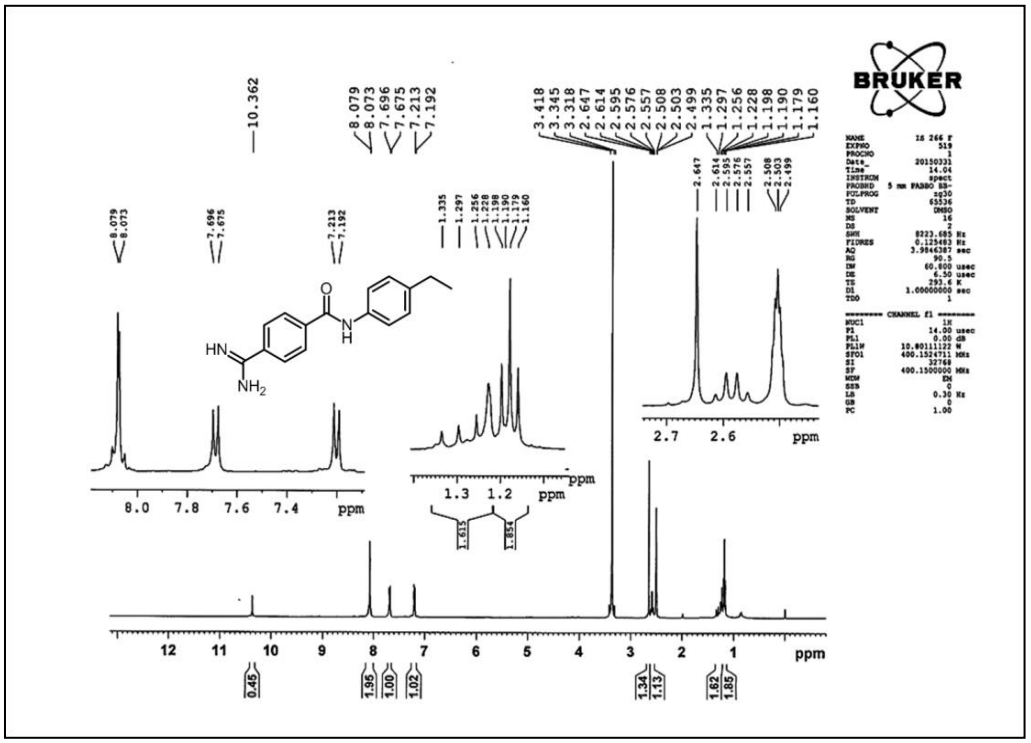

Figure 2.1.21: ^{1}H NMR spectra of 7j

^{13}C NMR of all the compounds (7a-7j):

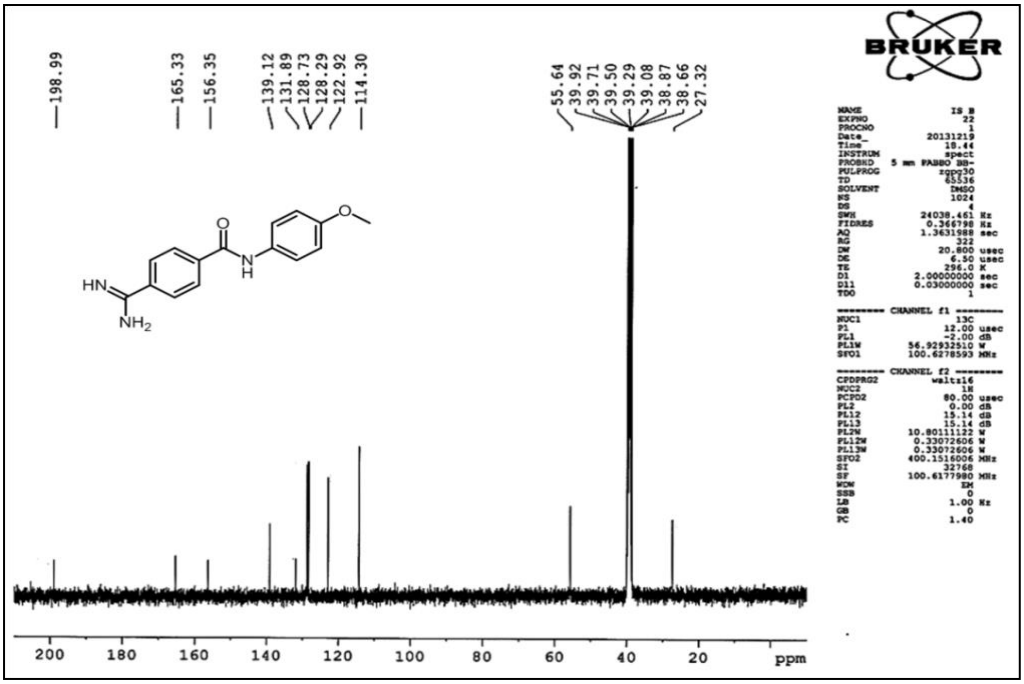

Figure 2.1.22: ^{13}C NMR spectra of 7a

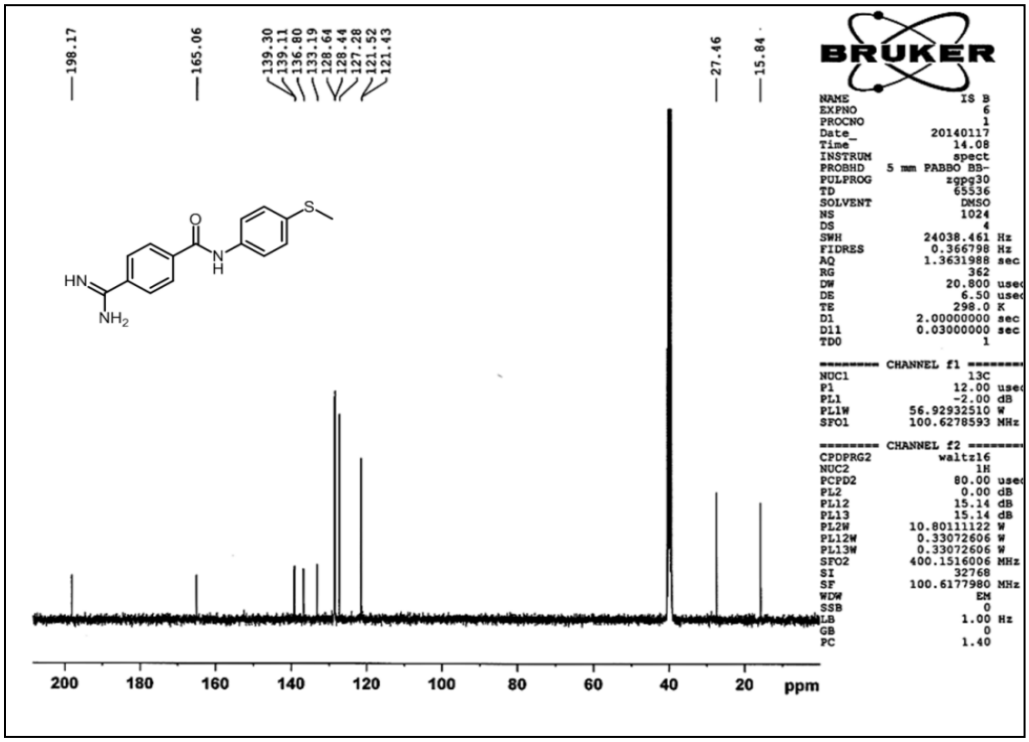

Figure 2.1.23: ^{13}C NMR spectra of 7b

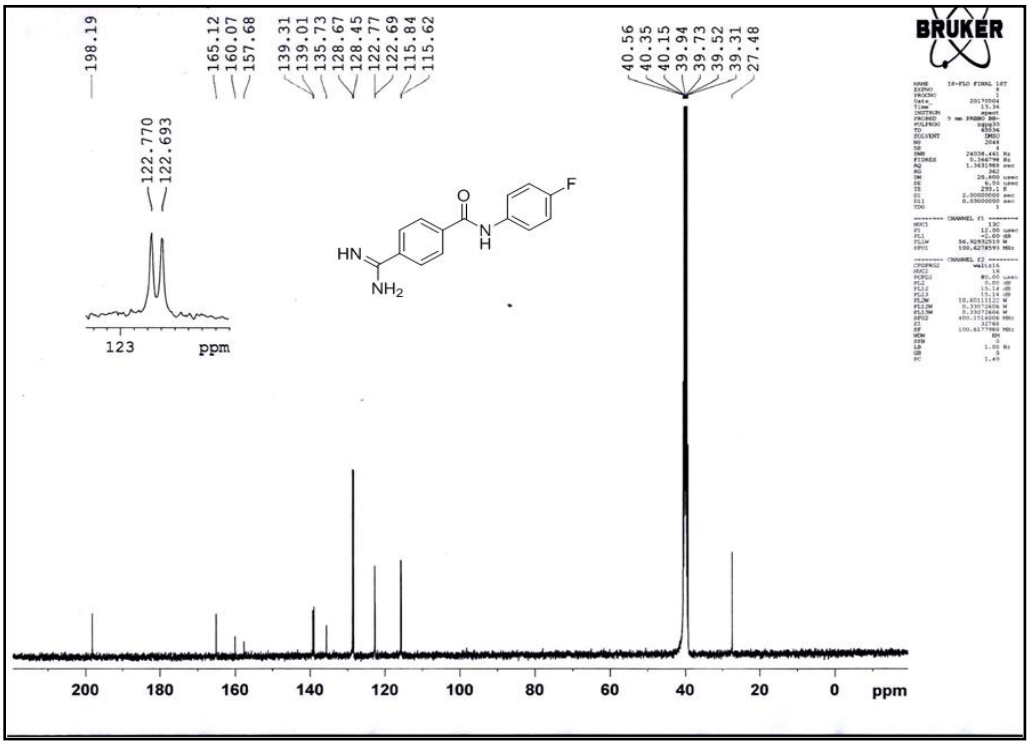

Figure 2.1.24: ^{13}C NMR spectra of 7c

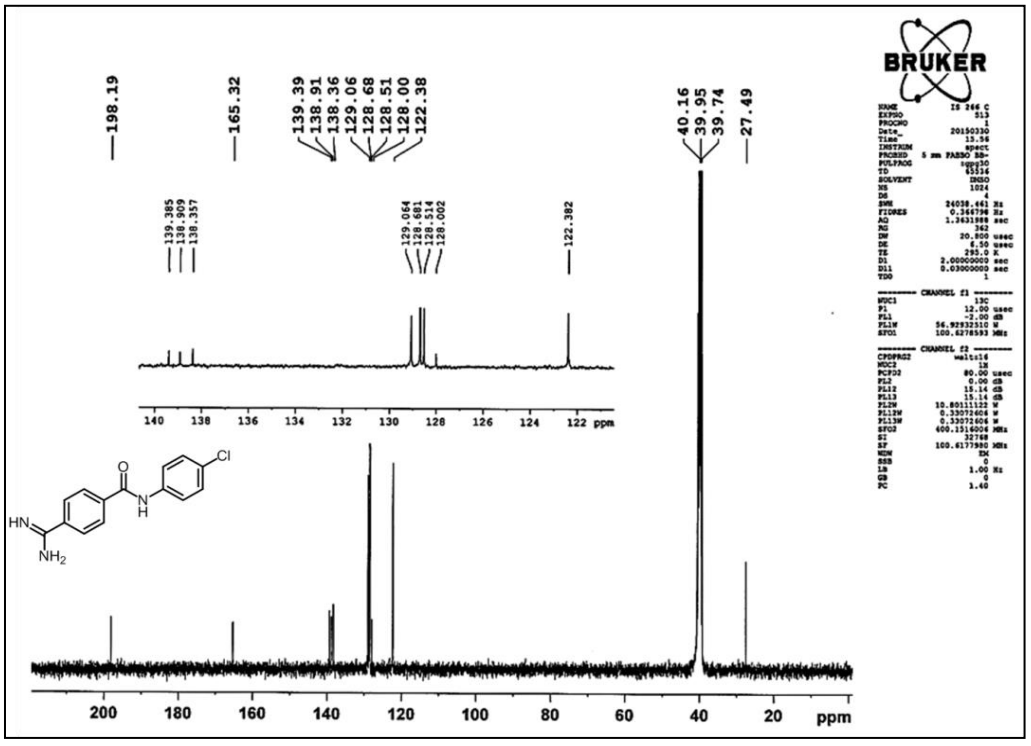

Figure 2.1.25: ^{13}C NMR spectra of 7d

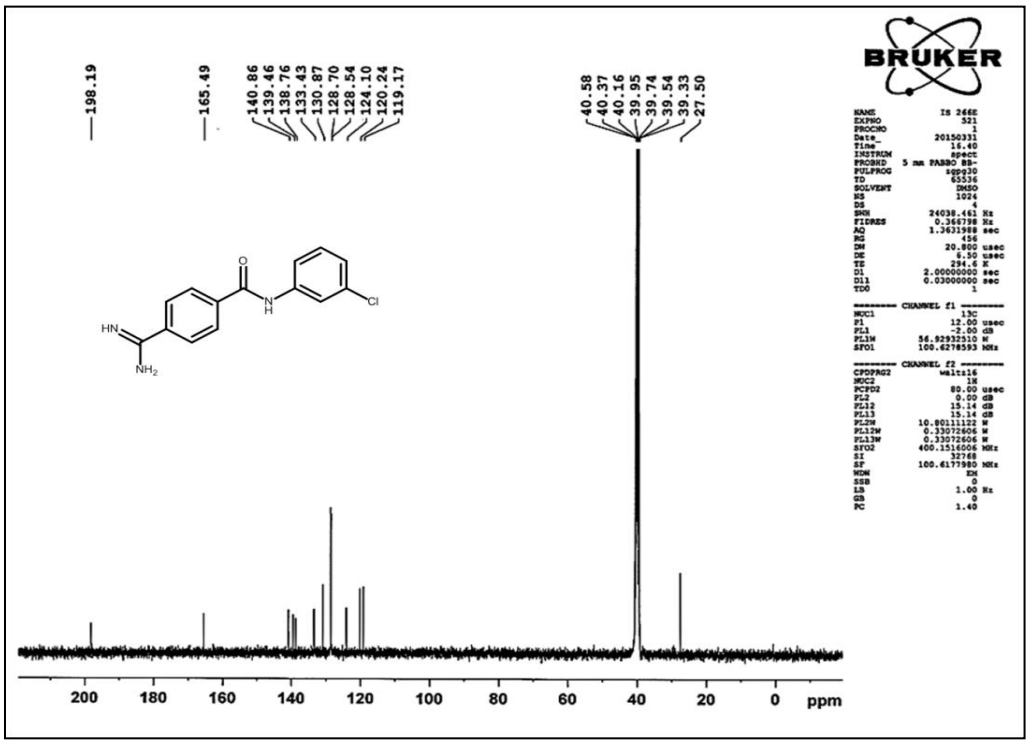

Figure 2.1.26: ^{13}C NMR spectra of 7e

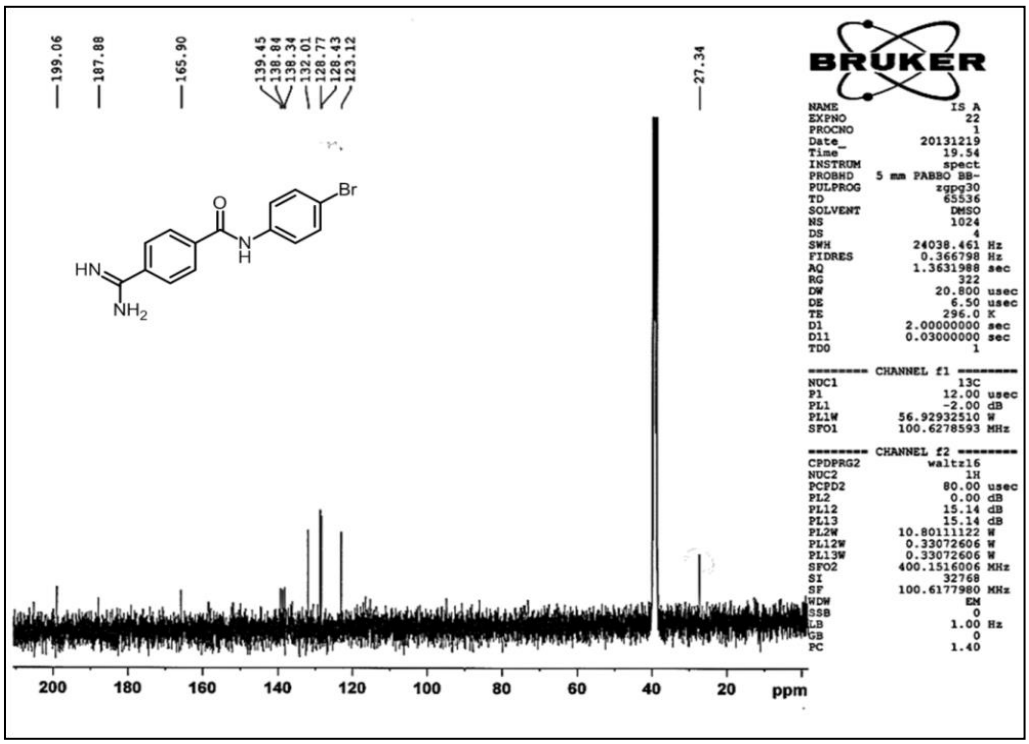

Figure 2.1.27: ^{13}C NMR spectra of 7f

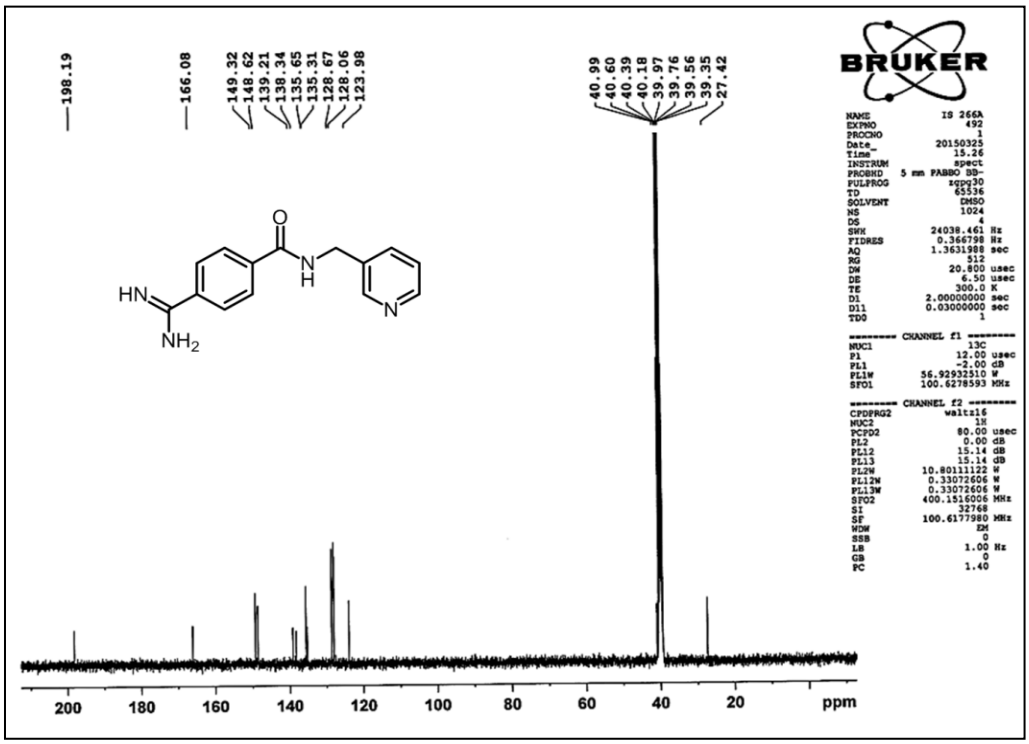

Figure 2.1.28: ^{13}C NMR spectra of 7g

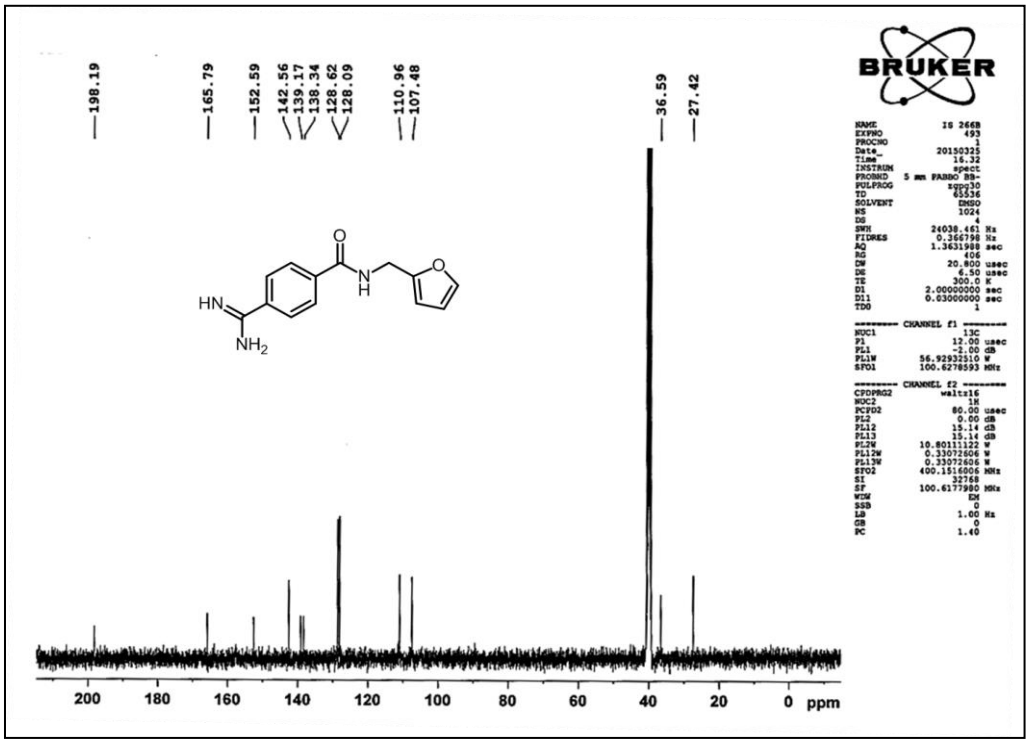

Figure 2.1.29: ^{13}C NMR spectra of 7h

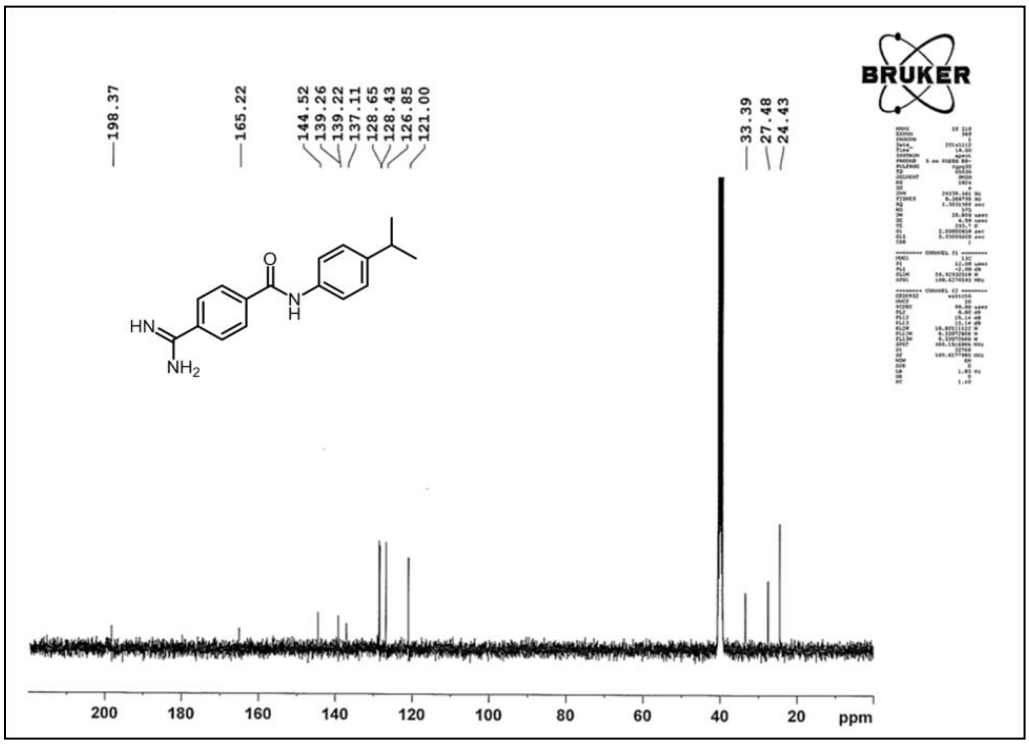

Figure 2.1.30: ^{13}C NMR spectra of 7i

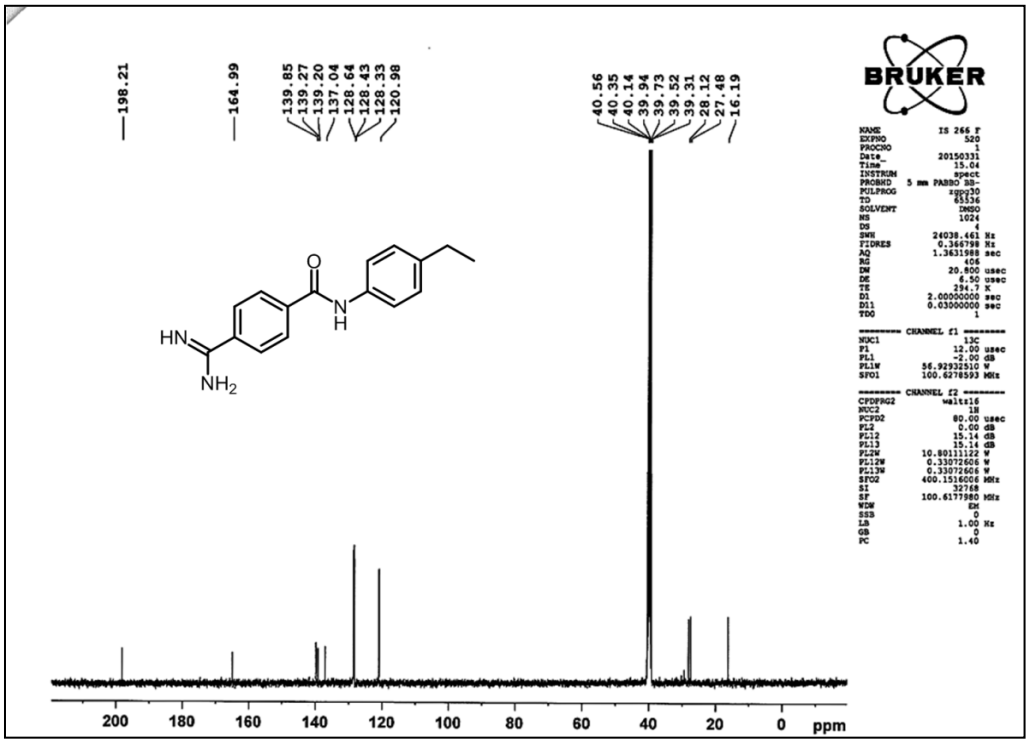

Figure 2.1.31: ^{13}C NMR spectra of 7j

IR Spectra of all the compounds

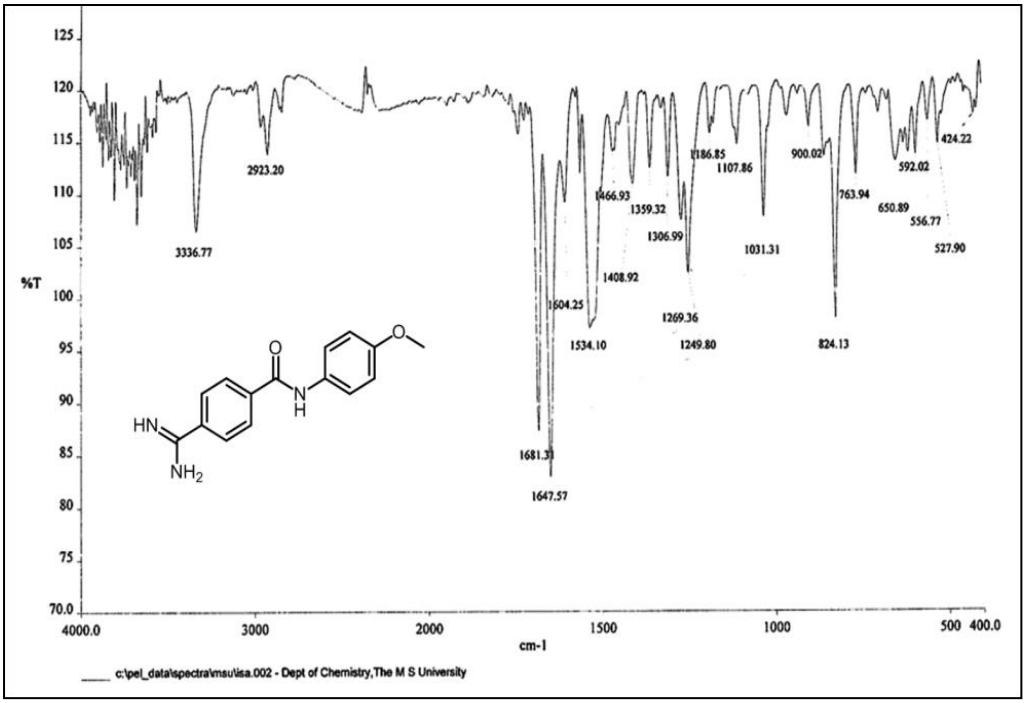

Figure 2.1.32: IR spectra of 7a

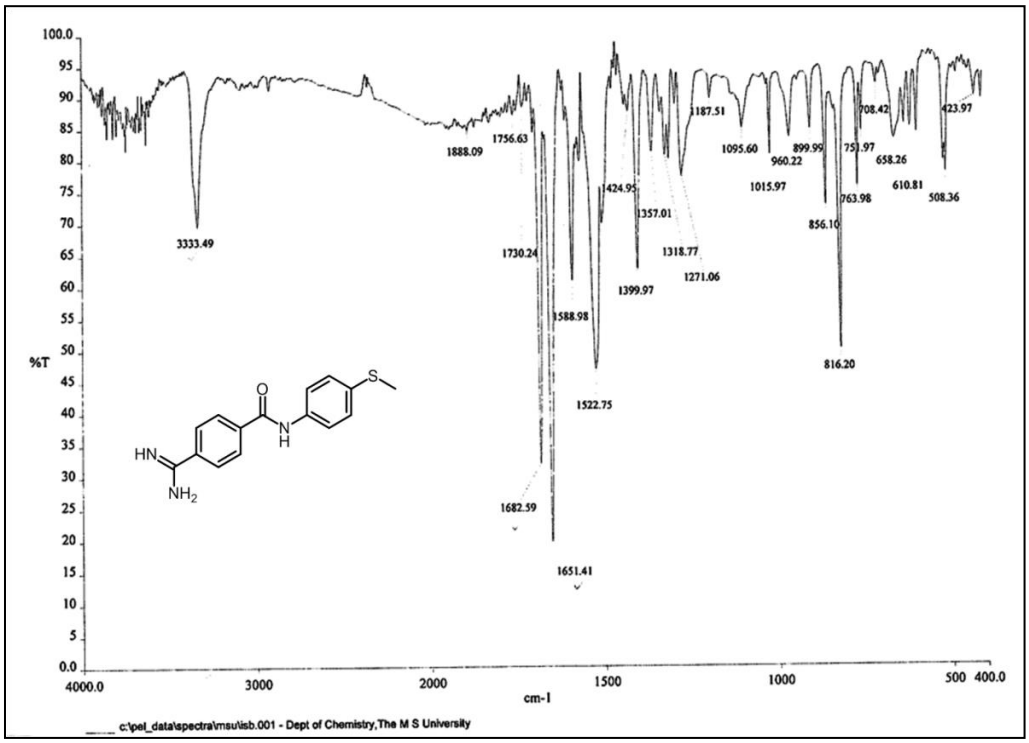

Figure 2.1.33: IR spectra of 7b

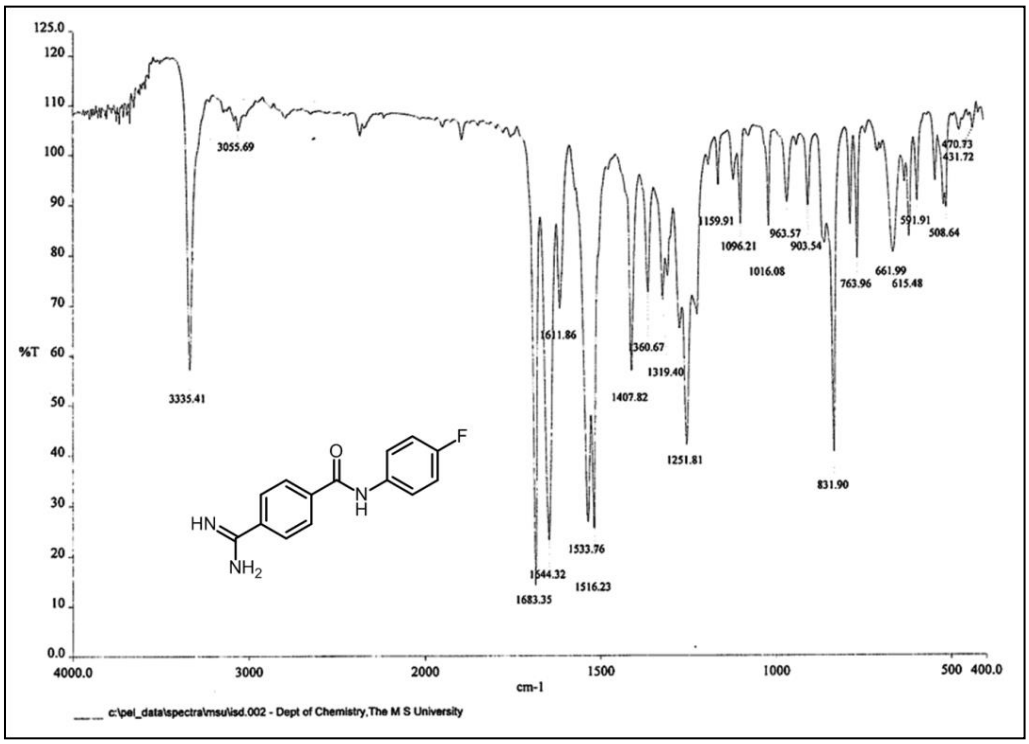

Figure 2.1.34: IR spectra of 7c

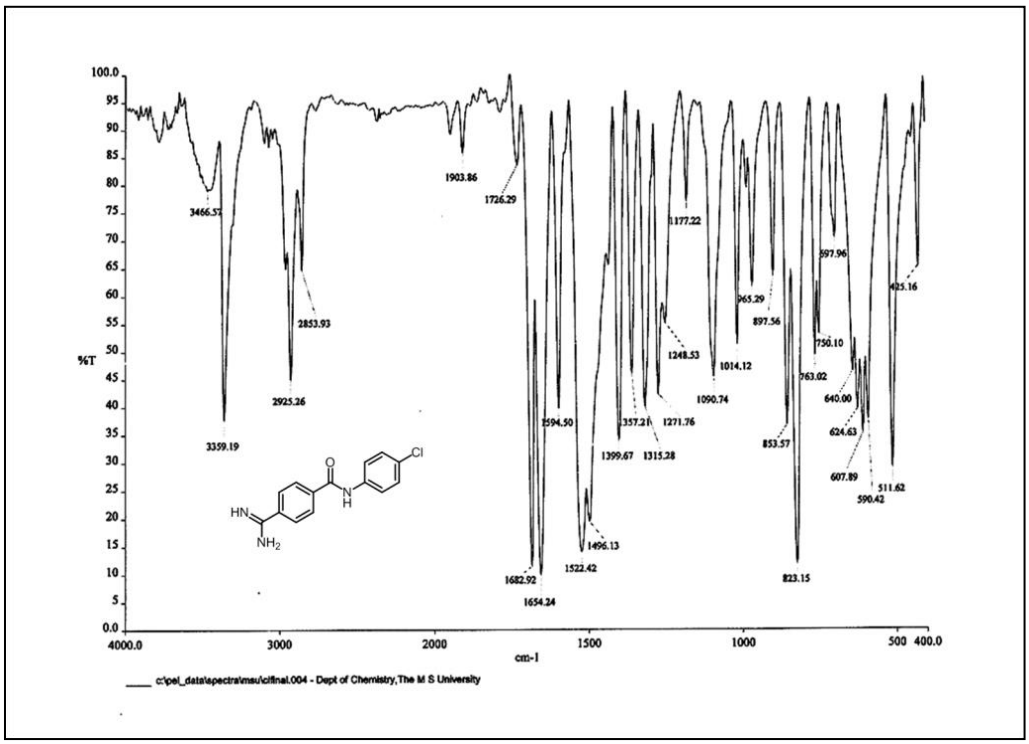

Figure 2.1.35: IR spectra of 7d

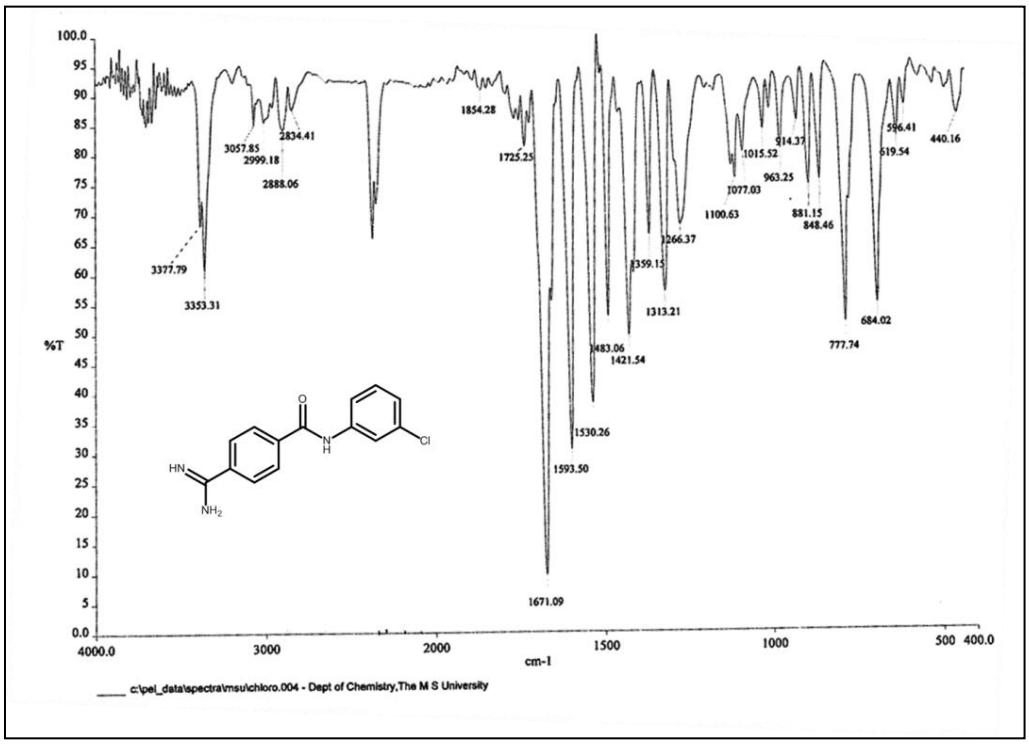

Figure 2.1.36: IR spectra of 7e

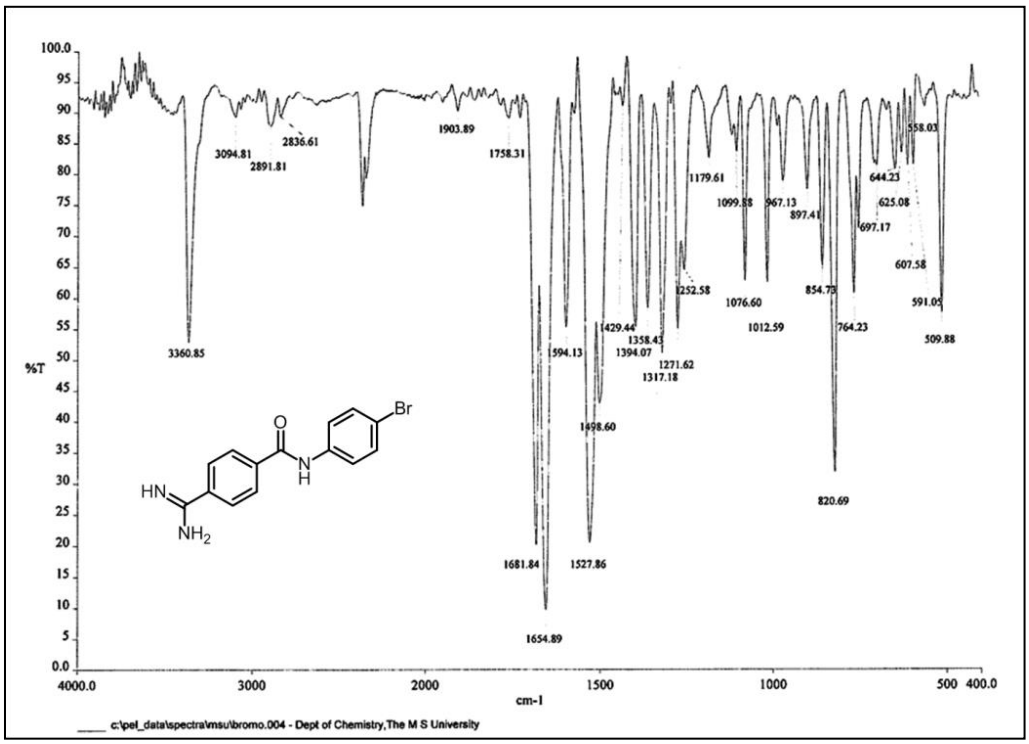

Figure 2.1.37: IR spectra of 7f

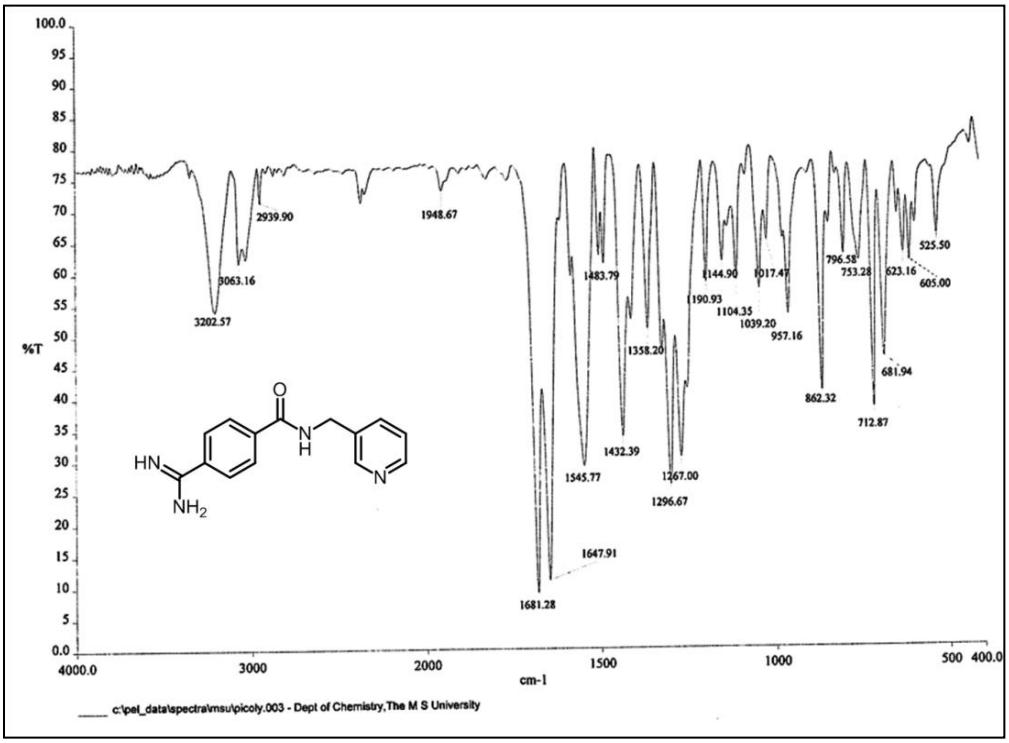

Figure 2.1.38: IR spectra of 7g

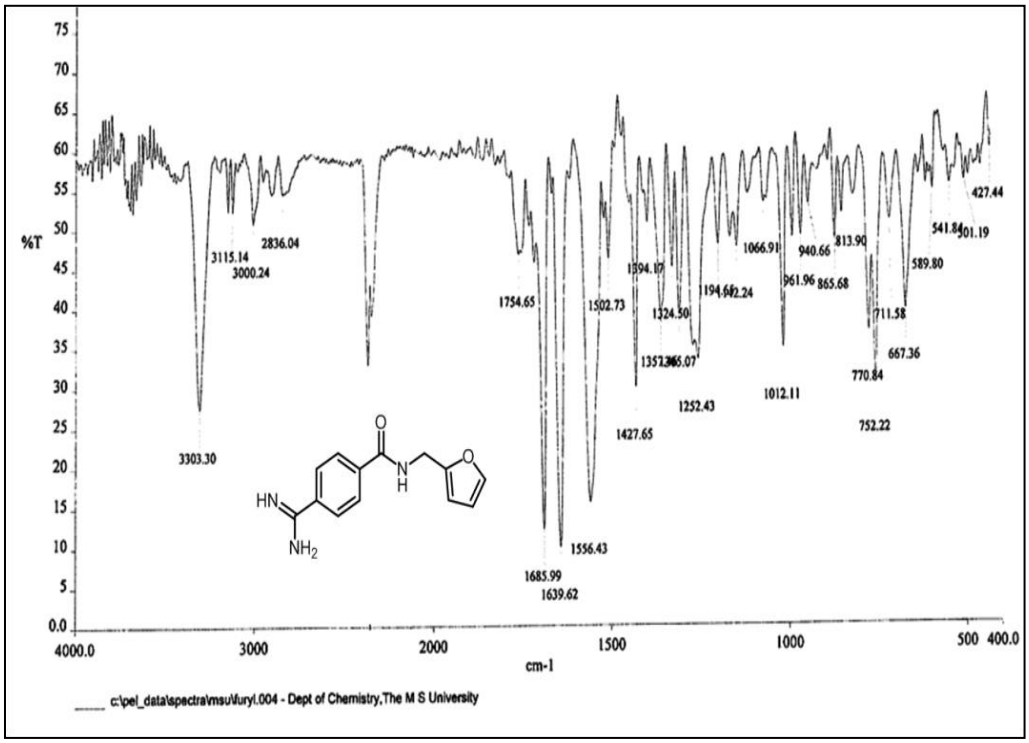

Figure 2.1.39: IR spectra of 7h

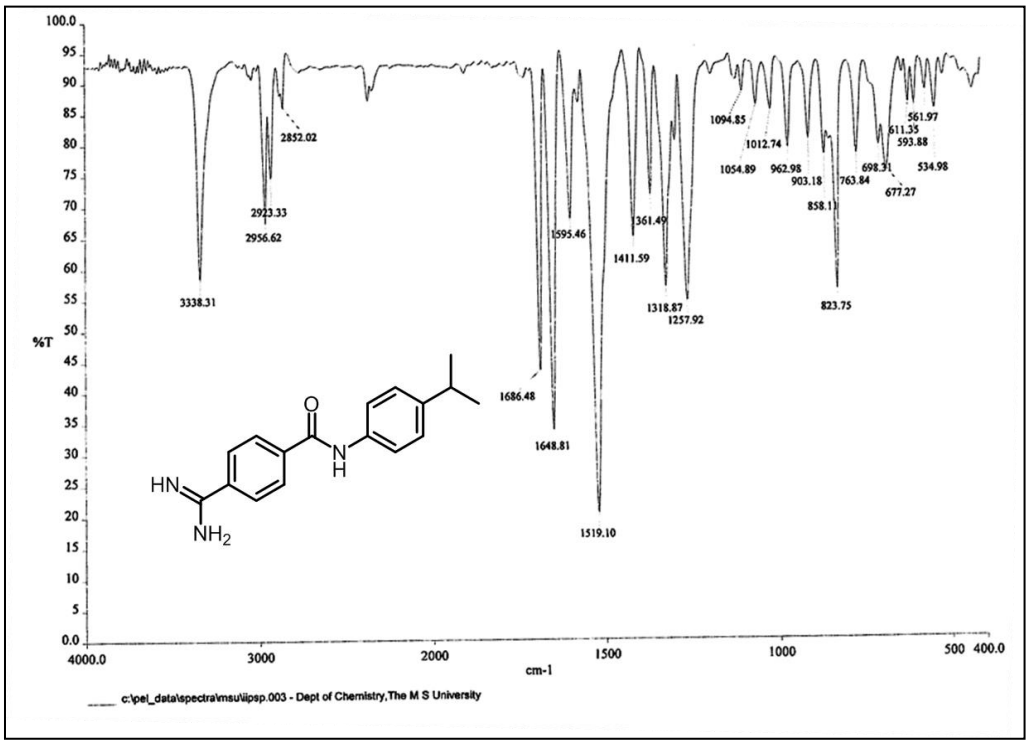

Figure 2.1.40: IR spectra of 7i

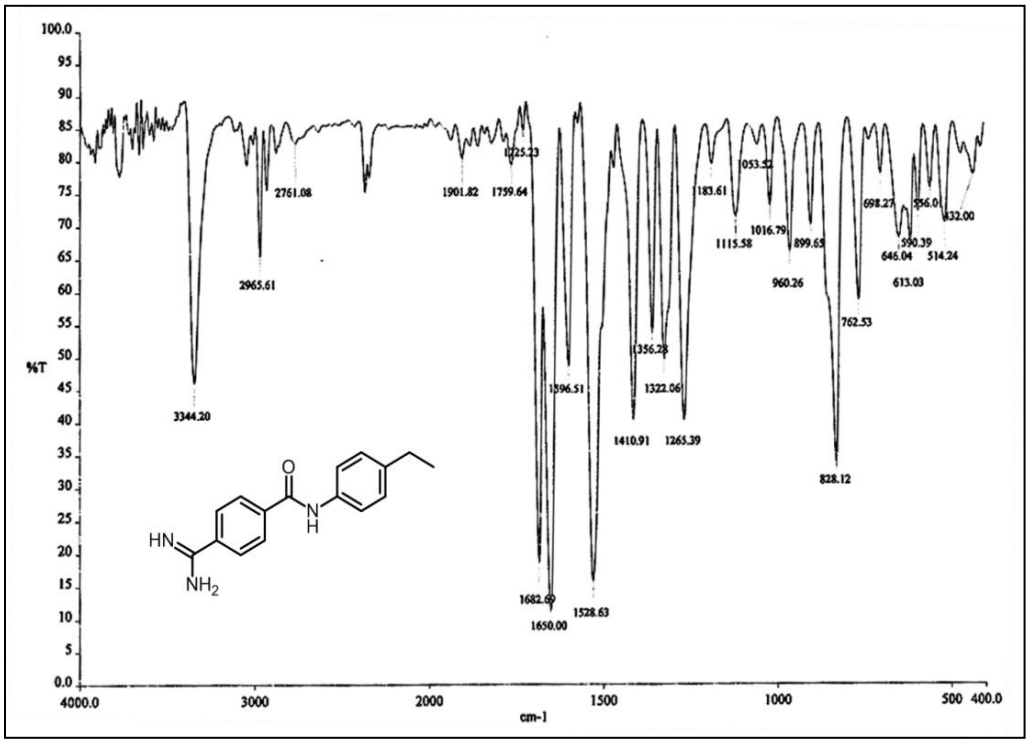

Figure 2.1.41: IR spectra of 7j

Mass spectra of all the compounds:

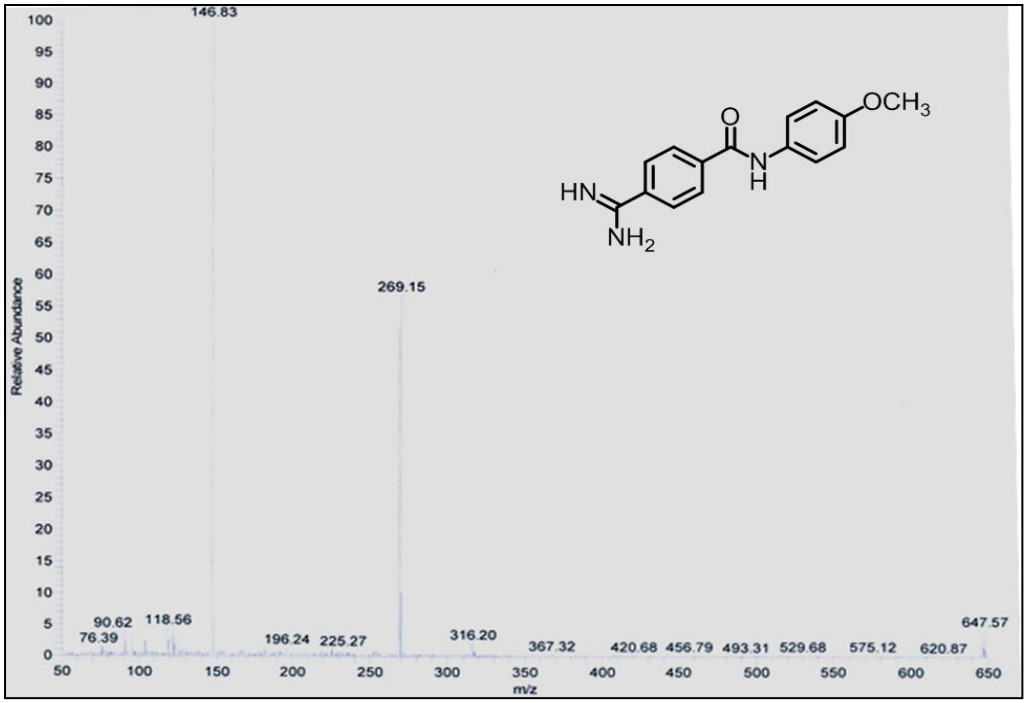

Figure 2.1.42: Mass spectra of 7a

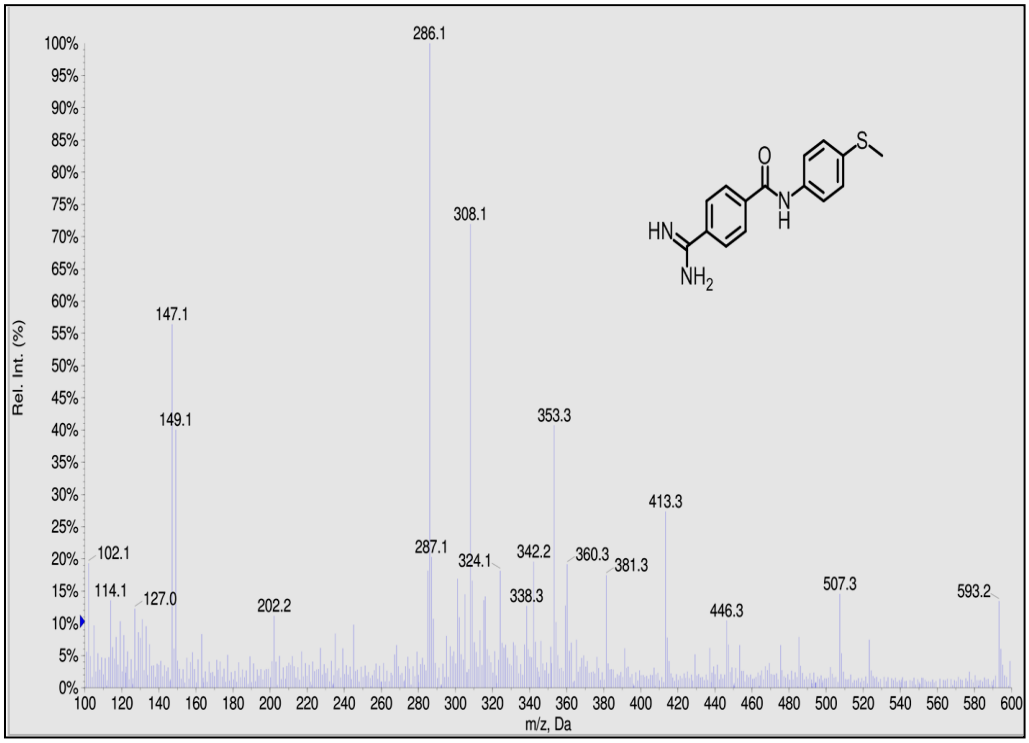

Figure 2.1.43: Mass spectra of 7b

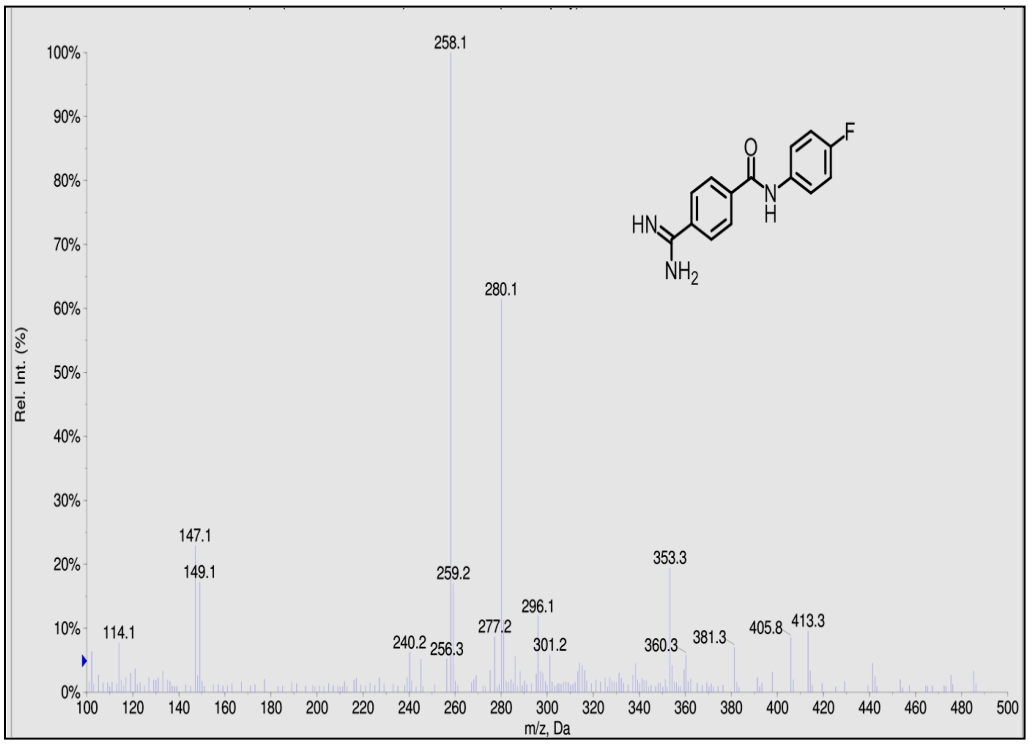

Figure 2.1.44: Mass spectra of 7c

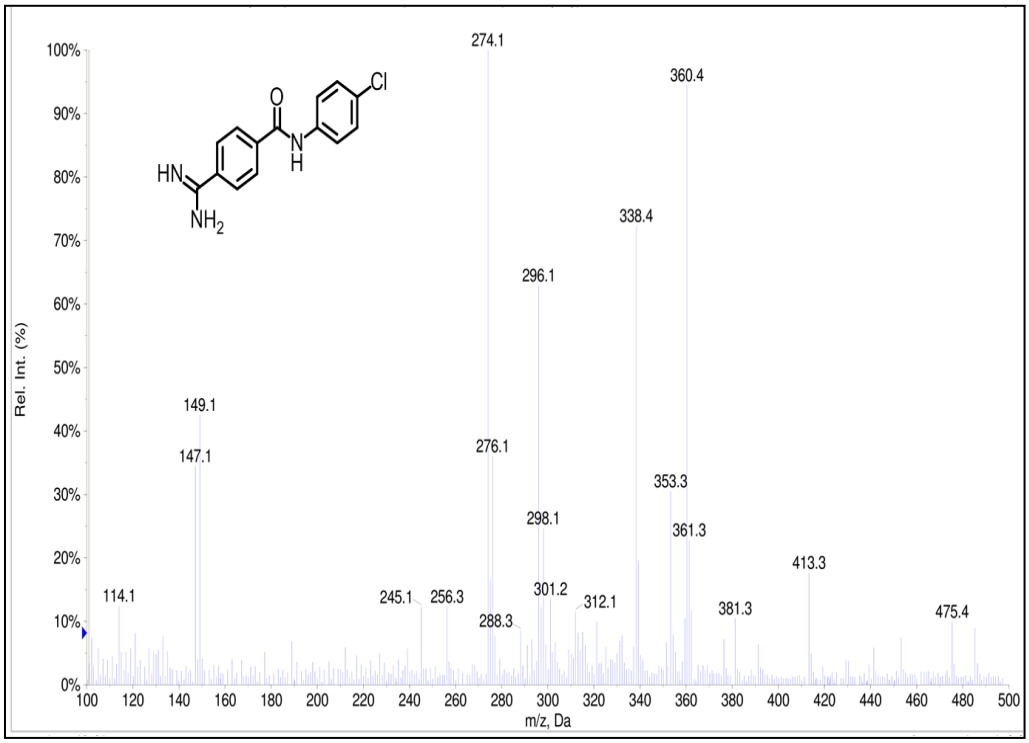

Figure 2.1.45: Mass spectra of 7d

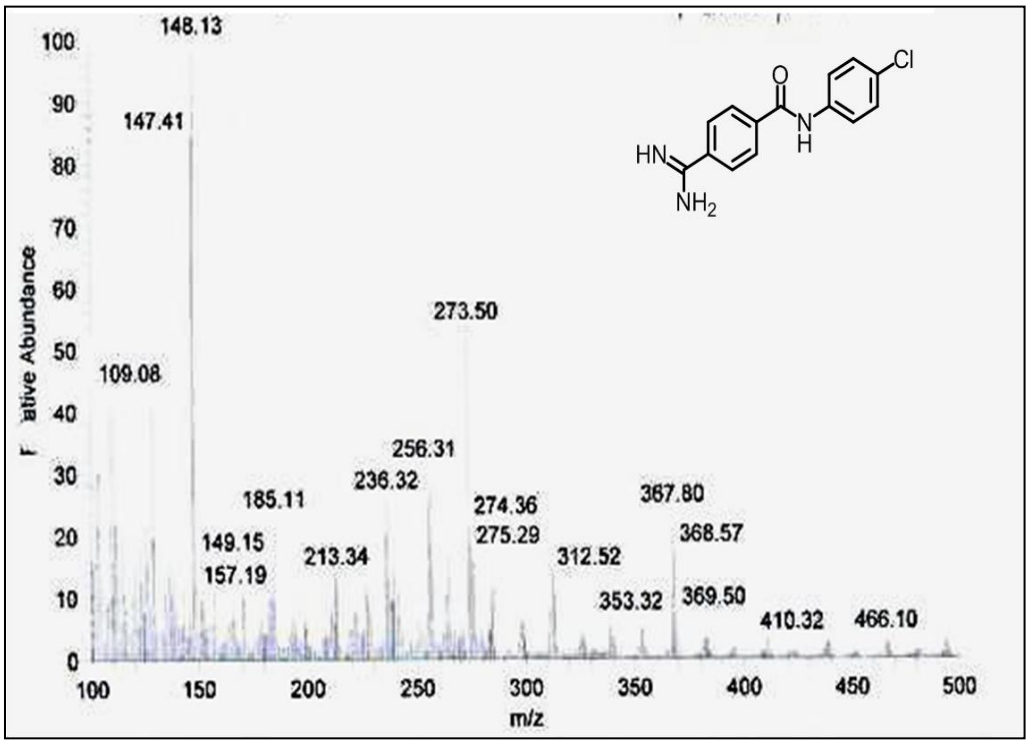

Figure 2.1.46: Mass spectra of 7e

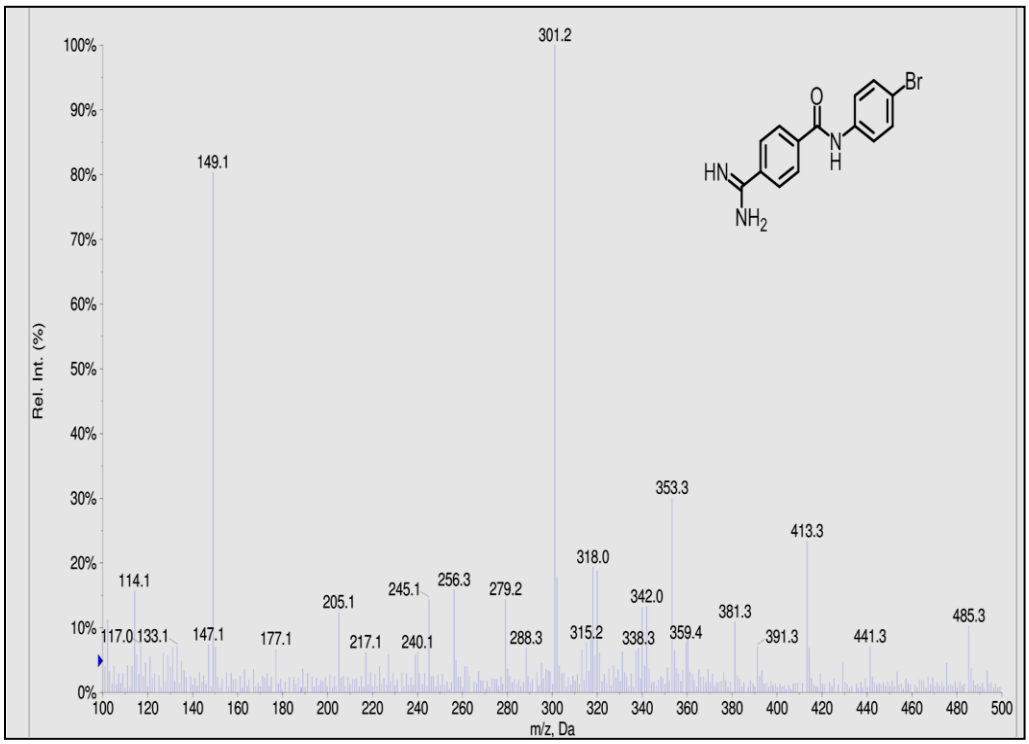

Figure 2.1.47: Mass spectra of 7f

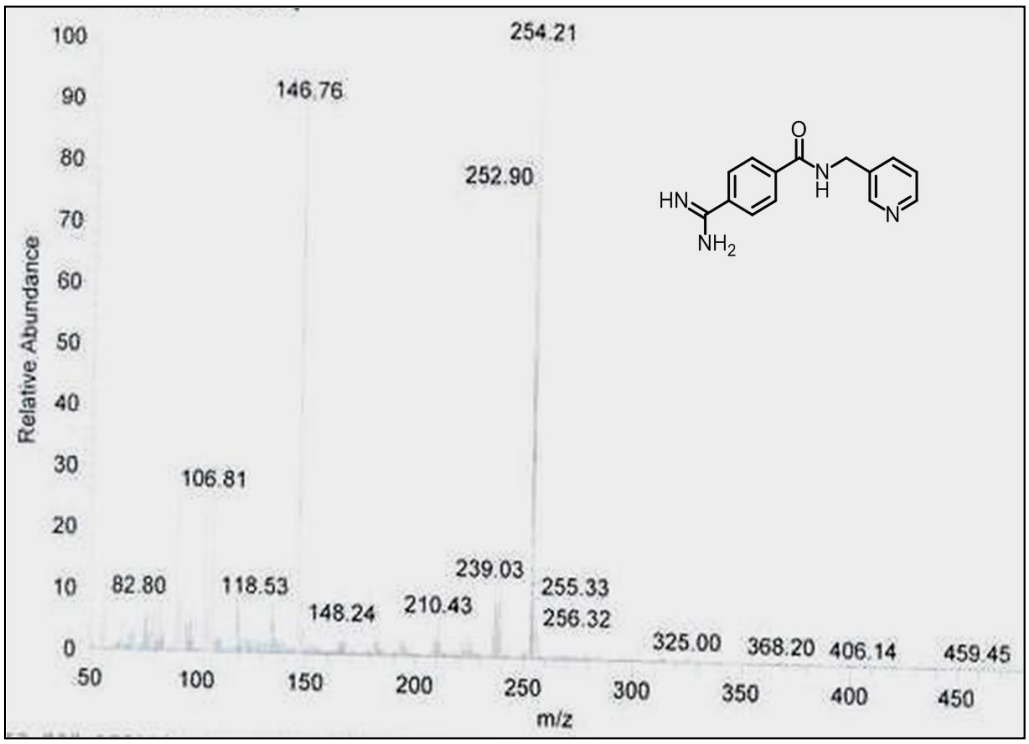

Figure 2.1.48: Mass spectra of 7g

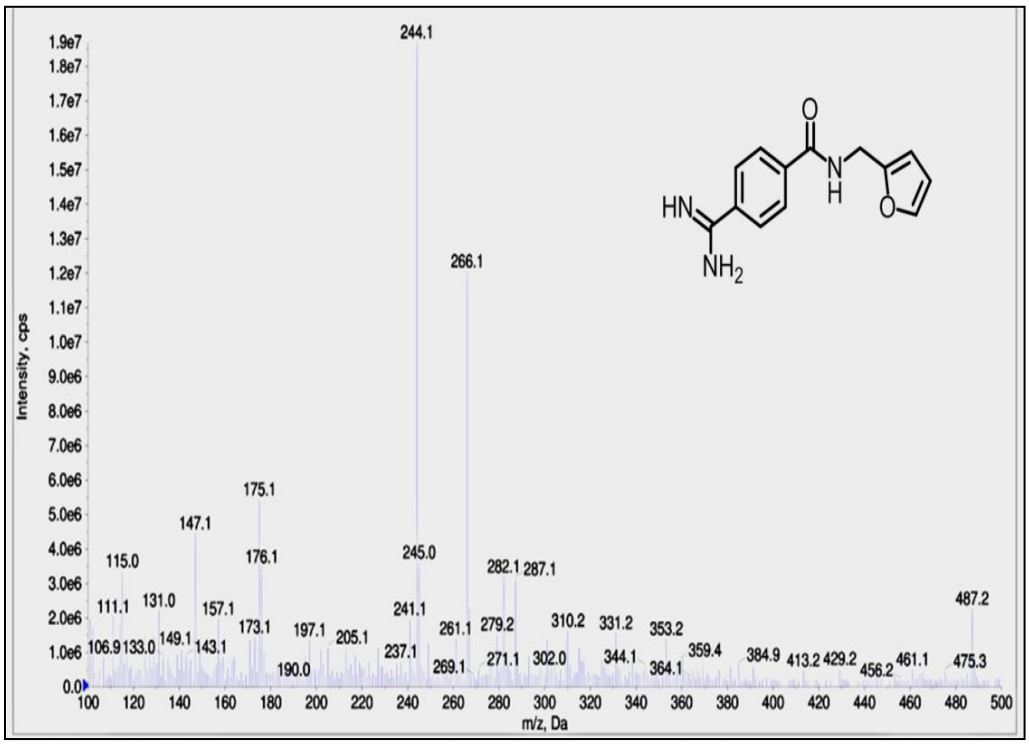

Figure 2.1.49: Mass spectra of 7h

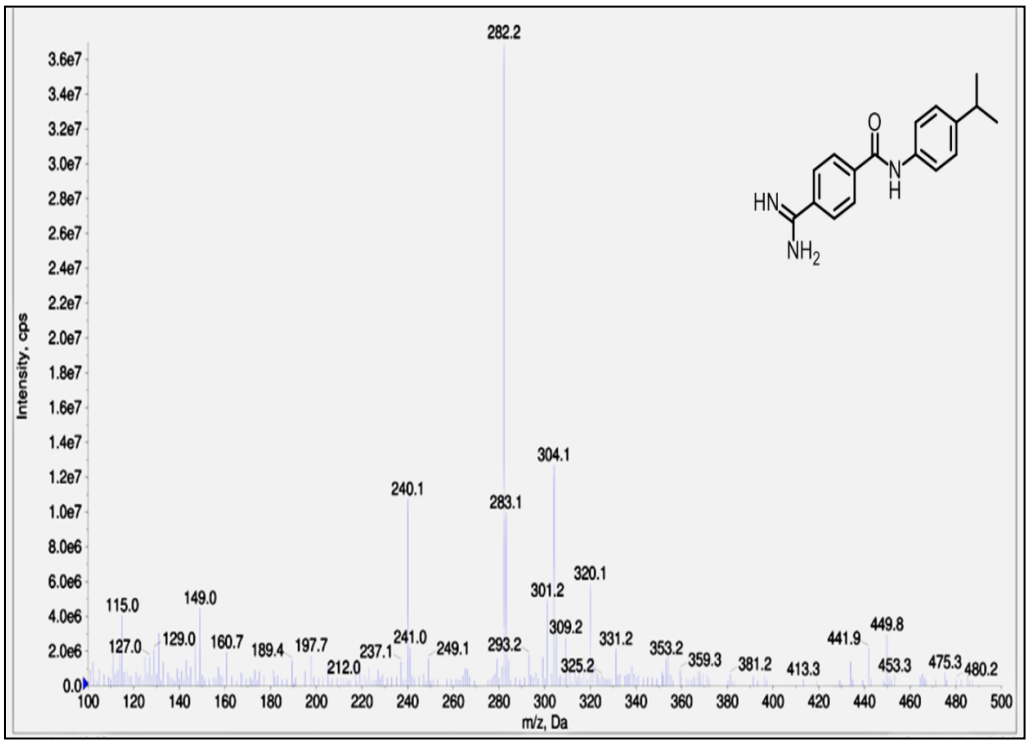

Figure 2.1.50: Mass spectra of 7i

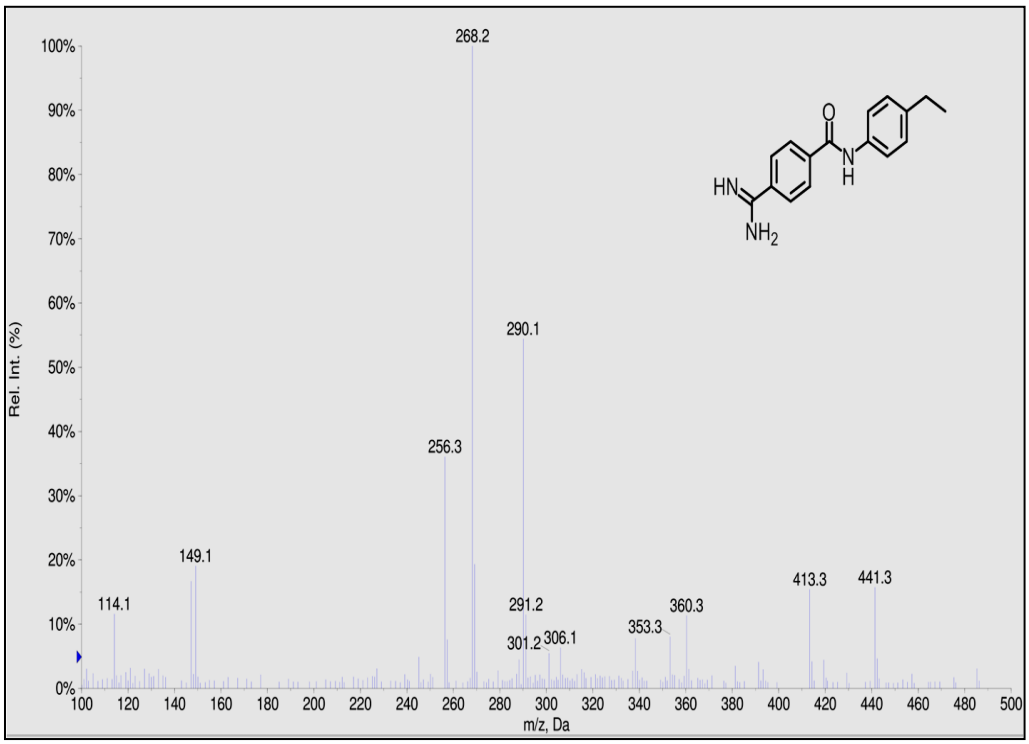

Figure 2.1.51: Mass spectra of 7j

TG-DTA

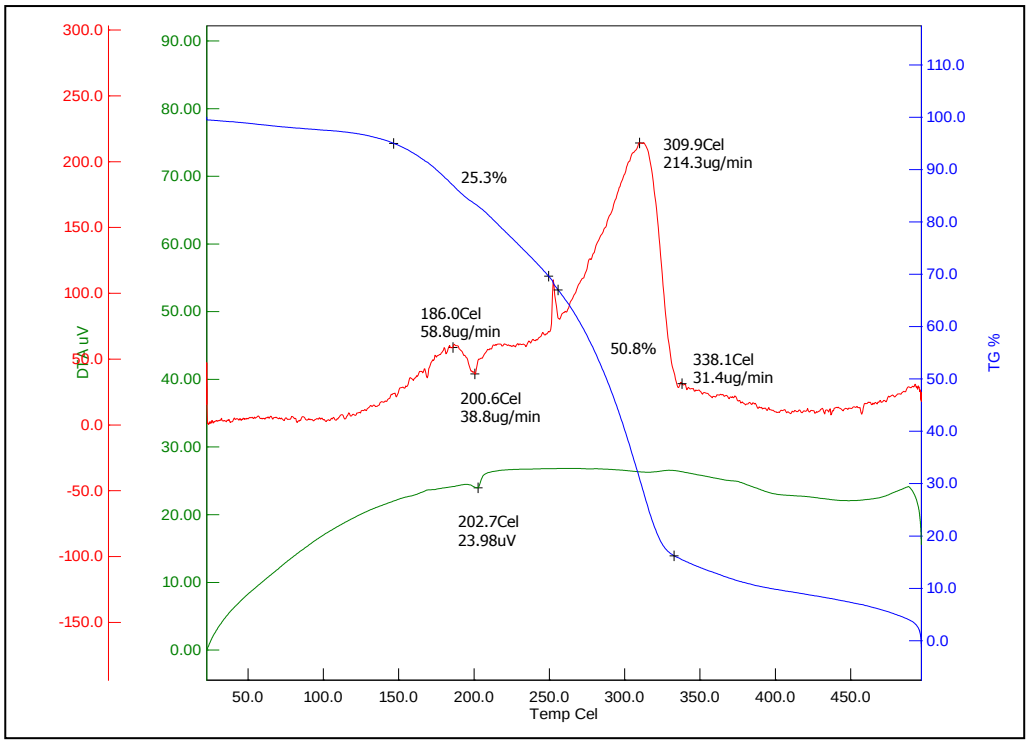

Figure 2.1.52: TG-DTA graph of 7a

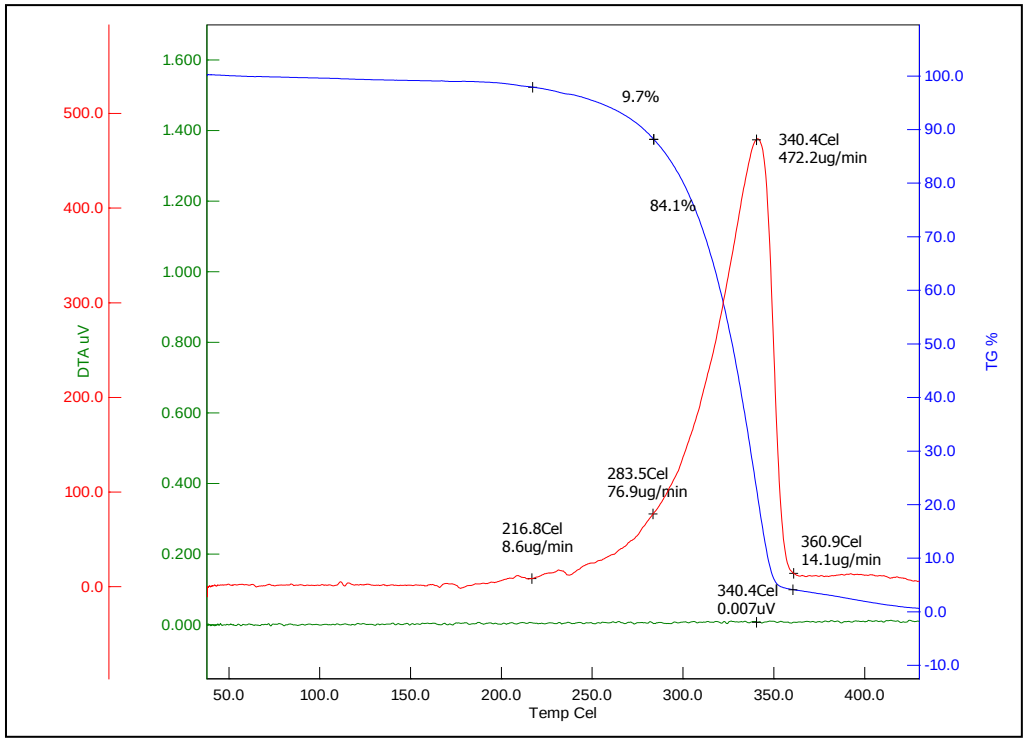

Figure 2.1.53: TG-DTA graph of 7b

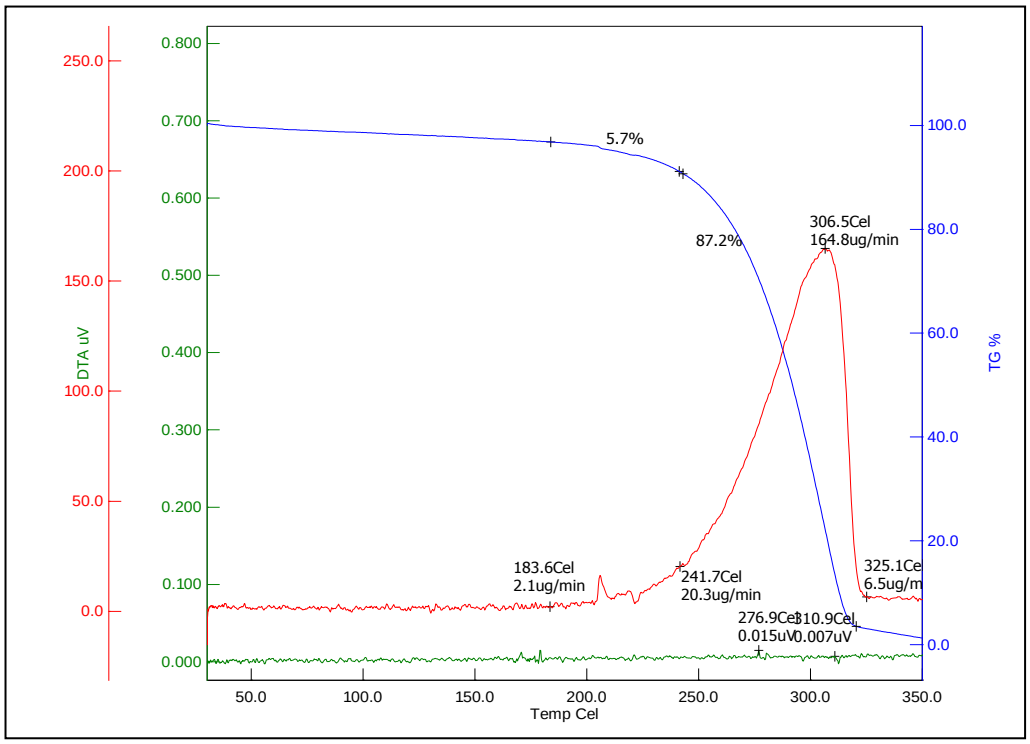

Figure 2.1.54: TG-DTA graph of 7d

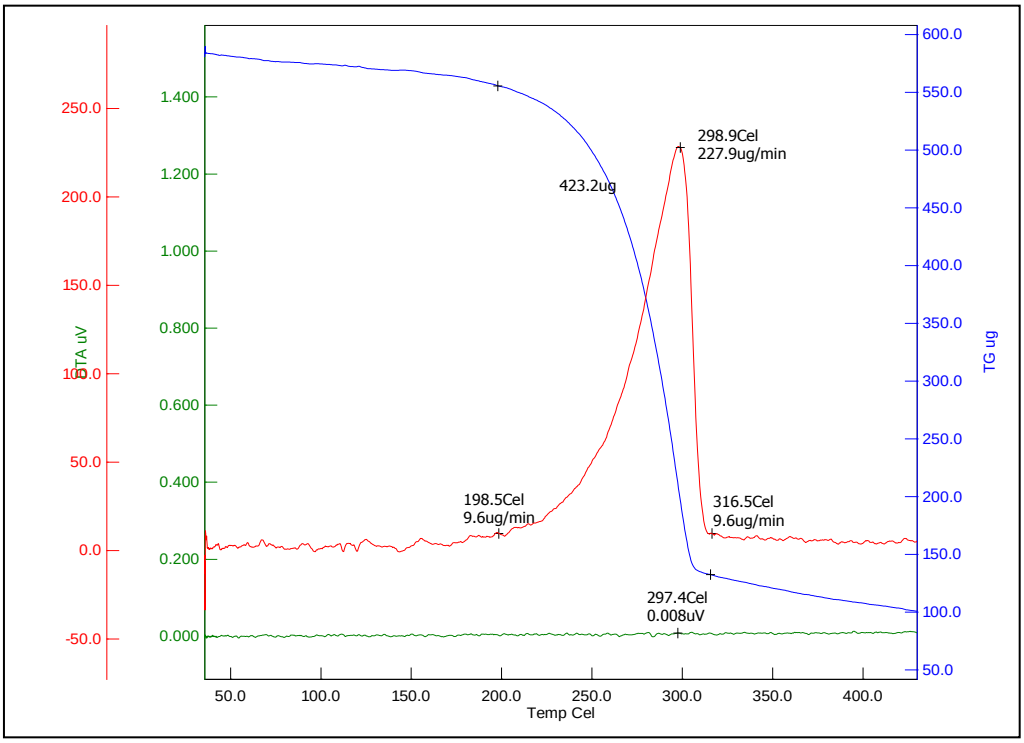

Figure 2.1.55: TG-DTA graph of 7e

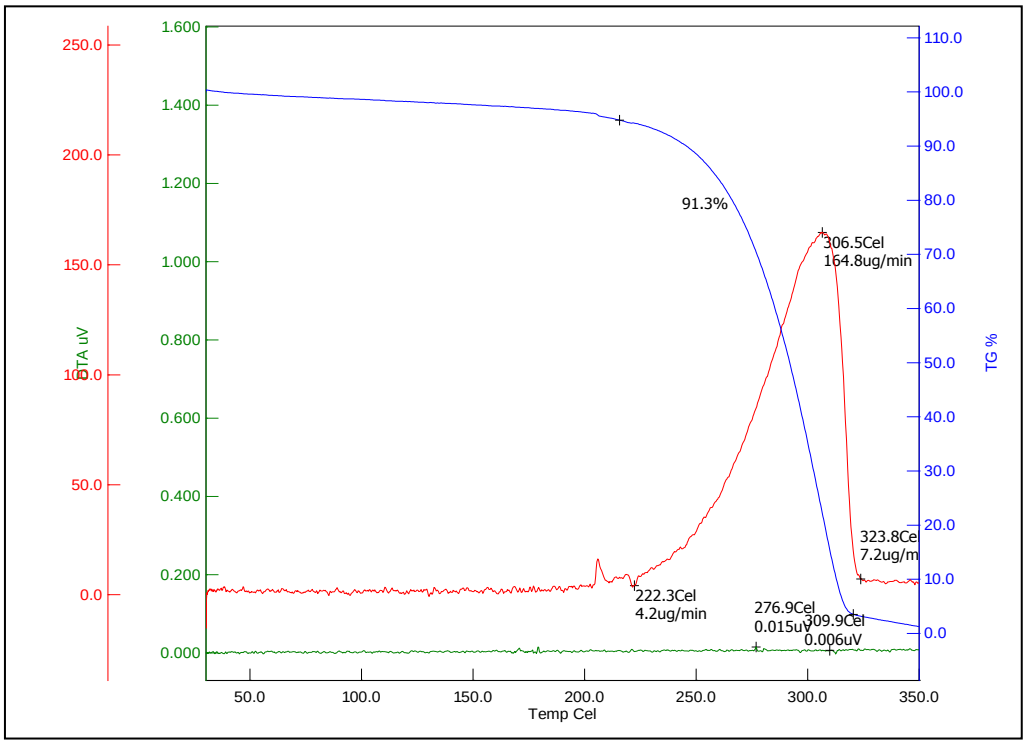

Figure 2.1.56: TG-DTA graph of 7f

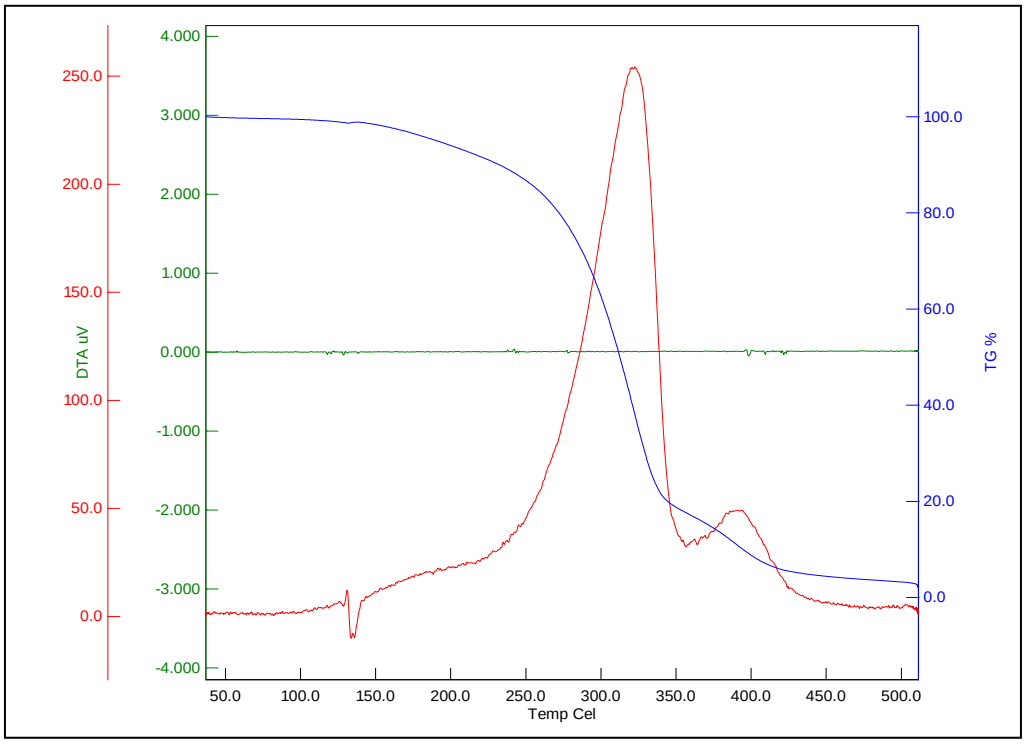

Figure 2.1.57: TG-DTA graph of 7g

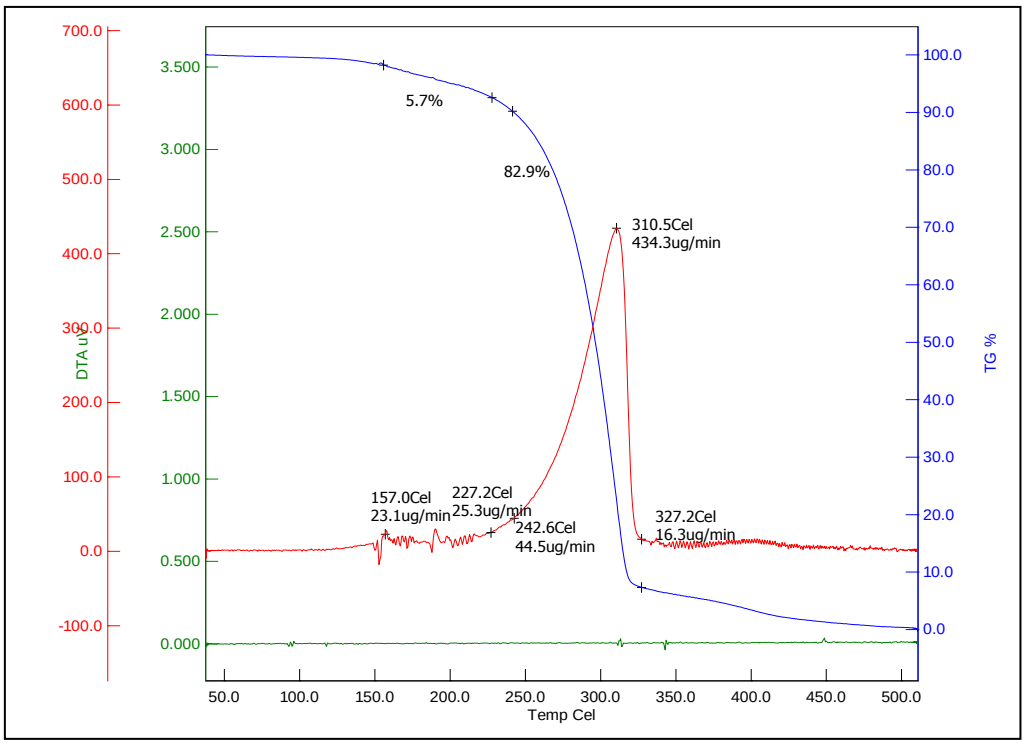

Figure 2.1.58: TG-DTA graph of 7i

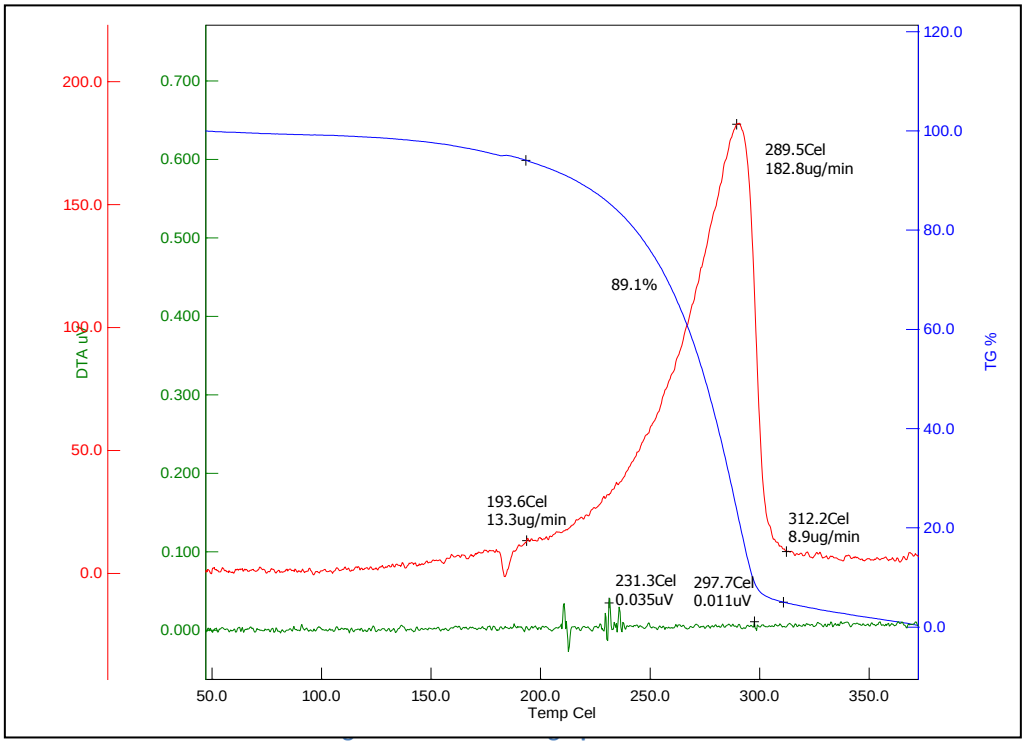

Figure 2.1.59: TG-DTA graph of 7j

2.1.7 References:

[1] Wei, H.; Mundade, R.; Lange, K.; Lu, T. *Cell Cycle*, **2014**, *13*, 32-41.

[2] Wang, C.; Jiang, H.; Jin, J.; Xie, Y.; Chen, Z.; Zhang, H.; Lian, F.; Liu, Y. C.; Zhang, C.; Ding, H.; Chen, S. *Journal of Medicinal Chemistry*, **2017**, *60*, 8888-8905.

[3] Hu, H.; Owens, E. A.; Su, H.; Yan, L.; Levitz, A.; Zhao, X.; Henary, M.; Zheng, Y. G. *Journal of Medicinal Chemistry*, **2015**, *58*, 1228-1243.

[4] Thomas, D.; van Ommeren, R.; Lakowski, T. M.; Frankel, A.; Martin, N. I. *MedChemComm*, **2012**, *3*, 1235-1244.

[5] Obianyo, O.; Causey, C. P.; Osborne, T. C.; Jones, J. E.; Lee, Y. H.; Stallcup, M. R.; Thompson, P. R. *ChemBioChem*, **2010**, *11*, 1219-1223.

[6] Osborne, T.; Weller Roska, R. L.; Rajski, S. R.; Thompson, P. R. *Journal of the American Chemical Society*, **2008**, *130*, 4574-4575.

[7] Spannhoff, A.; Machmur, R.; Heinke, R.; Trojer, P.; Bauer, I.; Brosch, G.; Schüle, R.; Hanefeld, W.; Sippl, W.; Jung, M. *Bioorganic & medicinal chemistry letters*, **2007**, *17*, 4150-4153.

[8] Spannhoff, A.; Heinke, R.; Bauer, I.; Trojer, P.; Metzger, E.; Gust, R.; Schüle, R.; Brosch, G.; Sippl, W.; Jung, M. *Journal of medicinal chemistry*, **2007**, *50*, 2319-2325.

[9] Ragno, R.; Simeoni, S.; Castellano, S.; Vicidomini, C.; Mai, A.; Caroli, A.; Tramontano, A.; Bonaccini, C.; Trojer, P.; Bauer, I.; Brosch, G. *Journal of medicinal chemistry*, **2007**, *50*, 1241-1253.

[10] (a) Chu, X. Q.; Cao, W. B.; Xu, X. P.; Ji, S. J. *J. Org. Chem.* **2017**, 82, 1145-1154 ; (b) Ma, B.; Wang, Y.; Peng, J.; Zhu, Q. *J. Org. Chem.* **2011**, 76, 6362-6366 ;(c) Doise, M.; Blondeau, D.; Sliwa, H. *Synth. Commun*. **1992**, *22*, 2891-2901.

[11] (a)Yan, L.; Yan, C.; Qian, K.; Su, H.; Kofsky-Wofford, S. A.; Lee, W. C.; Zhao, X.; Ho, M. C.; Ivanov, I.; Zheng, Y. G. *J. Med. Chem.* **2014**, 57, 2611 ;(b) Wang, J.; Xu, F.; Cai, T.; Shen, Q. *Org. Lett.* **2008**, 10, 445-448 ;(c) Cortes-Salva, M.; Garvin, C.; Antilla, J. C. *J. Org. Chem*. **2011**, 76, 1456-1459.

[12] Oxley, P.; Partridge, M. W.; Short, W. F. *J. Chem. Soc*. **1947**, 209. Amidines. Part VII, 1110-1116.

[13] (a) Garigipati, R. S. *Tet. Lett.* **1990**, 31, 1969-1972 ;(b) Grivas, J. C.; Taurins, A. *Can. J. Chem*, **1961**, *39*, 761-764.

[14] Pinner, A.; Klein, F. *Eur. J. Inorg. Chem.* **1877,** 10, 1889-1897.

[15] Boeré, R. T.; Oakley, R. T.; Reed, R. W. *J. Organometallic Chem.* **1987**, 331, 161-167.

[16] Ullapu, P. R.; Ku, S. J.; Choi, Y. H.; Park, J. Y.; Han, S. Y.; Baek, D. J.; Lee, J. K.; Pae, A. N.; Min, S. J.; Cho, Y. S. *Bulletin of the Korean Chem. Soc.* **2011**, 32(spc8), 3063-3073.

[17] (a) Cornell, E. F. *J. Am. Chem. Soc.* **1928**, 50, 3311-3318 ;(b) Schaefer, F. C.; Krapcho, A. P. *JOC*, **1962**, 27, 1255-1258.

[18] Newbery, G.; Webster, W. *J. Chem. Soc.* **1947**, 738-742.

[19] Nadrah, K.; Dolenc, M. S. *Synlett*, **2007**, 8, 1257-1258.

[20] (a)Yang, E. G.; Mustafa, N.; Tan, E. C.; Poulsen, A.; Ramanujulu, P. M.; Chng, W. J.; Yen, J. J.; Dymock, B. W. *J. Med. Chem.* **2016**, 59, 8233-8262 ;(b)Yang, S.Y. *Drug Discovery Today* **2010**, 15, 444-450.

[21] Zhang, X.; Cheng, X. *Structure* **2003**, 11, 509-520.

[22] Spannhoff, A.; Sippl, W.; Jung, M. *Int.J.Biochem.Cell.Biol*. **2009**, 41, 4-11.

[23] Yan, L.; Yan, C.; Qian, K.; Su, H.; Wofford, S.A.K.; Lee, W.; Zhao, X.; Ho, M.; Ivanov, I.; Zheng, G. Y. *J. Med. Chem.* **2014**, 57, 2611-2622.

[24] Vartale, S. P.; Pawar, Y. D.; Halikar, N. K. *Heteroletters* **2012**, 2,71-78.

[25] Hwang, S.; Choi, S. Y.; Lee, J. H.; Kim, S.; In, J.; Ha, S. K.; Lee, E; Kim, T. Y.; Kim, S. Y.; Choi, S.; Kim, S. *Bioorg Med. Chem*. **2010**, 18, 5602-5609.

[26] Amin, K. M.; Gawad, N. M. A.; Rahman, D. E. A.; EI Ashry, M. K. *Bioorg Chem*. **2014**, 52, 31-43.

[27] Baell, J.; Walters, M. A. *Nature* **2014**, 513, 481.

[28] Massorotti, A.; Aprile, S.; Mercalli, V.; Grosso, E. D.; Grosa, G.; Sorba, G.; Tron, G. C. *ChemMedChem.* **2014**, 9, 2497-2508.

[29] Hunter, C. A., & Sanders, J. K. (1990). *Journal of the American Chemical Society*, *112*(14), 5525-5534.

[30] Mosmann, T *J. Immun. Methods*, **1983**, 65, 55-63.

[31] (a) Hu, H.; Owens, E. A.; Su, H.; Yan, L.; Levitz, A.; Zhao, X.; Henary, M.; Zheng, Y. G. *J. Med. Chem.* **2015**, 58, 1228 ;(b) Hart, P.; Thomas, D.; van Ommeren, R.; Lakowski, T. M.; Frankel, A.; Martin, N. I. *Med. Chem. Commun.* **2012**, 3, 1235-1244 ;(c) Spannhoff, A.; Heinke, R.; Bauer, I.; Trojer, P.; Metzger, E.; Gust, R.; Schule, R.; Brosch, G.; Sippl, W.; Jung, M. *J. Med. Chem*. **2007**, 50, 2319-2325 ;(d) Ragno, R.; Simeoni, S.; Castellano, S.; Vicidomini, C.; Mai, A.; Caroli, A.; Tremontano, A.; Bonaccini, C.; Trojer, P.; Bauer, I.; Brosch, G. *J. Med. Chem*. **2007**, 50, 1241-1253

[32] Medina-Franco, J. L.; Giulianotti, M. A.; Welmaker, G. S.; Houghten, R. A. *Drug Discovery Today* **2013**, 18, 495-501.

[33] Duganath, N.; Sridhar, C.; Jayaveera, K. N. *RJPBCS* **2014**, 5, 1044.

[34] Sellarajah, S.; Lekishvili, T.; Bowring, C.; Thompsett, A. R.; Rudyk, H.; Birkett, C. R.; Brown, D. R.; Gilbert, I. H. *J. Med. Chem.* **2004**, 47, 5515.

[35] Zheng, Q.; Zhang, F.; Cheng, K.; Yang, Y.; Chen, Y.; Qian, Y.; Zhang, H.; Li, H.; Zhou, C.; An, S.; Jiao, Q.; Zhu, H. *Bioorg. Med. Chem*. **2010**, 18, 880.

[36] Li, X.; Li, C.; Zhang, W.; Lu, X.; Han, S.; Hong, R. *Org. Lett*. **2010**, 12, 1696.

[37] Vartale, S. P.; Pawar, Y. D.; Halikar, N. K. *Heteroletters* **2012**, 71, 1.

[38] (a) Hwang, S.; Choi, S. Y.; Lee, J. H.; Kim, S.; In, J.; Ha, S. K.; Lee, E; Kim, T. Y.; Kim, S. Y.; Choi, S.; Kim, S. *Bioorg Med. Chem.* **2010**, 18, 5602. (b) Ando, H.; Ryu, A.; Hashimoto, A.; Oka, M.; Ichihashi, M. *Arch. Dermatol. Res*. **1998**, 290, 375. (c) Imokawa, G.; Kawai, M.; Mishima, Y.; Motegi, I. *Arch. Dermatol. Res*. **1986**, 278, 352.

[39] (a) Amin, K. M.; Gawad, N. M. A.; Rahman, D. E. A.; Ashry, M. K. M. EI. *Bioorg Chem*. **2014**, 52, 31-43. (b) A.M. Errichetti, J. Ansell, *Arch. Int. Med.* **1984**, 144, 1966.

[40] Berridge, M. V.; Tan, A. S. *Arch. Biochem. Biophys.*, **1993**, *303*(2), 474.

[41] Berridge, M.; Tan, A.; McCoy, K.; Wang, R. *Biochemica,* **1996**, *4*, 14.

[42] Marshall, N. J.; Goodwin, C. J.; Holt, S. *J. Growth Regul.*, **1995**, *5*(2), 69.

Chapter 2: Part II

Pharmacophore: II. Benzimidazole and Triazole Adducts

Contents

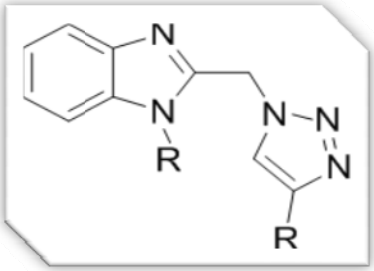

Abstract:

One pot Click chemistry is employed to link trizole and benzimidazole pharmacophore to get *N*-((1-((1*H*-benzo[*d*]imidazol-2-yl)methyl)-1*H*-1,2,3-triazol-4-yl)methyl)aniline and its derivatives. Flexible linkages in the form of $–CH_2$-R or –O-R/ -N-R were designed during synthesis. All the eleven newly synthesized compounds were characterized by FT-IR and NMR spectroscopy as well as high resolution mass spectrometry. ^{1}H NMR study showed interesting fluxional rotation in one of the molecules due to intramolecular hydrogen bonding. Selected compounds were screened for *in vitro* anti-proliferative activity using NCI (National Cancer Institute)-60-human-tumor-cell line-screening program. The most potent structure *N*-((1-((1*H*-benzo[*d*]imidazol-2-yl)methyl)-1*H*-1,2,3-triazol-4-yl)methyl)-4-chloroaniline **7e** showed 40% growth inhibition in renal cancer cell line (UO-31) at 10µM concentration.

Keywords: Benzimidazole, Click Reaction, 1,2,3-triazole, anti-proliferative.

2.2.1 Introduction

Pharmacophore driven synthesis for achieving biological activity is well known in literature. But designing efficient, high yielding regio-specific synthesis with more than one pharmacophore in a single molecule still remained challenge.

The broad and the potent activity of triazoles and benzimidazoles have established them as pharmacologically significant scaffolds[1-4] in an array of drug categories such as anti-microbial, anti-inflammatory, analgesic, anti-peptic, anti-viral, anti-neoplastic, anti-tubercular, anti parkinsons, anti-diabetic, anti-depressant (*Figure 2.2.1*).

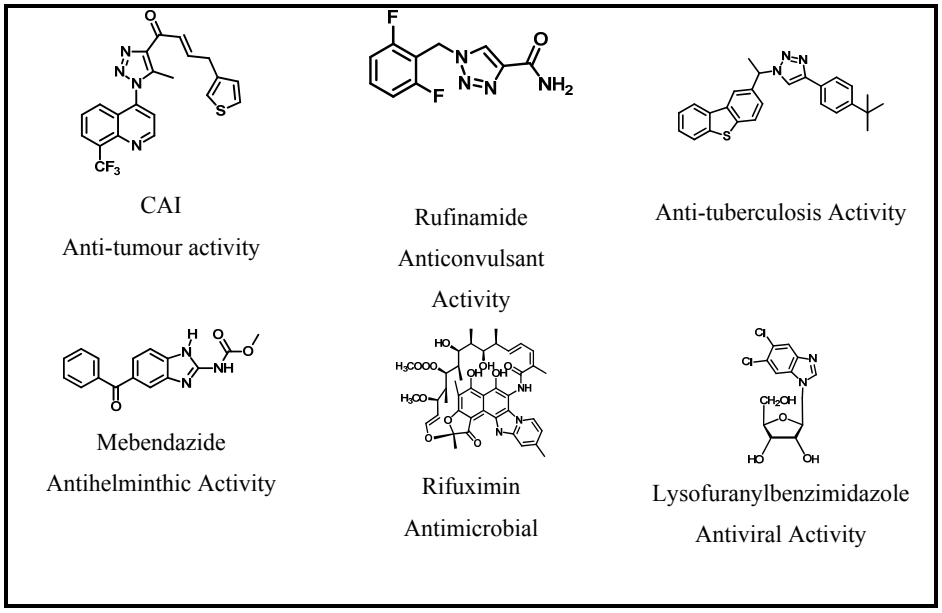

Figure 2.2.1: FDA approved drugs with benzimidazole and triazole in their core structure

Over the last decade 1,2,3-triazoles[5-9] have received increasing attention in medicinal chemistry[10-14] and this was made possible because of the discovery of the highly useful and widely applicable 1,3-dipolar cycloaddition reaction between azide and alkynes (click chemistry) [15] catalysed by copper salts and ruthenium complexes[16]. The most striking features of considering 1,2,3-triazoles as drug candidate[17-20], schematically shown in Figure 2, are (i) formation of hydrogen bonds for improving solubility and ability to interact with biomolecular targets (hydrogen bond acceptor sites- N_2 and N_3 centers, and hydrogen bond donor site - C_5 center); (ii) can act as intercalating agent via π–π stacking interactions; (iii) can participate in C-H hydrogen bonding

interactions; (iv) can substitute for an amide linkage without altering the binding pose; (v) are highly stable to metabolic degradation as compared to other compounds containing three adjacent nitrogen (*N*) atoms can be metabolically inert (1,2,4-triazoles) [21-23].

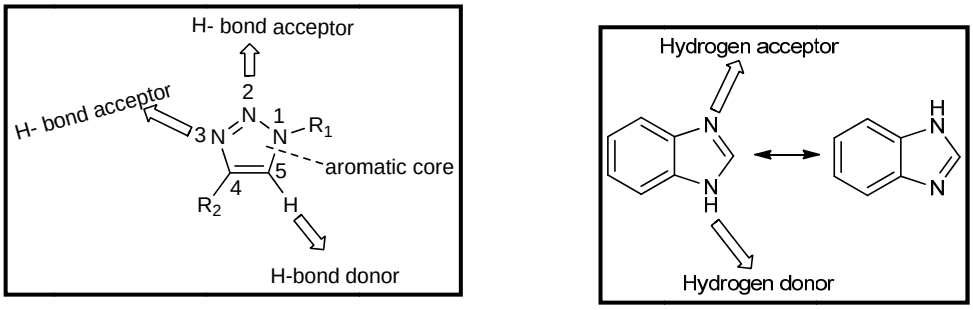

Figure 2.2.2: Donor acceptor property of the triazole and benzimidazole

On the other hand, benzimidazole, a heterocyclic aromatic organic compound, is an important pharmacophore [24-25] and a privileged structure in medicinal chemistry, especially for anti-cancer activity[26-30]. It is observed that, hydrogen bond donor and acceptor site i.e N_1 and N_3 in the benzimidazole molecule (*Figure 2.2.2*), which exhibits tautomerism,[31] play a critical role in binding to the biological targets.

2.2.2 Our Strategy:

Keeping above literature survey in mind, our efforts were focused on the synthesis of benzimidazole and triazole adducts (*Figure 2.2.3*).

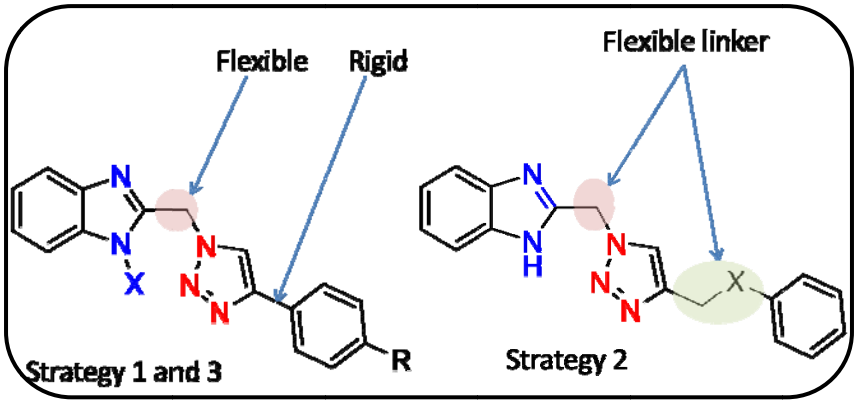

Figure 2.2.3: Our strategy for the synthesis

2.2.3 Results and Discussion:

A. Synthesis:

Our efforts were focused on synthesizing new triazole linked benzimidazole molecules and checking its anti proliferative activity, keeping PAINS (Pan Assay Interference Compounds) [32] structure in mind. Most PAINS function as reactive chemicals rather than discriminating drugs. The designing of compounds, see *Figure 2.2.3*, was driven by three basic principles: (i) inserting flexible linker between benzimidazole and triazole pharmacophore: use of methylene bridge; (ii) Derivatizing triazole at C_4 position with flexible group: CH_2-O/ CH_2-N; and (iii) increasing solubility and/or bioavailability by derivatizing benzimidazole pharmacophore: N-ethylation. Interestingly, this design strategy forced us to use three different synthetic routes, for synthesizing eleven new compounds, as discussed below.

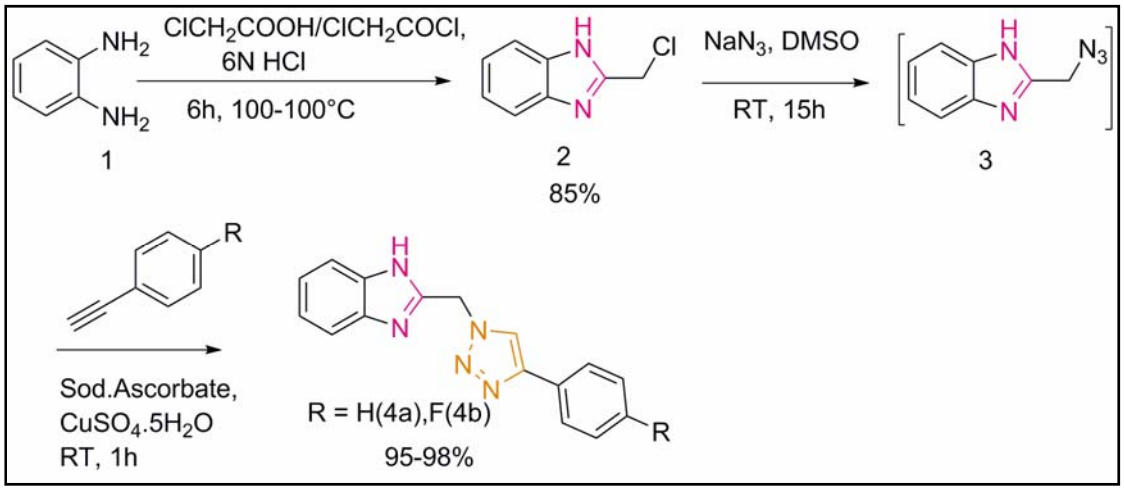

Scheme 2.2.1: Synthesis of 2-((4-phenyl-1*H*-1,2,3-triazol-1-yl)methyl)-1*H*-benzo[*d*]imidazole (4a and 4b)

Strategy 1: 2-Chloro benzimidazole, **2**, was synthesized by reacting *o*-phenylenediamine with two different reagents 1) 2-chloro acetyl chloride and 2) 2-chloro acetic acid[33-35](Scheme 1). Both these reactions gave comparable yield. **2** was transformed into 2-(azidomethyl)-1*H*-benzo[*d*]imidazole, **3**, using sodium azide in dry DMSO [33]. The reaction condition, especially solvent selection, was optimized to get the best yields. In accordance with theory, DMSO, aprotic polar solvent proved choice of solvent, since it favors conversion of **2** to **3**, S_N2 reaction, as well as 1,3-dipolar cycloaddition. Without isolating compound **3**, *in situ,* alkyne derivative was added to obtain final compound **4**.

Fluorine is known for its pharmacophorical activity therefore its addition on triazole nucleus was planned and carried out similar to *Scheme 2.2.1*.

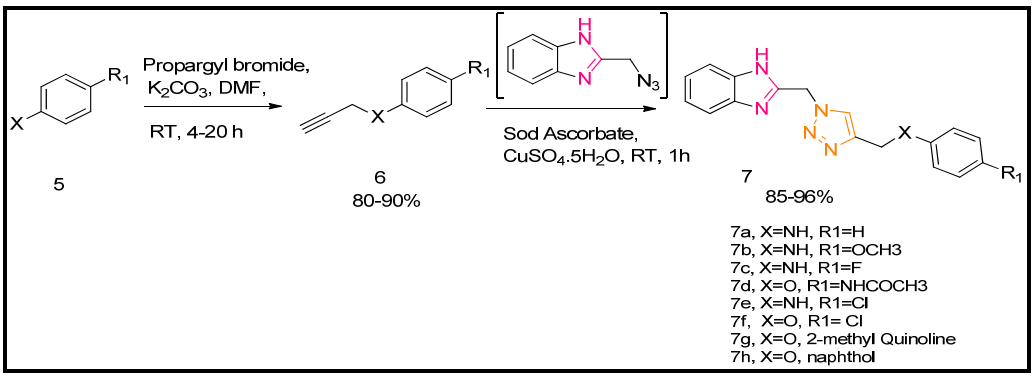

Scheme 2.2.2: Synthesis of *N*-((1-((1*H*-benzo[*d*]imidazol-2-yl)methyl)-1*H*-1,2,3-triazol-4-yl)methyl)aniline and its derivatives

Strategy 2: Our aim in this strategy is to derivatise triazole ring at C_4 position using the N-(prop-2-yn-1-yl) aniline/phenolic groups. Substituted phenol and aniline derivatives were allowed to react with propargyl bromide in the presence of K_2CO_3base and DMF as solvent [36-37] (*Scheme 2.2.2*).Terminal alkynes is known to provide an efficient method for the synthesis of triazole [38]. Krim and co-workers [39] reported (Prop-2-ynyloxy) benzene as an intermediate, for the synthesis of triazole via Huigen dipolar cycloaddition method using click chemistry, which is followed in the present study.

To extend our study, we thought of using paracetamol as an additional pharmacophore. We synthesized, **7d**, where phenolic group of paracetomol was attached at C_4 position of triazole.

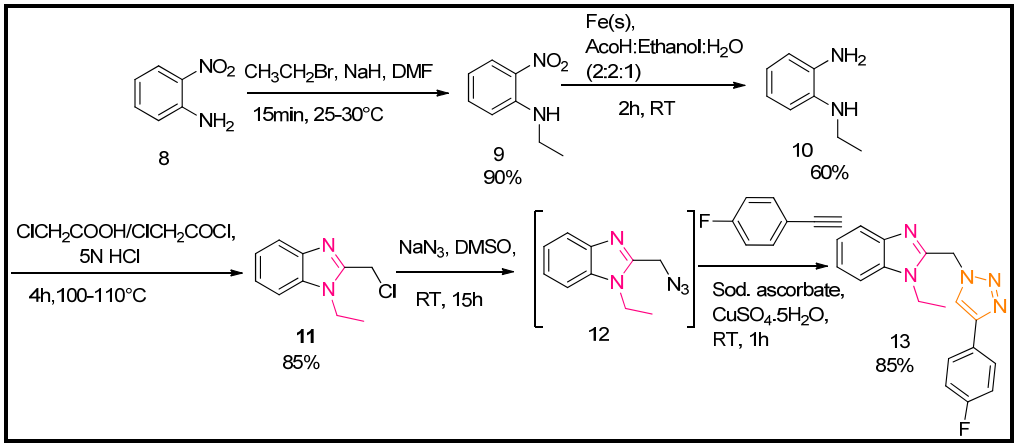

Scheme 2.2.3: Synthesis of 1-ethyl-2-((4-(4-fluorophenyl)-1*H*-1,2,3-triazol-1-yl)methyl)-1*H*-benzo[*d*]imidazole

Strategy 3: Bioavailability and solubility of benzimidazole can be increased by inserting ethyl or methyl groups at N_3 position. Therefore, we carried out direct methlylation/ethylation of compound **2**. But all the attempts resulted in difficult to characterize polymeric product. Hence, N-ethylation is carried out initially; on *o*-nitro aniline (*Scheme 2.2.3*). *o*-Nitro aniline was converted to N-ethyl derivative using ethyl iodide as per the reported procedure[40]. Further, compound **9** was reduced to compound **10** using iron powder [41]. All the further steps were followed according to *Scheme 2.2.1*.

All column purified eleven new molecules with triazole linked benzimidazole pharamacophore, were characterized by standard spectroscopic techniques. Literature showed hydrogen bonding ability of C_3 proton in triazole molecule [21]. Interestingly, we observed dramatic upfield shift of 0.63 ppm for the same proton in ^{1}H NMR spectra for **13** and not in **4b**, as shown in Figure 5. This implies that intramolecular hydrogen bonding in **13** forces rotation of benzimidazole molecule, a fluxional rotation, for fixing geometry. The NMR result for **13** is paving our path to understand the molecular aspect of this compound (role of ethyl group). Constant efforts are being put in this direction to understand this phenomenon which will be published later.

B. Characterization:

Spectral Analysis

All the new compounds were characterized by FT-IR, ^{1}H NMR, ^{13}C NMR and HR-MS. Spectra analyses were consistent with the assigned structures. Details of each structure with its characterization are presented in the experimental section.

Single crystal XRD analysis

The crystallographic data, details of data collection and some important features of the refinement for compound **7g** is given in *Table 2.2.1*. Crystals of suitable size of the **7g** were obtained by slow evaporation of solvent. The data were collected on Oxford X-CALIBUR-S diffractometer with MoKα radiation (λ = 0.71073) at 293K. The data interpretations were processed with CrysAlis Pro, Agilent Technologies, Version 1.171.35.19. An absorption correction based on multi-scan method was applied. All

structures were solved by direct methods and refined by the full matrix least-square based on F^2 technique using SHELXL-97 program package. All calculations were carried out using WinGX system Ver-1.64 [43-45].

We present a method in this chapter for selectively controlling polymorph growth utilizing co crystallization methodology. By introducing a second component into the crystallization environment in addition to the solvent, it is possible to grow different polymorphs. The concept here is, using different templates one can grow crystals in different space groups. Such type of polymorphism is termed as conformational polymorphism. The two templates which are used here are nickel nitrate (coformer 1) and zinc nitrate (coformer 2).

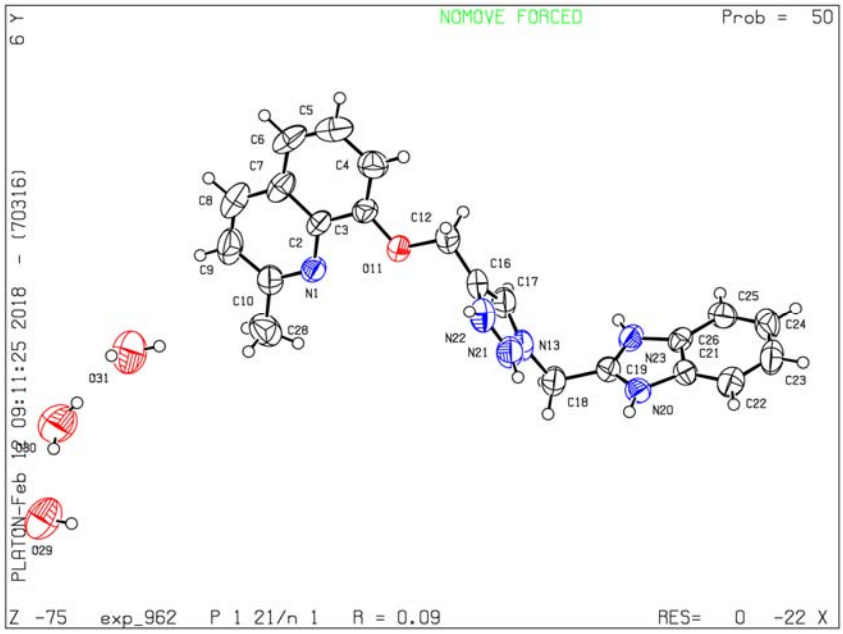

Figure 2.2.4: Molecular view of compound 7g (Structure A) having thermal ellipsoid are shown with 50% probability

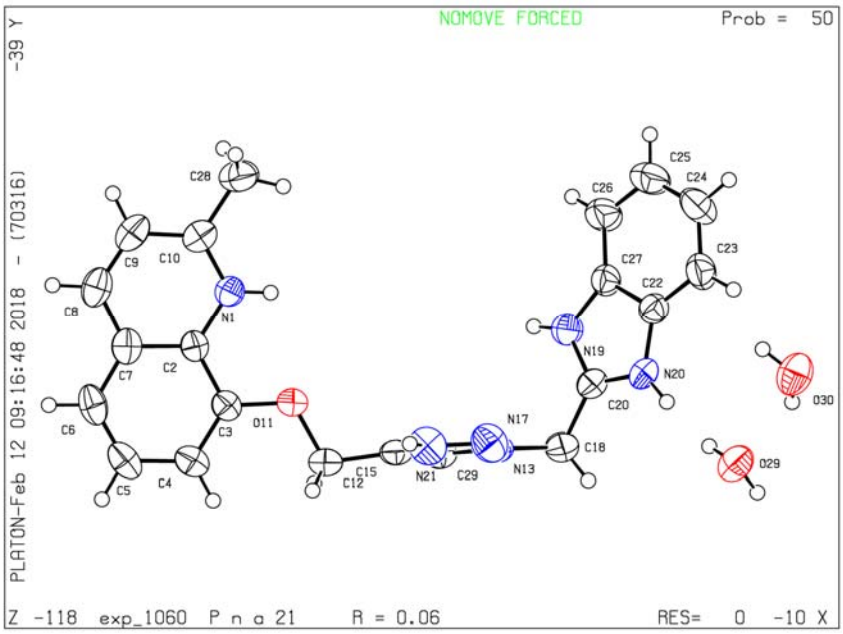

Figure 2.2.5: Molecular view of compound 7g (Structure B) having thermal ellipsoid are shown with 50% probability

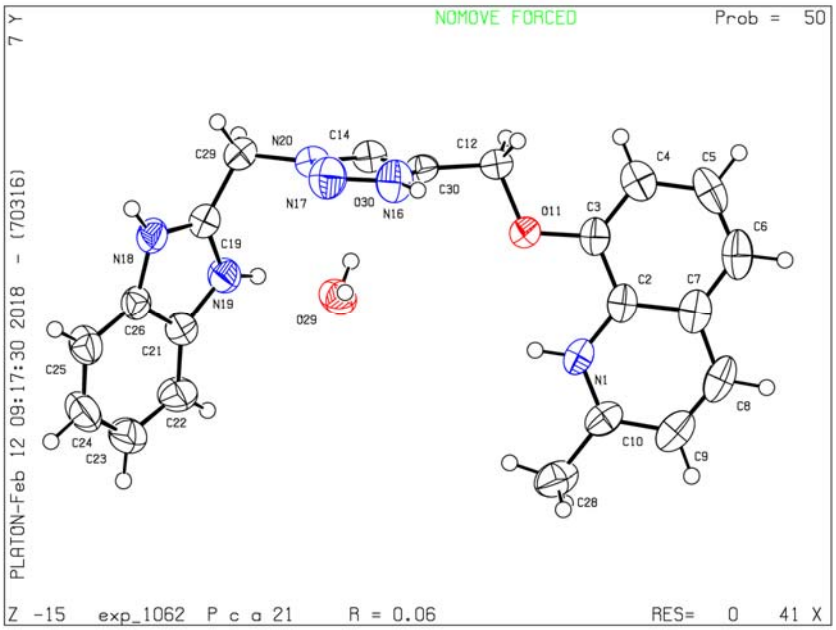

Figure 2.2.6: Molecular view of compound 7g (Structure C) having thermal ellipsoid are shown with 50% probability

Table 2.2.1: Crystallographic data and structure refinements for 7g (Structure A, B and C)

	Structure A	Structure B	Structure C
CCDC	1828841	1828842	1828853
Crystal Description	Needle	Needle	Needle
Empirical formula	$C_{21}H_{27}N_6O_4$	$C_{21}H_{25}N_6O_3$	$C_{21}H_{25}N_6O_3$
Formula weight	427.49	409.47	409.47
Temperature/K	293	293	293
Crystal system	Orthorhombic	Orthorhombic	Orthorhombic
Space group	$P2_1/n$	$Pna2_1$	$Pca2_1$
a/Å	9.083(3)	13.3708(12)	31.817(5)
b/Å	12.928(4)	31.766(3)	4.7536(7)
c/Å	18.593(6)	4.7835(4)	13.343(2)
α/°	90	90	90
β/°	90	90	90
γ/°	90	90	90
Volume/Å^3	2183.4(11)	2031.7(3)	2018.1(6)
Z	4	4	4
ρ_{calc}g/cm^3	1.3003	1.3386	1.3476
μ/mm^{-1}	0.093	0.093	0.094
F(000)	908.4	868.4	868.4
Radiation	Mo Kα (λ = 0.71073)	Mo Kα (λ = 0.71073)	Mo Kα (λ = 0.71073)
2Θ range for data collection/°	6.3 to 58.72	7.1 to 57.76	7.68 to 57.42
Index ranges	$-12 \le h \le 11$, $-16 \le k \le 16$, $-18 \le l \le 24$	$-17 \le h \le 17$, $-40 \le k \le 42$, $-6 \le l \le 5$	$-40 \le h \le 40$, $-6 \le k \le 6$, $-16 \le l \le 15$
Reflections collected	6999	15285	6660
Independent reflections	4020 [R_{int} = 0.0729, R_{sigma} = 0.0835]	4540 [R_{int} = 0.0402, R_{sigma} = 0.0468]	3710 [R_{int} = 0.0318, R_{sigma} = 0.0625]
Data/restraints/parameters	4020/0/289	4540/0/277	3710/0/277
Goodness-of-fit on F^2	1.077	0.933	0.862
Final R indexes [I>=2σ (I)]	R_1 = 0.0852, wR_2 = 0.2323	R_1 = 0.0569, wR_2 = 0.1457	R_1 = 0.0568, wR_2 = 0.1434
Final R indexes [all data]	R_1 = 0.1410, wR_2 = 0.3086	R_1 = 0.0835, wR_2 = 0.1667	R_1 = 0.0992, wR_2 = 0.1797

NH−O and OH−N type hydrogen bonds are important in many fields of chemistry and biology. The hydrogen-bonded clusters of benzimidazole and triazole are of interest as model systems due to several facts. First of all the water molecule(s) are able to attach at different positions of the solute. Second, even small water clusters may form cyclic structures, due to the close vicinity of proton-donating and proton-accepting groups in the solute. Both triazole and benzimidazole contain proton-donating and proton-accepting functional groups, as well as an aromatic π-system. All three regions are potential sites for the binding of one or more water molecules.

C. Antiproliferative Assay:

NCI 60 cell line screen:

All the molecules were initially screened for anti-proliferative activity *in silico* by National Cancer Institute (NCI), USA. Compound **4b**, **7d, 7e** and **13** were further selected for actual screening anti-proliferative activity at 10µM concentration. *Figure 2.2.7* shows comparative study of compound **4b**, **7d, 7e** and **13** on selected cell lines SR(Leukamia), SNB-75(CNS), A498(kidney), UO-31(kidney). **7e** shows 40% growth inhibition in UO-31 renal cancer cell line (mean growth inhibition) at 10μM concentration. Although this activity is moderate, the structure of **7e** can help in developing or designing novel drug candidates.

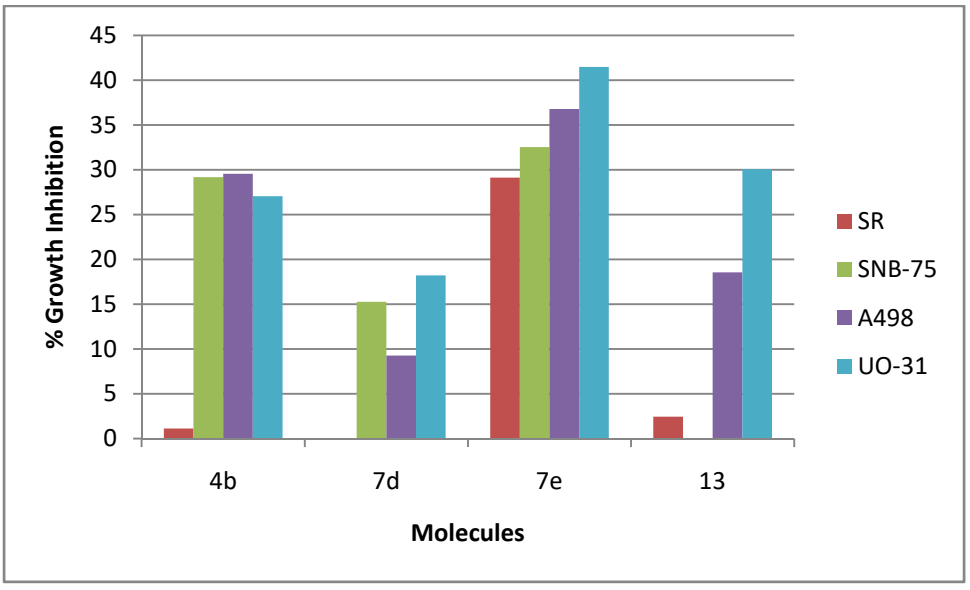

Figure 2.2.7: % Growth Inhibition on selected cell lines at 10µM concentration

2.2.4 Conclusion:

In conclusion, *in situ* click reaction can conjoin two pharmacophores triazole with benzimidazole in a faster and efficient method. The reaction proceeds without isolation of azide intermediate without compromising in good yields. Commercially available *o*-phenylenediamine was used during the synthesis of eleven novel derivatives of *N*-((1-((1*H*-benzo[*d*]imidazol-2-yl)methyl)-1*H*-1,2,3-triazol-4-yl)methyl)aniline compounds. The *in-vitro* anticancer activity of selected compounds using NCI-60 human cell line screening program revealed that most of the title compounds showed moderate bioactivity at 10μM concentration. Flexible structured molecule, **7e**, *N*-((1-((1*H*-benzo[*d*]imidazol-2-yl)methyl)-1*H*-1,2,3-triazol-4-yl)methyl)-4-chloroaniline showed a 40% growth inhibition in human renal cancer cell line (UO-31) which needs further investigation. Crystal of **7g** was developed and solved. Conformational polymorphism was also studied. Crystal structure revealed that very interesting hydrogen bonding between NH-O and OH-N is observed.

2.2.5 Experimental

2.2.5.1 Materials and Methods:

All the compounds were purified using column chromatography (2000- 400 mesh silica) before characterization. TLC analysis was done using pre-coated silica on aluminum sheets. Melting points were recorded in Thiele's tube using paraffin oil and are uncorrected. FT-IR (KBr pellets) spectra were recorded in the 4000-400 cm^{-1} range using a Perkin-Elmer FT-IR spectrometer. The NMR spectra were obtained on a Bruker AV-III 400 MHz spectrometer using TMS as an internal standard. The chemical shifts were reported in parts per million (ppm), coupling constants (*J*) were expressed in hertz (Hz) and signals were described as singlet (s), doublet(d), triplet(t), broad (b) as well as multiplet (m). The microanalysis was carried out using a Perkin-Elmer IA 2400 series elemental analyzer. The mass spectra were recorded on Thermo scientific DSQ-II. All chemicals and solvents were of commercial grade and were used without further purification. Single crystal data was collected with Xcalibur, EoS, Gemini.

2.2.5.2 Synthesis of compounds:

Synthesis of 2-(chloromethyl)-1*H*-benzo[*d*]imidazole 2:

The title compound was synthesized according to the literature procedure [36-38]. Commercially available o-Phenylenediamine (5.4 g), chloroacetic acid (7.1 g) and 4N hydrochloric acid (50 ml) were heated under reflux for 45 minutes. The mixture was allowed to stand overnight, filtered, diluted with 100 ml. of water, cooled and carefully neutralized with solid bicarbonate. The yellow solid was filtered, washed well with cold water and dried over vacuum (*Scheme 2.2.1*).

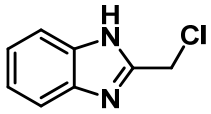 2 $C_8H_7N_2Cl$ (166.5)	White solid. Yield: 80%.

General method for synthesis of 2-((4-phenyl-1*H*-1,2,3-triazol-1-yl)methyl)-1*H*-benzo[*d*]imidazole 4a :

Synthesis of compound **4a** was done in single step. A mixture of compound **2** (0.500g, 3mmol) and sodium azide (0.195g, 3mmol) was charged in DMSO (5mL) at room temperature for 15-16hrs [22]. Reaction completion was monitored using thin layer chromatography (TLC, EtOAc:PET, 7:3). After *in situ* formation of compound **3**, the respective alkyne derivative (0.321g, 3.14mmol) was added and mixture of $CuSO_4.5H_2O$ (0.112g, 0.4mmol) and sodium ascorbate (0.267g, 1.35mmol) in water (0.5mL) was added as shown in Scheme 1 [25-26]. The reaction was stirred at room temperature and its completion was monitored by TLC. Compound **4a** was then isolated and further purified by column chromatography using various concentrations of ethyl acetate and petroleum ether to afford the desired compound **4a** as a white solid.

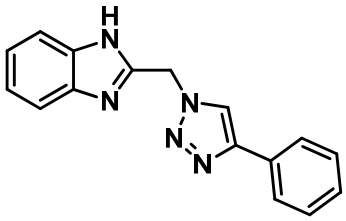 4a $C_{16}H_{13}N_5$ (298)	White solid. **Yield:** 78%; **M.P:** 198-200°C ; **^{1}H NMR(400MHz,DMSO-d6) δ**: 5.93(2H, s,), 7.19(2H, m) , 7.35(1H, m), 7.45(2H, t, *J*=8Hz), 7.50 (1H, d, *J*=7.6Hz), 7.61(1H, d, *J*=7.6Hz), 7.89(2H, d, *J*=8Hz), 8.71 (1H, s), 12.69(1H, s) ppm **^{13}C NMR (100MHz, DMSO-d6) δ**: 52.7, 127.4, 130.4, 133.3, 134.2, 135.7, 151.8, 153.5 ppm **FT-IR (KBr) *ɣ:*** 690.52(Mono substitution), 738.74(o-substitution), 1089.78(C-N stretch), 1276.88(C-N stretch), 1442.75(N=N), 1587.42(C=N), 3095.75(N-H stretch) cm^{-1} **HR-MS (ESI+) [$C_{16}H_{13}N_5$+Na]**: Calculated-298.1069, Observed-298.1064 (*Figure 2.2.8, 2.2.19, 2.2.30, 2.2.41*)

2-((4-(4-fluorophenyl)-1*H*-1,2,3-triazol-1-yl)methyl)-1*H*-benzo[*d*]imidazole 4b(Scheme1):

Synthesis of compound **4b** was done in single step. A mixture of compound **2** (0.500g, 3mmol) and sodium azide (0.195g, 3mmol) was charged in DMSO at room temperature for 15-16hrs [33]. Reaction completion was monitored using TLC. After *in situ* formation of compound 3, the respective alkyne derivative (0.321g, 3.14mmol) was added and mixture of $CuSO_4.5H_2O$ (0.112g, 0.4mmol) and sodium ascorbate (0.267g, 1.35mmol) in water was added as shown in Scheme 1. The reaction was stirred at room temperature and its completion of reaction was monitored by TLC. Compound **4b** was then isolated and further purified by column chromatography.

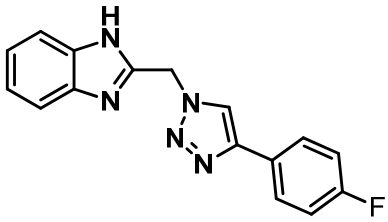 4b $C_{16}H_{15}FN_5$ (316)	Off-white solid. **Yield**: >98% **^{1}H NMR (400 MHz, DMSO-d6) δ**: 5.92(2H, s), 7.20(2H, m), 7.31(2H, t, *J*=9.2),7.55(2H, s), 7.92(2H, m), 8.71(1H, s) ppm **^{13}C NMR (100MHz, DMSO-d6) δ**: 48.1, 116.2, 116.4, 122.6, 127.7, 127.7, 146.2, 148.8 ppm **FT-IR (KBr) γ**: 736.81(o-substitution), 829.39(p-substitution), 1093.64(C-N stretch), 1224.80(C-N stretch), 1498.69(N=N), 1564.27(C=N), 3105.39(N-H) cm^{-1} **HR-MS (ESI+) [$C_{16}H_{12}FN_5$+Na]**: Calculated-316.0974, Observed-316.0977 (*Figure 2.2.9, 2.2.20, 2.2.31, 2.2.42*)

Synthesis of N-(prop-2-yn-1-yl) aniline 6a (Scheme 2):

The title compound was synthesized according to the literature procedure [36-37]. Starting with aniline derivative (0.500g, 3.9 mmol), potassium carbonate was charged. Now slowly propargyl bromide (0.4g, 3.9 mmol) was slowly charged in it (scheme 3). The compound was then isolated and further purified by column chromatography to afford desired compound **6a** as a white to pale yellow solid.

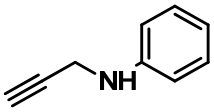 6a C_9H_9N (131)	White solid. **Yield**: 80-90%. **Melting point**: 158-160°C (literature melting point: 160-161°C)

Using the above procedure of compound **6a** rest of its derivatives was synthesized.

***N*-((1-((1*H*-benzo[*d*]imidazol-2-yl)methyl)-1*H*-1,2,3-triazol-4-yl)methyl)aniline 7a:**

The title compound was synthesized as per the procedure reported for compound **4a** (with respective alkyne derivative **6a**) and isolated as a brown gummy mass which solidifies after 15-20 h.

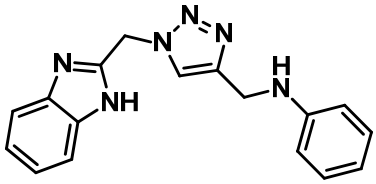 **7a** $C_{17}H_{16}N_6$ (327)	Brown glassy solid. **Yield**: >98% **^{1}H NMR (400 MHz, DMSO-d6) δ**: 4.28(2H, d, *J*=5.6), 5.82(2H, s), 6.06(1H, t), 6.53(1H, t, *J*= 7.6), 6.64(2H, d, *J*=8.4), 7.06(2H, t, *J*=8), 7.19(2H, t, *J*=6.4), 7.50(1H, d, *J*=7.6), 7.59(1H, d, *J*=7.6), 8.07(1H, s), 12.65(1H, s) ppm **^{13}C NMR (100MHz, DMSO-d6) δ**: 38.9, 477, 112.1, 114.2, 119.4, 119.8, 122.1, 123.2, 123.9, 129.0, 134.8, 143.3, 146.1, 147.7, 148.8 ppm **FT-IR (KBr) γ**: 650.03, 688.61 (mono substitution), 744.55(o-substitution), 804.34(para substitution, 1024.24(C-H stretch), 1224.84(C-N stretch), 1413.82(N=N), 1504.53(C-N stretch),1604.83, 1732.13(C=N), 3053.42(N-H) cm^{-1} **HR-MS (ESI+) [$C_{17}H_{16}N_6$+Na]**: Calculated-327.1334, Observed-327.1337. (*Figure 2.2.11, 2.2.21, 2.2.33, 2.2.43*)

***N*-((1-((1*H*-benzo[*d*]imidazol-2-yl)methyl)-1*H*-1,2,3-triazol-4-yl)methyl)-4-methoxyaniline 7b:**

The title compound was synthesized based as per the procedure reported for compound **4a** and isolated as yellow gummy mass which solidifies after 15-20 h.

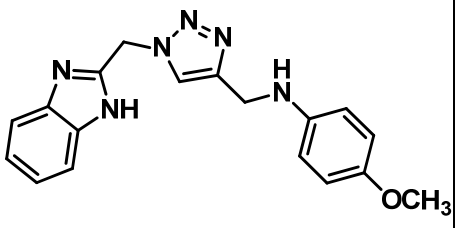 **7b** $C_{18}H_{18}N_6O$ (357)	Brown glassy solid. **Yield**: >98% **^{1}H NMR (400 MHz, DMSO-d6) δ**: 3.62(3H, s), 4.25(2H, s), 5.83(2H, s), 6.17(2H, d, *J*=3.2), 6.72(2H, d, *J*=4.4), 7.19(2H, b), 7.49(1H, d, *J*=7.6), 7.59(1H, d, *J*=7.6), 8.07(1H, s), 12.67(1H, s) ppm **^{13}C NMR (100MHz, DMSO-d6) δ**: 47.7, 55.7, 112.1, 113.9, 114.9, 119.4, 122.1, 123.1, 123.8, 143.0, 146.8, 148.8, 151.4 ppm **FT-IR (KBr) γ**: 752.26 (o-substitution), 823.63, 1022.31, 1039.67, 1180.47 (C-O stretch), 1251.84, 1274.99 (C-N stretch), 1506.46(C-N stretch), 2829.67(C-H stretch), 3093.92(N-H) cm^{-1} **HR-MS (ESI+) [$C_{18}H_{18}N_6O$+Na]**: Calculated-357.1440, Observed-357.1441 (*Figure 2.2.12, 2.2.22, 2.2.34, 2.2.44*)

***N*-((1-((1*H*-benzo[*d*]imidazol-2-yl)methyl)-1*H*-1,2,3-triazol-4-yl)methyl)-4-fluoroaniline 7c:**

The title compound was synthesized as per the procedure reported for compound **4a** and isolated as yellow gummy mass which solidifies after 15-20 h.

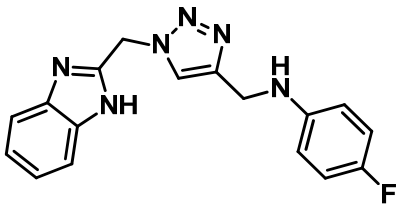 **7c** $C_{17}H_{15}N_6F$ (345)	Brown glassy solid. **Yield**: >98% **^{1}H NMR (400 MHz, DMSO-d6) δ** : 4.27(2H, s), 5.83(2H, s), 6.01(1H, s), 6.63(2H, m), 6.91(2H, m), 7.20(2H, s), 7.54(2H, s), 8.08(1H, s), 12.66(1H, s) ppm **^{13}C NMR (100MHz, DMSO-d6) δ**: 47.7, 113.5, 113.6, 115.6, 115.8, 123.9, 145.5, 146.4, 148.8, 153.8, 156.1 ppm **FT-IR (KBr) γ**: 740.67(o-substitution), 813.96(p-substitution), 1220.94(C-Nstretch), 1442.75(N=N), 1508.33(-C=N), 3099.61(N-H) cm^{-1} **HR-MS (ESI+) [$C_{17}H_{15}N_6F$+Na]**: Calculated-345.1240, Observed-345.1236 (*Figure 2.2.13, 2.2.23, 2.2.35, 2.2.45*)

***N*-(4-((1-((1*H*-benzo[*d*]imidazol-2-yl)methyl)-1*H*-1,2,3-triazol-4-yl)methoxy)phenyl)acetamide 7d:**

The title compound was synthesized as per the procedure reported for compound **4a** and isolated as yellow gummy mass which solidifies after 15-20 h.

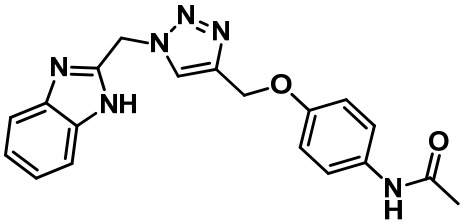 **7d** $C_{19}H_{18}N_6O_2$ (385)	Brown glassy solid. **Yield**: >98% **^{1}H NMR (400 MHz, DMSO-d6) δ**: 1.99(3H, s), 5.15 (2H, s), 5.95(2H, s), 6.97(2H, d, *J*=12), 7.18(2H, s), 7.50 (4H, m), 8.40 (1H, s), 10.00 (1H,s), 12.96(1H, s) ppm **^{13}C NMR (100MHz, DMSO-d6) δ**: 24.3, 61.5, 115.0, 120.9, 125.8, 133.4, 143.4, 148.8, 154.2, 168.3 ppm **FT-IR (KBr) γ**: 522.71(aromatic ring), 744.52(o-substitution), 825.53(p-substitution), 1012.63(C-H stretch), 1217.08(N-H stretch), 1413.82(N=N), 1508.33(N-H of acetyl), 1548.84(amide 1), 1658.78(amide 2), 3103.46(N-H), 3282.84(-CONH-) cm^{-1} **HR-MS (ESI+) [$C_{19}H_{18}N_6O_2$+Na]** : Calculated-385.1389, Observed-385.1386 (*Figure 2.2.14, 2.2.24, 2.2.36, 2.2.46*)

***N*-((1-((1*H*-benzo[*d*]imidazol-2-yl)methyl)-1*H*-1,2,3-triazol-4-yl)methyl)-4-chloroaniline 7e:**

The title compound was synthesized as per the procedure reported for compound **4a** and isolated as yellow gummy mass which solidifies after 15-20 h.

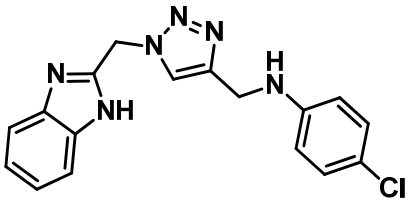 **7e** $C_{17}H_{15}ClN_6$ (361)	Brown glassy solid. **Yield**: >98% **^{1}H NMR (400 MHz, DMSO-d6) δ**: 4.29(2H, d, J=6), 5.83(2H, s), 6.29(1H, t, J=6), 6.65(2H, d, J=8.8), 7.08(2H, d, J=8.8), 7.19(2H, b), 7.53(2H, b), 8.08(1H,s), 12.68 (1H, s) ppm **^{13}C NMR (100MHz, DMSO-d6) δ**: 38.9, 47.7, 114.2, 119.8, 123.9, 128.9, 146.1, 147.7, 148.8 ppm **FT-IR (KBr) γ**: 628.79(C-Cl stretch), 738.74(o-substitution), 812.03(p-substitution), 1060.85(C-H stretch), 1224.80(C-N stretch), 1448.54(N=N), 1598.99(C=N), 3045.60(N-H) cm^{-1} **HR-MS (ESI+) [$C_{17}H_{15}ClN_6$+Na]**: Calculated-361.0944, Observed-361.0948 (*Figure 2.2.15, 2.2.25, 2.2.37, 2.2.47*)

2-((4-((4-chlorophenoxy)methyl)-1*H*-1,2,3-triazol-1-yl)methyl)-1*H*-benzo[*d*]imidazole 7f :

The title compound was synthesized as per the procedure reported for compound **4a** and isolated as plae yellow gummy mass which solidifies after 15-20 h.

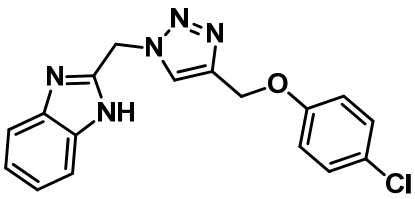 **7f** $C_{17}H_{14}ClN_5O$ (362)	Brown glassy solid. **Yield**: >98% **^{1}H NMR (400 MHz, DMSO-d6) δ**: 5.16(2H, s), 5.89(2H, s), 7.07(2H, d, J=12.4), 7.19(2H, t, J=10.4), 7.33(2H, d, J=12.8), 7.51(1H, d, J=7.2), 7.59(1H, d, J=7.6), 8.37(1H, s), 12.70(1H, s) ppm **^{13}C NMR (100MHz, DMSO-d6) δ**: 47.8, 61.7, 116.9, 125.0, 126.0, 129.7, 143.1, 148.8, 157.3 ppm **FT-IR (KBr) γ**: 740.67(o-substitution), 817.82(p-substitution), 997.20(C-O stretch), 1060.85(C-Cl stretch), 1226.73(C-N), 1440.83(N=N), 1489.05(C=N), 2956.87(C-H stretch), 3097.68(N-H stretch) cm^{-1} **HR-MS (ESI+) [$C_{17}H_{14}ClN_5O$+Na]**: Calculated-362.0785, Observed-362.0784 (*Figure 2.2.16, 2.2.26, 2.2.38, 2.2.48*)

8-((1-((1*H*-benzo[*d*]imidazol-2-yl)methyl)-1*H*-1,2,3-triazol-4-yl)methoxy)-2-methylquinoline 7g:

The title compound was synthesized as per the procedure reported for compound **4a** and isolated as brown gummy mass which solidifies after 15-20 h.

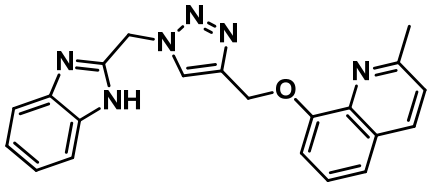 **7g** $C_{21}H_{18}N_6O$ (393)	Brown glassy solid. **Yield**: >98% **^{1}H NMR (400 MHz, DMSO-d6) δ**: 2.61(3H, s), 5.37(2H, s), 5.92(2H, s), 7.17(2H, t, *J*=9.6), 7.42(4H,m), 7.52(1H, d, *J*=7.6), 7.62(1H, d, *J*=7.6), 8.19(1H, d, *J*=8.4), 8.45(1H, s), 12.72(1H, s) ppm **^{13}C NMR (100MHz, DMSO-d6) δ**: 25.4, 47.8, 62.0, 110.6, 112.0, 119.4, 120.3, 122.1, 122.9, 123.1, 126.1, 126.2, 127.8, 134.8, 136.5, 139.6, 143.3, 143.4, 148.8, 153.8, 157.8 ppm **FT-IR (KBr) γ**: 736.81(o-substitution), 827.46(p-substitution), 1103.28(C-O, stretch), 1230.58(C-N stretch), 1255.66(C-N stretch), 1440.83(N=N), 1564.27(C=N), 3020.58(N-H stretch) cm^{-1} **HR-MS (ESI+) [$C_{21}H_{18}N_6O$+Na]**: Calculated-393.1440, Observed-393.1439 (*Figure 2.2.17, 2.2.27, 2.2.39, 2.2.49*)

2-((4-((naphthalen-2-yloxy)methyl)-1*H*-1,2,3-triazol-1-yl)methyl)-1*H*-benzo[*d*]imidazole 7h:

The title compound was synthesized as per the procedure reported for compound **4a** and isolated as brown gummy mass which solidifies after 15-20 h.

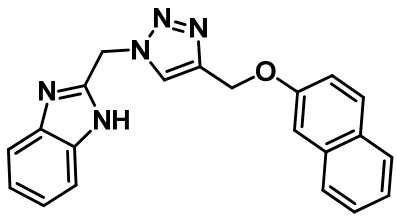 **7h** $C_{21}H_{17}N_5O$ (378)	Brown glassy solid. **Yield**: >98% **^{1}H NMR (400 MHz, DMSO-d6) δ**: 5.29(2H, s), 5.91(2H, s), 7.20 (3H, m), 7.34(1H,s), 7.50 (3H, m), 7.60 (1H, d), 7.82(3H, m), 8.43(1H, s), 12.70(1H, s) ppm **^{13}C NMR (100MHz, DMSO-d6) δ**: 47.8, 61.5, 107.6, 112.1, 119.1, 119.4, 122.1, 123.1, 124.2, 126.0, 126.9, 127.2, 127.9, 129.0, 129.8, 134.6, 143.3, 156.4 ppm **FT-IR (KBr) γ**: 738.74(o-substitution), 1006.84(C-O stretch), 1176.58(C-O stretch), 1213.23(C-N stretch), 1442.75(N=N), 1597.06(C=N), 3178.69(N-H) cm^{-1} **HR-MS (ESI+) [$C_{21}H_{17}N_5O$+Na]**: Calculated-378.1331, Observed-378.1330 (*Figure 2.2.18, 2.2.28, 2.2.40, 2.2.50*)

2-(chloromethyl)-1-ethyl-1*H*-benzo[*d*]imidazole 11 (Scheme 3):

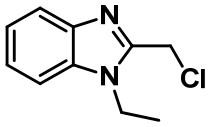

For the synthesis of the title compound, initially **8** was converted to compound **9**, N-ethyl derivative by using the literature procedure [40]. Then compound **9** was further reduced to compound **10** using Fe [41]. Finally the cyclisation step was performed to yield the title compound **11** as a yellow solid. As shown in Scheme 2.

Overall yield: 45%.

1-ethyl-2-((4-(4-fluorophenyl)-1*H*-1,2,3-triazol-1-yl)methyl)-1*H*-benzo[*d*]imidazole 13:

Title compound was synthesized following the same procedure as reported for compound **4a** and isolated as white solid.

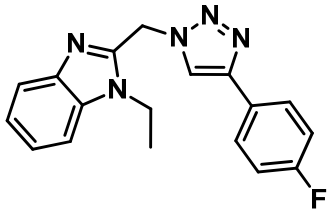 **13** $C_{18}H_{16}FN_5$ (344)	White solid **Yield**: >98% **^{1}H NMR (400 MHz, DMSO-d6) δ**: 1.21(3H, t, *J*=7.2Hz), 4.40(2H, q, *J*=7.2Hz), 6.08(2H, s), 7.22(1H, d, *J*=7.2Hz), 7.28(3H, t, *J*=8.8Hz), 7.62(2H, t, *J*=6.8Hz), 7.93(2H, t, *J*=5.2Hz), 8.08(1H, s) ppm **^{13}C NMR (100MHz, DMSO-d6) δ**: 15.3, 38.8, 46.6, 111, 116.2, 116.4, 119.7, 122.4, 122.6, 123.2, 127.5, 127.5, 127.7, 127.8, 135.2, 142.5, 146.3, 148.3, 161.1, 163.5 ppm **FT-IR (KBr) γ**: 734.88 (o-substitution), 829.39(p-substitution), 1228.66(C-N stretch), 1458.18(N=N), 1496.76(-C=N of benzimidazole), 2972.31(-C-H)cm^{-1} **HR-MS (ESI+) [$C_{18}H_{16}FN_5$+Na]**: Calculated-344.1287, Observed-344.1284 (*Figure 2.2.10, 2.2.29, 2.2.32, 2.2.51*)

2.2.5.3 Methodology for invitro cancer screen:

As mentioned earlier that 60 human cancer cell line screen for selected molecules was performed by NCI. Following procedure is adapted from web page of NCI: www.dtp.nci.nih.gov. The human tumor cell lines of the cancer screening panel are grown in RPMI 1640 medium containing 5% fetal bovine serum and 2 mM L-glutamine. For a typical screening experiment, cells are inoculated into 96 well microtiter plates in 100 µl at plating densities ranging from 5,000 to 40,000 cells/well depending on the doubling time of individual cell lines. After cell inoculation, the microtiter plates are

incubated at 37 °C, 5% CO_2, 95% air and 100% relative humidity for 24 h prior to the addition of experimental drugs (Chaudhary et al., 2011). After 24 h, two plates of each cell line are fixed in situ with TCA, to represent a measurement of the cell population for each cell line at the time of drug addition (Tz). Experimental drugs are solubilized in dimethyl sulfoxide at 400-fold the desired final maximum test concentration and stored frozen prior to use. At the time of drug addition, an aliquot of frozen concentrate is thawed and diluted to twice the desired final maximum test concentration with complete medium containing 50 µg/ml gentamicin. Additional four, 10-fold or ½ log serial dilutions are made to provide a total of five drug concentrations plus control. Aliquots of 100 µl of these different drug dilutions are added to the appropriate microtiter wells already containing 100 µl of medium, resulting in the required final drug concentrations. Following drug addition, the plates are incubated for an additional 48 h at 37 °C, 5% CO_2, 95% air, and 100% relative humidity. For adherent cells, the assay is terminated by the addition of cold TCA. Cells are fixed in situ by the gentle addition of 50 µl of cold 50% (w/v) TCA (final concentration, 10% TCA) and incubated for 60 min at 4°C. The supernatant is discarded, and the plates are washed five times with tap water and air dried. Sulforhodamine B (SRB) solution (100 µl) at 0.4% (w/v) in 1% acetic acid is added to each well, and plates are incubated for 10 min at room temperature. After staining, unbound dye is removed by washing five times with 1% acetic acid and the plates are air dried. Bound stain is subsequently solubilized with 10 mM trizma base, and the absorbance is read on an automated plate reader at a wavelength of 515 nm. For suspension cells, the methodology is the same except that the assay is terminated by fixing settled cells at the bottom of the wells by gently adding 50 µl of 80% TCA. The values are the mean of three independent observed values (www.dtp.nci.nih.gov).

2.2.6 Selected Spectra

^{1}H NMR

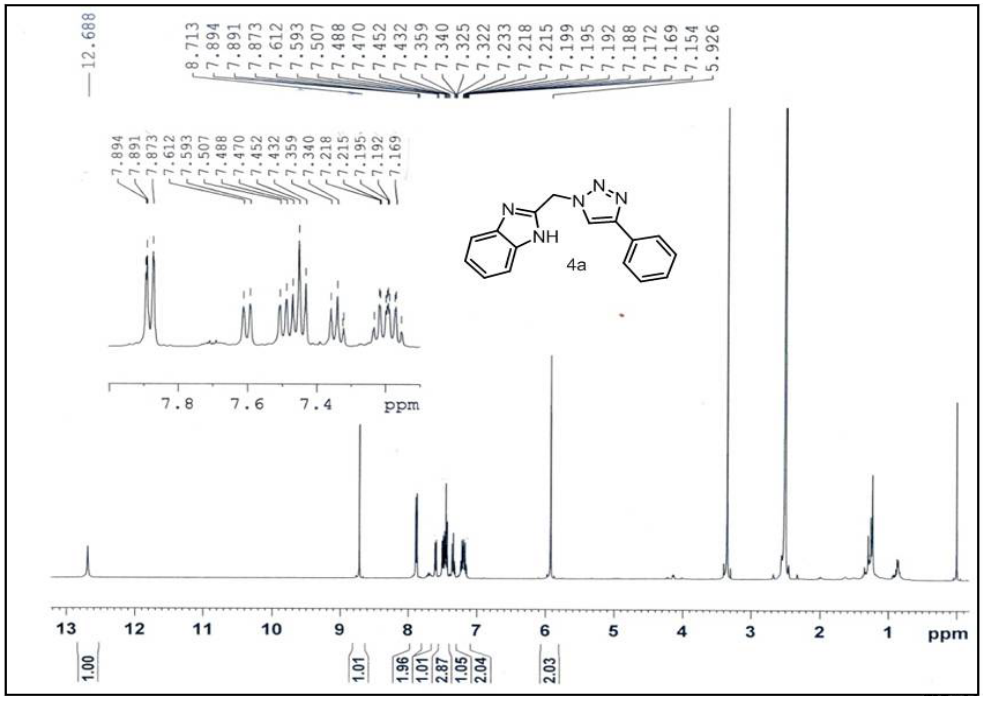

Figure 2.2.8: ^{1}H NMR spectra of 4a

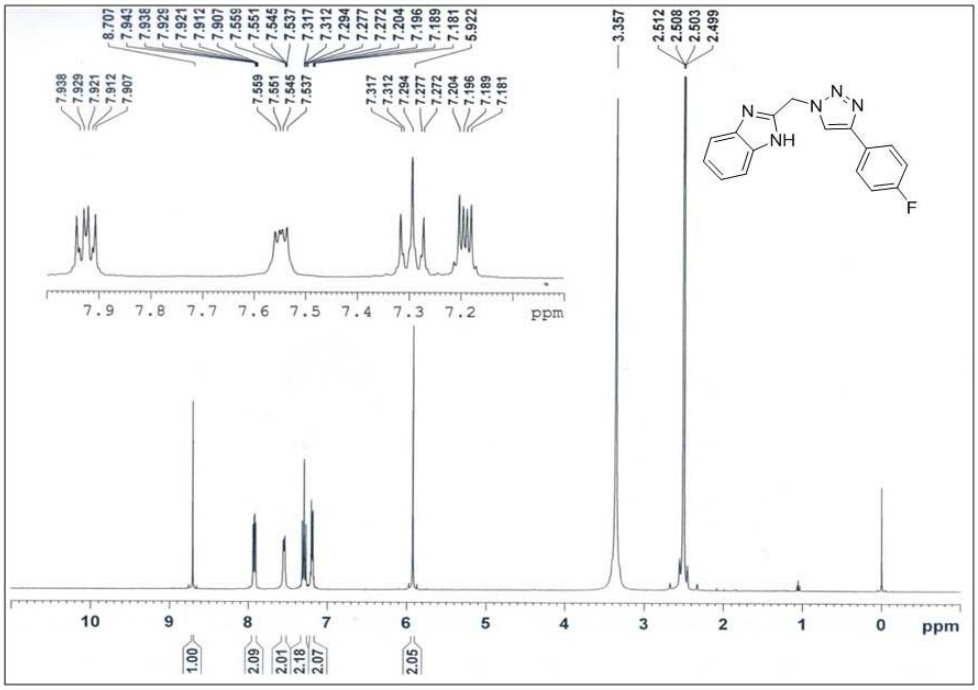

Figure 2.2.9: ^{1}H NMR spectra of 4b

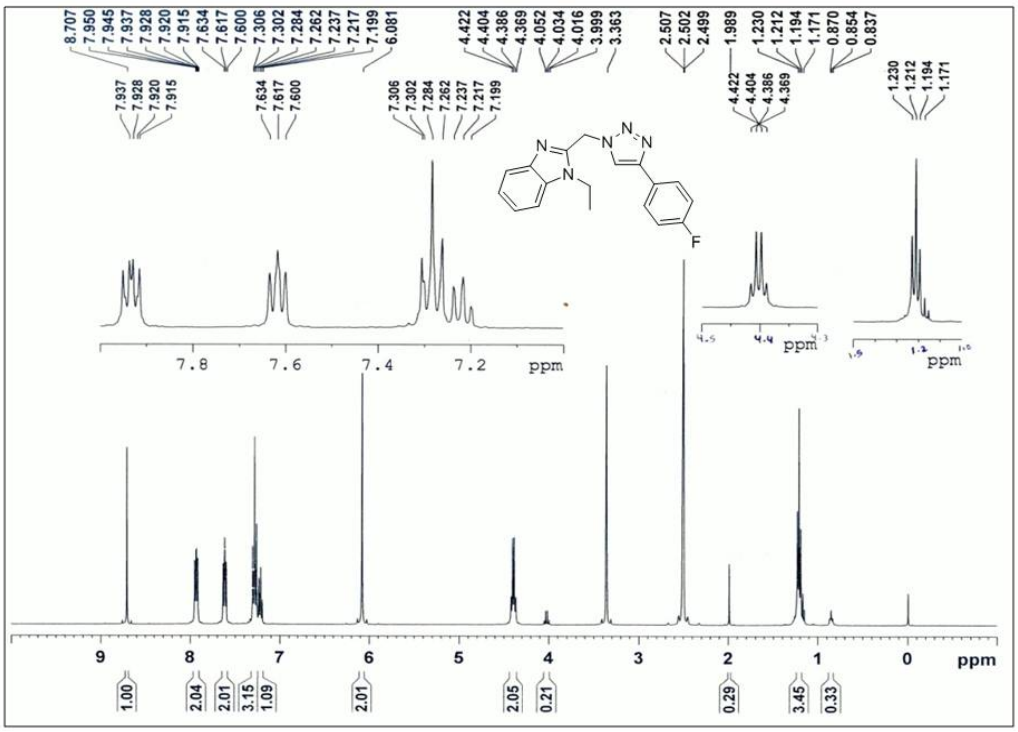

Figure 2.2.10: ^{1}H NMR spectra of 13

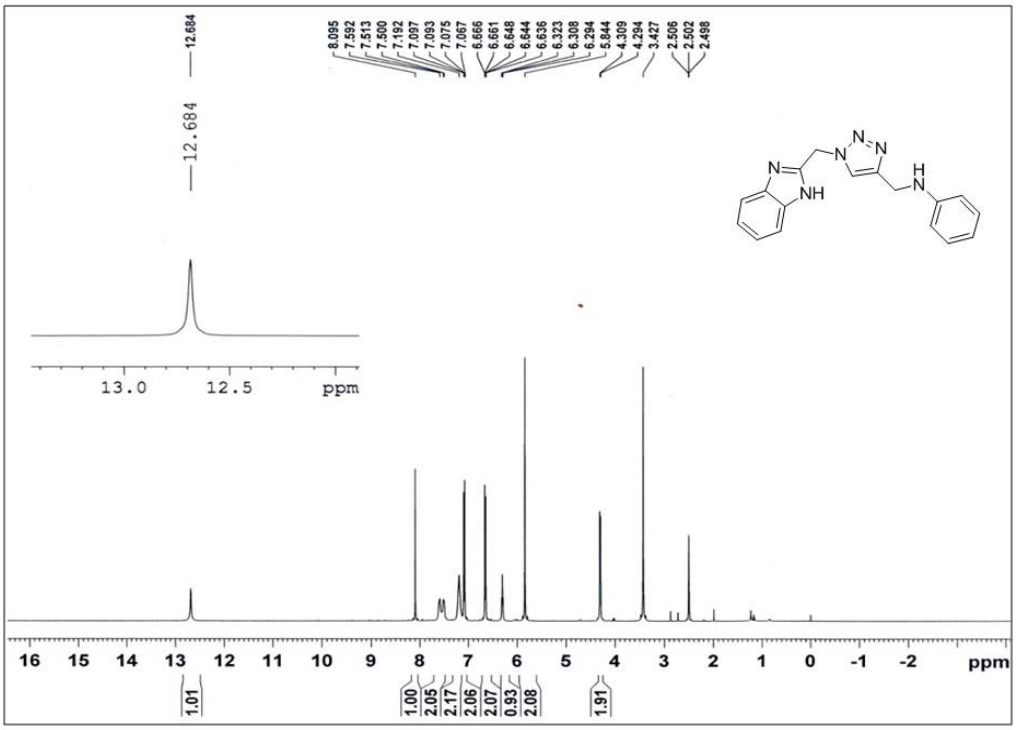

Figure 2.2.11: ^{1}H NMR spectra of 7a

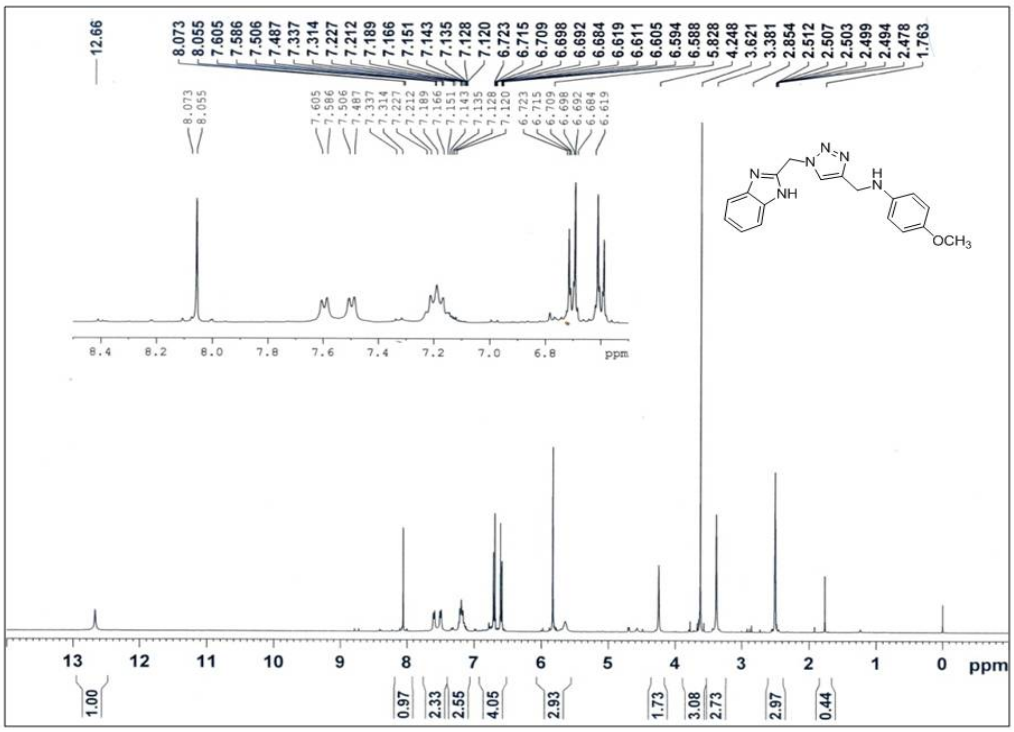

Figure 2.2.12: ^{1}H NMR spectra of 7b

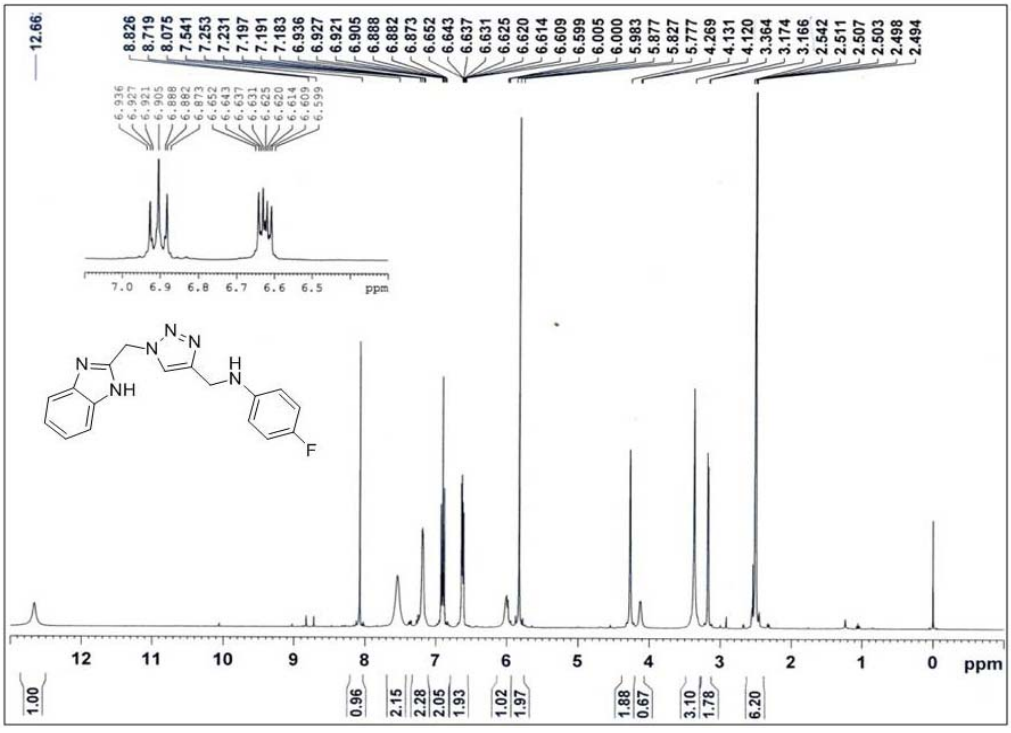

Figure 2.2.13: ^{1}H NMR spectra of 7c

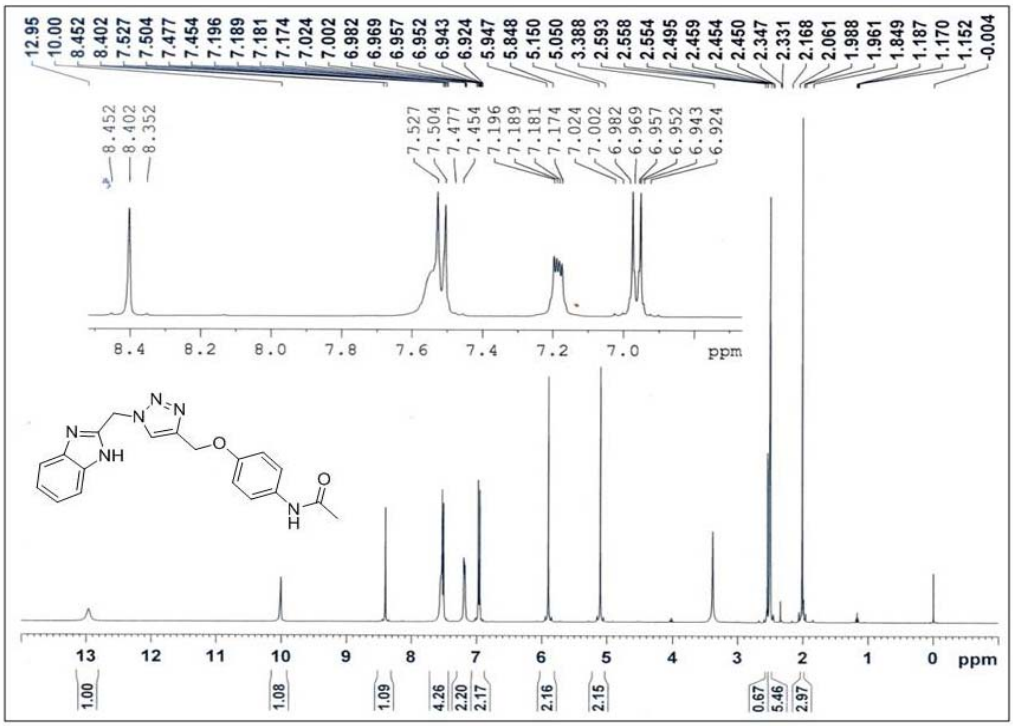

Figure 2.2.14: ^{1}H NMR spectra of 7d

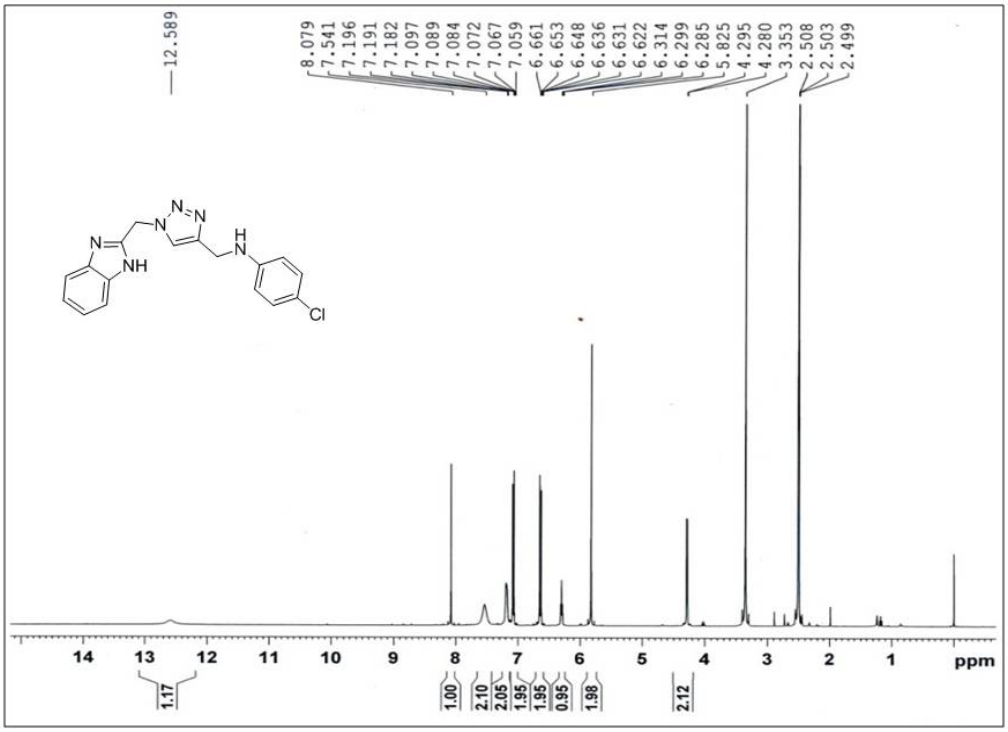

Figure 2.2.15: ^{1}H NMR spectra of 7e

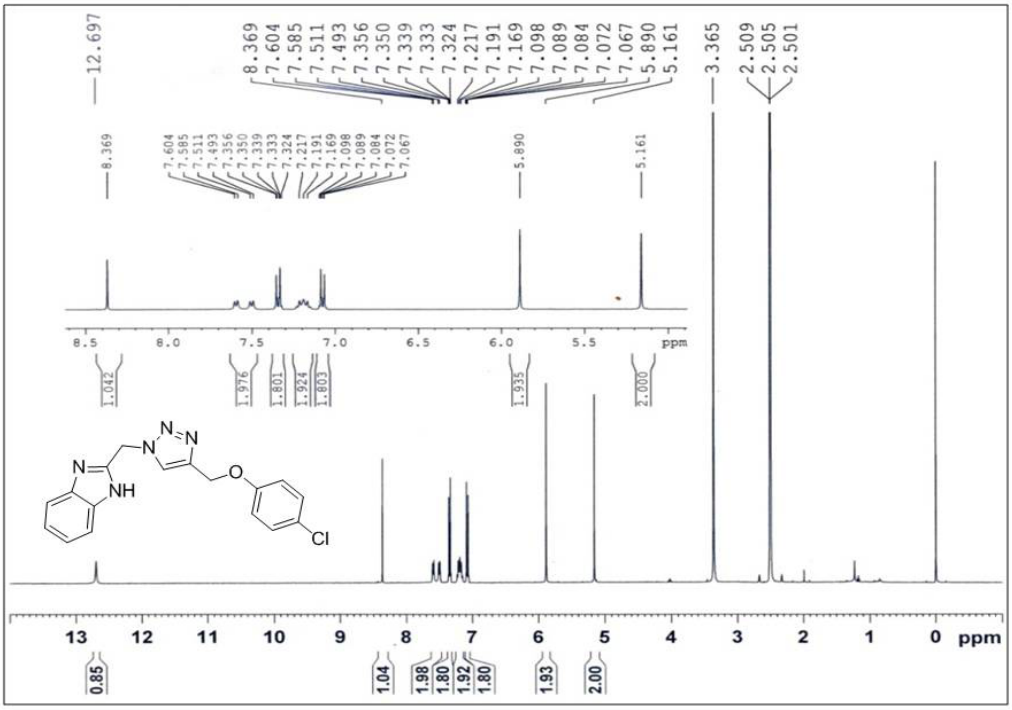

Figure 2.2.16: ^{1}H NMR spectra of 7f

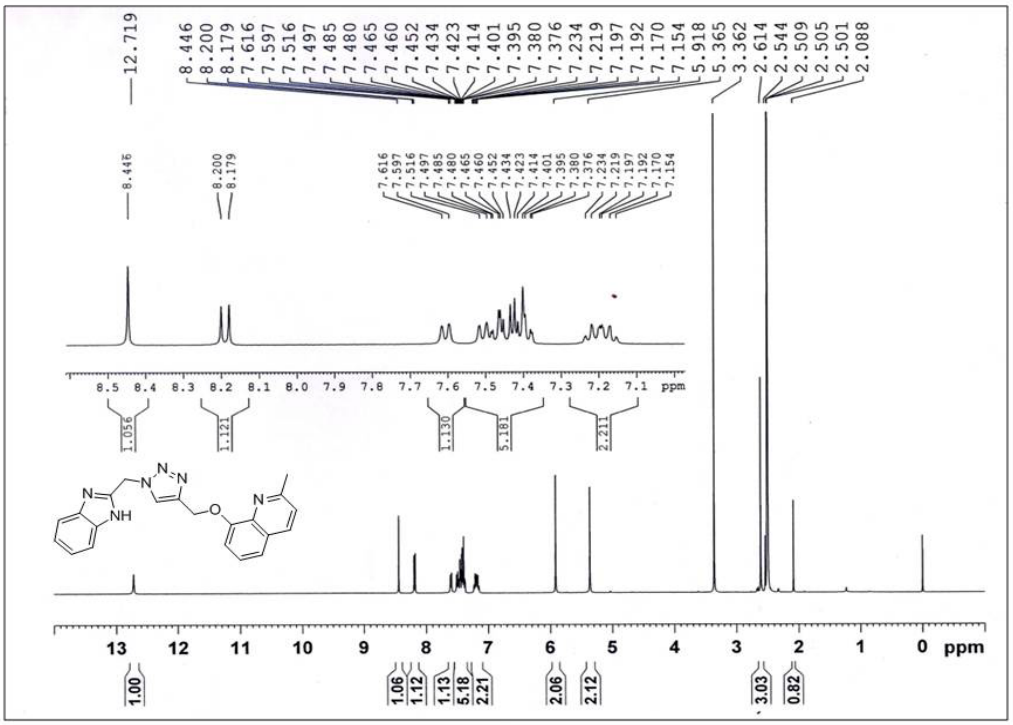

Figure 2.2.17: ^{1}H NMR spectra of 7g

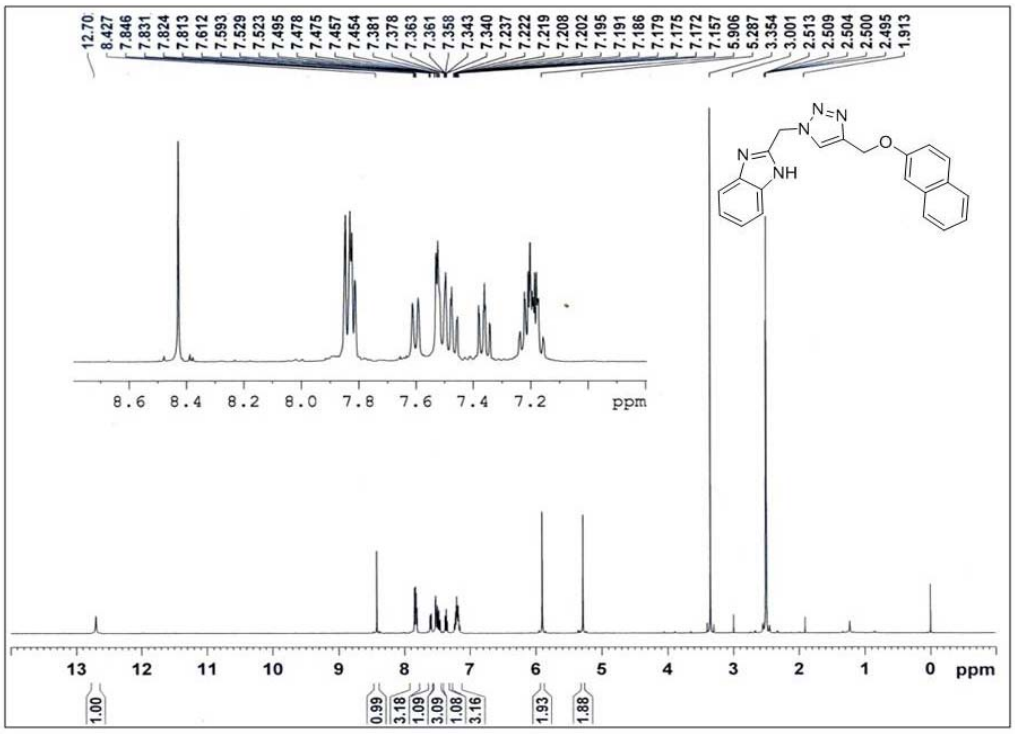

Figure 2.2.18: ^{1}H NMR spectra of 7h

^{13}C NMR:

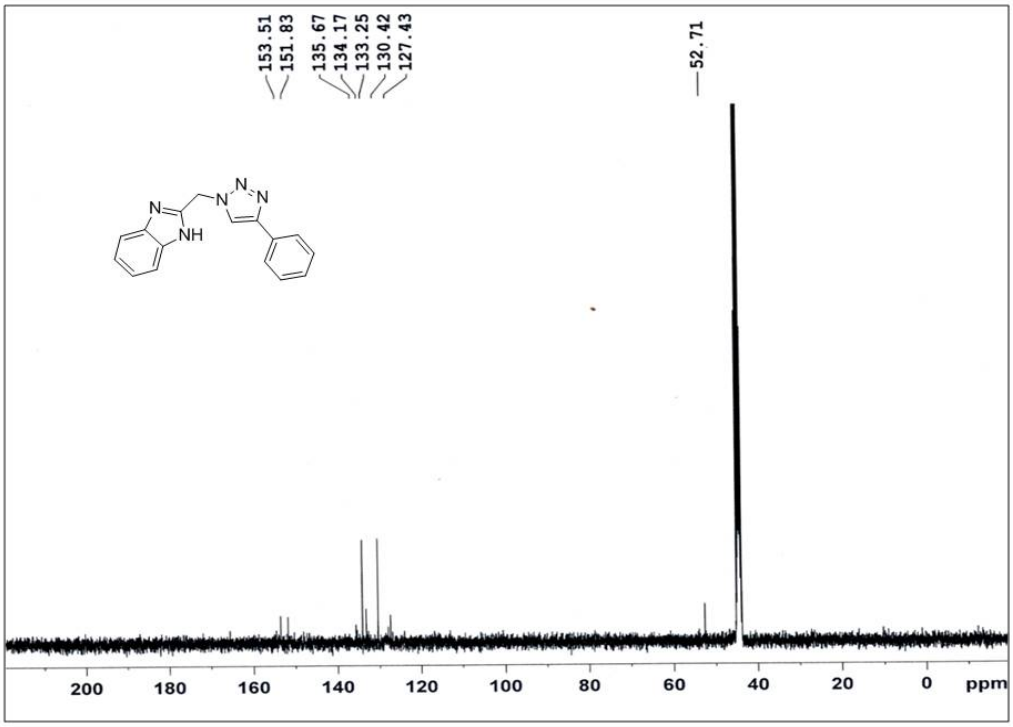

Figure 2.2.19: ^{13}C NMR spectra of 4a

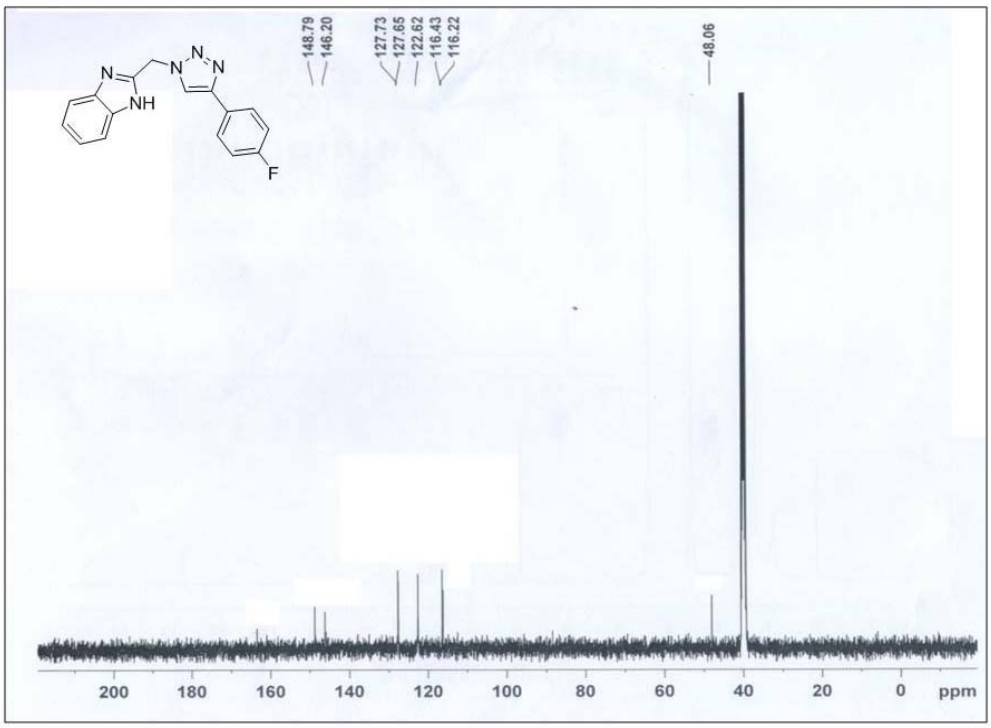

Figure 2.2.20: ^{13}C NMR spectra of 4b

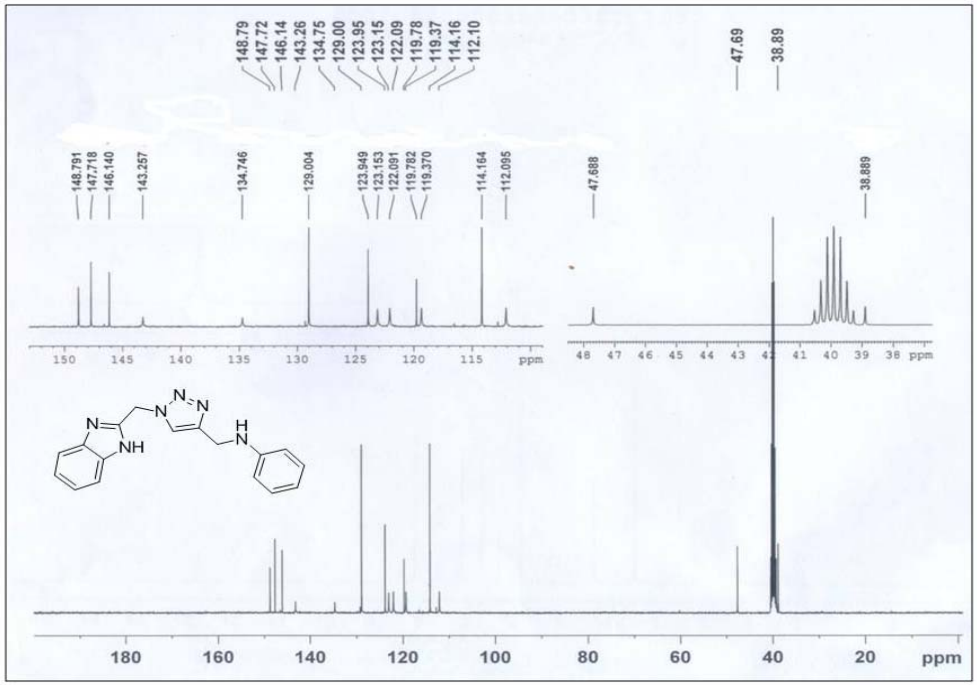

Figure 2.2.21: ^{13}C NMR spectra of 7a

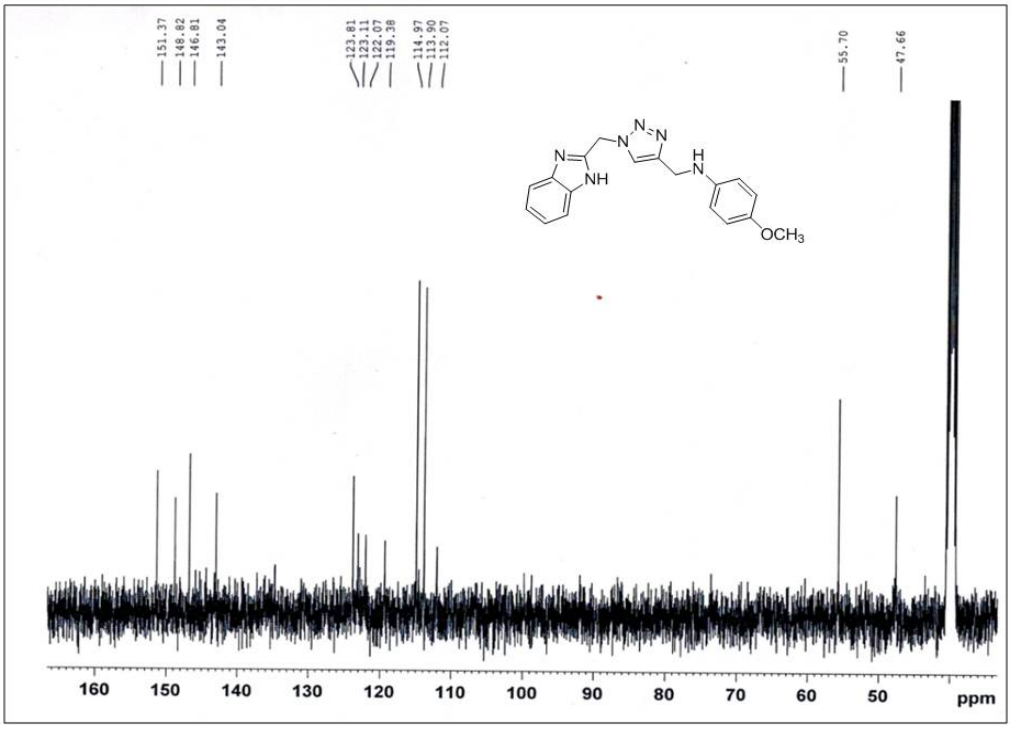

Figure 2.2.22: ^{13}C NMR spectra of 7b

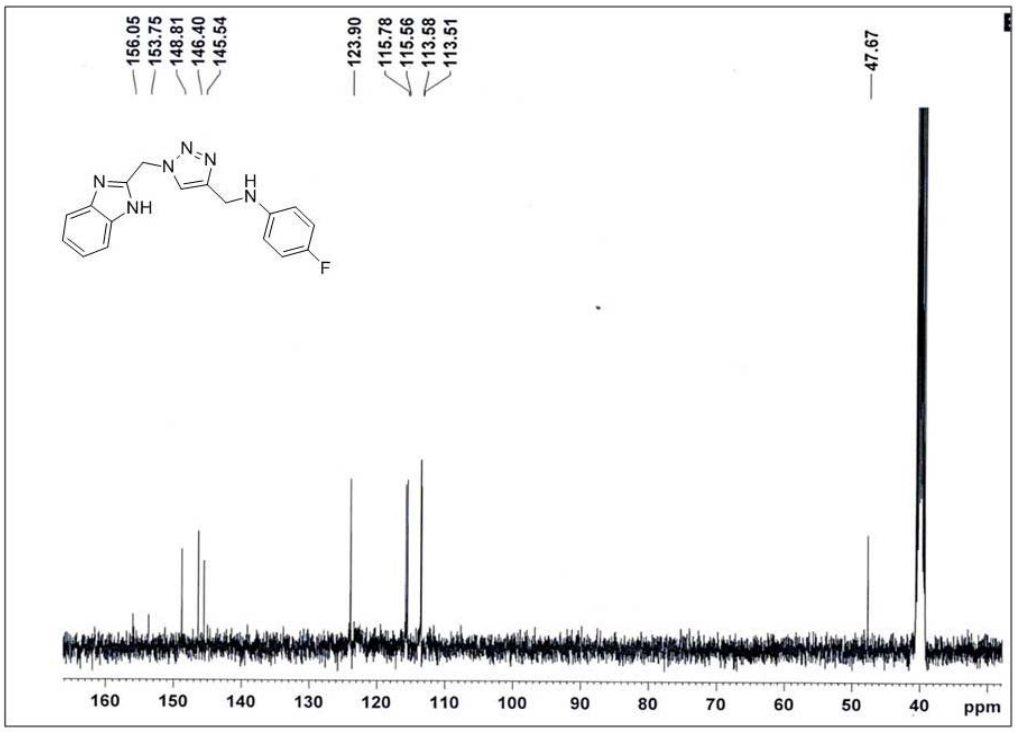

Figure 2.2.23: ^{13}C NMR spectra of 7c

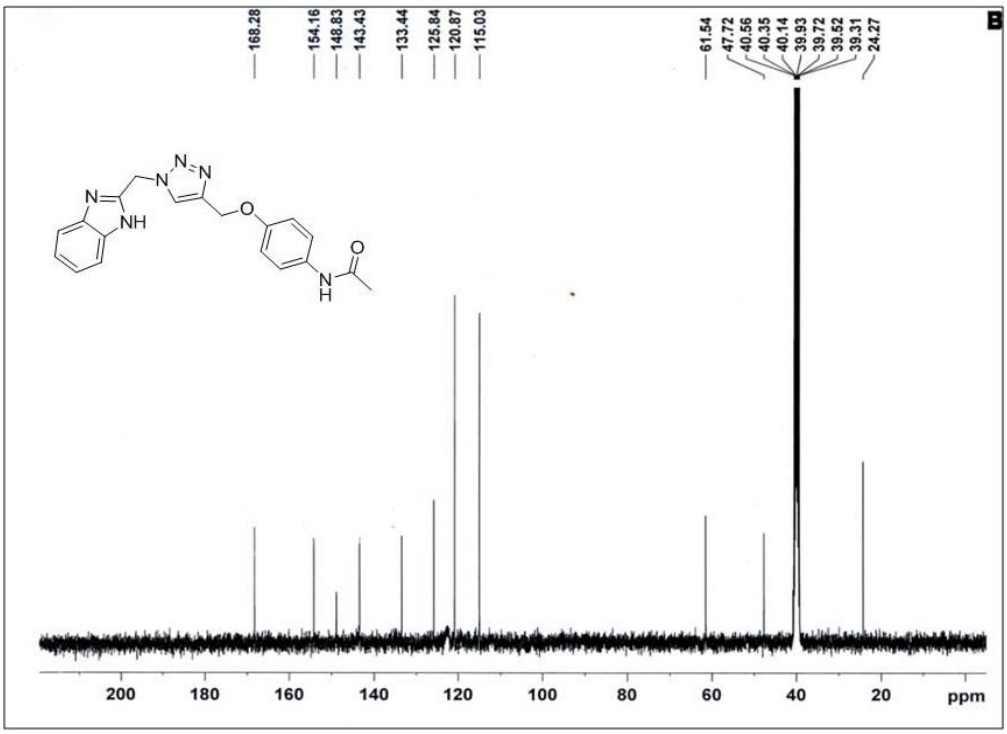

Figure 2.2.24: ^{13}C NMR spectra of 7d

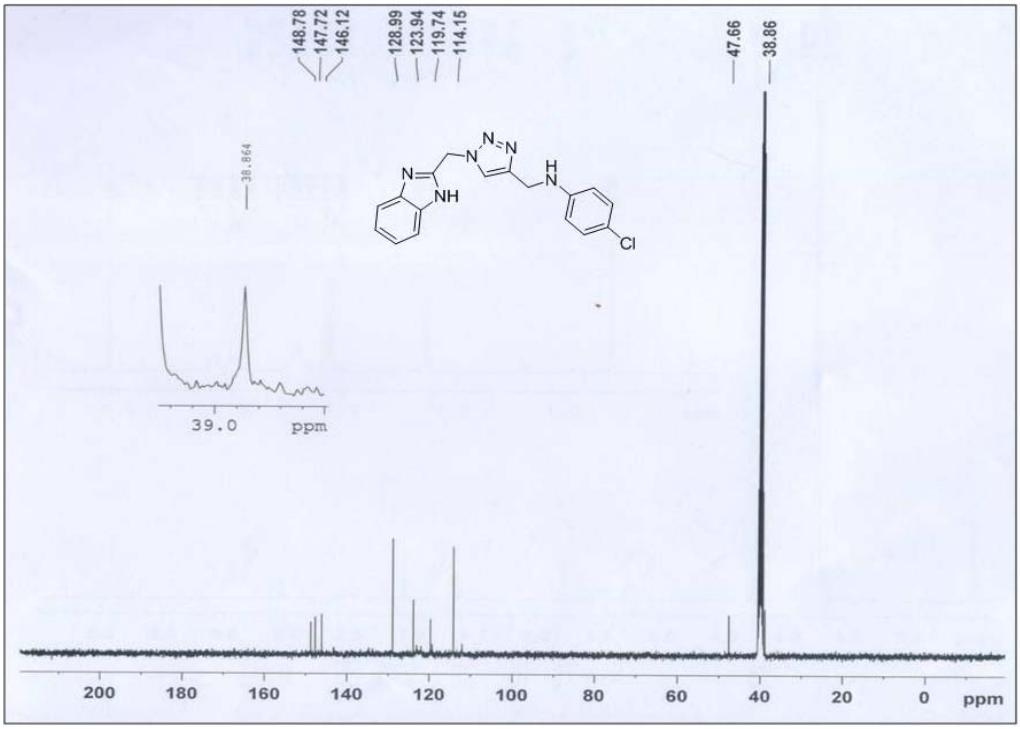

Figure 2.2.25: ^{13}C NMR spectra of 7e

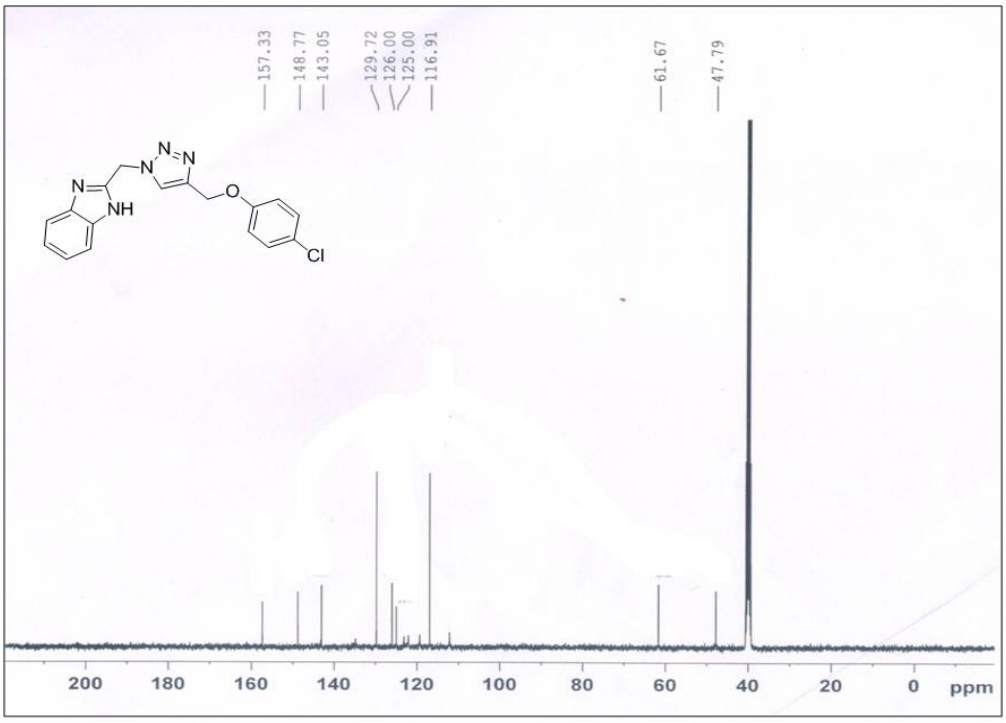

Figure 2.2.26: ^{13}C NMR spectra of 7f

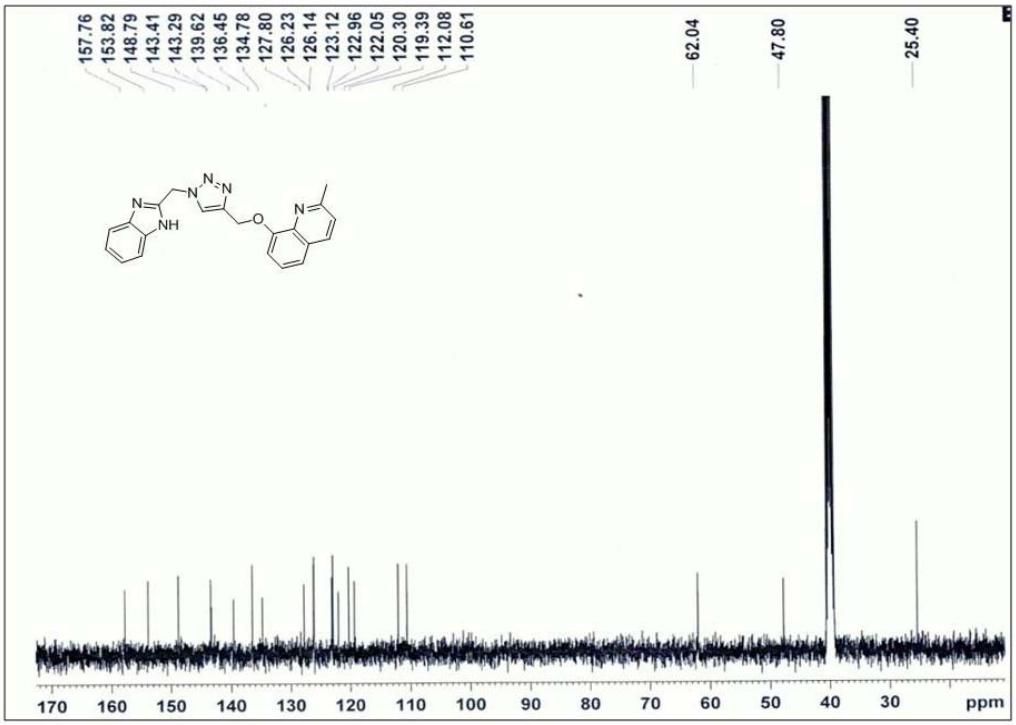

Figure 2.2.27: ^{13}C NMR spectra of 7g

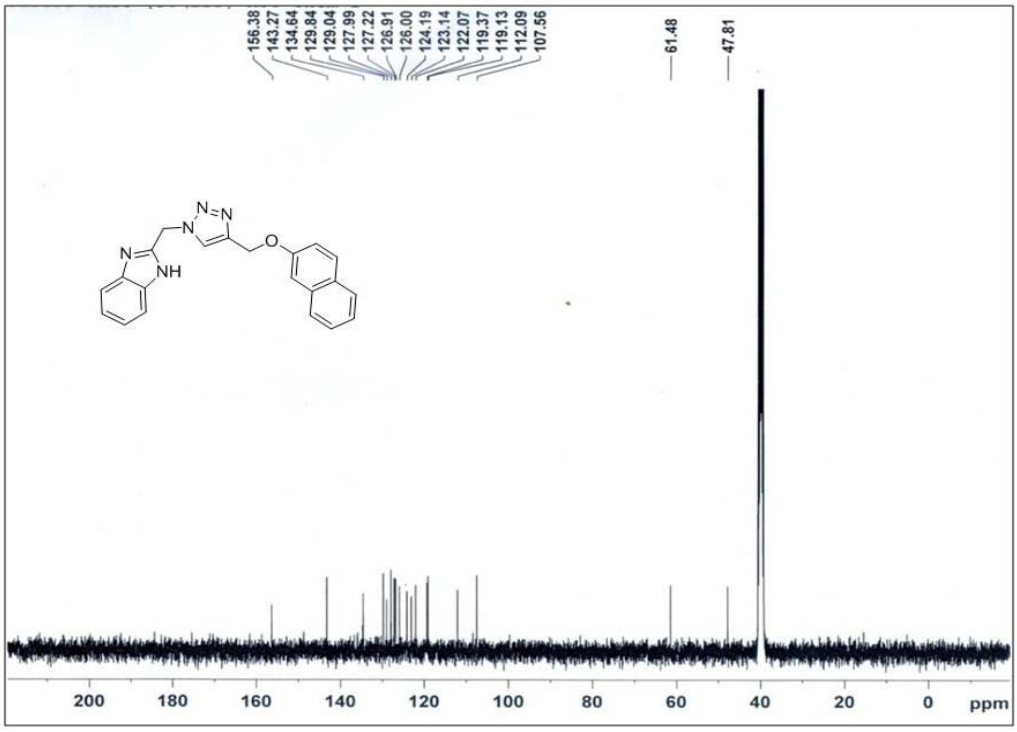

Figure 2.2.28: ^{13}C NMR spectra of 7h

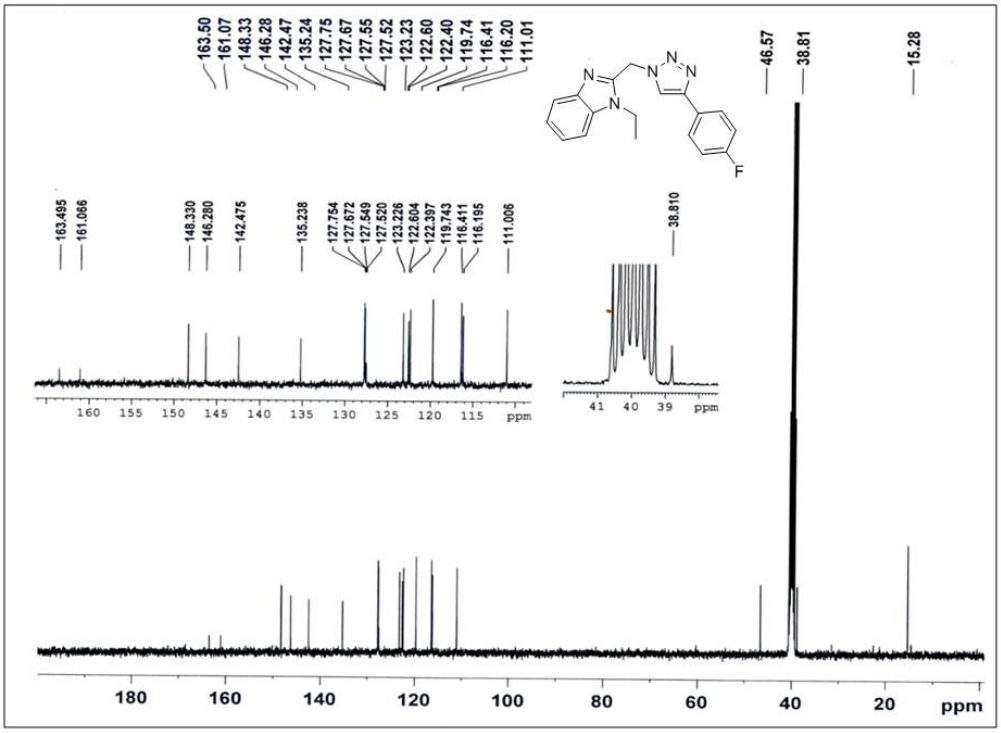

Figure 2.2.29: ^{13}C NMR spectra of 13

FT-IR-Spectra of all the compounds

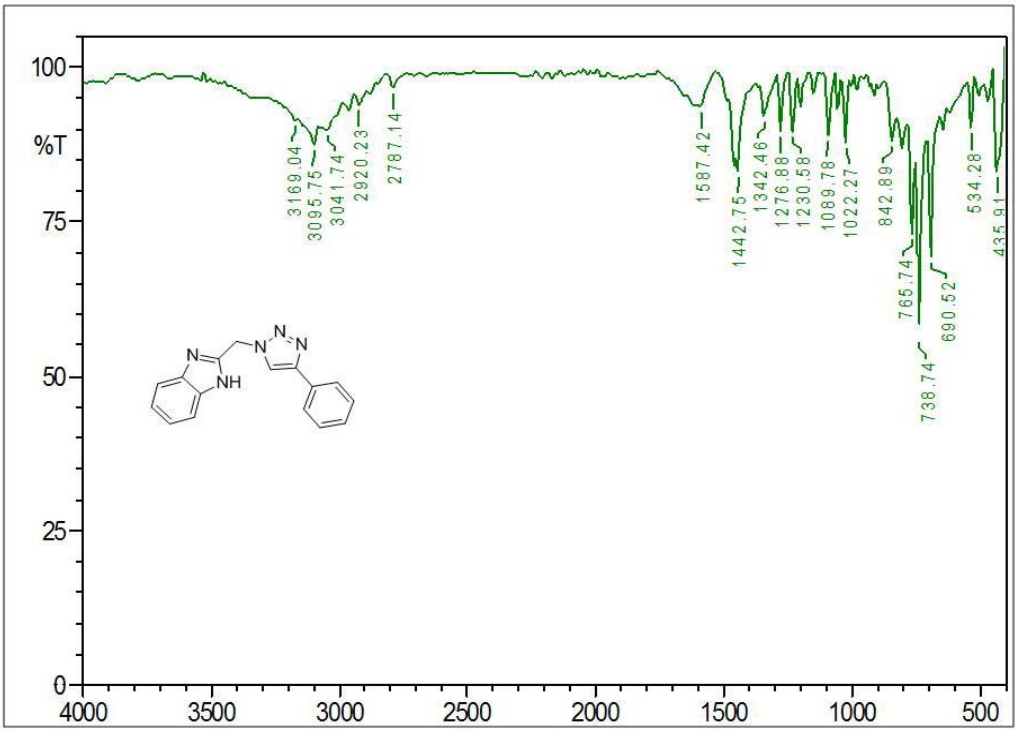

Figure 2.2.30: FT-IR spectra of 4a

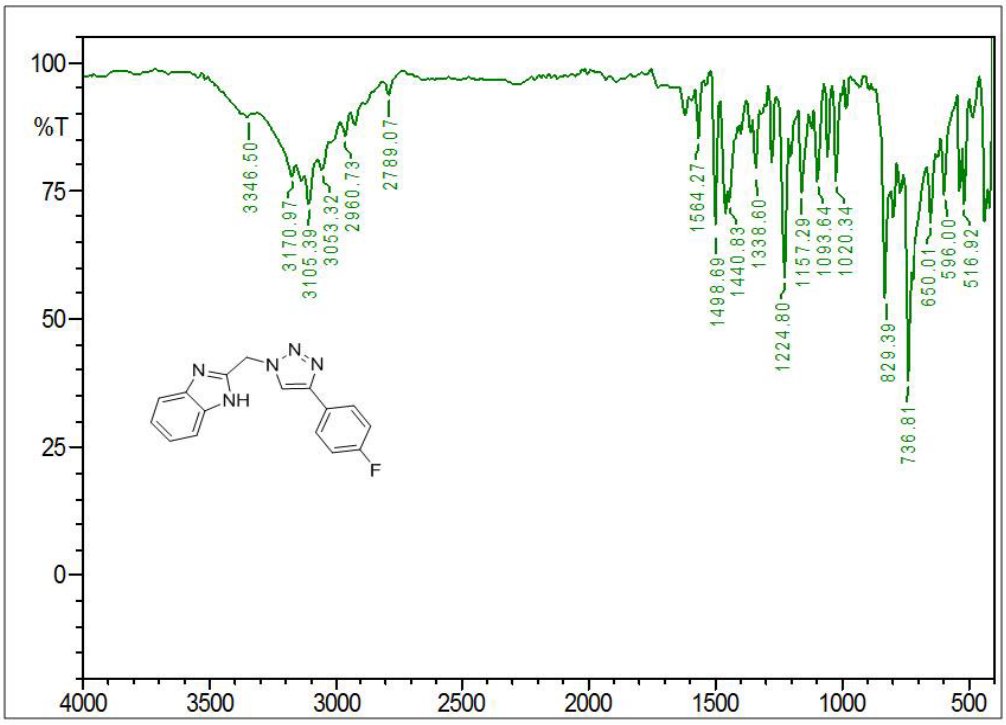

Figure 2.2.31: FT-IR spectra of 4b

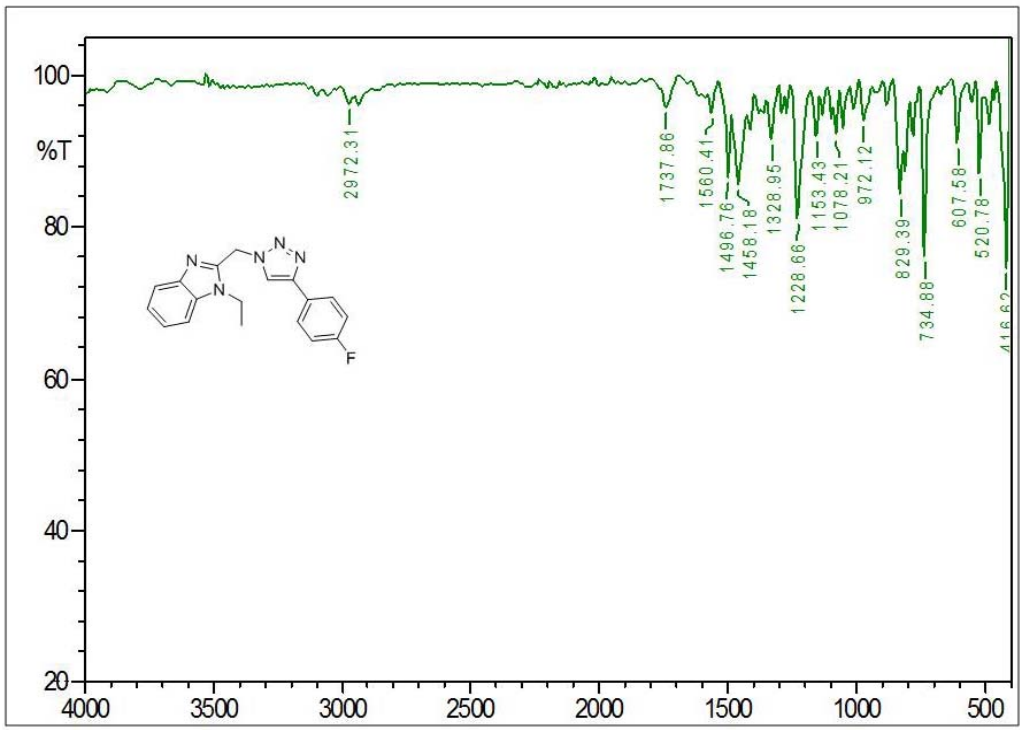

Figure 2.2.32: FT-IR spectra of 13a

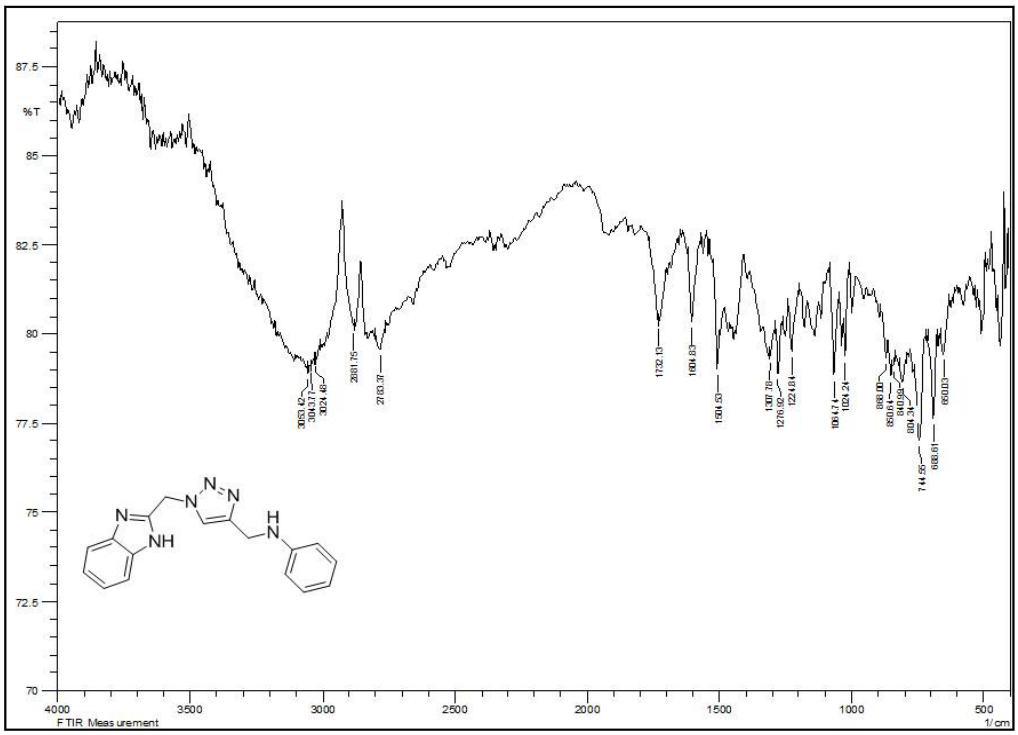

Figure 2.2.33: FT-IR spectra of 7a

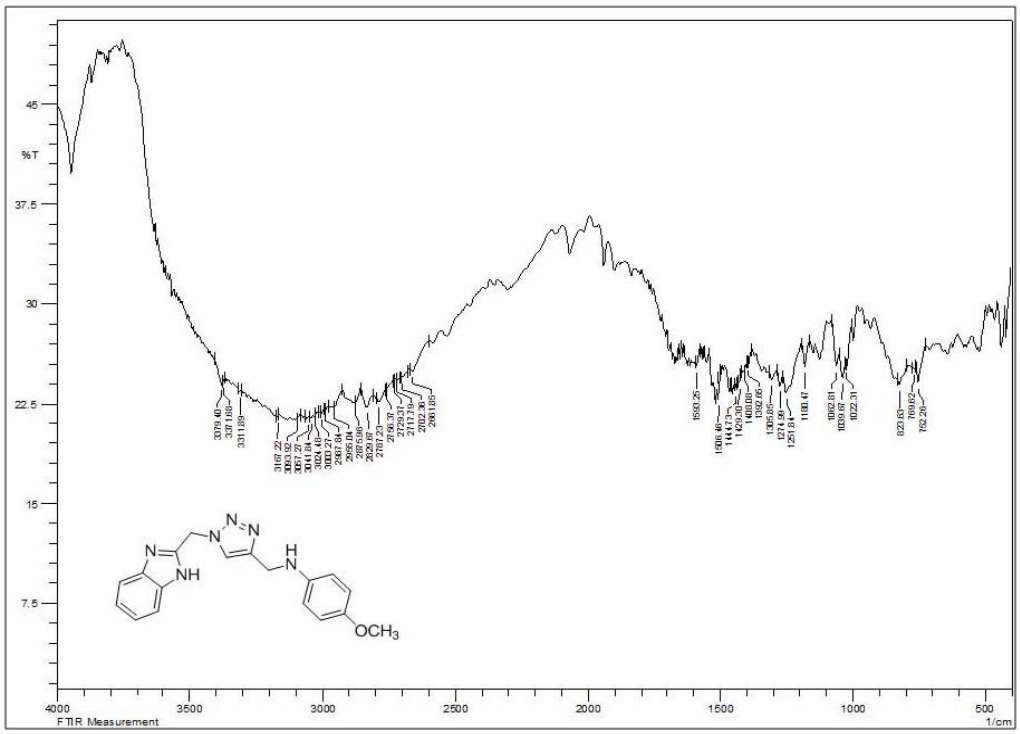

Figure 2.2.34: FT-IR spectra of 7b

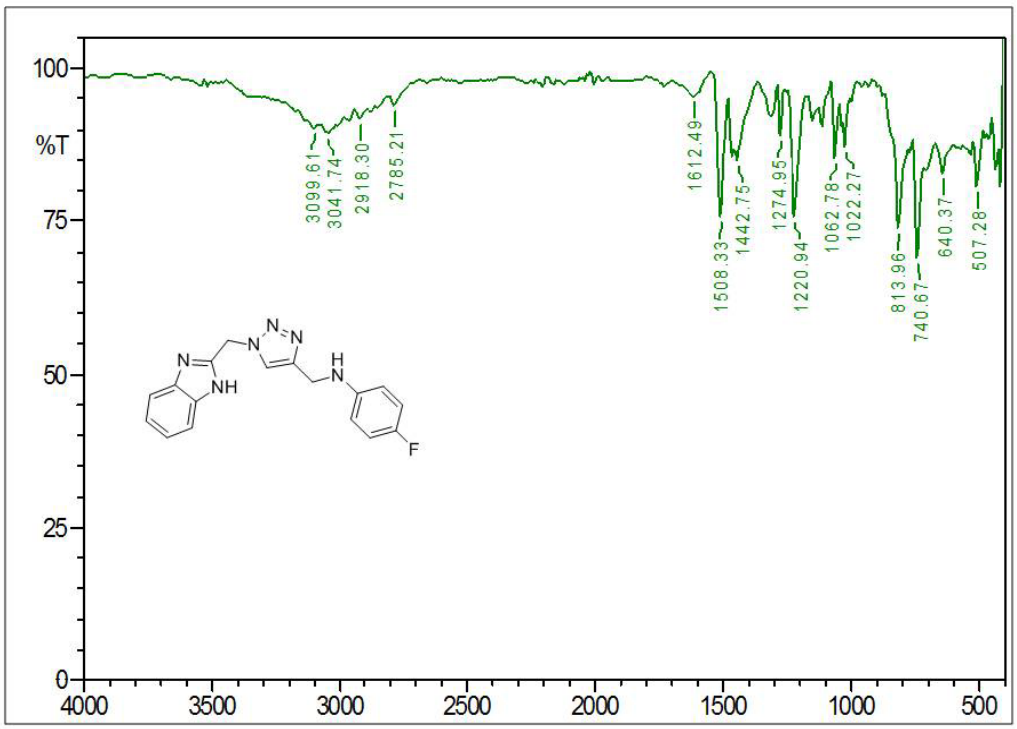

Figure 2.2.35: FT-IR spectra of 7c

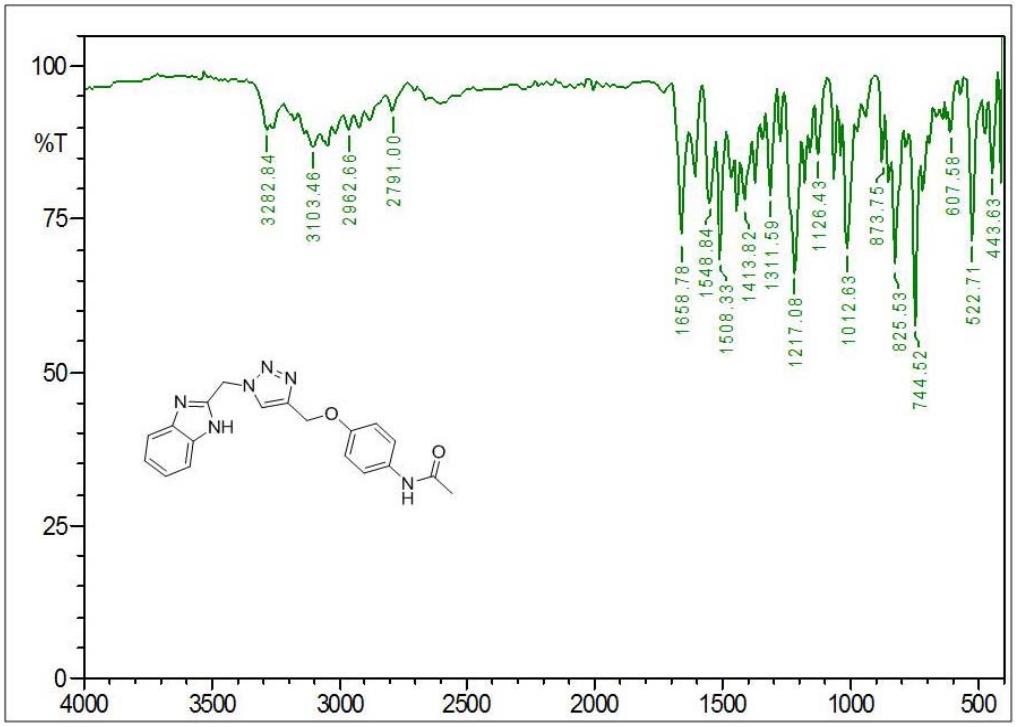

Figure 2.2.36: FT-IR spectra of 7d

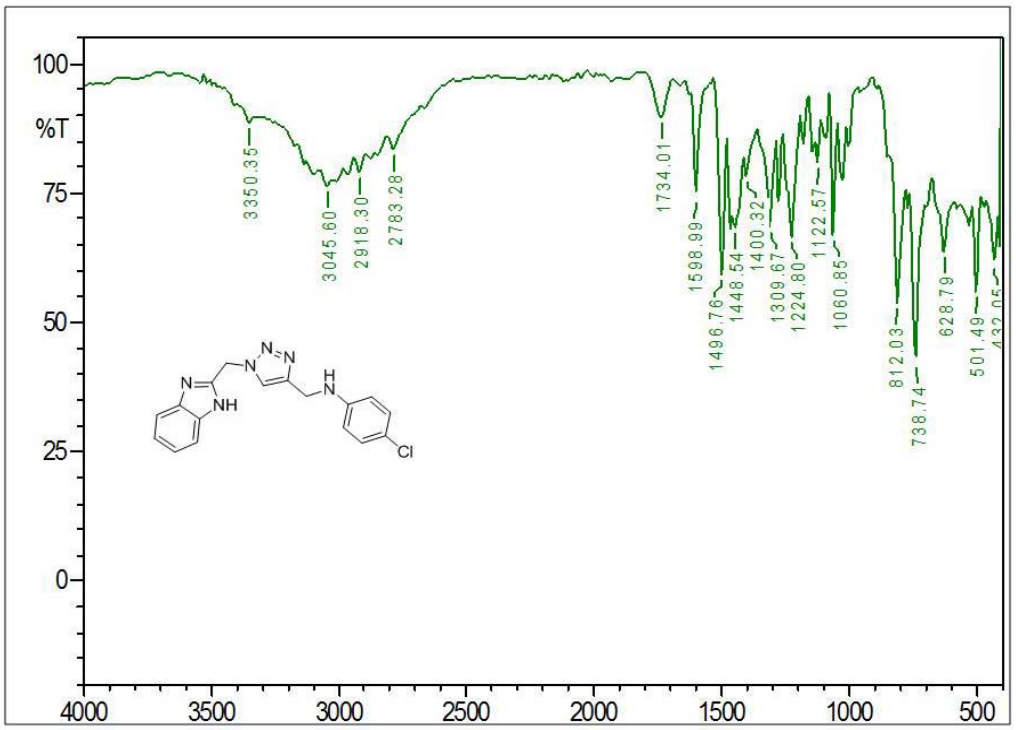

Figure 2.2.37: FT-IR spectra of 7e

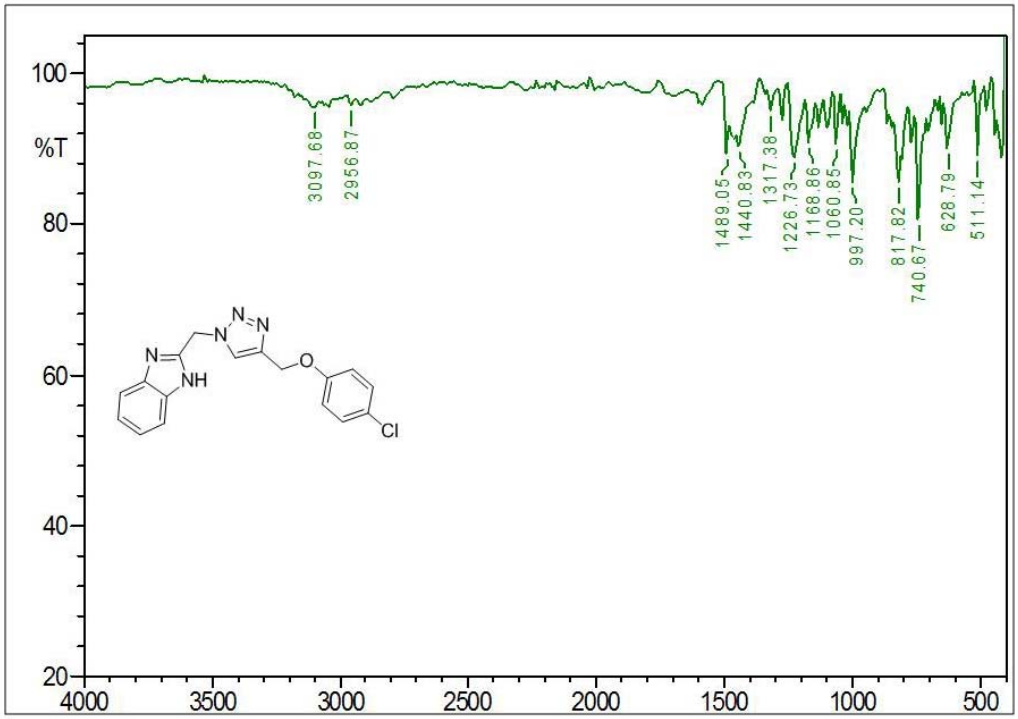

Figure 2.2.38: FT-IR spectra of 7f

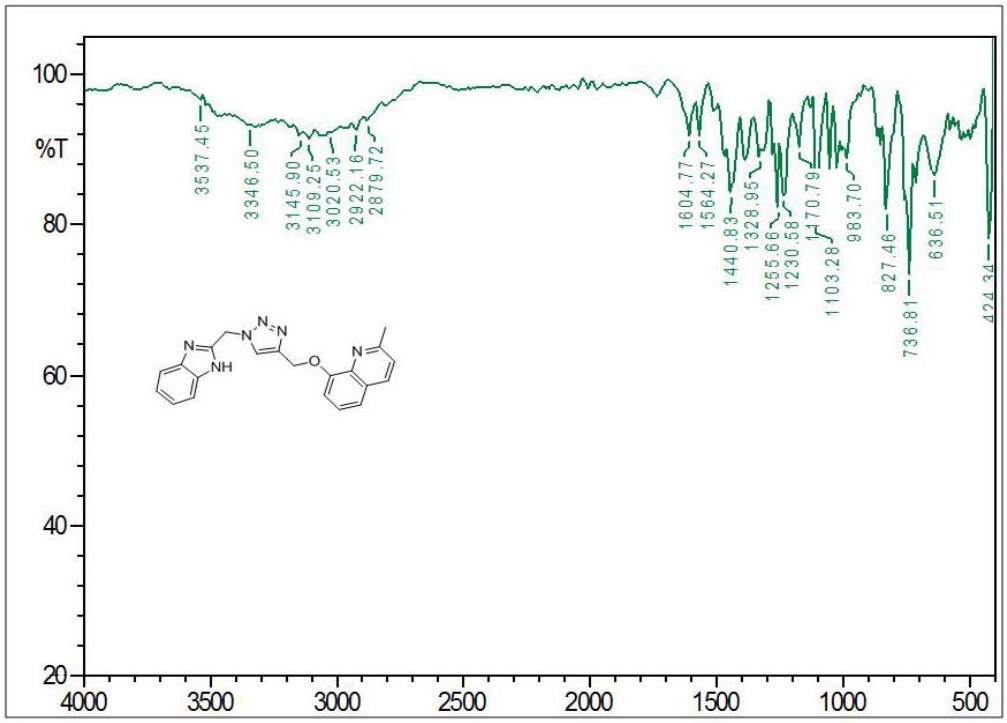

Figure 2.2.39: FT-IR spectra of 7g

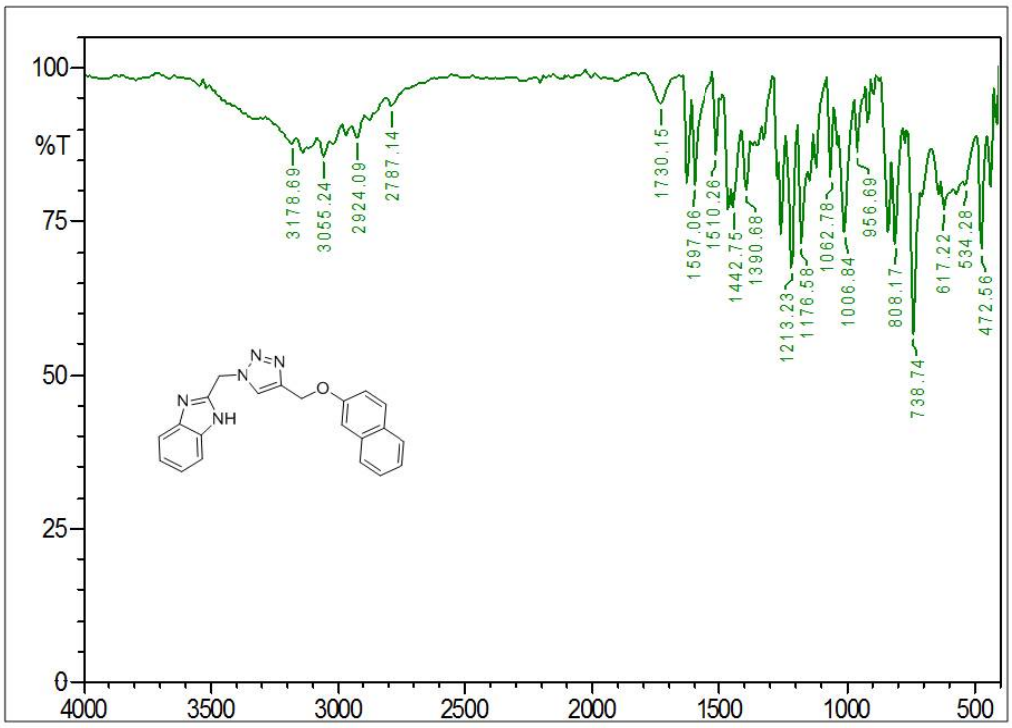

Figure 2.2.40: FT-IR spectra of 7h

HR-MS:

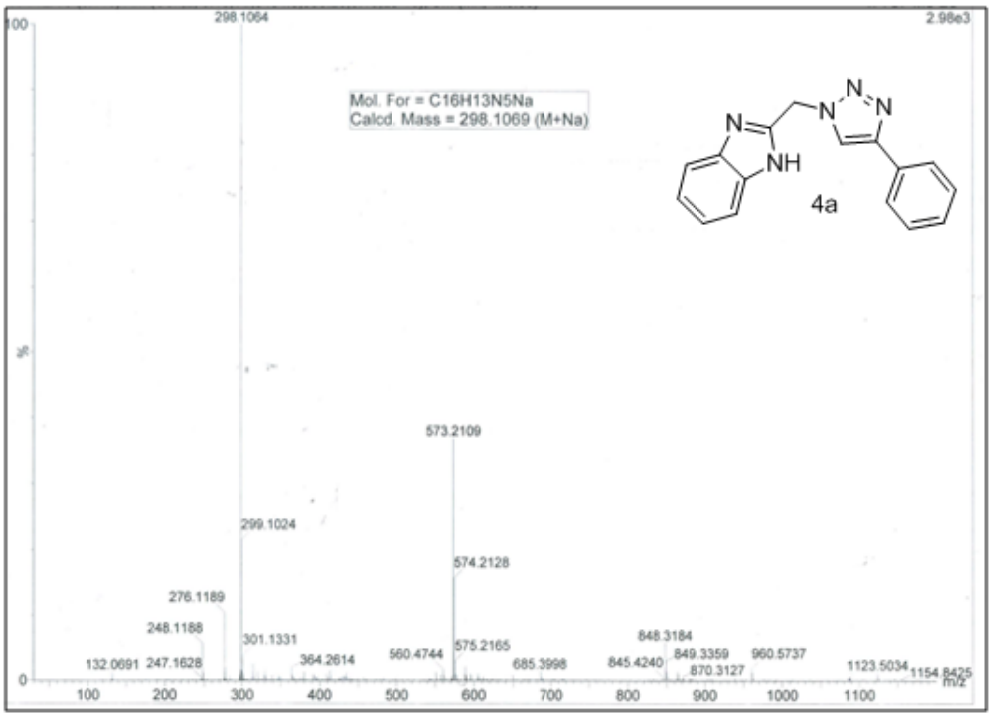

Figure 2.2.41: HR-MS spectra of 4a

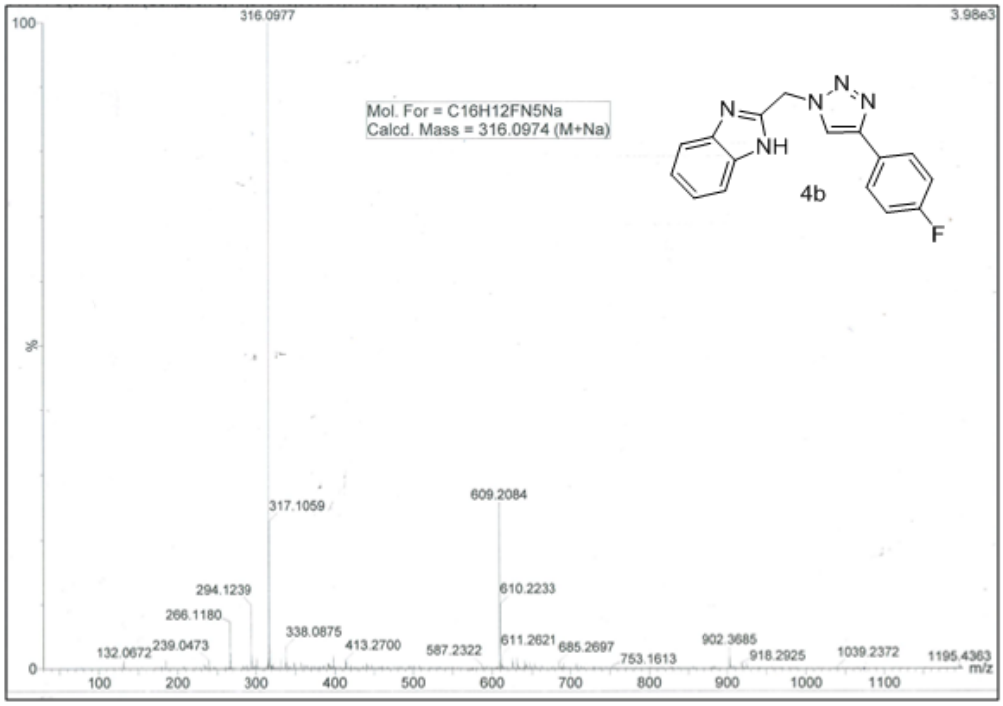

Figure 2.2.42: HR-MS spectra of 4b

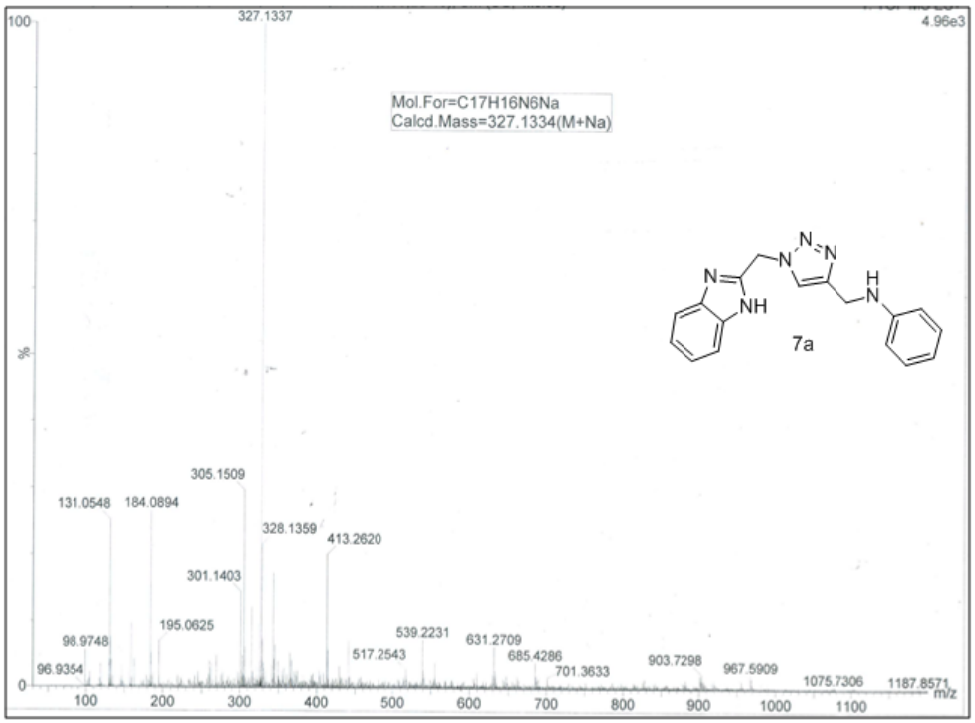

Figure 2.2.43: HR-MS spectra of 7a

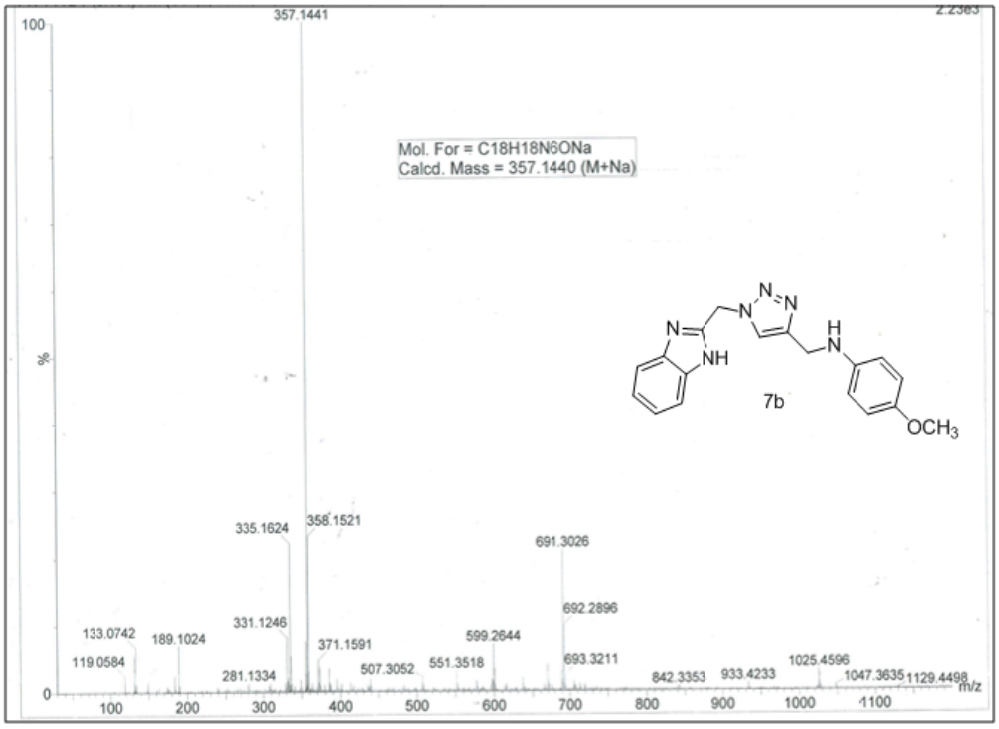

Figure 2.2.44: HR-MS spectra of 7b

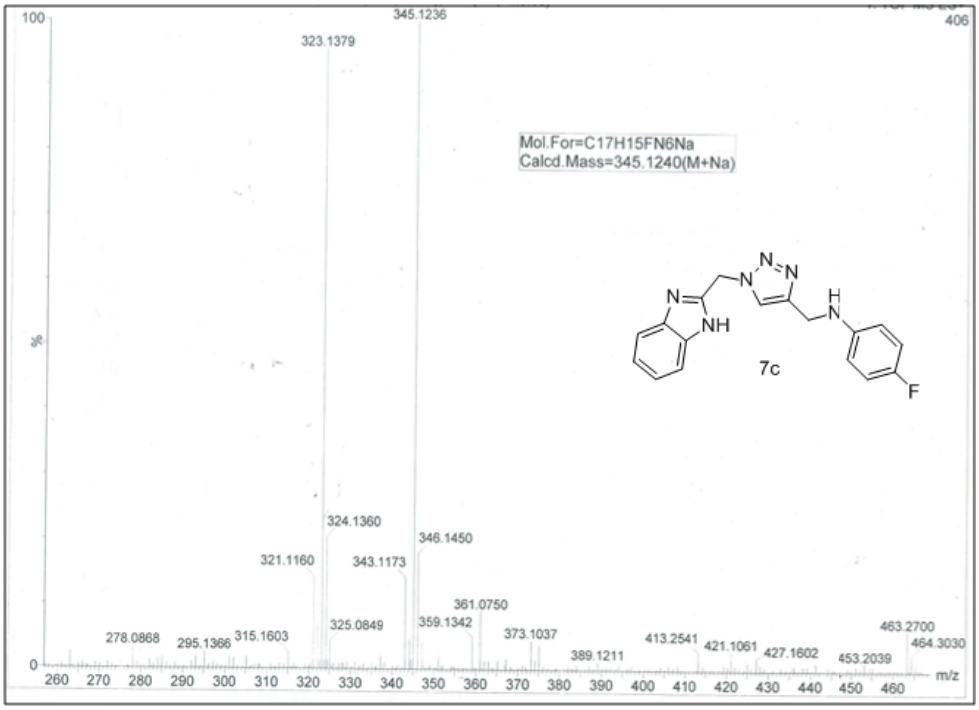

Figure 2.2.45: HR-MS spectra of 7c

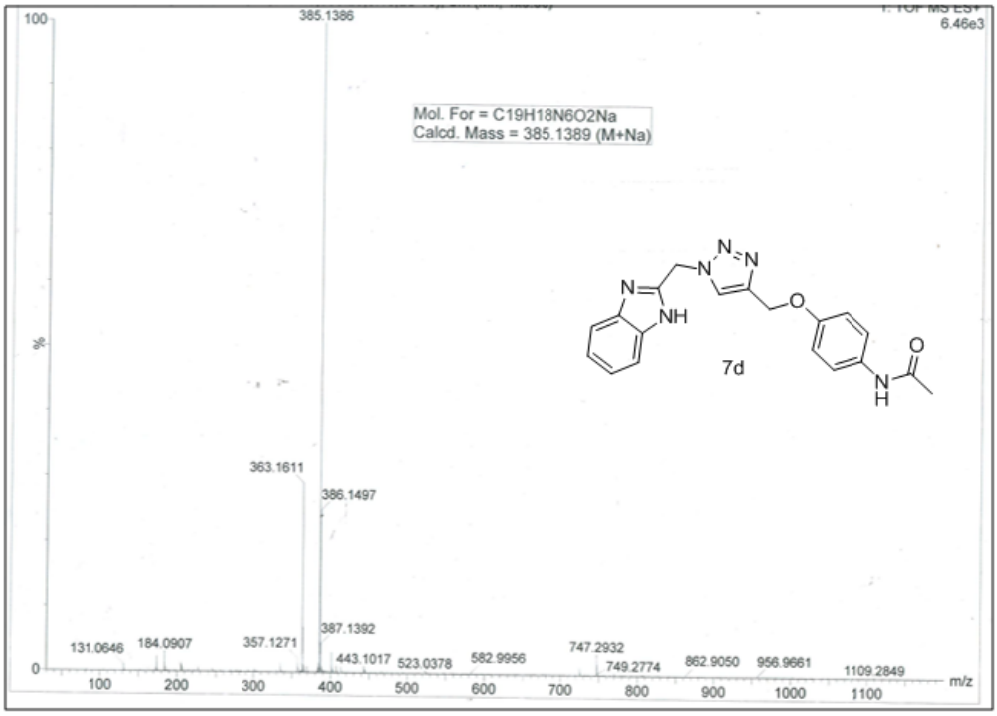

Figure 2.2.46: HR-MS spectra of 7d

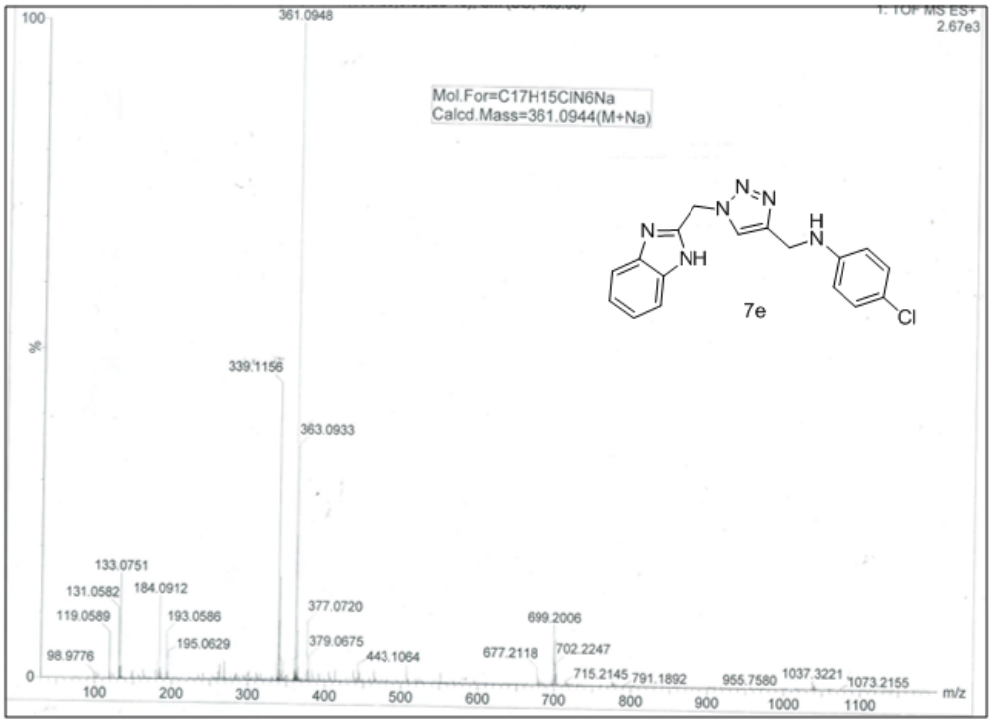

Figure 2.2.47: HR-MS spectra of 7e

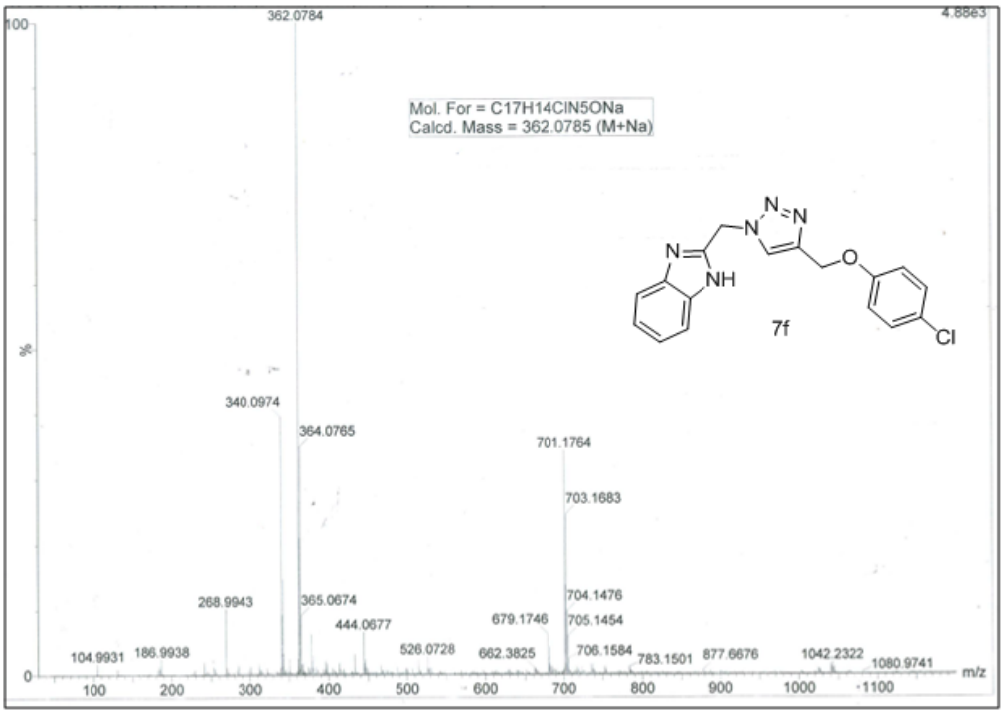

Figure 2.2.48: HR-MS spectra of 7f

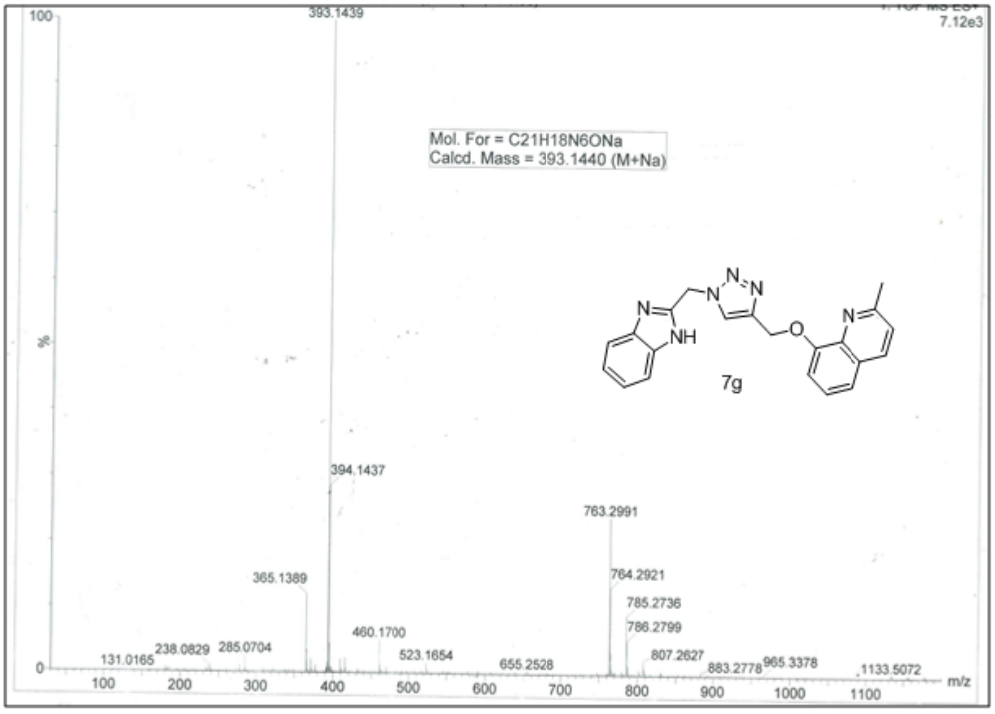

Figure 2.2.49: HR-MS spectra of 7g

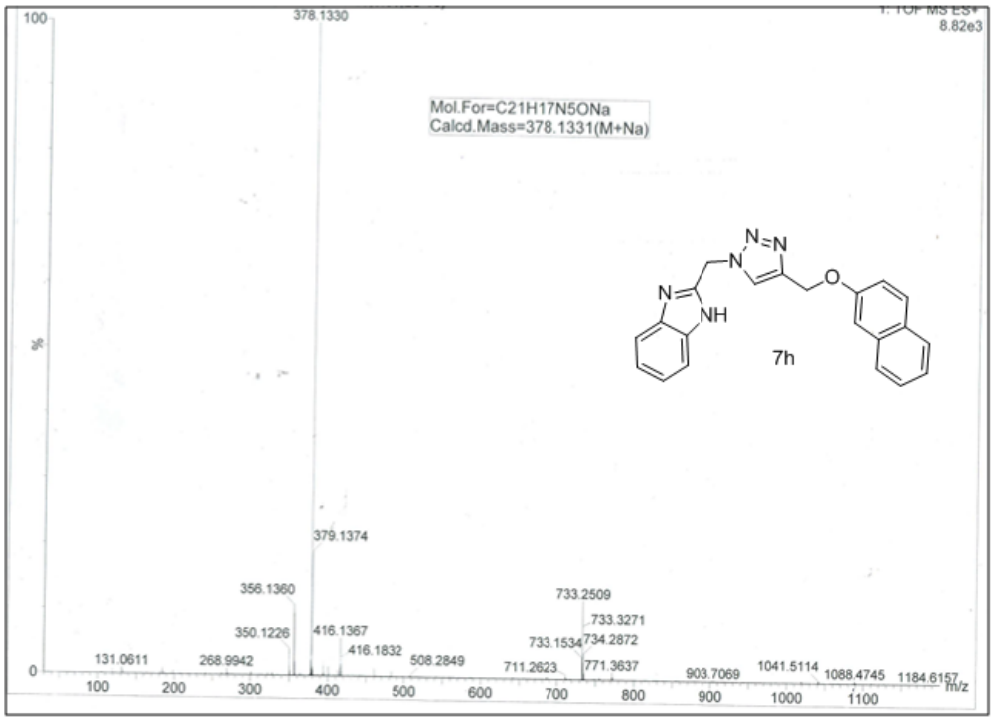

Figure 2.2.50: HR-MS spectra of 7h

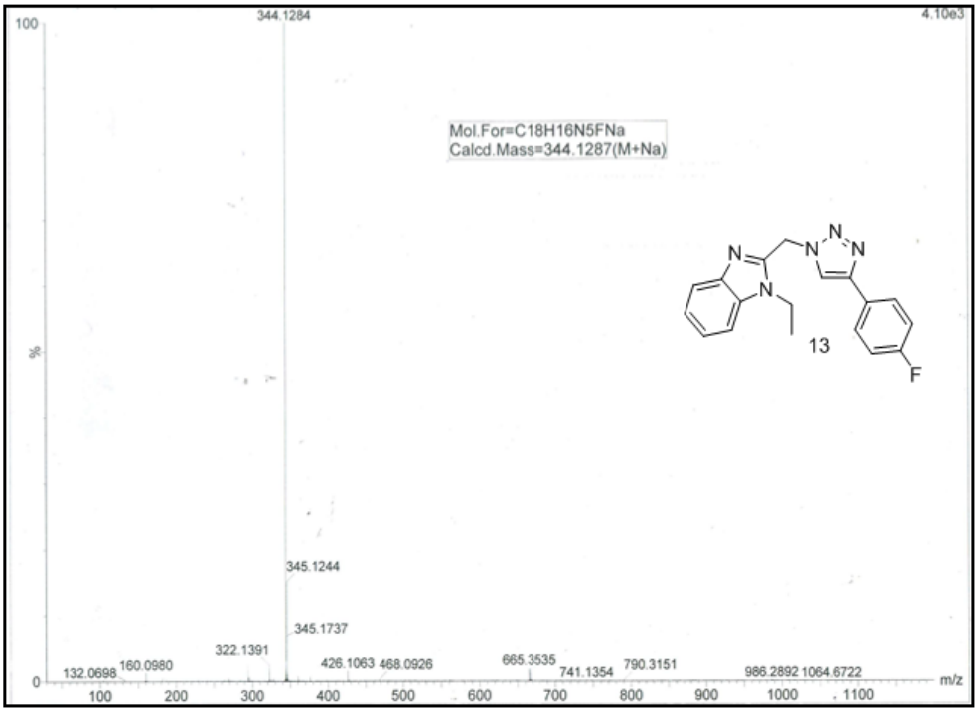

Figure 2.2.51: HR-MS spectra of 13

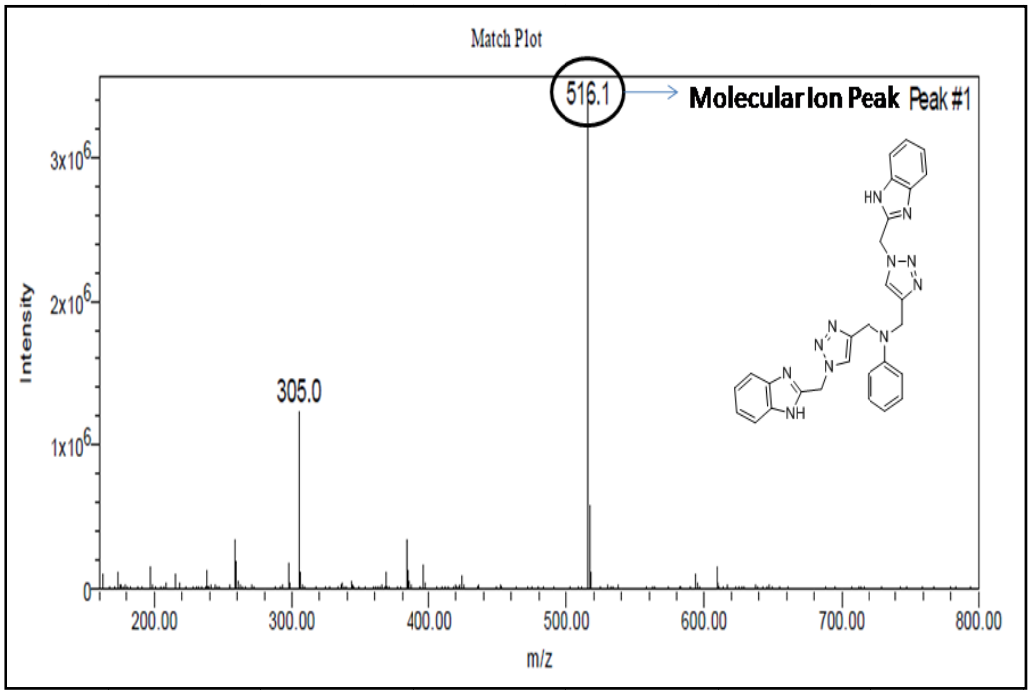

Figure 2.2.52: Mass spectra spectra of N,N-bis((1-((1H-benzo[d]imidazol-2-yl)methyl)-1H-1,2,3-triazol-4-yl)methyl)aniline

2.2.7 References:

[1] Ekhardt, S. *Curr. Med. Chem. Anti. Canc. Agents.* **2002**, *2*, 419-439.

[2] Medina, J. C.; Shan, B.; Beckmann, H.; Farrell, R. P.; Clark,D. L.; Marc Learned, R.; Roche, D.; Li, A.; Baichwal, V.; Case, C. *Bioorg. Med. Chem. Lett.***1998**, *8*, 2653-2656.

[3] Alaa, A.M. *Eur. J. Med. Chem.***2007**, *42*, 614-626.

[4] El-Nezhawy, A. O. H.; Eweas, A. F.; Radwan, M. A. A.; El-Naggar, T. B. A. *J. Heterocyclic Chem.***2016**, *53*, 271-279.

[5] (a) Bai, S.; Li, S.; Xu, J.; Peng, X.; Sai, K.; Chu, W.; Tu, Zhude.; Zeng, C.; Mach, R. H. *J. Med. Chem.***2014**, *57*, 4239-4251. (b) Saeedi, M.; Ansari, S.; Mahdavi, M.; Sabourian, R.; Akbarzadeh, T.; Foroumadi, A.; Shafiee, A. *Syn Comm*, **2015**, *20*, 2311-2318.

[6] Hou, J.; Li, Z.; Fang, Q.; Feng, C.; Zhang, H.; Guo, W.; Wang, H.; Gu, G.; Tian, Y.; Liu, P.; Liu, R.; Lin, J.; Shi, Yi-K.; Yin, Z.; Shen, J.; Wang, P. G. *J. Med. Chem*. **2012**, *55*, 3066-3075.

[7] Guo, L.J.; Wei, C. X.; Jia, J. H.; Zhao, L. M.; Quan, Z. S.*Eur. J. Med. Chem*. **2009**, *44*, 954-958.

[8] Kumar, S. S.; Kavitha, H. P.*Mini. Rev. Org. Chem.***2013**, *10*, 40-65.

[9] Penthala, N. R.; Madhukuri, L.; Thakkar, S.; Madadi, N. R.; Lamture, G.; Eoff, R. L.; Crook, P. A. *Med. Chem. Commun*. **2015**, *6*, 1535-1543.

[10] Mareddy, J.; Nallapati, S. B.; Anireddy, J.; Devi, Y. P.; Mangamoori, L. N.; Kapavarapu, R.; Pal, S. *Bioorg. Med. Chem. Lett.* **2013**, *23,* 6721-6727.

[11] Praveena, K. S. S.; Durgadas, S.; Babu, N. S.; Akkenapally, S.; Kumar, C. G.; Deora, G. S.; Murthy, N.Y.S.; Mukkanti, K; Pal, S. *Bioorg.Chem.* **2014**, *53*, 8-14.

[12] Babu, P. V.; Mukherjee, S.; Gorja, D. R.; Yellanki, S.; Medisetti, R.; Kulkarni, P.; Mukkanti, K.; Pal, M. *RSC Advances* **2014**, *4*, 4878-4882.

[13] Kuntala, N.; Telu, J. R.; Banothu, V.; Nallapati, S. B.; Anireddy, J. S.; Pal, S. *MedChemComm*, **2015**, *6*, 1612-1619.

[14] Pingaew, R.; Prachayasittikul, V.; Mandi, P.; Nantasenamat, C.; Prachayasittikul, S.; Ruchirawat, S.; Prachayasittikul, V. *Bioorg.Med.Chem.* **2015**, *23*, 3472-3480.

[15] Kolb, H. C.; Finn, M. G.; Sharpless, K. B. *Angew. Chem. Int. Ed*. **2001**, *40*, 2004-2021.

[16] Rostovtsev, V. V.; Green, L. G.; Fokin, V. V.; Sharpless, K. B.*Angew. Chem. Int. Ed*. **2002**, *41*, 2596.

[17] Nallapati, S. B.; Sreenivas, B. Y.; Bankala, R.; Parsa, K. V.; Sripelly, S.; Mukkanti, K.; Pal, M. *RSC Advances,* **2015,** *5*, 94623-94628.

[18] Sri Shanthi Praveena, K.; Veera Venkat Shivaji Ramarao, E.; Poornachandra, Y.; Ganesh Kumar, C.; Suresh Babu, N.; Yadagiri Sreenivasa Murthy, N.; Pal, S. *Lett. Drug Design. Discovery*, **2016**, *13*, 210-219.

[19] Neeraja, P.; Srinivas, S.; Mukkanti, K.; Dubey, P. K.; Pal, S. *Bioorg. Med. Chem. Lett.* **2016**, *26*, 5212-5217.

[20] Agalave, S. G.; Maujan, S. R.; Pore, V. S. *Chem.–An Asian Journal*, **2011**, *6*, 2696-2718.

[21] Massaroti, A.; Aprile, S.; Mercalli, V.; Grosso, E. D.; Grosa, G.; Sorba, G.; Tron, G. S. *Chem. Med. Chem.***2014**, *9*, 2497-2508.

[22] Prachayasittikul, V.; Pingaew, R.; Anuwongcharoen, N.; Worachartcheewan, A.; Nantasenamat, C.; Prachayasittikul, S.; Ruchirawat, S.; Prachayasittikul, V. *Springer Plus* **2015**, *4*, 571.

[23] Totobenazara, J.; Burke, A. J. Tet.Lett. **2015**, *56*, 2853-2859.

[24] VijayaáBabu, P. *Org. Biomol. Chem.* **2014**, *12*, 6800-6805.

[25] Harkala, K. J.; Eppakayala, L.; Maringantiz, T. C. *Org. Med. Chem. Lett.* **2014**, *4*, 14.

[26] Abdelgawad, M. A.; Abdellatif, K. R. A.; Ahmed, O. M. *Med. Chem*. **2014**, S1, 001.

[27] Youssef, A. M.; Malki, A.; Badr, M. H.; Elbayaa, R. Y.; Sultan, A. S. *Med. Chem*. **2012**, *8*, 151-162.

[28] Torres, F. C.; García-Rubiño, M. E.; Lozano-López, C.; Kawano, D. F.; Eifler-Lima, V. L.; Von-Poser, G. L.; Campos, J. M. *Curr. Med. Chem*. **2015**, *22*, 1312-1323.

[29] Bailly, C. *Curr. Med. Chem*. **2000**, *7*, 39-58.

[30] Gellis, A.; Kovacic, H.; Boufatah, N.; Vanelle, P. *Eur. J. Med. Chem*. **2008**, *43*, 1858-1864.

[31] Chawla, A.; Kaur, G.; Sharma, A. K. *Int.J.Pharm. Phytopharmacol.Res.***2012**, *2*, 148-159.

[32] Baell, J.; Walter, M. A. *Nature,***2014**, *513*, 481-483.

[33] Hou, J.; Li, Z.; Fang, Q.; Feng, C.; Zhang, H.; Guo, W.; Wang, H.; Gu, G.; Tian, Y.; Liu, P.; Liu, R.; Lin, J.; Shi, Yi-K.; Yin, Z.; Shen, J.; Wang, P. G. *J. Med. Chem.***2012**, *55*, 3066-3075.

[34] Chen, P. J.; Yang, A.; Gu, Y. F.; Zhang, X. S.; Shao, K. P.; Xue, D. Q.; He, P.; Jiang, T. F.; Zhang, Q. R.; Liu, H. M. *Bioorg. Med. Chem. Lett*. **2014**, *24*, 2741-2743.

[35] Gu, S. J.; Lee, J. K.; Pae, A. N.; Chung, H. J.; Rhim, H.; Han, S. Y.; Min, Sun-J.; Cho, Y. S. *Bioorg. Med. Chem.Lett.***2010**, *20*, 2705-2708.

[36] Pal, M.; Parasuraman, K.; Yeleswarapu, K. R. *Org.Lett.***2003**, *5*, 349-352.

[37] Hong, L.; Shao, Y.; Zhang, L.; Zhou, X. *Chem. Eur. J.***2014**, *20*, 8551-8555.

[38] Agag, T.; Takeichi, T. *Macromolecules* **2001**, *34*, 7257-7263.

[39] Krim, J.; Sillahi, B.; Taourirte, M.; Rakib, E. M.; Engels, J. W. *Arkivoc* **2009**, *8*, 142-152.

[40] Chattopadhyay, P.; Nagpal, R.; Pandey, P. S.; *Aus. J. Chem*. **2008**, *61*, 216-222.

[41] Gamble, A. B.; Garner, J.; Gordon, C. P.; Conner, S. M. J.; Keller, P. A. *Syn. Comm*. **2007**, *37*, 2777-2786.

[42] Nagesh, H. N.; Suresh, A.; Reddy, M. N.; Suresh, N.; Subbalakshmi, J.; Sekhar, K. V. G. C. *RSC Advances* **2016**, *6*, 15884-15894.

[43] Miller, G. J.; Lin, J. I.; Young, V. *Acta Crystallographica Section C*, **1993**, *49*(10), 1770-1773.

[44] Sheldrick, G. M. SHELX-2014, University of Gottingen: Gottingen, Germany, 2014.

[45] Farrugia, L. J. *Journal of Applied Crystallography*, **1999**, *32*(4), 837-838.

Chapter 2: PartIII

Pharmacophore III: Pyrimidine and Aniline adducts

Contents

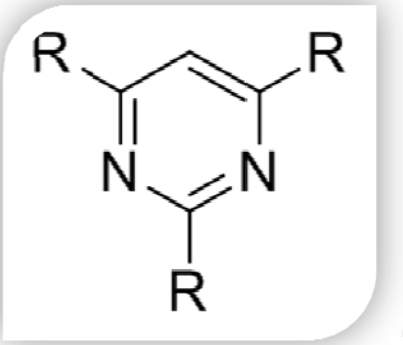

Abstract:

Here four pyrimidine linked aniline compounds have been synthesized. Pyrimidine drugs are used for the treatment of three main disease classes: anti-infective, cardiovascular, and oncological. The designing of molecule was driven by three different ways: (i) 2,4-linked pyrimidine derivatives with dimethyl amine group fixed at position 2; (ii) 4,6-linked pyrimidine derivatives with dimethyl amine fixed at position 4 and (iii) Use of derivatives of aniline in both the above cases. Overall synthesis was carried out in two steps. In the first step 2,4 or 4,6 dichloropyrimidine were treated with aniline and 4-methoxy aniline under ambient conditions. In the second step, S_NAr reaction was performed to insert dimethyl amine group either by direct insertion or by *in situ* formation. Single crystal of one of the derivatives shows the complete planar structure. Thus, present study concludes that N^2,N^2-dimethyl-N^4-phenylpyrimidine-2,4-diamine and its derivatives can be synthesized with high yields using the above strategy.

2.3.1: Introduction

Pyrimidine drugs are used for the treatment of three main disease classes: anti-infective, cardiovascular, and oncological [1]. Tyrosine kinase inhibitors like imatinib [2] have since been approved as oncological drugs, containing a pyrimidine group (dasatinib [3], pazopanib [4], and nilotinib [5]) are extensively used. Rosuvastatin, a top-selling pyrimidine drug with multibillion-dollar sales per year, is a member of the statin family [6]. Pyrimidine substitution pattern analysis reveals that the C2- (orange) and C4-positions (green) (*Figure 2.3.1*) are strongly favored, with 94% and 81% substitution frequency, respectively [1]. There is close to an even distribution of mono-, di-, tri- and tetrasubstituted pyrimidines. Almost all pyrimidine drugs contain a nitrogen substituent (88%) of which 38% are a 2-amino group and another 38% are 2,4-diamino groups.

Rilpivirine and etravirine [7] are the example of drugs with pyrimidine in core structure and with two nitrile groups, are the anti-HIV drugs. Many of the pyrimidine drugs contain multiple rings connected linearly. Minoxidine and etravirine are structurally remarkable for the fact that not only is the pyrimidine core tetrasubstituted but all of the substitutents are heteroatoms [1].

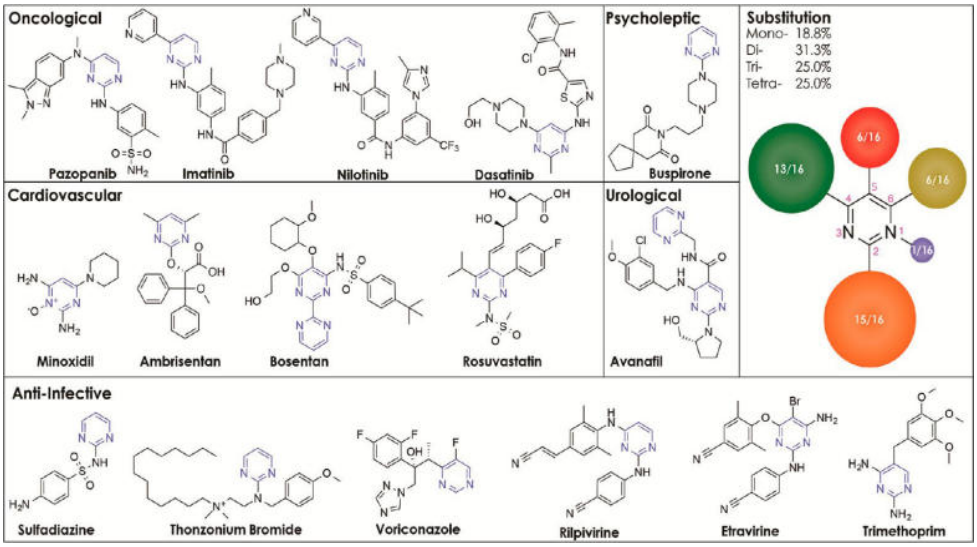

Figure 2.3.1: Pyrimidine core containing anti-cancer drugs in market. Fig adapted from ref [1]

2.3.2 Our Strategy

Our efforts were focused on synthesizing new pyrimidine linked aniline derivatives at one end and dimethyl amine on the other end, keeping PAINS (Pan Assay Interference Compounds) [8] structure in mind. Most PAINS function as reactive chemicals rather than discriminating drugs. The designing of compounds (*Figure 2.3.2*) were driven by three basic principles: (i) 2,4-linked pyrimidine derivatives with dimethyl amine group fixed at position 2; (ii) 4,6-linked pyrimidine derivatives with dimethyl amine fixed at position 4 and (iii) Derivatizing aniline derivatives in both the cases (*Figure 2.3.3*). Final product was obtained by two different reactions conditions (i) *in situ* formation of N, N-dimethyl amine and (ii) direct insertion of N, N- dimethyl amine.

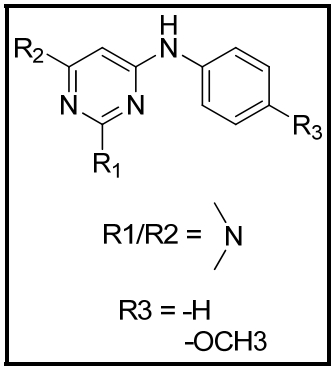

Figure2.3.2: Designing Strategy

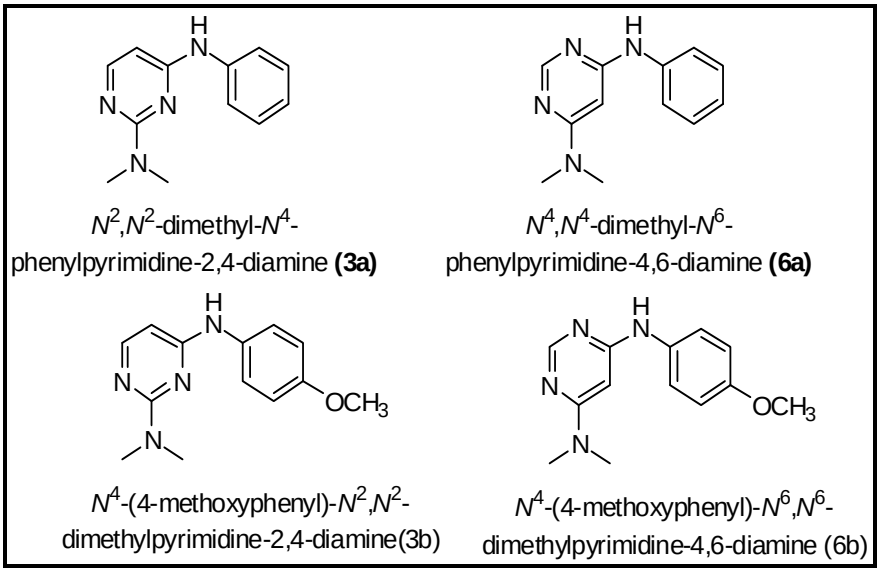

Figure 2.3.3: Synthesized four molecules in this chapter

2.3.3: Results and Discussion

Synthesis:

As discussed above in section 2.3.2, each strategy will be taken in detail now.

Strategy 1: The first strategy deals with the amination of the 2,4-dichloro pyrimidine at 4^{th} position using aniline. **2a** is synthesized by reacting 2,4-dichloro pyrimidine with aniline in presence of triethyl amine used as a base [9]. The solvent used for this reaction is ethanol. The reaction conditions, especially the solvent, are optimized to get the best yields. Reaction is performed at ambient conditions in an open vessel. Selective substitution at C-4 of pyrimidine is obtained. Owing to the inherent tendency towards 4-substitution of 2,4-dichloro pyrimidine, this is the only product obtained after reaction completion. The mole ratio of aniline:pyrimidine in reaction was maintained to be 1:1. In the first step, triethylamine was used as a base since, in this case, it proved better than any other base. The next step deals with the amination at second position. For this S_NAr reaction the two mechanisms were proposed by J.Muzart [10] as shown in *Figure 2.3.4*. This conversion of formation of compound **3** was achieved by the two different methods. Method 1: In this DMF was used as a solvent as well as the source of $N(Me)_2$. Potassium carbonate was used as the base. Reaction completion for different substrates was achieved in 20-24h and at high temperatures of 110-120°C [11]. Method 2: This method deals with the direct addition of dimethylamine, used slightly in excess. DIPEA (N,N-Diisopropylethylamine) proved to be the best bet in this case. Solvent trials showed that the best yields were obtained with THF (Tetrahydrofuran). Reaction completion was achieved at 70-75°C for 8-10h. Comparing the two above methods, method 2 proved to be slightly high yielding as compared to method 1. This is because in method one, amine is getting generated in situ, while in method 2 we are directly adding amine externally.

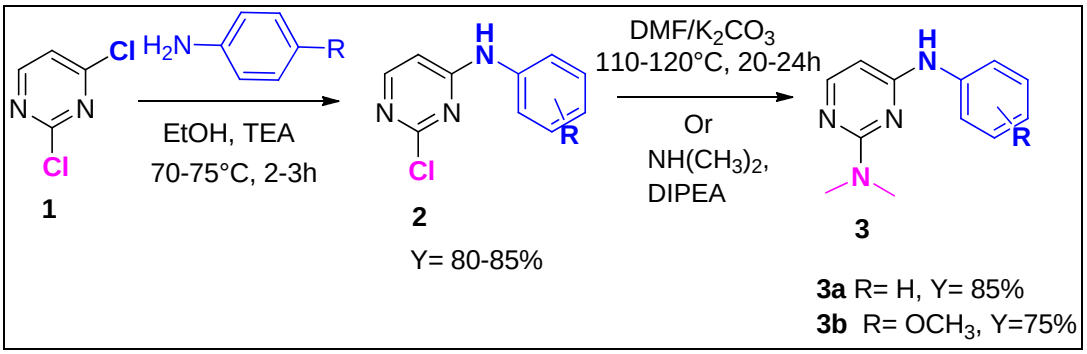

Scheme 2.3.1: Synthesis of 2,4 amine substituted pyrimidine

Mechanism:

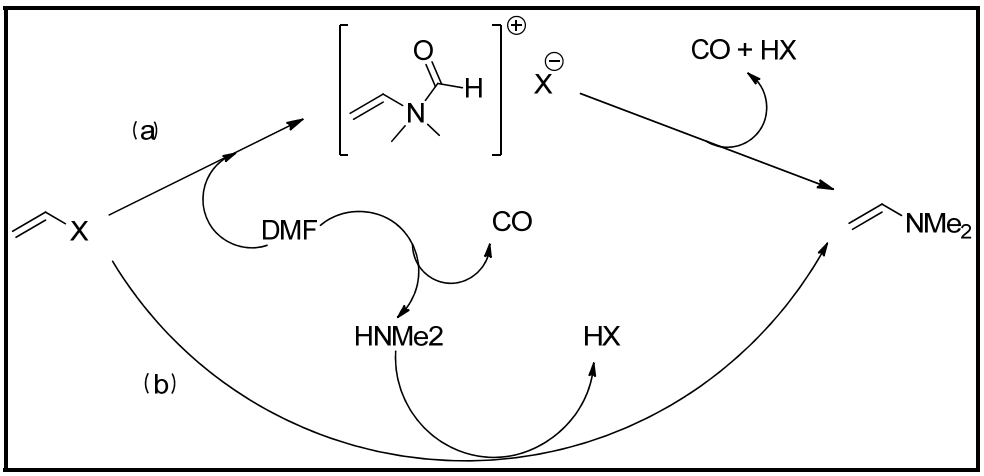

Figure2.3.3: Mechanism of $N(Me)_2$ insertion (adapted from reference 10)

Substitution reactions of aryl halides leading to dimethyl amines were carried out using DMF as the solvent and reactant as reported in the literature [11]. The two plausible mechanistic pathways were proposed by J.Muzart [10]. Path a gives the aminated product by direct attack of DMF on the aryl halide and then removal of carbon monoxide was achieved. On the other hand, path b involves the direct attack of dimethyl amine on aryl halide generated from the degeneration of the DMF due to high temperature (*Figure 2.3.4*).

Strategy 2: This strategy is planned to use 4,6-dichloro pyrimidine as the basic core. Keeping in mind the importance of substituting 4^{th} and 6^{th} positions of pyrimidine in

pharmaceutical drugs this was planned (*Scheme 2.3.2*). The reaction proceeds in a similar way as was discussed in strategy 1. The yields are slightly better in this case as compared to strategy 1.

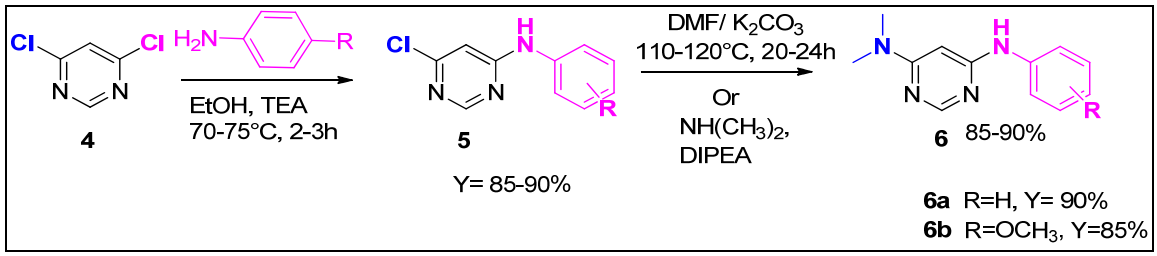

Scheme 2.3.2: Synthesis of 4,6 amine substituted pyrimidine

Strategy 3: In this we planned to derivatize the aniline system in search to get the best biologically active compounds. For derivatizing 4-methoxy aniline was used. The derivatives are listed as shown in Chart 1.

Spectral Analysis

^{1}H NMR spectra for all the compounds showed appropriate peaks for all the newly synthesized compounds. As expected, the only difference in the 2,4 and 4,6 substituted products will be clear cut two doublets observed for prior and two singlets observed for latter. The two doublets for 2,4 substituted derivatives appeared at 7.91-7.84 and 6.00-5.91 ppm. Similarly, the two singlets for 4,6 derivatives appeared at 8.16 and 5.82 ppm. Proton sandwiched in between the two nitrogens of the pyrimidine ring appears to be up field. The six methyl protons of the N-methyl amine appeared at 2.99-3.06 ppm.

^{13}CNMR spectra for all the compounds showed appropriate peaks for all the newly synthesized compounds.

Single Crystal Analysis

The crystallographic data, details of data collection and some important features of the refinement for compound 3a is given in *Table 2.3.1*. Crystals of suitable size of the molecule 3a were obtained by slow evaporation of the solvent. The data was collected on Oxford X-CALIBUR-S diffractometer with MoKα (λ = 0.71073) at 100K. The data interpretations were processed with CrysAlis Pro, Agilent Technologies, Version 1.171.35.19. An absorption correction based on multi-scan method was applied. All structures were solved by direct methods and refined by the full matrix least-square based on F^2 technique using SHELXL-97 program package. All calculations were carried out using WinGX system Ver- 1.64.

N^2,N^2-dimethyl-N^4-phenylpyrimidine-2,4-diamine **3a** got crystallized in orthorhombic crystal system with *Pbca* space group, with only one molecule in an asymmetric unit (*Figure 2.3.4*).

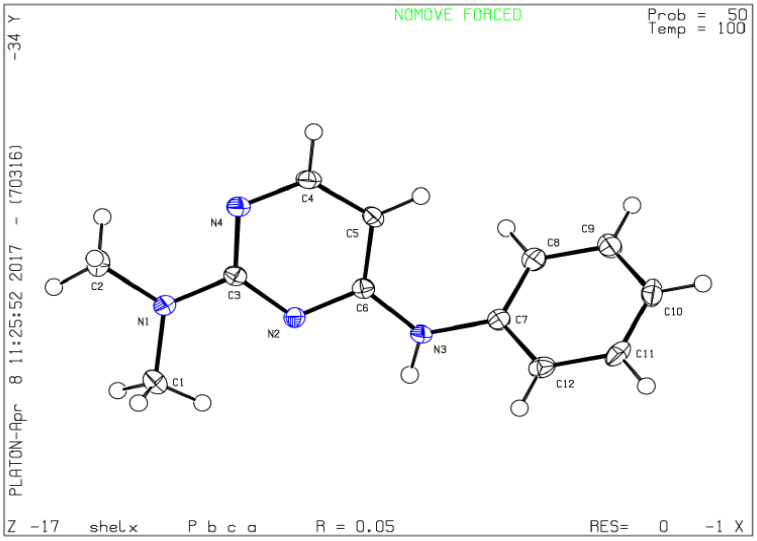

Figure 2.3.4: Molecular view of 3a having thermal ellipsoid are shown with 50% probability

Table 2.3.1:Crystallgraphic data and structure refinements for 3a

	3a
CCDC	1544619
Empirical formula	$C_{12}H_{14}N_4$
Formula weight	214.27
Temperature/K	100(2)
Crystal system	Orthorhombic
Space group	Pbca
a/Å	6.9596(4)
b/Å	11.4096(6)
c/Å	27.9387(16)
α/°	90
β/°	90
γ/°	90
Volume/Å^3	2218.5(2)
Z	8
ρ_{calc}g/cm^3	1.283
μ/mm^{-1}	0.081
F(000)	912.0
Crystal size/mm^3	0.5 × 0.4 × 0.2
Radiation	MoKα (λ = 0.71073)
2Θ range for data collection/°	6.54 to 55.234
Index ranges	$-9 \le h \le 9$, $-14 \le k \le 14$, $-36 \le l \le 36$
Reflections collected	55975
Independent reflections	2580 [R_{int} = 0.0780, R_{sigma} = 0.0323]
Data/restraints/parameters	2580/0/147
Goodness-of-fit on F^2	1.030
Final R indexes [I>=2σ (I)]	R_1 = 0.0522, wR_2 = 0.1067
Final R indexes [all data]	R_1 = 0.0757, wR_2 = 0.1164
Largest diff. peak/hole / e Å^{-3}	0.28/-0.44

2.3.3: Conclusion:

Four new molecules with two pharmacophore were conjoined together; pyrimidine linked aniline molecules were synthesized and thoroughly characterized. Designing of the molecules were done by the three strategies. Single crystal of one of the new derivative was obtained. Synthesis was achieved in two steps with high yields. The reaction was performed under ambient conditions.

2.3.4: Experimental Section:

Materials and methods:

All reactions were carried out in oven-dried glassware with magnetic stirring. Purification of reaction products was carried out by column chromatography using silica gel (60-120 mesh). Thin layer chromatography was performed on TLC Silica Gel 60 F254 (Merck). The spots were visualized under UV light or with iodine vapour. 1H-NMR spectra were recorded on Bruker Avance II 400 NMR spectrometer (400 MHz) and were run in CDCl3 unless otherwise stated. Signal multiplicity is denoted as singlet (s), doublet (d), doublet of doublets (dd), triplet (t), quartet (q), and multiplet (m). Mass spectra were recorded on Thermo-Fischer DSQ II GCMS instrument. Melting points were recorded in Thiele's tube using paraffin oil and are uncorrected.

Solvents were dried and purified by distillation under reduced pressure and stored on molecular sieves. All chemicals were purchased from Sigma-Aldrich Chemicals Limited, SD Fine, Sisco, Qualigens, Avara Chemicals Limited etc., and used without further purification.

Synthesis:

Synthesis of 2-chloro-*N*-phenylpyrimidin-4-amine (2a):

A three necked oven dried flask was charged with absolute ethanol (10ml). In that flask 2,4 dichloro pyrimidine (0.5g, 3.35mmol), aniline (0.32g, 3.35mmol) and triethyl amine (0.51g, 5.03mmol) were added and stirred at room temperature (30-35°C) for 15 mins. Then slowly, temperature of the reaction mass was raised to 70-75°C and maintained at

that temperature till completion via TLC (2h). After completion, solvent was evaporated using vacuum distillation. Water was added to the reaction mass and extracted with ethyl acetate (3 x 25ml). The organic layer was washed with water (2 x 10ml) and dried over sodium sulfate. The solution was then concentrated under reduced pressure to obtain a semi solid mass, which was purified by column chromatography on neutral alumina and petroleum ether-ethyl acetate mixture as eluent to give pure product.

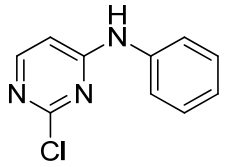 2a $C_{10}H_8ClN_3$ 205.6	White solid **Yield**: 85%; **^{1}H NMR (400MHz, CDCl3) δ** : 9.92 (s, 1H, NH), 8.10-8.09 (d, *J*=5.88Hz, 1H, H^6 Pyrimidine), 7.59-7.57 (d, *J*=7.96Hz, 2H, $H^{2,6}$ of aniline), 7.36-7.32 (t, *J*=7.56Hz, 2H, $H^{3,5}$ of aniline), 7.09-7.06 (t, *J*=7.36Hz, 1H, H^4 of aniline), 6.74-6.73 (d, *J*=5.88Hz, 1H, H^5 of Pyrimidine) ppm **MS(m/z):** 205.5 (M+, 100)

Synthesis of 2-chloro-*N*-(4-methoxyphenyl) pyrimidin-4-amine (2b):

A three necked oven dried flask was charged with absolute ethanol (10ml). In that flask 2,4 dichloropyrimidine (0.5g, 3.35mmol), 4-methoxyaniline (0.41g, 3.35mmol) and triethyl amine (0.51g, 5.03mmol) were added and stirred at room temperature (30-35°C) for 15 mins. Then slowly, temperature of the reaction mass was raised to 70-75°C and maintained at that temperature till completion via TLC (3h). After completion solvent was evaporated using vacuum distillation. Water was added to the reaction mass and extracted with ethyl acetate (3 x 25ml). The organic layer was washed with water (2 x 10ml) and dried over sodium sulfate. The solution was then concentrated under reduced pressure to obtain a semi solid mass, which was purified by column chromatography on neutral alumina and petroleum ether-ethyl acetate mixture as eluent to give pure product.

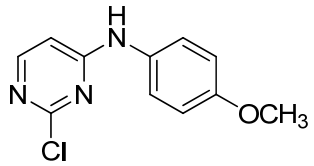 2b $C_{11}H_{10}ClN_3O$ 235.6	White solid **Yield**: 80%; **MS(m/z):** 235.5 (M^+, 100)

Synthesis of 6-chloro-*N*-phenylpyrimidin-4-amine (5a)

A three necked oven dried flask was charged with absolute ethanol (10ml). In that flask 2,4 dichloro pyrimidine (0.5g, 3.35mmol), aniline (0.31g, 3.35mmol) and triethyl amine (0.51g, 5.03mmol) were added and stirred at room temperature (30-35°C) for 15 mins. Then slowly, temperature of the reaction mass was raised to 70-75°C and maintained at that temperature till completion via TLC (2h). After completion, solvent was evaporated using vacuum distillation. Water was added to the reaction mass and extracted with ethyl acetate (3 x 25ml). The organic layer was washed with water (2 x 10ml) and dried over sodium sulfate. The solution was then concentrated under reduced pressure to obtain a semi solid mass, which was purified by column chromatography on neutral alumina and petroleum ether-ethyl acetate mixture as eluent to give pure product.

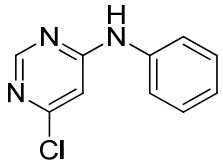 5a $C_{10}H_8ClN_3$ 205.6	White solid **Yield**: 90%; **^{1}H NMR (400MHz, CDCl3) δ** : 9.92 (s, 1H, NH), 8.10-8.09 (d, *J*=5.88Hz, 1H, H^6 Pyrimidine), 7.59-7.57 (d, *J*=7.96Hz, 2H, $H^{2,6}$ of aniline), 7.36-7.32 (t, *J*=7.56Hz, 2H, $H^{3,5}$ of aniline), 7.09-7.06 (t, *J*=7.36Hz, 1H, H^4 of aniline), 6.74-6.73 (d, *J*=5.88Hz, 1H, H^5 of Pyrimidine) ppm **MS(m/z):** 205.5 (M+, 100)

Synthesis of 6-chloro-*N*-(4-methoxyphenyl) pyrimidin-4-amine (5b)

A three necked oven dried flask was charged with absolute ethanol (10ml). In that flask 2,4 dichloro pyrimidine (0.5g, 3.35mmol), 4-methoxyaniline (0.41g, 3.35mmol) and triethyl amine (0.51g, 5.03mmol) were added and stirred at room temperature (30-35°C) for 15 mins. Then slowly, temperature of the reaction mass was raised to 70-75°C and maintained at that temperature till completion via TLC (3h). After completion, solvent was evaporated using vacuum distillation. Water was added to the reaction mass and extracted with ethyl acetate (3 x 25ml). The organic layer was washed with water (2 x 10ml) and dried over sodium sulfate. The solution was then concentrated under reduced pressure to obtain a semi solid mass, which was purified by column chromatography on neutral alumina and petroleum ether-ethyl acetate mixture as eluent to give pure product.

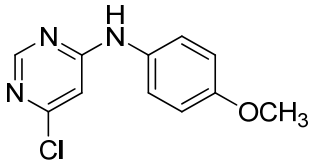 5b $C_{11}H_{10}ClN_3O$ 235.6	White solid **Yield**: 85%; **^{1}H NMR (400MHz, CDCl3) δ** : 9.92 (s, 1H, NH), 8.10-8.09 (d, *J*=5.88Hz, 1H, H^6 Pyrimidine), 7.59-7.57 (d, *J*=7.96Hz, 2H, $H^{2,6}$ of aniline), 7.36-7.32 (t, *J*=7.56Hz, 2H, $H^{3,5}$ of aniline), 7.09-7.06 (t, *J*=7.36Hz, 1H, H^4 of aniline), 6.74-6.73 (d, *J*=5.88Hz, 1H, H^5 of Pyrimidine) ppm **MS (EI) m/z** : 235.5 (M+, 100)

Synthesis of N^2,N^2-dimethyl-N^4-phenylpyrimidine-2,4-diamine (3a)

Synthesis of the title molecule was achieved via two procedures, stated below:

Strategy 1: In a three necked oven dried flask was charged with dried DMF (15ml). In that flask 2a (1g, 4.86 mmol) and potassium carbonate (2.78g, 14.59 mmol) was added. Under nitrogen atmosphere the reaction mass was stirred at room temperature (30-35°C) for 10-15mins. Slowly temperature was raised to 110-120°C. Maintained at that temperature till completion of the reaction monitored via TLC (22-24h). Cooled reaction

mass and then poured into cold water and extracted with ethyl acetate (3 x 25ml). The organic layer was washed with water (2 x 10ml) and dried over magnesium sulfate. The solution was then concentrated under reduced pressure to obtain a semi solid mass, which was purified by column chromatography on neutral alumina and petroleum ether-ethyl acetate mixture as eluent to give the desired compound.

Strategy 2: In a three necked oven dried flask was charged with isopropyl alcohol (10ml). In that flask 2a (1g, 4.86 mmol), K_2CO_3 (2.68g, 19.4 mmol) and dimethyl amine hydrochloride (0.79g, 9.72 mmol) was charged. Stirred reaction mass at room temperature (30-35°C) for 15 mins. Then slowly temperature of the reaction mass was raise to 70-75°C and maintained at that temperature till completion via TLC (8h). After completion solvent was evaporated under high vacuum. Water was added to the reaction mass and extracted with ethyl acetate (3 x 25ml). The organic layer was washed with water (2 x 10ml) and dried over magnesium sulfate. The solution was then concentrated under reduced pressure to obtain a semi solid mass, which was purified by column chromatography on neutral alumina and petroleum ether-ethyl acetate mixture as eluent to give pure product.

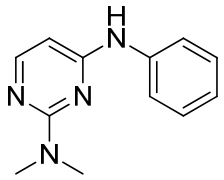 3a $C_{12}H_{14}N_4$ 214.2	Yellowish white solid **Yield**: 85%; **^{1}H NMR (400MHz, DMSO-d$_6$) δ** : 9.20 (s, 1H, NH), 7.91-7.89 (d, *J*=6Hz, 1H, H^6 Pyrimidine), 7.71-7.69 (d, *J*=7.6Hz, 2H, $H^{2,6}$ of aniline), 7.30-7.26 (t, *J*=7.6Hz, 2H, $H^{3,5}$ of aniline), 6.95-6.92 (t, *J*=7.6Hz, 1H, H^4 of aniline), 6.00-5.99(d, *J*=5.6Hz, 1H, H^5 of Pyrimidine), 3.09 (s, 6H, $N(CH_3)_2$) ppm **^{13}C NMR (100MHz, DMSO-d$_6$) δ**: 162.1, 160.6, 156.3, 140.9, 129.0, 121.8, 119.5, 96.2, 37.1 ppm **MS (EI) m/z** : 214.26(M+, 100) (*Figure 2.3.5, 2.3.6, 2.3.7*)

Synthesis of N^4,N^4-dimethyl-N^6-phenylpyrimidine-4,6-diamine (6a)

Synthesis of the title molecule was achieved following the same procedure as described for 3a.

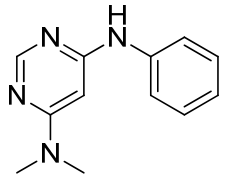 6a $C_{12}H_{14}N_4$ 214.2	Yellowish white solid **Yield**: 85%; **^{1}H NMR (400MHz, DMSO-d$_6$) δ** : 9.03 (s, 1H, NH), 8.16(s, 1H, H^2 Pyrimidine), 7.60-7.58 (d, *J*=7.6Hz, 2H, $H^{2,6}$ of aniline), 7.27-7.23 (t, *J*=7.6Hz, 2H, $H^{3,5}$ of aniline), 6.93-6.89 (t, *J*=7.6Hz, 1H, H^4 of aniline), 5.82(s, 1H, H^5 of Pyrimidine), 2.98 (s, 6H, $N(CH_3)_2$) ppm **^{13}C NMR (100MHz, DMSO-d$_6$) δ**: 162.6, 161.0, 157.5, 141.3, 129.1, 121.6, 120.2, 119.7, 83.6, 37.0 ppm **MS (EI) m/z** : 214.26(M+, 100) (*Figure 2.3.8, 2.3.9, 2.3.10, 2.3.11*)

Synthesis of N^4-(4-methoxyphenyl)-N^2,N^2-dimethylpyrimidine-2,4-diamine (3b)

Synthesis of the title molecule was achieved following the same procedure as described for **3a**.

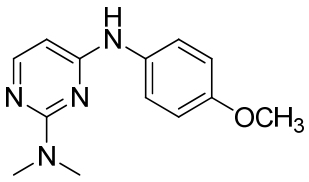 3b $C_{13}H_{16}N_4O$ 244.2	Off-white solid **Yield**: 85% **^{1}H NMR (400MHz, DMSO-d$_6$) δ** : 9.02 (s, 1H, NH), 7.85-7.84 (d, *J*=6Hz, 1H, H^6 Pyrimidine), 7.58-7.56 (d, *J*=8.8Hz, 2H, $H^{2,6}$ of aniline), 6.89-6.86 (d, *J*=9.2Hz, 2H, $H^{3,5}$ of aniline), 5.92-5.91(d, *J*=5.6Hz, 1H, H^5 of Pyrimidine),3.71(s, 3H, OCH_3), 3.06 (s, 6H, $N(CH_3)_2$) ppm **^{13}C NMR (100MHz, DMSO-d$_6$) δ**: 162.2, 160.6, 156.0, 154.6, 134.01, 121.4, 114.2, 95.7, 55.5, 37.1 ppm **MS (EI) m/z**: 244.29(M+, 100) (*Figure 2.3.12, 2.3.13, 2.3.14, 2.3.15*)

Synthesis of N^4-(4-methoxyphenyl)-N^6,N^6-dimethylpyrimidine-4,6-diamine (6b):

Synthesis of the title molecule was achieved following the same procedure as described for **3a**.

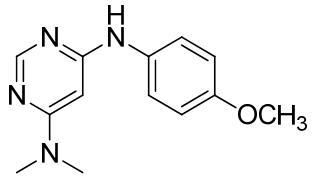 6b $C_{13}H_{16}N_4O$ 244.2	Reddish white solid **Yield**: 85% **^{1}H NMR (400MHz, DMSO-d$_6$) δ** : 8.76 (s, 1H, NH), 8.11 (s, 1H, H^2 Pyrimidine), 7.44-7.42 (d, *J*=8.8Hz, 2H, $H^{2,6}$ of aniline), 6.87-6.85 (d, *J*=8.8Hz, 2H, $H^{3,5}$ of aniline), 5.70(s, 1H, H^5 of Pyrimidine), 3.71 (s, 3H. – OCH_3), 2.50 (s, 6H, $N(CH_3)_2$) ppm **^{13}C NMR (100MHz, DMSO-d$_6$) δ**: 162.6, 161.3, 157.5, 154.9, 134.1, 122.1, 114.4, 82.5, 55.6, 37.0 ppm (*Figure 2.3.16, 2.3.17*)

2.3.5 Selected Spectral Data

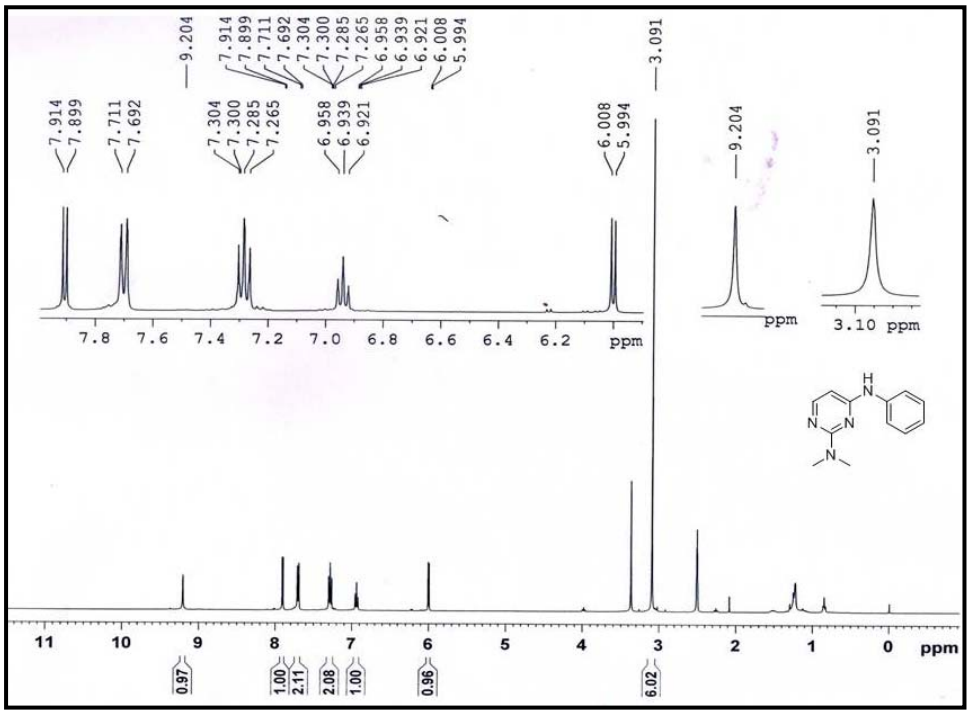

Figure 2.3.5: ^{1}H NMR spectra of 3a

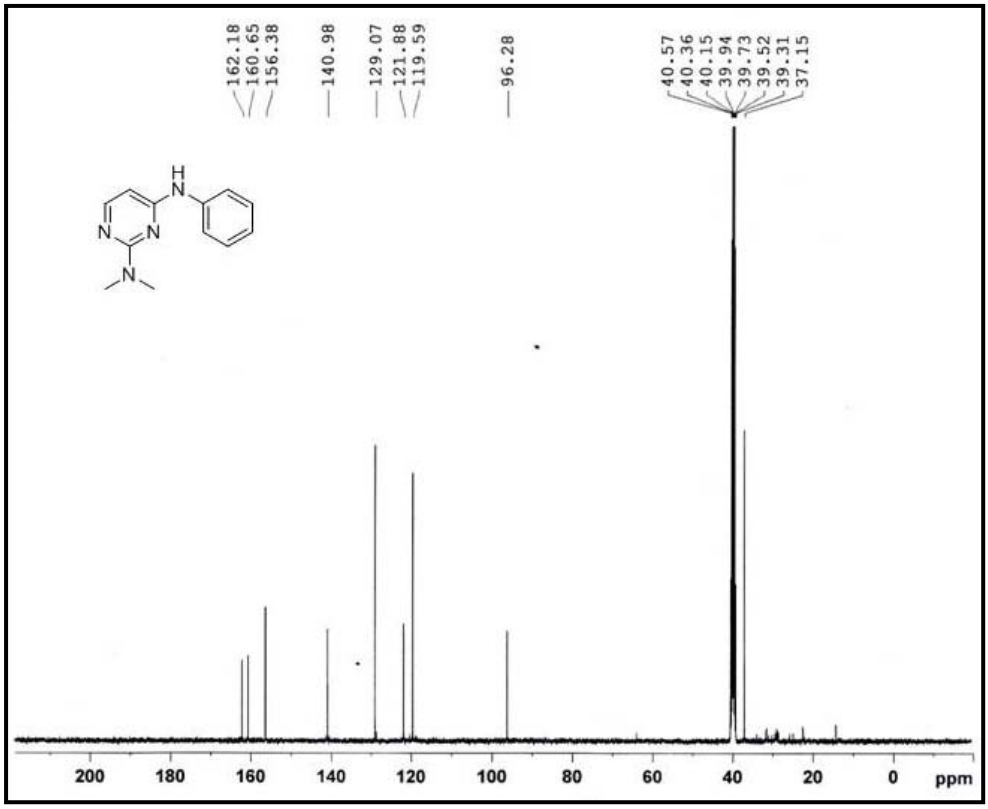

Figure2.3.6: ^{13}C NMR spectra of 3a

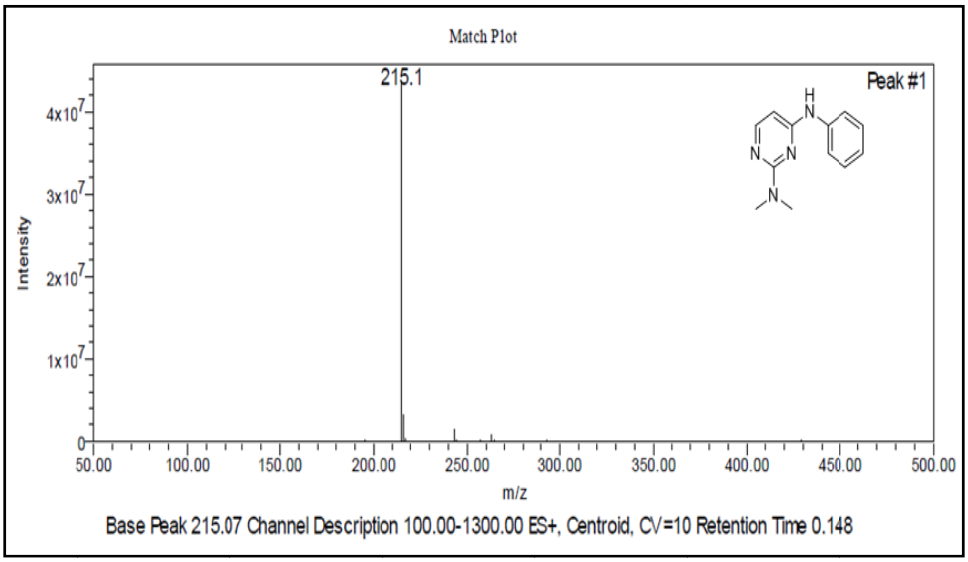

Figure 2.3.7: Mass spectra of 3a

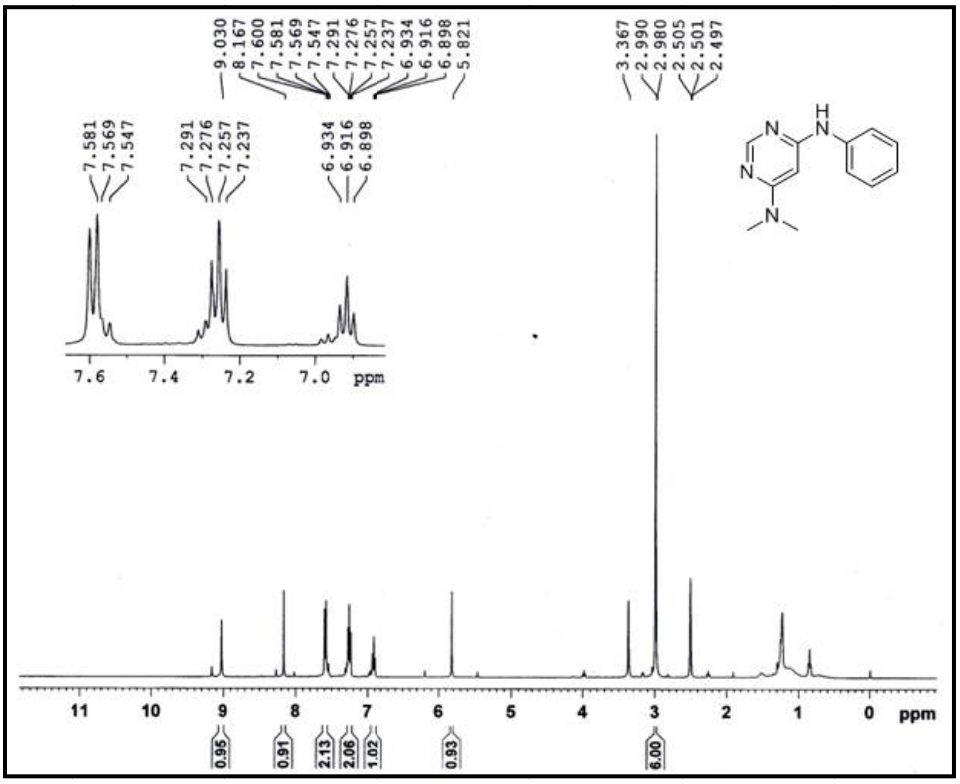

Figure 2.3.8: ^{1}H NMR spectra of 6a

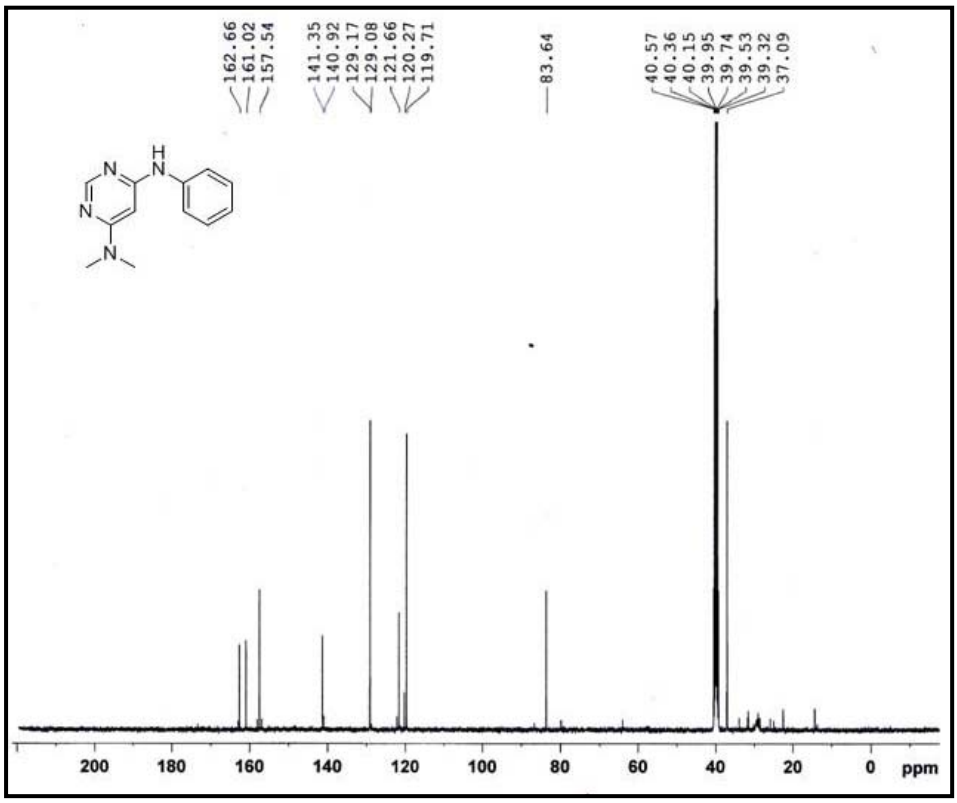

Figure 2.3.9: ^{13}C NMR spectra of 6a

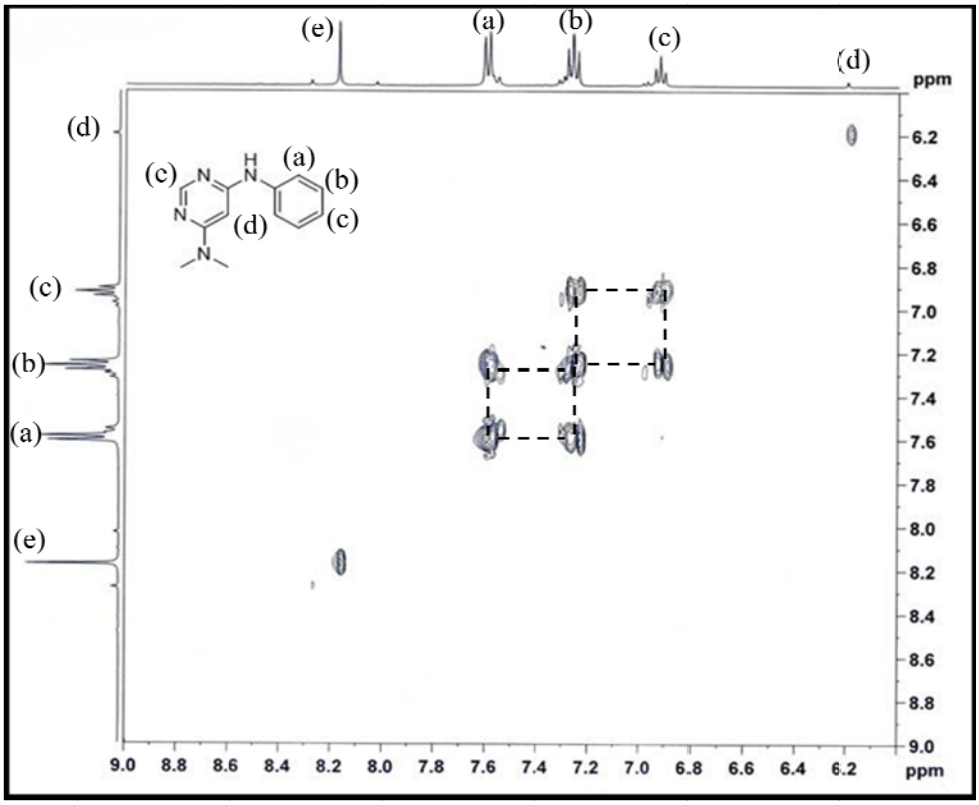

Figure 2.3.10: COSY Spectra of 6a

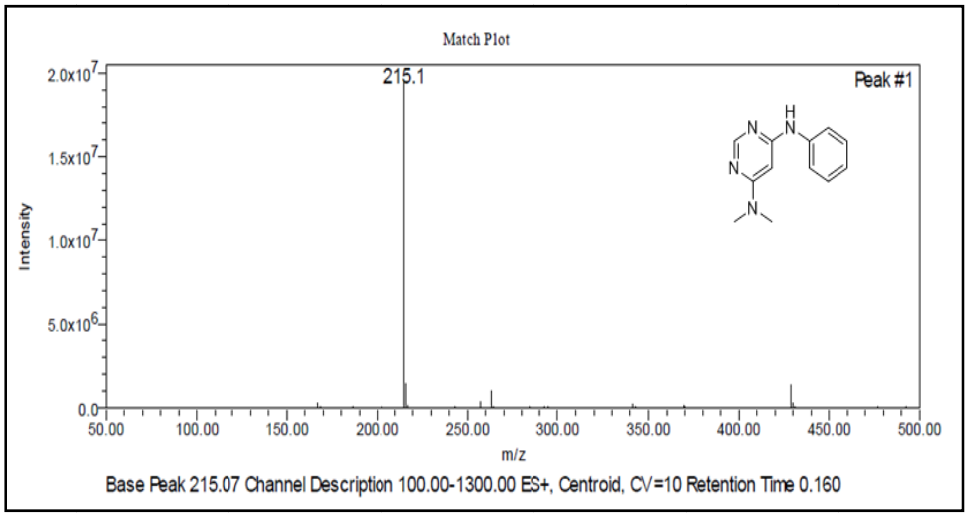

Figure 2.3.11: Mass spectra of 6a

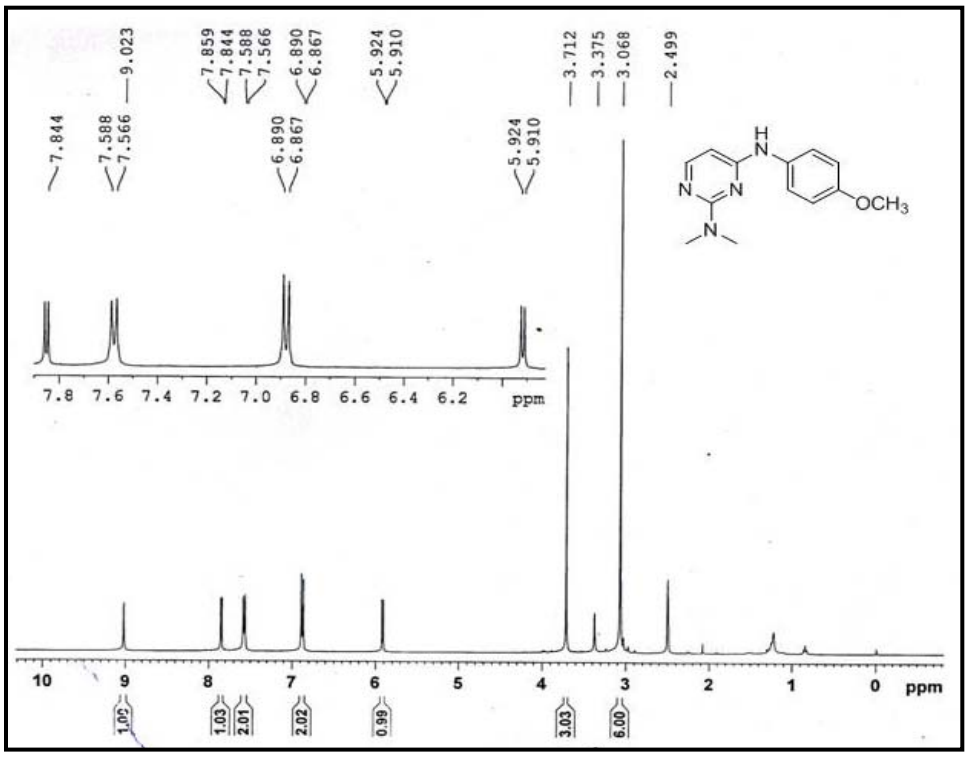

Figure 2.3.12: [1]HNMR spectra of 3b

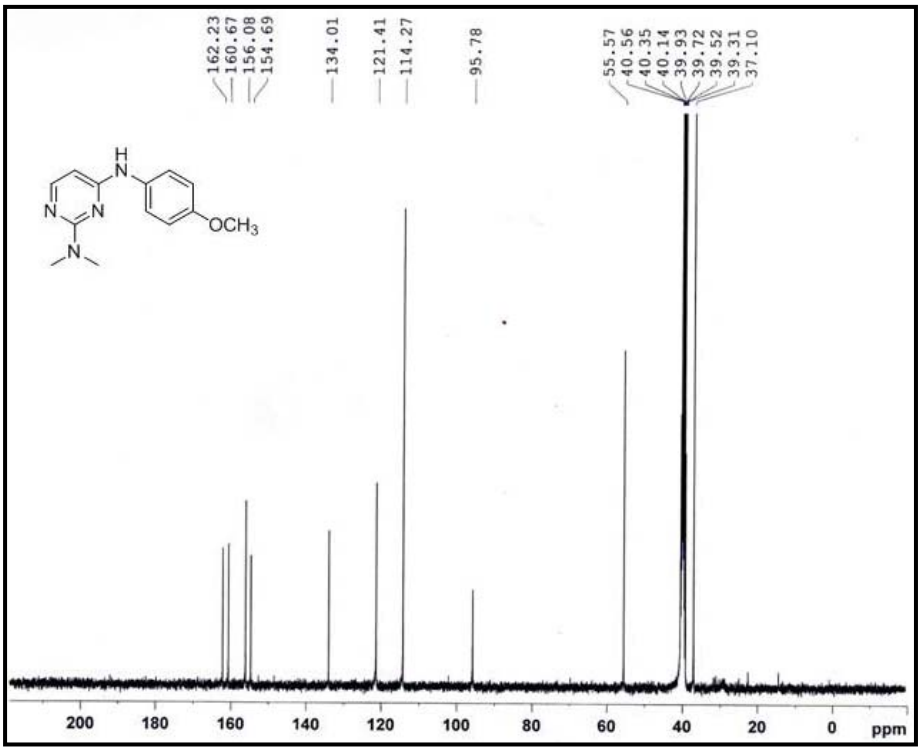

Figure 2.3.13: [13]C NMR spectra of 3b

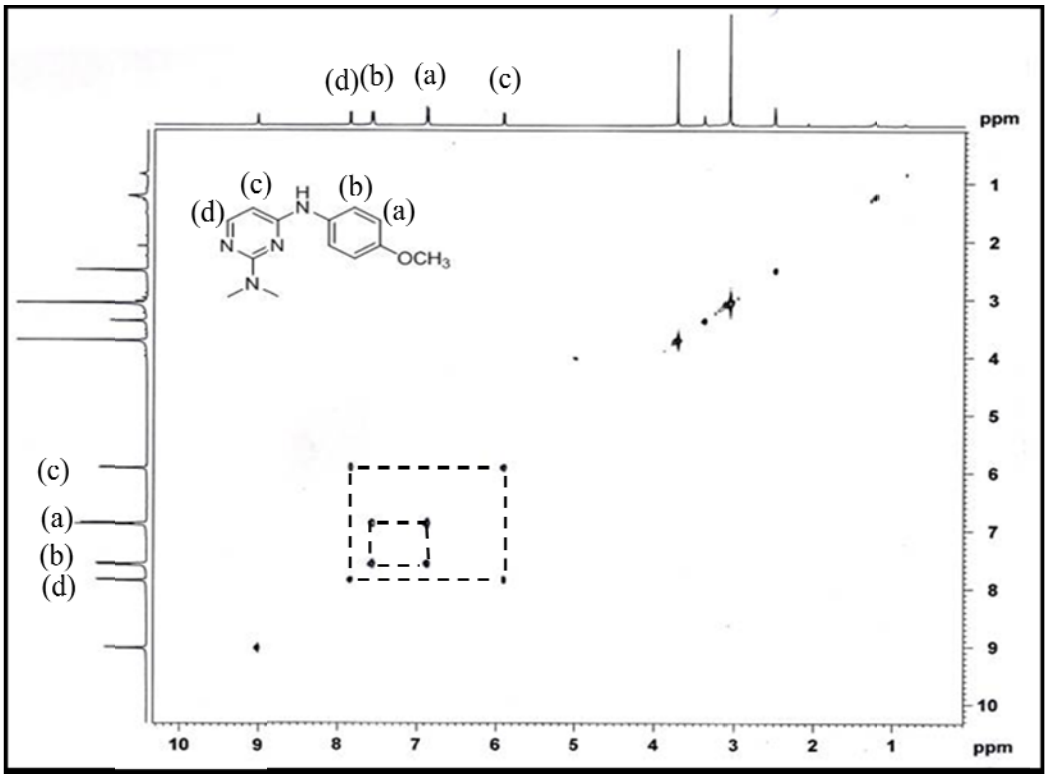

Figure 2.3.14: COSY spectra of 3b

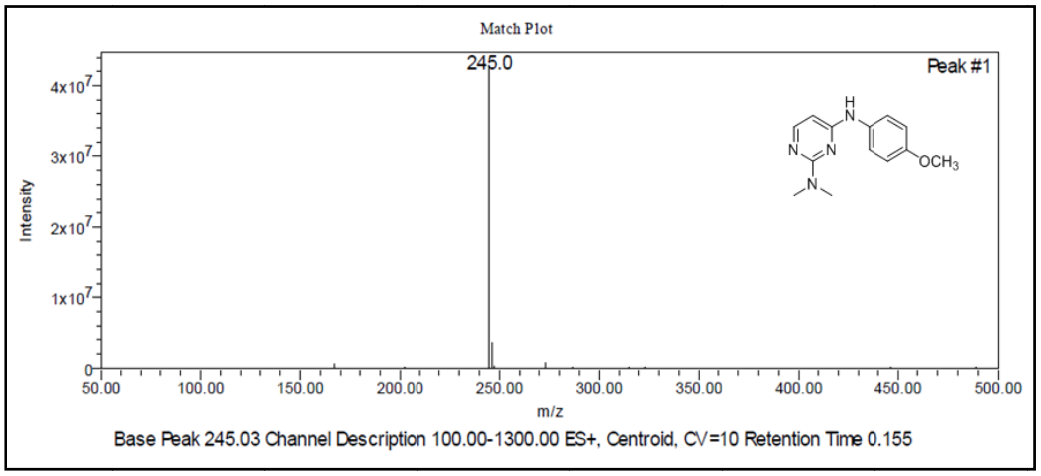

Figure 2.3.15: Mass spectra of 3b

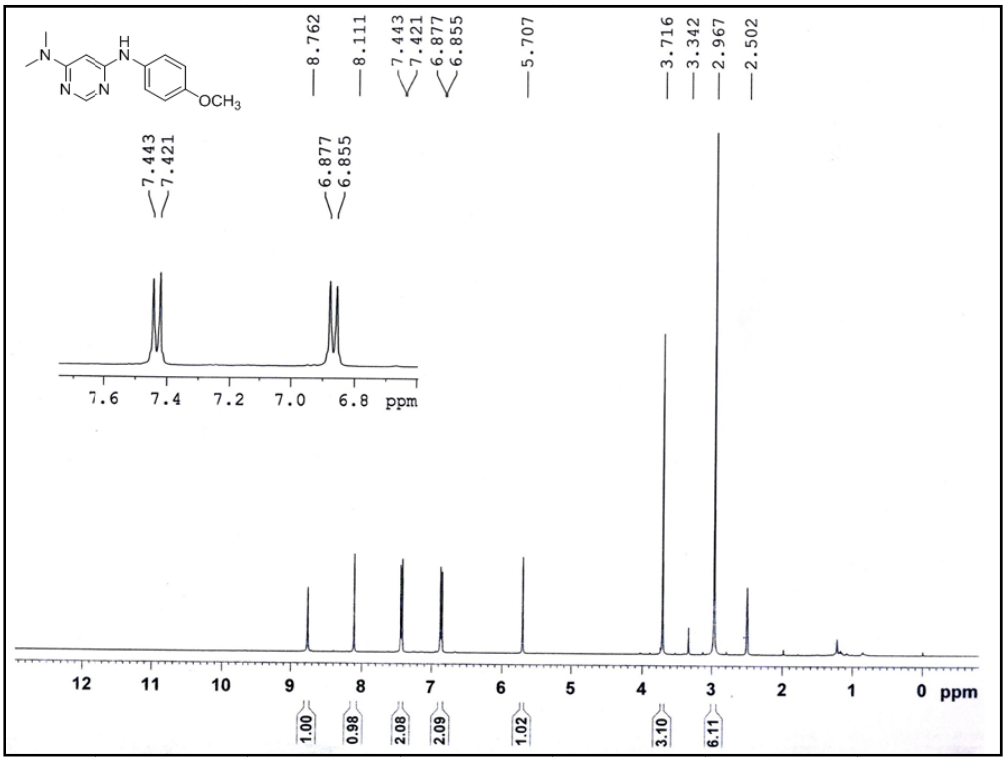

Figure 2.3.16: ^{1}H NMR spectra of 6b

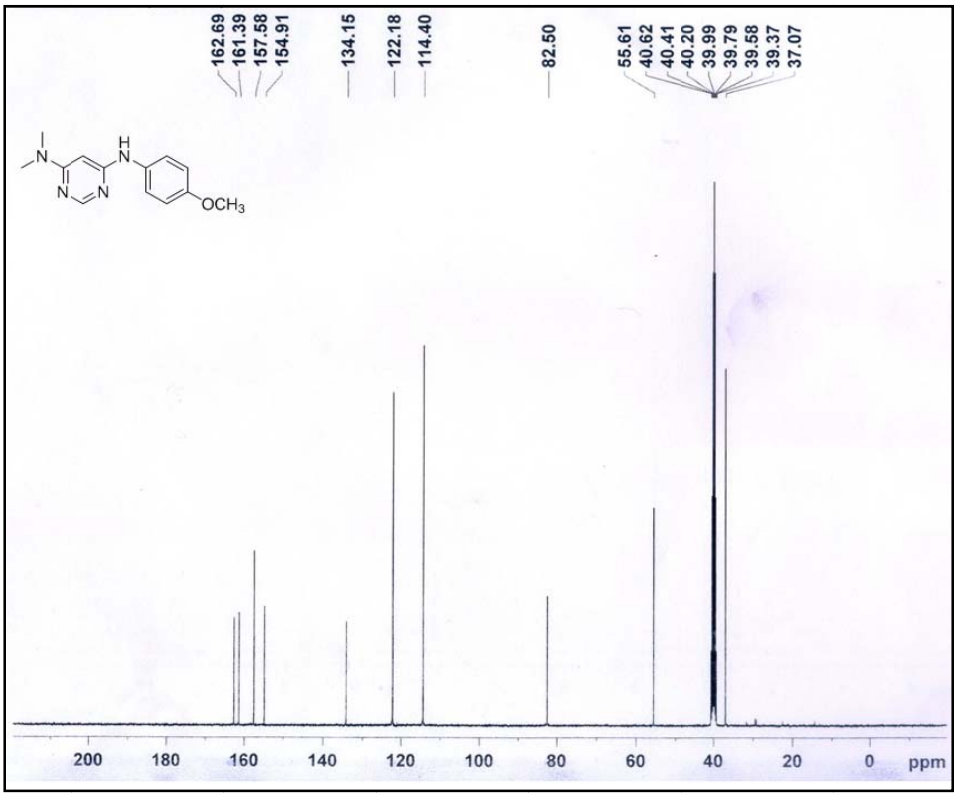

Figure 2.3.57: ^{13}C NMR spectra of 6b

2.3.6: References:

[1] Vitaku E.; Smith D. T.; Njardarson J. T. *J. Med. Chem.*, **2014**, 57, 10257-10274.

[2] Manley, P. W.; Cowan-Jacob, S. W.; Buchdunger, E.; Fabbro, D.; Fendrich, G.; Furet, P.; Meyer, T.; Zimmermann, J. *European Journal of Cancer*, **2002**, *38*, S19-S27.

[3] Christiansson, L.; Söderlund, S.; Mangsbo, S.; Hjorth-Hansen, H.; Höglund, M.; Markevärn, B.; Richter, J.; Stenke, L.; Mustjoki, S.; Loskog, A.; Olsson-Strömberg, U. *Molecular cancer therapeutics*, **2015**, *14*, 1181-1191.

[4] Sonpavde, G.; Hutson, T. E. *Current oncology reports*, **2007**, *9*, 115-119.

[5] (a) Le Coutre, P.; Ottmann, O. G.; Giles, F.; Kim, D. W.; Cortes, J.; Gattermann, N.; Apperley, J. F.; Larson, R. A.; Abruzzese, E.; O'Brien, S. G.;Kuliczkowski, K. *Blood*, **2008**, *111*, 1834-1839. (b) Kantarjian, H. M.; Giles, F.; Gattermann, N.; Bhalla, K.; Alimena, G.; Palandri, F.; Ossenkoppele, G. J.; Nicolini, F. E.; O'Brien, S. G.; Litzow, M.; Bhatia, R. *Blood*, **2007**, *110*, 3540-3546.

[6] Kim, Y. S.; Ahn, Y.; Hong, M. H.; Kim, K. H.; Park, H. W.; Hong, Y. J.; Kim, J. H.; Kim, W.; Jeong, M. H.; Cho, J. G.; Park, J. C. *Journal of cardiovascular pharmacology*, **2007**, *49*, 376-383.

[7] Fulco, P. P.; McNicholl, I. R. *Pharmacotherapy: The Journal of Human Pharmacology and Drug Therapy*, **2009**, *29*, 281-294.

[8] Baell, J.; Walters, M. A. *Nature* **2014**, 513, 481.

[9] Breault, G. A.; Pease, J. E. PCT Int Appl WO 2000012485. In *Chem Abstr* **2000**, *132*, 194385.

[10] Muzart, J. *Tetrahedron*, **2009**, *65*, 8313-8323.

[11] Agarwal, A.; Chauhan, P. M. *Synthetic Communications*, **2004**, *34*, 2925-2930.

Chapter 2: Part IV

Pharmacophore:IV. Benzimidazole and Aniline Adducts

Contents

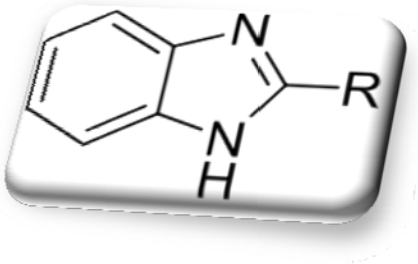

Abstract:

This chapter presents the synthesis of three novel benzimidazole linked aniline derivatives. Cyclisation of respective diamine group followed by two substitution reactions to give the required product molecules is the overall strategy. Construction of *N*-((1*H*-benzo[*d*]imidazol-2-yl)methyl)-4-methyl-*N*-(4-methylbenzyl)aniline and its derivatives were achieved in high yields.

2.4.1 Introduction:

Benzimidazole and its derivatives are an important class of compounds, not only for their pharmaceutical uses but also for their industrial applications such as chemical UVB filters [1], pigments[2], optical brighteners[3] and thermo stable membranes[4] for fuel cells[5].

The importance of benzimidazole in the pharmaceutical industry is due to its structural similarity with various biological compounds such as purine base of the DNA and vitamin B_{12}. This similarity is believed to help its easy recognition by various biological systems. Therefore, benzimidazole has been termed as 'privileged structures' for drug design [6]. Its affinity for various enzymes and protein receptors keeps biological chemists interested in exploring the new derivatives. So far many Benzimidazole compounds have been successfully developed as clinical drugs such as antihistaminic astemizole, anti-anabrotic Omeprazole, antiparasiticalbendazole and anti-hypertensive Candesartan, and have been prevalently used in the treatment of various diseases (*Figure 2.4.1*).

Benzimidazole can be viewed as a benzene fused imidazole structure, which can readily interact with various active targets in biological system via diverse non-covalent interactions like hydrogen bonds, coordination, ion-dipole, cation-π, π-π, stacking and hydrophobic effect as well as Van der Waals force [7], thus resulting in observed bioactivities.

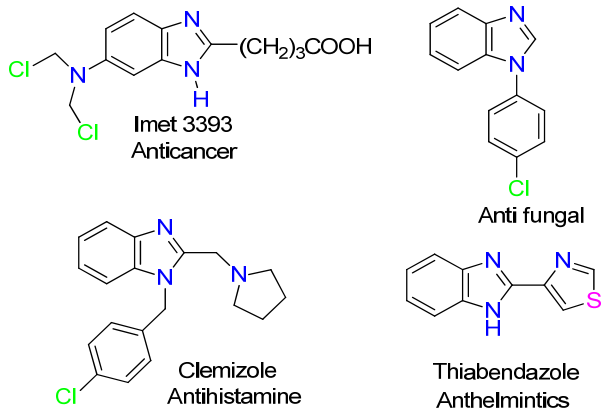

Figure 2.4.1: FDA approved benzimidazole derivatives as drug candidates

2.4.2 Our Strategy:

Continuing with the discovery of new biologically active compounds, the efforts in this chapter are focused on benzimidazole linked aniline derivatives (*Figure 2.4.2*).After zooming in on the target molecule, retro synthetic strategy was employed for choosing starting materials by FGI and disconnections. The overall synthesis was divided into two parts: (i) synthesis of electrophilic synthon viz cyano benzyl or toluyl methyl ring (*Part-B in Figure 2.4.2*). (ii) Synthesis of benzimidazole ring with electrophilic centre at its second position for nucleophilic substitution reaction (*Part-A in Figure 2.4.2*).

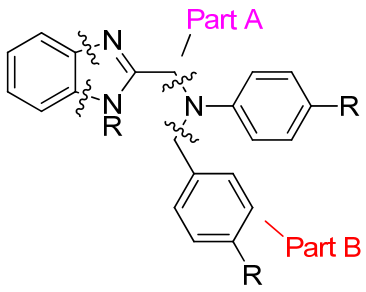

Figure 2.4.2: Retro synthesis of designing benzimidazole-aniline adducts

2.4.3 Results and Discussions:

2.4.3.1 Synthesis:

Efforts were focused on synthesizing new benzimidazole linked aniline derivatives, keeping PAINS (Pan Assay Interference Compounds) [9] structure in mind. Most PAINS function as reactive chemicals rather than discriminating drugs.

The synthesis of 2-methyl-1H-benzo[d]imidazole-5-carbonitrile **5** (*Scheme 2.4.1*) commenced by derivatizing *o*-nitoaniline. Among a range of iodination methods examined, the I_2/H_2O_2 method was found to be optimal; offering easy attachmentsto the direct benzene ring furnishing molecule **2.**Hydrogen peroxide was added as the oxidant and the reaction temperature was maintained at 25-30°C [10]. Direct iodination of o-phenylenediamine was also tried using various methods such as $I_2/NaIO_4$ and KI/KIO_3 but unfortunately the trial met failure every time. Following this, the next step was the nucleophilic substitution of iodo to cyano using eco friendly copper cyanidefurnishing

molecule **3** [11]. To generate *o*-phenylenediamine derivative **4**, reduction of nitro was performed using iron. Other possibility was to do reduction first, to get 4-iodobenzene-1,2-diamine and then perform cyanation reaction to yield 3,4-diaminobenzonitrile but no product was obtained. 2-methyl benzimidazole derivative **5** was formed by using the standard cyclisation method using acetic acid and hydrochloric acid[12]. Acetic acid reacts slowly with *o*- phenylene diamine derivative hence necessitating the addition of hydrochloric acid. Here we planned to further derivatize the methyl end of benzimidazole. The first step for this was to prepare the halo derivative, but unfortunately it met failure. The reason behind it may be the formation of amine salt after the generation of HCl which finally deactivates the molecule.

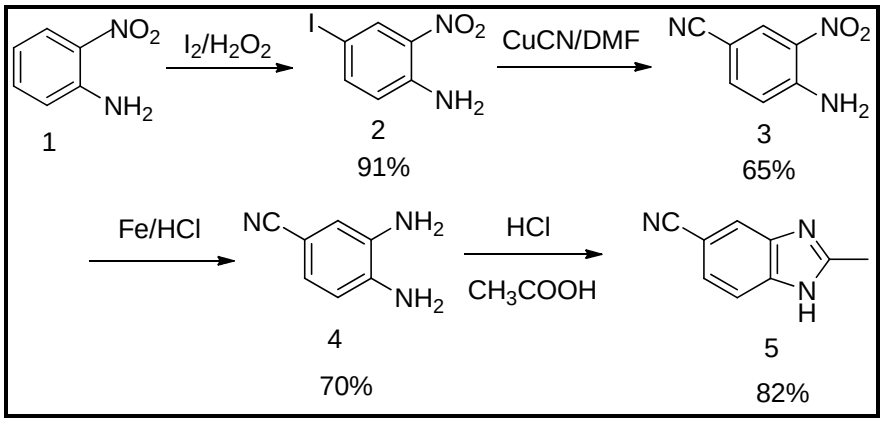

Scheme 2.4.1: Synthesis of 5-cyano-2-methyl benzimidazole

The strategy was designed to prepare 4-(bromomethyl)benzonitrile such that all the steps were high yielding (Scheme 2.4.2). Starting with the commercially available toludine, first step was the conversion of amine to iodo **6** using standard diazotization method [13]. The method for cyanation was the same as discussed above. It was the next step yielding molecule **7** [15]. To achieve the final step synthesis, bromobenzyl derivative **8**, starting material was treated with NBS [14].

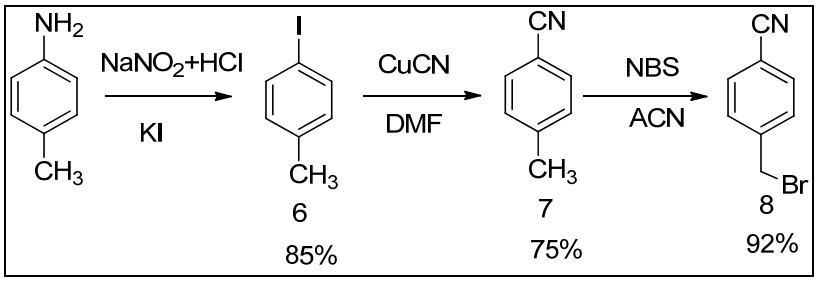

Scheme 2.4.2: Synthesis of 4-(bromomethyl)benzonitrile

The xylene bromination (*Scheme 2.4.3*) was also performed in a similar way as we have discussed for molecule **8**in the previous section (*Scheme 2.4.2*) [14].These synthesized bromo derivatives (**8, 9** and**10**) were further used in scheme 2.4.4 to get the novel benzimidazoles linked aniline adducts.

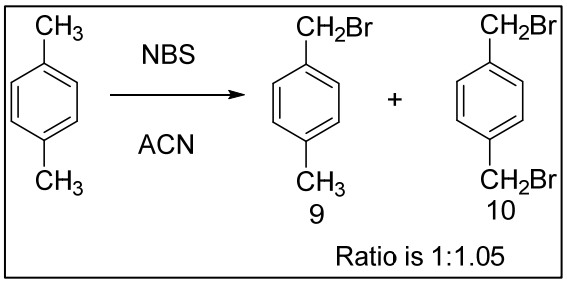

Scheme 2.4.3: Synthesis of bromo derivative of xylene

The ratio of the mono and di-derivative in the *scheme 2.4.3* for 9:10 was 20:21 by mole ratio. The mole ratio of NBS used was in slight excess. As per TLC, the two reactions proceed in competition with each other, resulting in the formation of both the products in the same time. The isolation step for this reaction was little tedious as the products formed were very volatile and lacrymatric and difficult to handle.

The overall synthesis of benzimidazole linked aniline adducts is shown in scheme 2.4.4. The synthesis of 2-chloro benzimidazole derivative **11**was obtained following the scheme *2.4.1* [11].Molecule **12** was synthesized via S_N2 reaction mechanism using *p*-toluidine [16]. The nucleophilic substitution of bromo derivatives (**8** and **9**) with 12 furnished the final product **13**, **14** and **15**. Interestingly we observed that for compound **12** when 4-methyl benzylbromide was subjected in the ratio of 1 or 1.5, both the products **13**and**14** were formed [16]. Hence, we can conclude that the reactions, di and mono substitution

are competing with each other. On the other hand, when we consider the cyano benzyl derivative**15**, the product formed was mono substituted cyano derivative, and the di product formed was comparatively very less with lot of other reaction products. Literature also showed synthesis of compounds similar to **13** and **15** [17].

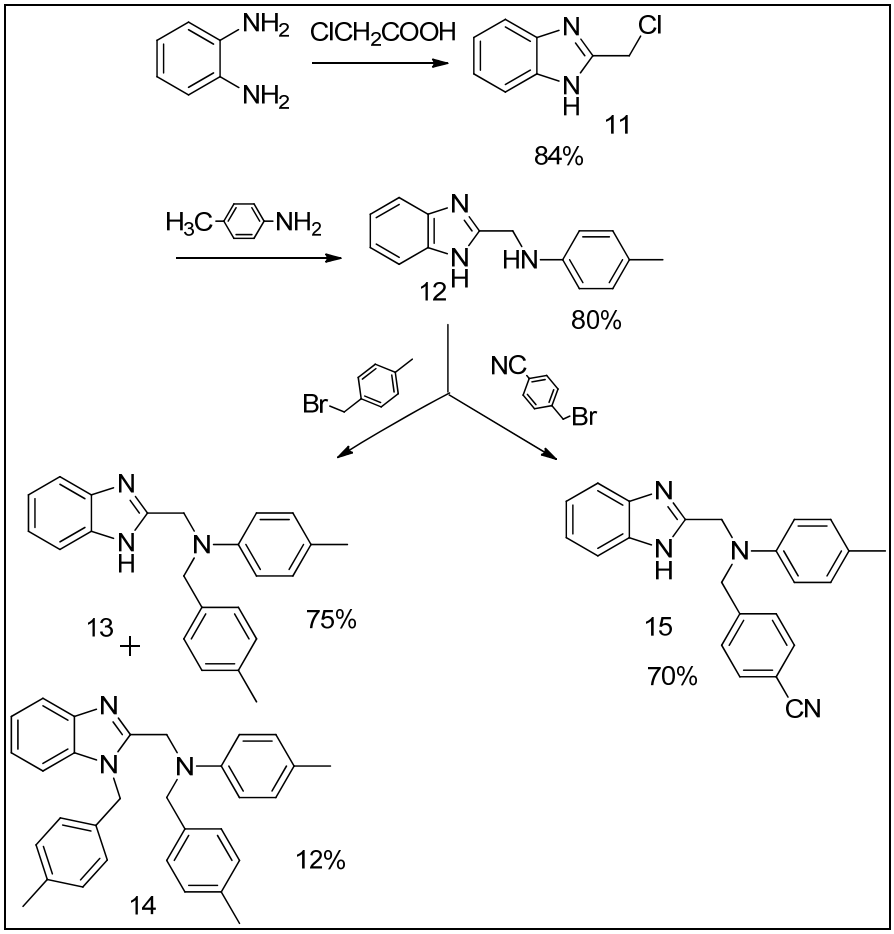

Scheme 2.4.4: Synthesis of *N*-((1*H*-benzo[*d*]imidazol-2-yl)methyl)-4-methyl-*N*-(4-methylbenzyl)aniline and its derivatives

2.4.3.2 Characterization:

All the new compounds were characterized by ^{1}HNMR and mass spectrometry. Spectra analyses were consistent with the assigned structures. Details of each structure with its characterization are presented in the experimental section.

2.4.4 Conclusion:

In summary, commercially available *o*-phenylenediamine was used to synthesize *N*-((1*H*-benzo[*d*]imidazol-2-yl)methyl)-4-methyl-*N*-(4-methylbenzyl)aniline and its derivatives. Novelty is the synthesis of three new molecules by conjoining two pharmacophores; benzimidazole and aniline together. Novel compounds are characterised by spectroscopic methods. The synthetic strategy has been designed in such a way so as to have the maximum yields from each step.

2.4.5Experimental

2.4.5.1 Materials and Methods:

All the compounds were purified using column chromatography (2000-400 mesh silica) before characterization. TLC analysis was done using pre-coated silica on aluminum sheets. Melting points were recorded in Thiele's tube using paraffin oil and are uncorrected. FT-IR (KBr pellets) spectra were recorded in the 4000-400 cm^{-1} range using a Perkin-Elmer FT-IR spectrometer. The NMR spectra were obtained on a Bruker AV-III 400 MHz spectrometer using TMS as an internal standard. The chemical shifts were reported in parts per million (ppm), coupling constants (J) were expressed in hertz (Hz) and signals were described as singlet (s), doublet(d), triplet(t), broad (b) as well as multiplet (m). The microanalysis was carried out using a Perkin-Elmer IA 2400 series elemental analyzer. The mass spectra were recorded on Thermo scientific DSQ-II. All chemicals and solvents were of commercial grade and were used without further purification. Single crystal data was collected with Xcalibur, EoS, Gemini.

2.4.5.2 Synthesis of compounds:

Synthesis of 4-iodo-2-nitro aniline (2):

To a solution of methanol (31ml) and water (6ml), slowly sulphuric acid (3ml) was added such that temperature of the reaction mixture was maintained at 25-30°C. 2-nitroaniline was then added to the reaction mass in one lot. Reaction mixture was stirred at 25-30°C

for 10mins. Then, iodine (4.6g) was added in one lot and stirred at 25-30°C for 2hrs. In ten minutes 30% H_2O_2 (3.3ml) was added. Reaction mixture was stirred at 25-30°C for 15-16h. Water (21.7 ml) was added and reaction mass was stirred at 25-30°C for 30mins to obtain white precipitate. Precipitate was filtered and washed with water, 5% sodium sulphite solution and again with water. Precipitate was further dried in high vacuum at 55-57°C for 2hrs.

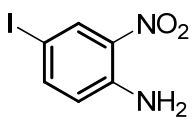 2 **$C_6H_5IN_2O_2$** **264**	**Yield:** 91% **M.P:** 115-117°C (literature melting point: 120-123°C) **MS(m/z):**263.37

Synthesis of 4-cyano-2-nitro aniline (3):

To a solution of 4-iodo-2-nitroaniline (5g, 18.9mmol) in dry DMF (15ml), CuCN (8.47g, 94.6mmol) was added. Reaction was heated to 140-150°C for 15-16 h. After completion, water (20ml) was added. Solid was obtained, filtered the solid and the filtrate was basified with K_2CO_3. The resulting solution was washed with ethylacetate (50ml x 3).The combined organic layer was washed with brine dried over Na_2SO_4 and concentrated in vacuo to give **6**. Analytically pure **6** were obtained by column purification.

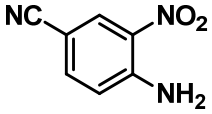 3 $C_7H_5N_3O_2$ 163	**Yield:** 65%

Synthesis of 4-cyano-*o*-phenylenediamine (4):

Compound **3** (1.4g, 8.58mmol) in solvent mixture CH_3COOH:CH_3OH:H_2O (2:2:1) (7ml) was stirred at 25-30°C for 5mins. After that iron powder (2.39g, 24.9mmol) was added to the reaction mass and sonicated for 1 hour such that temperature didn't exceed 35°C. After completion of the reaction, basified it with 2M KOH and extracted with ethyl acetate. Organic layer was then distilled and purified through column chromatography.

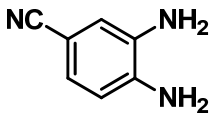 4 $C_7H_7N_3$ 133	**Yield:** 70% ; **M.P:** 140-142°C (literature melting point 144-148°C) **FT-IR(KBr) *γ*:** 3438.87, 3364.49, 3191.37, 2213.42 (-CN), 1631.40, 1579.58, 1514.17, 1314.75, 1150.23, 865.41, 812.15 cm^{-1}

Synthesis of 5-cyano-2-methyl benzimidazole (5):

In a round bottom flask compound **4** (5.4g, 0.03mol), water (20 ml) and glacial CH_3COOH (5.4g,0.09 mmol) were heated under reflux for 45 minutes. Reaction was cooled and basified with aqueous ammonia till pH 8-9, the precipitated product was filtered and recrystallized in 10% aqueous ethanol.

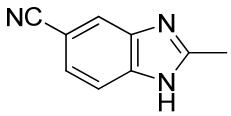 5 $C_9H_7N_3$ 157	**Yield:** 82%; **^{1}H NMR (400MHz,DMSO-d6) *δ*:**7.91(s,1H), 7.61(d, 1H, *J*=8Hz), 7.54(d, 1H, *J*=8Hz), 2.71(s, 3H) ppm

Attempted synthesis of 2-bromomethyl benzimidazole:

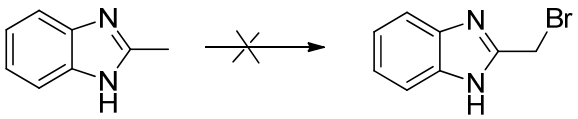

1g (0.0063mol) of compound 5 was charged in a round bottom flask. 1.7g (0.0095mol) of NBS and 20 ml of CCl_4 was added. Benzoylperoxide as an initiator was also added.

Method 1: Reaction mass was then stirred at 25-30°C in the presence of light (Tungstan filament lamp, 60W) for 15hrs. No product was obtained.

Method 2: Heated whole reaction mass at 80-85°C for 6hrs. No product formed.

Attempted synthesis of 2-bromomethyl benzimidazole:

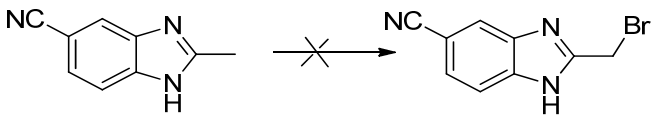

Compound 5 (1g, 6.3mmol) was charged in a round bottom flask. NBS (1.7g, 9.5mmol) and 20 ml of CCl_4 were added. Bezoylperoxide as an initiator was also added.

Method 1: Reaction mass was then stirred at 25-30°C in presence of light (Tungsten filament lamp, 60W) for 15hrs. No product obtained.

Method 2: Heated whole reaction mass at 80-85°C for 6hrs. No product found

Synthesis of 4-iodo toluene (6):

p-Toluidine (5g, 46.7mmol) was charged in a flask. Water (14.2ml) was added and the reaction mass was cooled to 0-5°C. Conc. HCl was added to it. The reaction mass was stirred for 5 to10 minutes at 0-5°C. After that $NaNO_2$(3.38g, 49.0mmol) solution in water was added such that temperature of the reaction doesn't exceed 5°C and stirred reaction mass for 5-10 minutes at the same temperature. In the above reaction mass slowly added KI (8.44g, 50.9mmol) solution in water such that temperature of the reaction mass should not exceed 10°C. [Evolution of nitrogen is observed]. Reaction mass was then allowed to stir at 25-30°C for 3 hours. Then, the reaction mass was slowly heated to 70-75°C and stirred at the same temperature for 30 minutes. Two layers were formed, separated out

thelower denser layer. Washed it with 10% NaOH solution, 5% sodium metabisulfite solutions and with distilled water. Distilled and column purified the product.

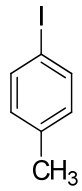 6 C_7H_7I 218	**Yield:** 85% **M.P:**207-209°C (literature value: 211.5°C)

Synthesis of 4-cyano toluene (7):

In a round bottom flask compound **7** (0.5g, 2.29mmol), CuCN (1.027g, 11.4mmol) and 5ml of DMF was charged. Heated the reaction mass to 120-130°C under inert atmosphere for 4hrs. After that 1.0 ml distilled water was added in reaction mass and basified with sodium carbonate. Product was then extracted in ethyl acetate and distilled. Crude mass was column purified to get the pure product.

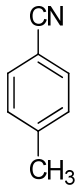 7 C_8H_7N 117	**Yield**: 75%; **B.P**: 215-217°C (Literature value: 217-218°C)

Synthesis of 4-(bromomethyl) benzonitrile (8):

In a round bottom flask, benzonitrile (0.05g, 0.426mmol) and N-bromosuccinamide (0.114g, 0.640mmol) were charged. Benzoyl peroxide as an initiator anddichloromethane (5ml) was added. Reaction was performed in the presence of light (Tungsten filament bulb, 60W) for 4-5 h. After that TLC was checked and extracted product in MDC. Organic layer was then distilled and degassed. Column purified to obtain the pure compound.

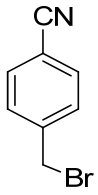 8 C_8H_6BrN 196	**Yield**: 92%; **M.P**: 110-112°C (Literature value: 115-117°C) **MS(m/z)(M^+):**195.42

Synthesis of 1-(bromomethyl)-4-methylbenzene and 1,4-bis(bromomethyl)benzene (Compound 9 and Compound 10):

p-Xylene (2g, 0.0188mol) and NBS (5.02g, 0.028mol) were chargedin R.B flask. Added 15 ml CCl_4 as a solvent and also added benzoyl peroxide as an initiator. Stirred reaction mass for 4-5 hrs at 25-30°C in the presence of light (Tungsten filament lamp, 60W).After that 20ml of water was added in reaction mass and extracted product in ethyl acetate. Distilled and degassed the organic layer. Compound was then purified using column chromatography. Ratio of compound 11:12 is 1:0.4.

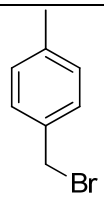 **9** C_8H_9Br	**Yield**: 92% **^{1}H NMR (400MHz,DMSO-d6) δ:**7.31 (d, 2H), 7.17 (d, 2H), 4.51(s, 2H), 2.37(s, 3H)ppm **MS(m/z)(M^+):**185.2

185	
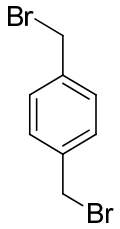 **10** $C_8H_8Br_2$ 264	**Yield**: 92% ; **^{1}H NMR (400MHz,DMSO-d6) δ:** 7.39(s, 4H), 4.50 (s,4H) ppm **MS(m/z)(M^+):**263.8

Synthesis of 2-(chloromethyl) benzimidazole (11):

5g (0.0462mol) *o*-phenylenediammine and 7.84g (0.069mol) 2-chloro acetic acid was charged in round bottom flask and stirred at room temperature for 5 minutes. Add 20ml of 5N hydrochloric acid as a solvent in it. Then heat the reaction mass to 110-130°C for 4-5 hours. Reaction was then cooled. Water was added and then basified with sodium carbonate and extracted with ethyl acetate.

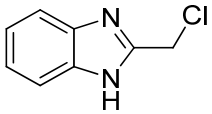 11 $C_8H_7ClN_2$ (166.6)	**Yield**:84% **M.P**: 145-147°C (Literature value: 146-148°C) **^{1}H NMR (400MHz, $CDCl_3$) δ**: 7.55(m,2H), 7.20(m,2H), 4.92(s,2H) ppm **MS(m/z)(M^+):**167

Synthesis of 2-(4-methylanilinomethyl)-1*H*-benzo[*d*]imidazole (12):

In round bottom flask DMSO (5ml) was charged. After that sodium hydride (0.82g, 0.034mol) was added and stirred reaction mass for 5 minutes. *p*-Toluidine (1.843g, 0.0172mol) was added and stirred reaction mass for 5 minutes at 25-30°C(color changes from brown to purple). 2g (0.0172mol) of **2** was added. Reaction was exothermic so maintained temperature such that it doesn't exceed 30°C. Stirred reaction mass for 15 minutes at 25-30°C and checked TLC. To quench reaction mass water was slowly added such that temperature doesn't exceed 30°C and product was then extracted in ethylacetate. The organic layer was distilled and degassed to obtain the crude mass. Column purification was done to obtain the required compound.

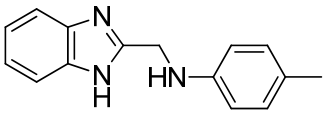 12 $C_{15}H_{15}N_3$ 237	**Yield**: 92% ; **^{1}H NMR (400MHz, $CDCl_3$)** δ: 7.57 (m,2H), 7.26 (m,2H), 6.98 (d, 2H), 6.57(d,2H), 4.64(s,2H), 2.23(s,3H) ppm. **MS(m/z) (M+1):**238

Synthesis of *N*-((1*H*-benzo[*d*]imidazol-2-yl)methyl)-*N*-(4-cyanobenzyl)-4-methylaniline (15):

In round bottom flask 0.05 g (0.21mmol) of **3** and 0.05g (0.316 mmol) of **9** were charged. 0.058g (0.422 mmol) dry $K_2CO_3$was added as a base and 5ml of ACN as a solvent. Refluxed reaction for 15-16 hrs at 80-85°C. Reaction was done under nitrogen atmosphere. After that 3ml of water was added in reaction mixture and extracted product in ethyl acetate. Organic layer was distilled and degassed under vacuum. Column was done to separate out the required spot.

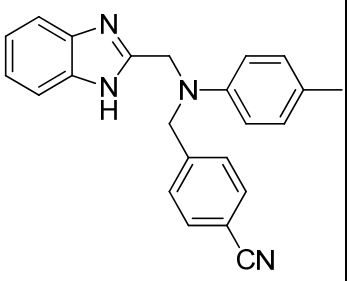 **15** $C_{23}H_{20}N_4$ 352	**Yield**: 92% ; **MS(m/z)(M^+)**:352.23

Synthesis of N-((1H-benzo[d]imidazol-2-yl)methyl)-4-methyl-N-(4-methylbenzyl)aniline and 4-methyl-N-(4-methylbenzyl)-N-((1-(4-methylbenzyl)-1H-benzo[d]imidazol-2-yl)methyl)aniline(Compound 13 and compound 14):

In round bottom flask 0.1g (0.422mmol) of compound3and 0.078g (0.422mmol) compound **20** was charged. 0.0875g (0.633mmol) of dry $K_2CO_3$was added as a base and 5ml of ACN as a solvent in the round bottom flask. Refluxed reaction mass for 15-16hrs Reaction was performed under nitrogen atmosphere. After that 3ml of water was added in reaction mixture and extracted product in ethyl acetate. Organic layer was distilled and degassed. Compound was column purified to separate molecule **16** and **17**.

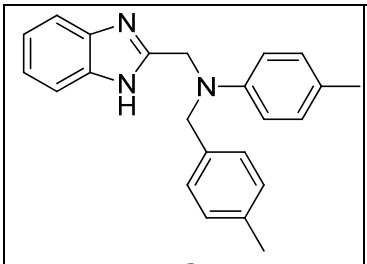 **13** $C_{23}H_{23}N_3$ 341	**Yield**:75% **^{1}H NMR (400MHz,DMSO-d6) *δ*:** 7.81 (m,1H), 7.51 (s,1H), 7.32 (m, 1H), 7.26 (m,1H), 7.17 (s,2H), 7.15 (s,1H), 7.03 (s,1H), 6.99 (m,2H), 6.77 (m,1H), 6.61(m,1H),5.41 (s,1H), 4.81(s,1H), 4.59 (s,1H), 4.46 (s,1H), 2.34 (s,3H), 2.24 (s,3H) ppm **MS(m/z) (M+1):** 342 (*Figure 2.4.5*)

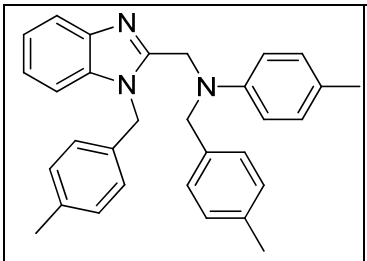 **14** $C_{31}H_{31}N_3$ 445	**Yield**:12%; **^{1}H NMR (400MHz,DMSO-d6) δ:**7.60 (m,1H), 7.44 (s,1H), 7.14 (m, 8H), 6.96(d,2H), 6.84(d,2H), 6.59(d,2H), 5.46 (s,2H), 4.76(s,2H), 4.56(s,2H), 2.249(s,3H), 2.243(s,3H), 2.10(s,3H) ppm **MS(m/z) (M+1):**446 (*Figure 2.4.3, 2.4.4*)

2.4.6 Selected Spectra:

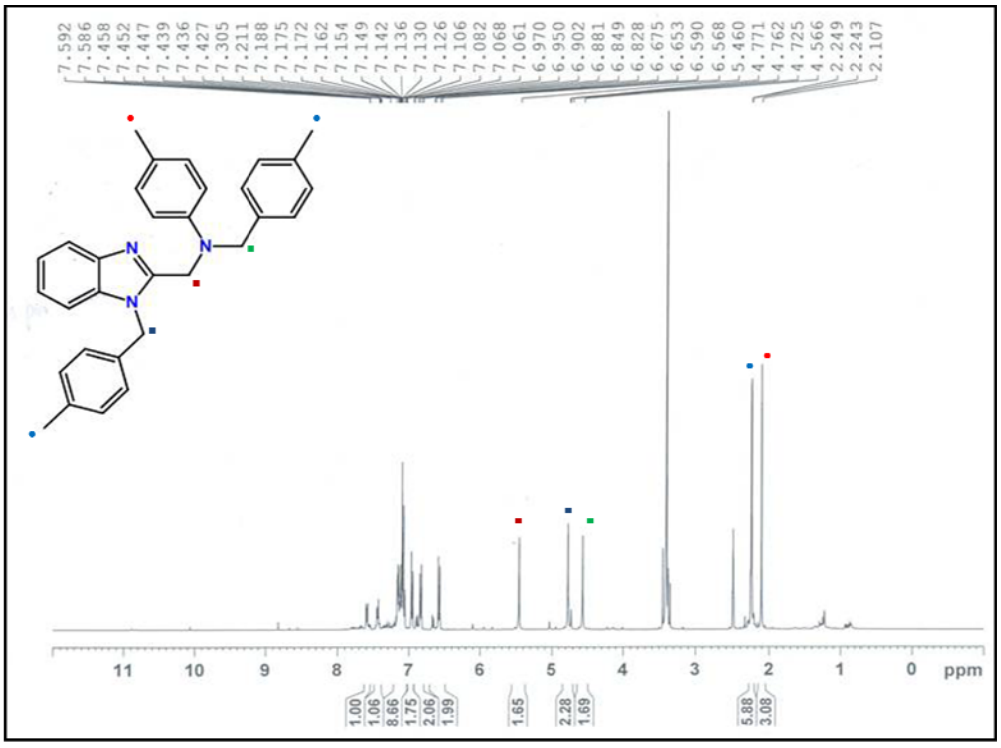

Figure 2.4.3: 1H NMR spectra of 14

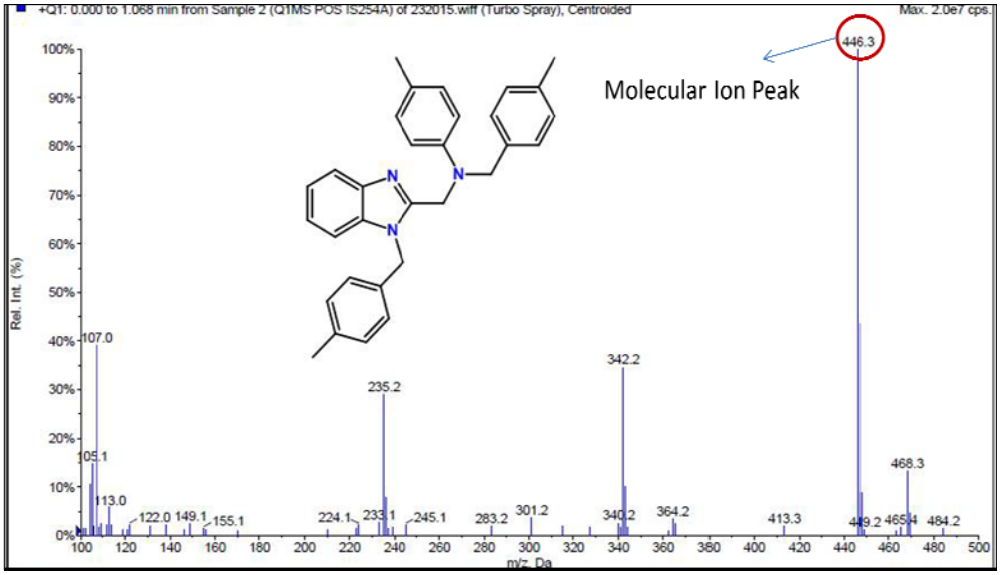

Figure 2.4.4: Mass spectra of 14

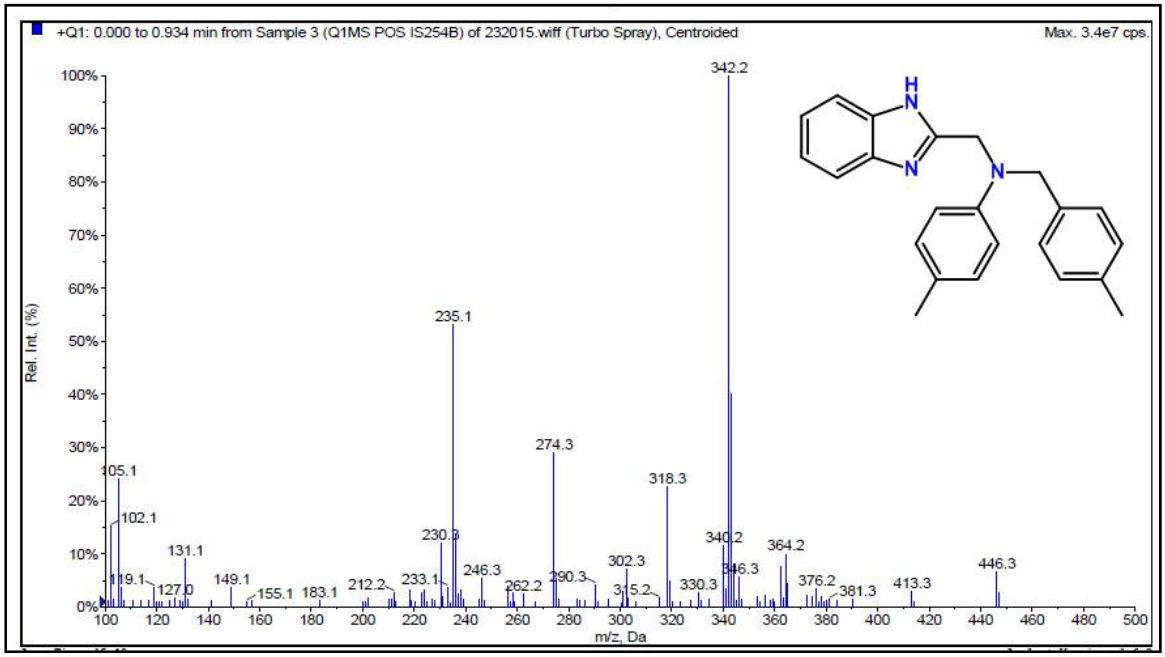

Figure 2.4.5: Mass spectra of 13

2.4.7 References:

[1] Fritsch, P. *Dermatologie Venerologie: Grundlagen. Klinik. Atlas*. Springer-Verlag, **2013**.

[2] Hille, T.; Irrgang, T.; Kempe, R. *Chemistry-A European Journal*, **2014**, *20*, 5569-5572.

[3] Chevalier, V.; Quest, M.*U.S. Patent No. 6,203,781*. Washington, DC: U.S. Patent and Trademark Office, **2001**.

[4] G. G. Scherer. Fuell Cells II, Springer Verlag, Berlin, **2008**, 65–120.

[5] Zhang, F.F.; Huang, G.; Wang, X.X.; Qin, Y.L.; Du, X.C.; Yin, D.M.; Liang, F.; Wang, L.M. *Chemistry-A European Journal*, **2014**, *20*, 17523-17529.

[6] S Panda, S.; Malik, R.; C Jain, S. Current Organic Chemistry, **2012**, *16*, 1905-1919.

[7] Zhang, H. Z.; Damu, G. L.; Cai, G. X.; Zhou, C. H. *European journal of medicinal chemistry*, **2013**, *64*, 329-344.

[8] Patel, M. O.; Prajapati, D. P. *International Journal for Research in Management and Pharmacy*, **2013**, *2*, 17-21.

[9] Baell, J.; Walter, M. A. *Nature*, **2014**, *513*, 481.

[10] Bo, S.; Fangsheng, J.; Pengpeng, W.; Jianjian, X. CN102936223 A, CN Applications, **2013**.

[11] Sahay, I. I.; Ghalsasi, P. S.; Singh, M.; Begum, R. *Synthetic Communications*, **2017**, *47*, 1400-1408.

[12] Brown, D. J.; Katritzky, A. R.; Rees, C. W. Comprehensive Heterocyclic Chemistry. *AR Katrizky (Ed.)*, **1984,** *2*, 150-189.

[13] Duganath, N.; Sridhar, C.; Jayaveera, K. N. *RJPBCS,* **2014**, *5*, 1044.

[14] Liu, P.; Chen, Y.; Deng, J.; Tu, Y. *Synthesis*, **2001**, 14, 2078-2080.

[15] (a) Hou, J.; Li, Z.; Fang, Q.; Feng, C.; Zhang, H.; Guo, W.; Wang, H.; Gu, G.; Tian, Y.; Liu, P.; Liu, R.; Lin, J.; Shi, Yi-K.; Yin, Z.; Shen, J.; Wang, P. G. *J. Med. Chem.***2012**, 55, 3066. (b) Chen, P. J.; Yang, A.; Gu, Y. F.; Zhang, X. S.; Shao, K. P.; Xue, D. Q.; He, P.; Jiang, T. F.; Zhang, Q. R.; Liu, H. M. *Bioorg. Med. Chem. Lett*. **2014**, 24, 2741. (c) Gu, S. J.; Lee, J. K.; Pae, A. N.; Chung, H.

J.; Rhim, H.; Han, S. Y.; Min, Sun-J.; Cho, Y. S. *Bioorg. Med. Chem.Lett.* **2010**, 20, 2705.

[16] Zhang, H. Z.; Cui, S. F.; Nagarajan, S.; Rasheed, S.; Cai, G. X.; Zhou, C. H. *Tetrahedron Letters*, **2014**, *55*, 4105-4109.

[17] Zhang, H. Z.; Damu, G. L.; Cai, G. X.;Zhou, C. H. *European journal of medicinal chemistry*, **2013**, *64*, 329-344.

Chapter 2: Part V

Pharmacophore V: Quinoxalinones

Contents

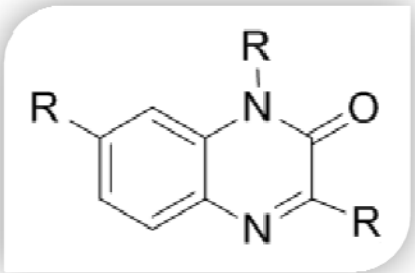

Abstract:

Quinoxalines and quinoxalinones are known to have antimicrobial, anti-inflammatory, anticancer and anti-HIV activities. Development of new molecules bearing this functionality is a challenging task of current interest. Synthesis of amidine-quinoxaline, a molecule with two pharmacophores, was planned with the help of two different retrosynthetic approaches. But end result was the combination of two different pharmacophores as a final product. In short, we report the short and simple synthesis of cyano bearing quinoxalinone. Reaction of cyano *o*-phenylenediamine with glyoxalic acid furnished quinoxalinone in 95% yield. The C-H bond activated Suzuki coupling reaction with boronic acid derivatives finally furnished the desired compound, 4-methyl-3-oxo-2-(p-tolyl)-3,4-dihydroquinoxaline-6-carbonitrile.

2.5.1 Introduction

As already discussed in chapter 2.1, the importance of amidines, here also we aimed to synthesize amidine and quinoxalinone adduct. The quinoxaline scaffold, which belongs to an important class of *N*-heterocycles, is incorporated in a large number of bioactive compounds which possess diverse biological properties (*Figure 2.5.1*). Among these compounds is the piperazinyl-substituted quinoxalinone, **1**, that has been reported to act as an antagonist for the histamine H4 receptor. This receptor plays an important role in immune modulatory and inflammatory functions in the human organism [1]. Similarly, *N*-alkylated quinoxalinone**2** was also suggested to act as a potent cancer chemotherapeutic agent [1]. Quinoxaline derivatives are effective antineoplastics [2], antivirals [3], antidepressants [4,5], and antibiotics [6,7]. In addition, they are used as dyes [8] and organic semi-conductors [9].

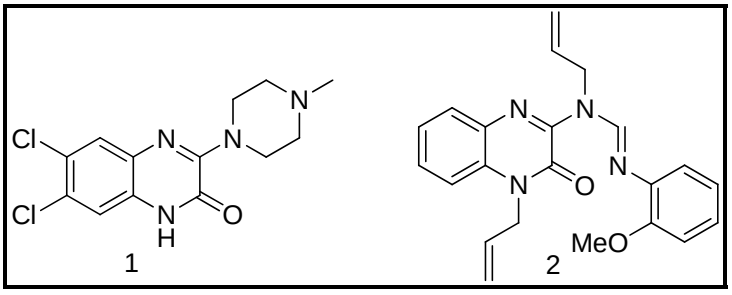

Figure 2.5.1: Biologically active quinoxalinones

2.5.2 Our Strategy:

Keeping the above literature survey in mind, our efforts were focused on the synthesis of amidine-quinoxalinone adducts. After designing of the target molecule, retrosynthetic disconnection approach was applied for efficient and economical starting materials. To obtain the target molecule two disconnection approaches (*Figure 2.5.2*) can be used, Path A: generating amidine from cyano group in the final step; functional group interconversion (FGI) and Path B: introducing amidine first and then quinoxalinone. The two paths use the two different synthons in the transformation steps.

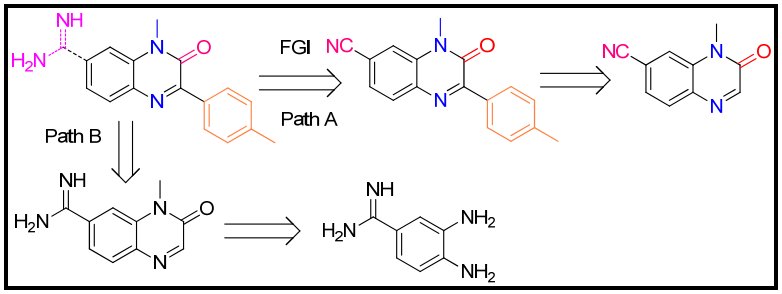

Figure 2.5.2: Retro synthesis for 4-methyl-3-oxo-2-(p-tolyl)-3,4-dihydroquinoxaline-6-carboximidamide

2.5.3 Results and Discussion:

2.5.3.1 Synthesis:

As seen in the previous section to synthesize target molecule C-H activated Suzuki Miyanura coupling reaction is an important step. For this synthesis of boronic acid, derivative is required for coupling reaction. Aryl bromide undergoes Grignard reaction to give the intermediate, magnesium bromide derivative, which further reacts with trimethoxy boron followed by hydrolysis to give boronic acid derivatives in good yields (*Scheme 2.5.1*) [10].

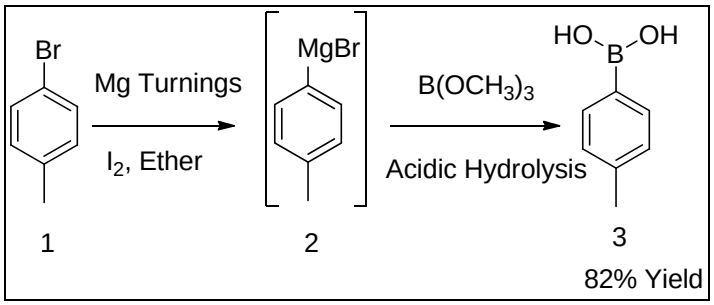

Scheme 2.5.1: Synthesis of *p*-tolylboronic acid

As discussed in chapter 2.4 the synthesis of 4-cyano-*o*-phenylenediamine compound **4** was achieved, as shown in scheme 2.5.2. Compound **4** in the first step was condensed with glyoxalic acid to form quinoxalinone **5**. The next step was the methylation of amide nitrogen of quinoxalinoneto furnish molecule **6**. The last step to achieve the target molecule was the C-H bond activated Suzuki coupling.Since the pioneering work of Suzuki and Miyaura [11], the use of organoboron reagents as nucleophilic coupling

partners with various organic electrophiles provides a powerful and general methodology for the formation of C-N and C-C coupled products. Amandine et al reported the C-3 arylation of quinoxalin-2(1*H*)-ones 1 with arylboronic acids using a catalytic amount of Pd (II) under oxygen atmosphere [12]. In this step the oxygen was used to oxidize Pd(0) to Pd(II), and keeps the reaction going[12].

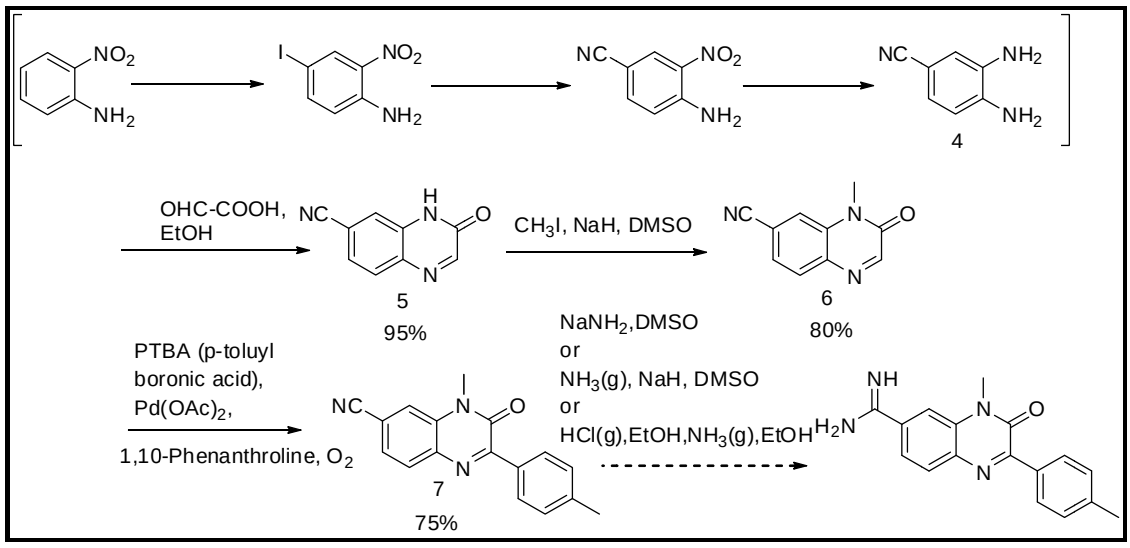

Scheme 2.5.2: Synthesis of 4-methyl-3-oxo-2- (*p*-tolyl)-3,4-dihydroquinoxaline-6-carbonitrile

Mechanistically:

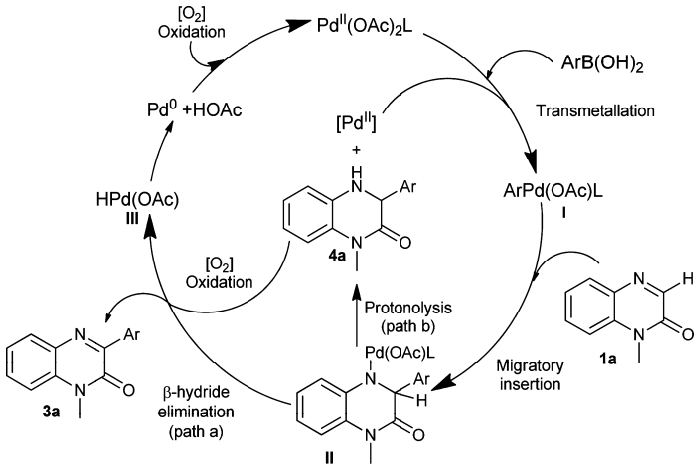

Figure 2.5.3: Plausible mechanism of C-3 annulation of quinoxalin-2-one[11]

Amandine et al, proposed the mechanism for the C-3 arylation of quinoxalinone where they have proposed the intermediate formation of the hydrated product 4a, which further undergoes oxidation to form the final desired product (*Figure 2.5.3*).

Attempted synthesis (Amidine formation; target molecule):

To synthesize our target molecule (*Figure 2.5.1*) one more strategy was tried (Path B). In this, molecule **9** was synthesized (*Scheme 2.5.3*). The idea was to introduce amidine pharmacophore first and then formation of quinoxalinone ring. The drawback of this synthesis was, after formation of amidine, cyclisation of diamino derivative to quinoxalinonewas never achieved (Multiple spots on TLC).

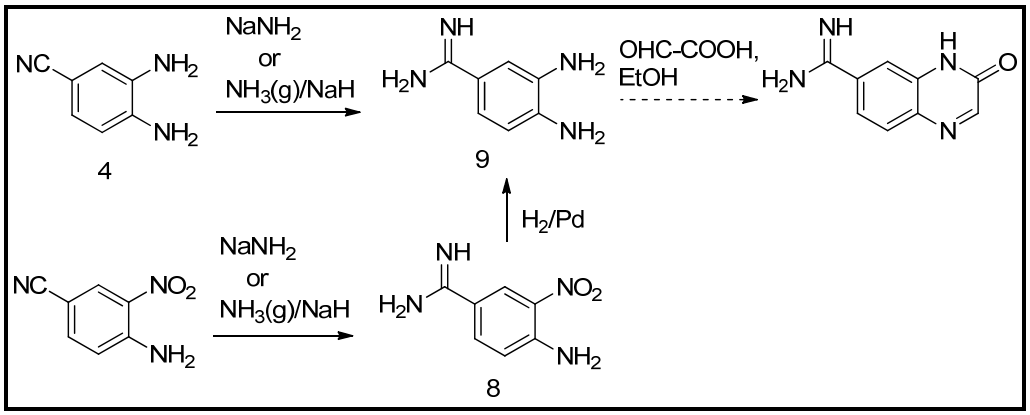

Scheme2.5.3: Attempted synthesis: Path B

2.5.3.2 Characterization:

All the new compounds were characterized by FT-IR, ^{1}HNMR and Mass spectrometry. Spectra analyses were consistent with the assigned structures. Details of each structure with its characterization are presented in the experimental section.

2.5.4 Conclusion:

In conclusion, strategy for conjoining two pharmacophores, amidine-quinoxalinone adduct was made, considering the best possible pathway. The synthesis of boronic acid derivative commenced from commercially available bromo toluene via Grignard reaction. Treatment of glyoxalic acid with cyano*o*-phenylenediamine gave quinoxalinone derivative. The final step is the Suzuki-Miyanura coupling reaction between boronic acid

and quinoxalinone derivatives. Conversion of cyano to amidine is practically feasible reaction but not when present in quinoxalinone ring. On the other hand, cyclisation of o-phenylenediamine in the presence of amidine functionality was also not observed. Hence, the overall synthesis of cyano-quinoxalinone was achieved in eight multiple steps with overall good yield.

2.5.5 Experimental

2.5.5.1 Materials and Methods:

All the compounds were purified using column chromatography (2000- 400 mesh silica) before characterization. TLC analysis was done using pre-coated silica on aluminum sheets. Melting points were recorded in Thiele's tube using paraffin oil and are uncorrected. FT-IR (KBr pellets) spectra were recorded in the 4000-400 cm^{-1} range using a Perkin-Elmer FT-IR spectrometer. The NMR spectra were obtained on a Bruker AV-III 400 MHz spectrometer using TMS as an internal standard. The chemical shifts were reported in parts per million (ppm), coupling constants (J) were expressed in hertz (Hz) and signals were described as singlet (s), doublet(d), triplet(t), broad (b) as well as multiplet (m). The mass spectra were recorded on Thermo scientific DSQ-II. All chemicals and solvents were of commercial grade and were used without further purification. Single crystal data was collected with Xcalibur, EoS, Gemini.

2.5.5.2 Synthesis of compounds:

Synthesis of 4-methylphenylboronic acid (3):

Title compound was prepared following the literature procedure [12,13]. The solution of 4- bromotoulene (12 ml, 0.1 mol) in dry THF (100 ml) was added slowly into the solution of magnesium (2.52 g, 0.10) in dry THF (100 ml). After addition, the reaction mass was refluxed for 1 h with stirring. In another flask trimethyl boronate (11.5 ml, 0.11mol) was charged and dry THF (100 ml) was added to it. The temperature of reaction mass was lowered to -78 ºC using liquid nitrogen, and the above prepared Grignard reagent was added dropwise to it with stirring. After stirring the reaction mass at -78 ºC for 1 h, 10%

sulfuric acid was added. The THF layer was separated and the aqueous layer was extracted 3 times with ethyl ether. The organic phase was combined and washed with water and dried to give the product in white powder. Re-crystallized from hot water to give pure 3 (8.7 g, 82%).

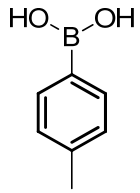 3 $C_7H_9BO_2$ (136)	**Yield:** 82% ; **M.P:** 250-252°C (literature melting point 256-258°C) **^{1}H NMR (400MHz,$CDCl_3$) δ:**8.16-8.14 (d, 2H, *J*=8Hz), 7.34-7.32 (d, 2H, *J*=8Hz), 2.46 (s, 3H) ppm **^{1}H NMR (400MHz,$CDCl_3$+ H_2O) δ:**8.16-8.14 (d, 2H, *J*=8Hz), 7.66-7.64 (d, 2H, *J*=8Hz), 7.34-7.32 (d, 2H, 8Hz), 7.25-7.23 (d, 2H, *J*=8Hz), 2.46 (s, 3H), 2.40 (s, 3H) ppm (*Figure 2.5.10*, *2.5.11*)

Synthesis of 3-oxo-3,4-dihydroquinoxaline-6-carbonitrile (5):

Title compound was prepared following the literature procedure [17]. To a solution of cyano *o*-phenylenediamine (2g)in absolute alcohol was added glyoxylic acid (50 %, 4.0 ml) and the reaction mixture was stirred under dry conditions for 3h. A white precipitate was obtained. The reaction mixture was concentrated in vacuum. Now added water and stirred at room temperature for further 1h. The precipitate was filtered, washed with cold absolute alcohol and oven dried at 55°C for 15-16h.

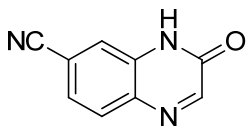 5 $C_9H_5N_3O$(171)	**Yield:** 70% ;

Synthesis of 4-methyl-3-oxo-3,4-dihydroquinoxaline-6-carbonitrile (6):

Title compound was prepared following the literature procedure [11]. Dry DMF (2ml) was charged, 60% NaH (91mg) was added. Reaction mass was cooled to 0°C. Compound **5** (200mg) was then added. After 5 mins methyl iodide 0.1ml was added. Stirred reaction mass at 0-20°C for 40mins.After completion of the reaction ice and chloroform were added. Separated out the organic layer and performed column chromatography to obtain the pure product.

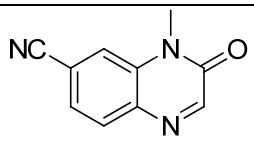 6 $C_{10}H_7N_3O$(185)	**Yield:** 70% ; **FT-IR(KBr)** ***γ*:**2924.82, 2225.68(-CN), 1717.93, 1662.83, 1608.02, 1559.00, 1306.93, 1059.05, 928.17, 831.27, 605.37 cm^{-1}. **^{1}H NMR(400MHz, $CDCl_3$)** ***δ*:**8.39 (s, 1H), 8.22 (s, 1H, *J*=5Hz), 7.86-7.84 (dd, 1H, *J*=1.6 Hz and 8.8Hz), 7.47-7.44 (d, 1H, *J*=8.8Hz), 3.727 (s, 3H) ppm **MS(m/z):** 184.89 (*Figure 2.5.4, 2.5.5, 2.5.6, 2.5.7*)

Synthesis of 4-methyl-3-oxo-2- (p-tolyl)-3,4-dihydroquinoxaline-6-carbonitrile(7):

Title compound was prepared following the literature procedure [11].To a solution of cyano methyl quinoxalinone (50mg) compound **6** in dry DMF was added 1,10-phenanthroline(7.3mg), $Pd(OAc)_2$ (6.06mg) and p-toluylboronic acid (55.11mg). Under oxygen atmosphere the reaction was stirred at 100-110°C for 20 h. After workup the crude residue was purified by silica gel column chromatography using a mixture of petroleum ether and ethyl acetate to furnish **7**.

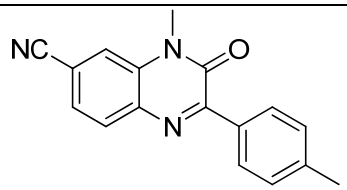 7 $C_9H_5N_3O$ (275)	**Yield:**72% **Anal. Calc. for $C_9H_5N_3O$:** C, 74.17, H, 4.76; N, 15.26 %, Found: C, 74.30, H, 4.65; N, 15.18 % **^{1}H NMR(400MHz, $CDCl_3$) δ:** 8.29-8.26 (d, 2H, *J*=8Hz), 8.25 (s, 1H, *J*=1.6Hz), 7.80-7.82(dd, 1H, *J*=2Hz and 8.8Hz), 7.42-7.40(d, 1H, *J*=8.8Hz), 7.33-7.31 (d, 2H, *J*=8Hz), 3.79 (s, 3H), 2.45 (s, 3H) ppm **MS (m/z):(M^+)** 275.09 (*Figure 2.5.8, 2.5.9*)

2.5.6 Selected Spectra

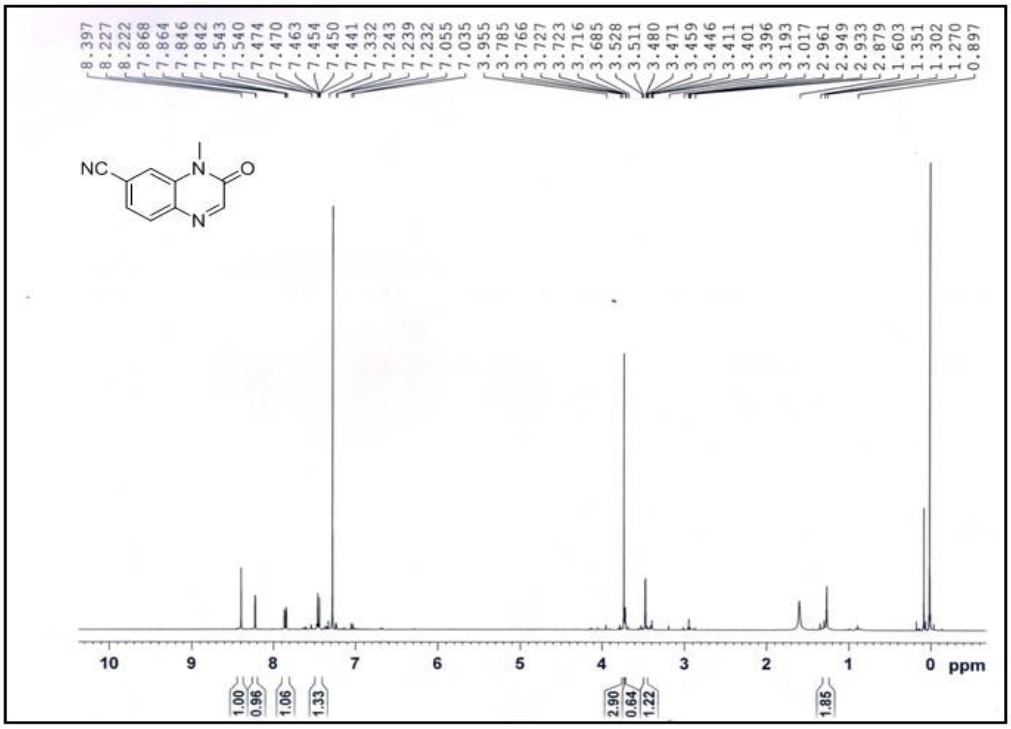

Figure 2.5.4: ^{1}H NMR spectra of 6

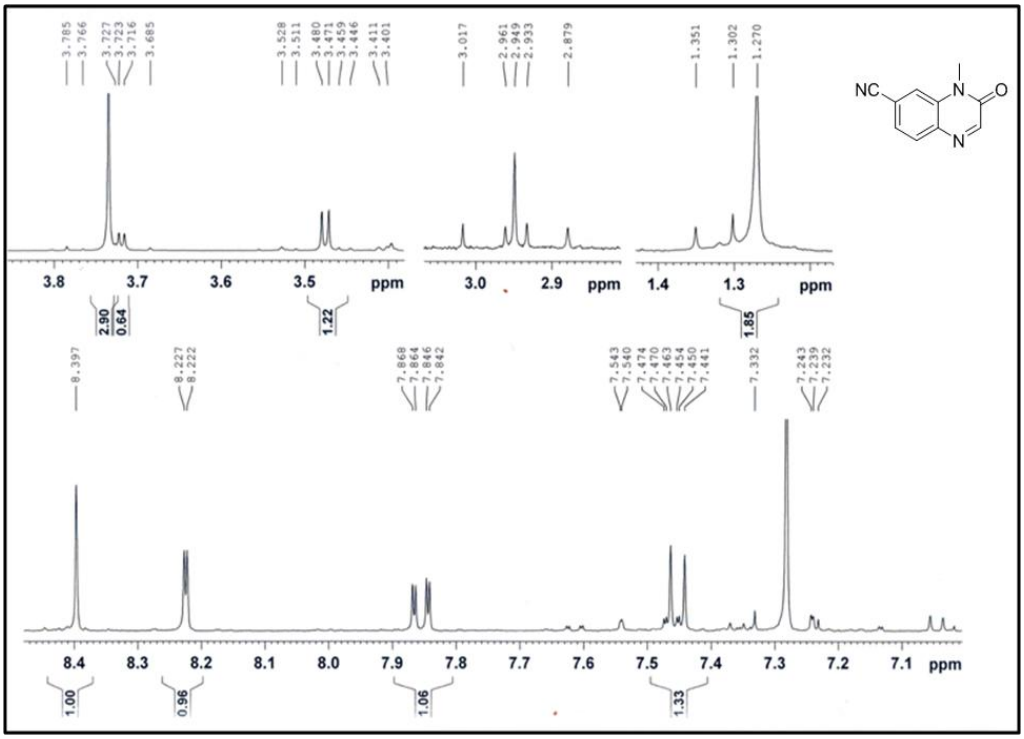

Figure 2.5.5: ^{1}H NMR spectra of 6 (Expansion)

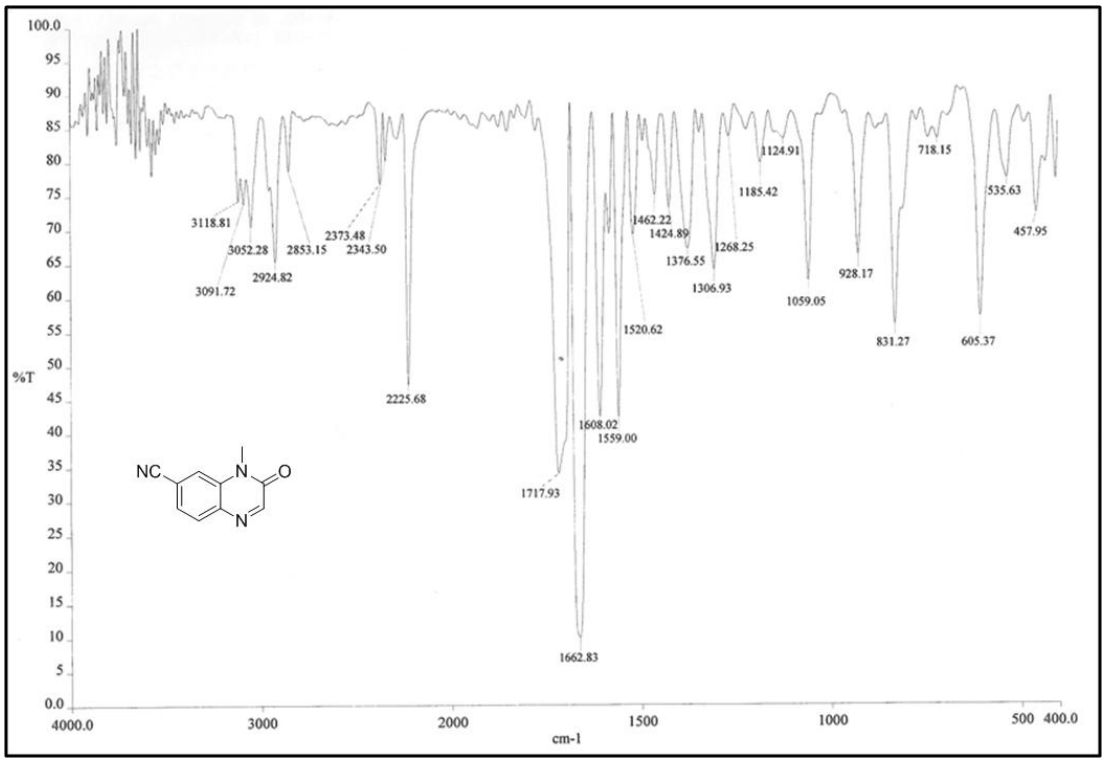

Figure 2.5.6: FT-IR spectra of 6

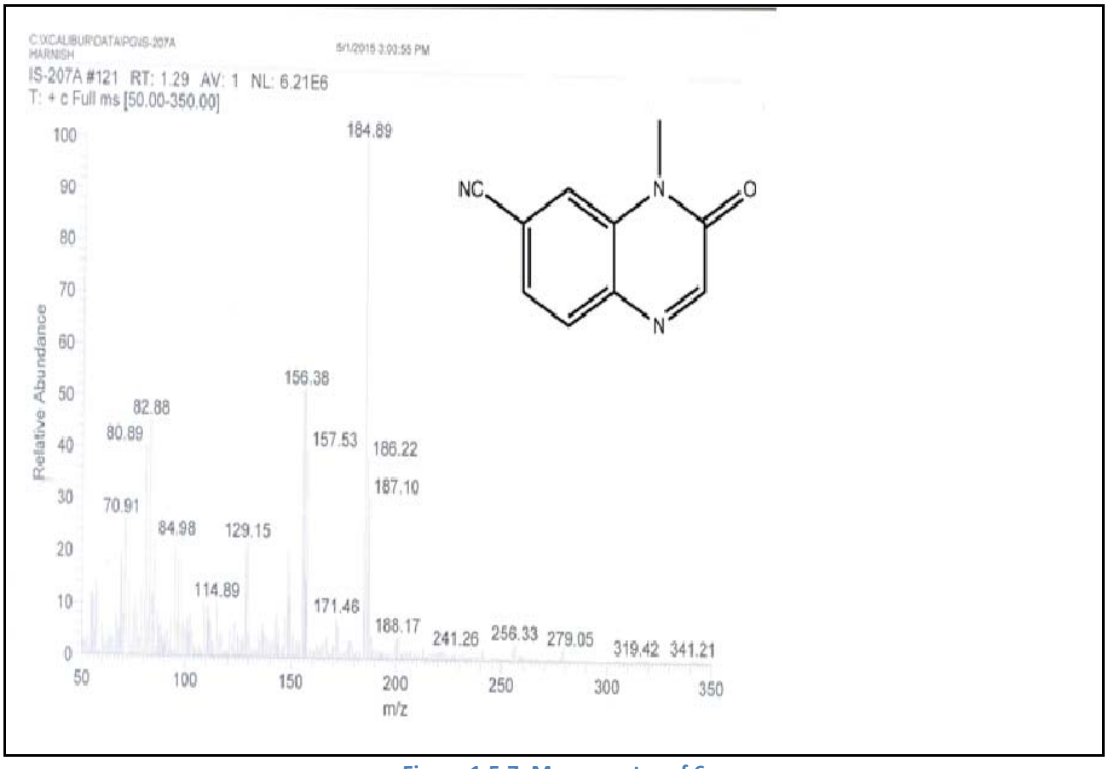

Figure 1.5.7: Mass spectra of 6

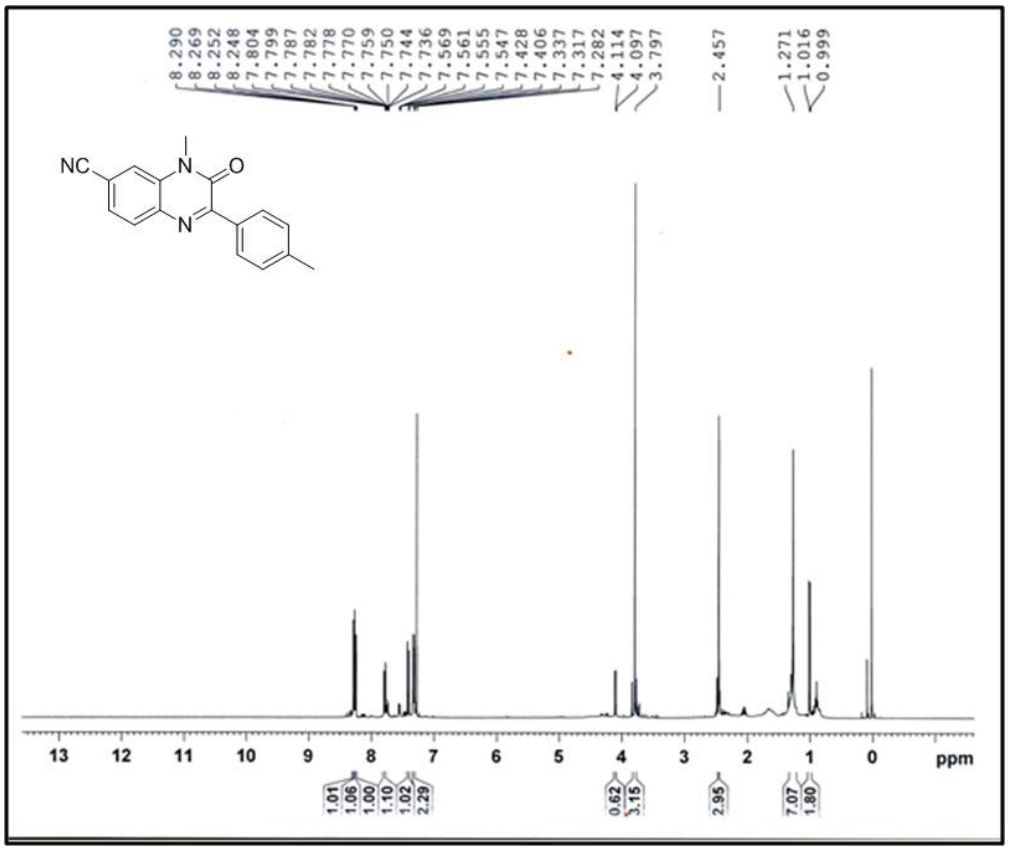

Figure 2.5.8: ^{1}H NMR spectra of 7

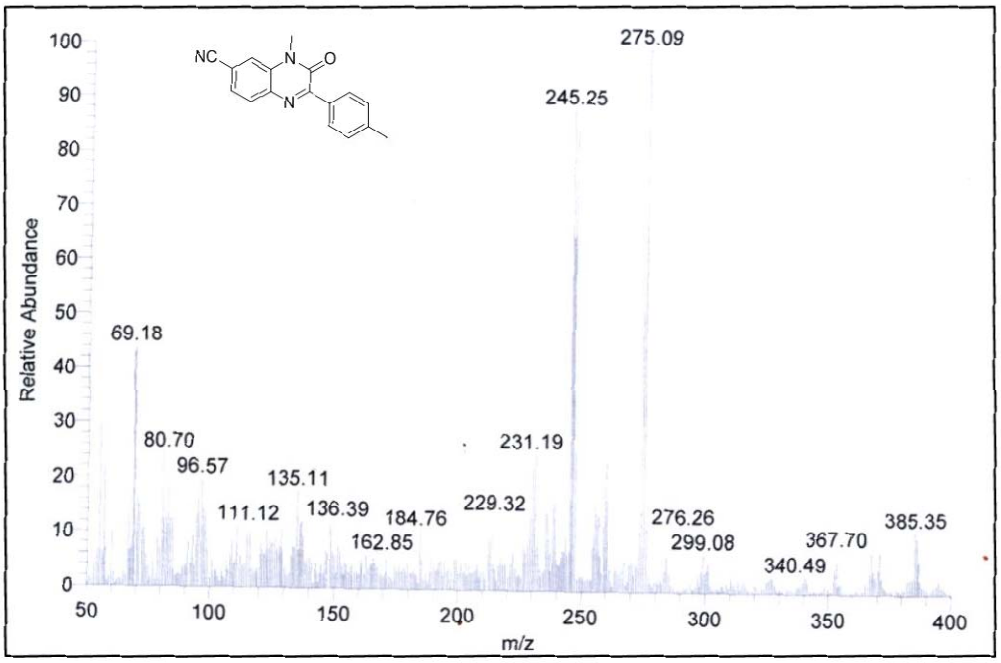

Figure 2.5.9: Mass spectra of 7

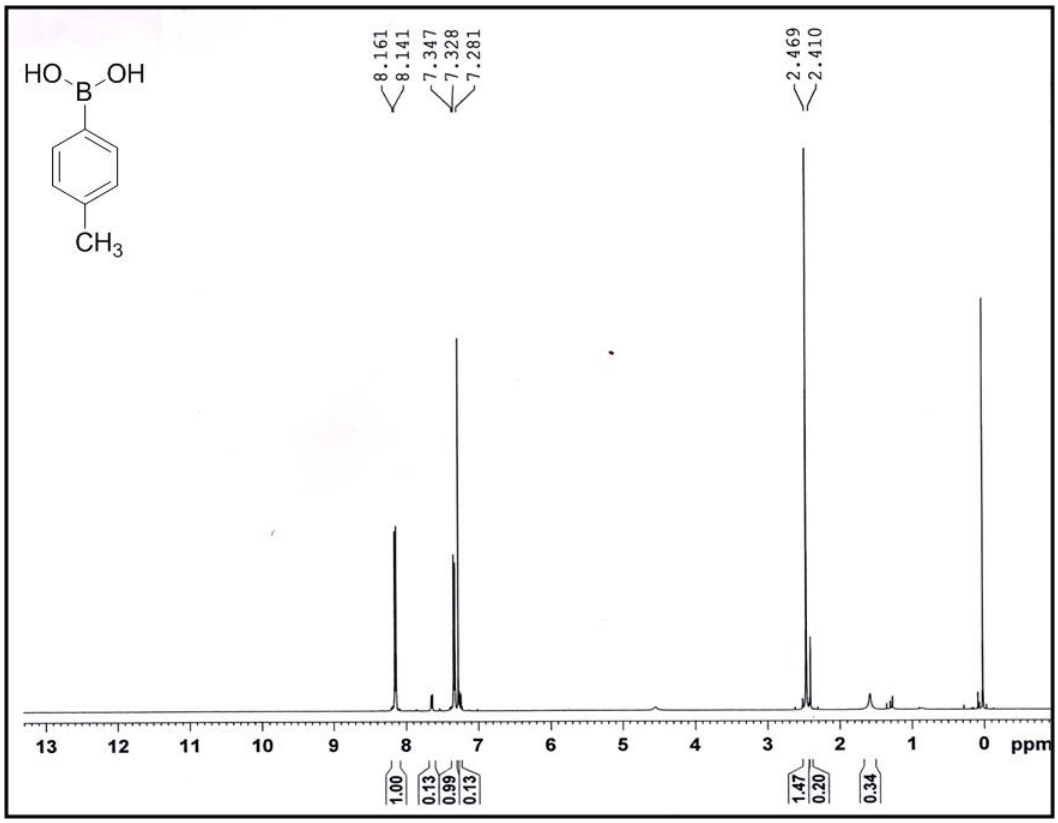

Figure 2.5.10: ^{1}H NMR spectra of 3

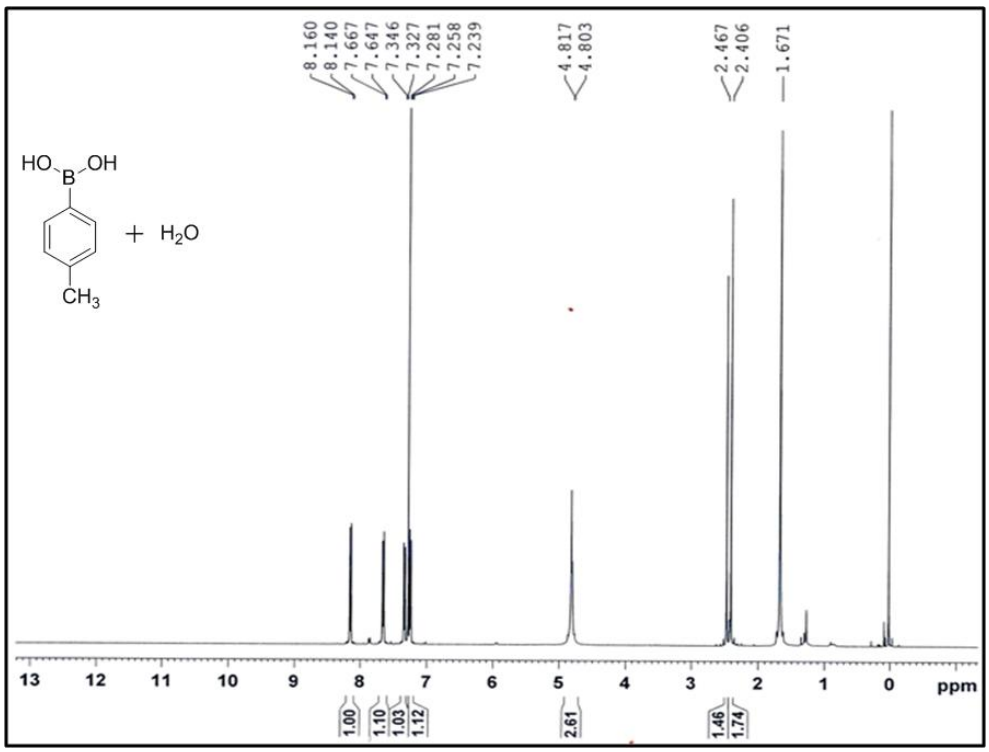

Figure 2.5.11: ^{1}H NMR of 3 with water

2.5.7 References:

[1] (a) Maichrowski, J.; Gjikaj, M.; Hübner, E. G.; Bergmann, B.; Müller, I. B.; Kaufmann, D. E. *European Journal of Organic Chemistry*, **2013**, *11*, 2091-2105.; (b) Smits, R.A.; Lim, H.D.; Hanzer, A.; Zuiderveld, O.P.; Guaita, E.; Adami, M.; Coruzzi, G.; Leurs, R.; de Esch, I.J.; *Journal of Medicinal Chemistry*, **2008**, *51*, 2457-2467.; (c) Smits, R.A.; Lim, H.D.; van der Meer, T.; Kuhne, S.; Bessembinder, K.; Zuiderveld, O.P.; Wijtmans, M.; de Esch, I.J.; Leurs, R. *Bioorganic & Medicinal Chemistry Letters*, **2012**, *22*, 461-467. (d) Galal, S.A.; Abdelsamie, A. S.; Tokuda, H.; Suzuki, N.; Lida, A.;ElHefnawi, M. M.; Ramadan, R. A.; Atta, M.H.; El Diwani, H. I. *European Journal of Medicinal Chemistry*, **2011**, *46* , 327-340.

[2] Undevia, S.D.; Innocenti, F.; Ramirez, J.; House, L.; Desai, A.A.; Skoog, L.A.; Singh, D.A.; Karrison, T.; Kindler, H.L.; Ratain, M.J. *European Journal of Cancer*, **2008**, *44*, 1684-1692.

[3] Briguglio, I.; Loddo, R.; Laurini, E.; Fermeglia, M.; Piras, S.; Corona, P.; Giunchedi, P.; Gavini, E.; Sanna, G.;Giliberti, G.; Ibba, C.*European Journal of Medicinal Chemistry*, **2015**, *105*, 63-79.

[4] Hille, T.; Irrgang, T.; Kempe, R. *Chemistry-A European Journal*, **2014**, *20*, 5569-5572.

[5] Pandit, R. P.; Kim, S. H.; Lee, Y. R. *Advanced Synthesis & Catalysis*,**2016**, *358*, 3586-3599.

[6] Gerchakov, S.; Schultz, H. P. *Journal of medicinal chemistry*, **1969**, *12*, 141-144.

[7] Jakubke, H.D.; Sewald, N. **2008**. *Peptides from A to Z: a concise encyclopedia*. John Wiley & Sons.

[8] Dailey, S.; Feast, W. J.; Peace, R. J.; Sage, I. C.; Till, S.; Wood, E. L. *Journal of Materials Chemistry*, **2001**, *11*, 2238-2243.

[9] O'brien, D.; Weaver, M. S.; Lidzey, D. G.; Bradley, D. D. C. *Applied Physics Letters*, **1996**, *69*, 881-883.

[10] Clary, J . W.; Singaram, B. WO2013016185 A1, **2013**.

[11] Miyaura, N.; Yamada, K.; Suzuki, A. *Tetrahedron Letters*, **1979**, *20*, 3437-3440.

[12] Carrër, A.; Brion, J. D.; Messaoudi, S.; Alami, M. *Organic letters*, **2013**, *15*, 5606-5609.

[13] Qu, D. H.; Wang, Q. C.; Ren, J.; Tian, H.*Organic letters*,**2004**, *6*(13), 2085-2088.

[14] Bo, S.; Fangsheng, J.; Pengpeng, W.; Jianjian, X., CN102936223 A, CN Applications, **2013**.

[15] Sahay, I. I., Ghalsasi, P. S., Singh, M., & Begum, R. *Synthetic Communications*, **2017**, *47*, 1400-1408.

[16] Chattopadhyay, P.; Nagpal, R.; Pandey, P. S.; *Aus. J. Chem*. **2008**, *61*, 216.

[17] Shahin, M. I.; El Ella, D. A. A.; Ismail, N. S.; Abouzid, K. A. *Bioorganic chemistry*, **2014**, *56*, 16-26.